



VNIVERSITATIS VALÈNCIA

Facultad de Medicina

Departamento de Fisiología

Programa de Doctorado en Medicina

PhD Thesis

**THE INTERPLAY BETWEEN METABOLOME,
EPIGENOME AND METABOLIC SYNDROME IN
SEVERE OBESITY: THE INFLUENCE OF SEX
AND AGE**

Presented by:

Serena Pisoni

Directors:

Dr. Daniel Monleón Salvadó

Dr. Vannina Elena González Marrachelli

Dr. Anna Maria Di Blasio

Tutor:

Dr. Consuelo Borrás Blasco

Valencia, December 2022

INFORME DIRECTORES/AS Y TUTOR/A PARA DEPÓSITO DE TESIS

Director (es) / Codirector (es):

1.- Apellidos y nombre: Monleón Salvadó, Daniel N.I.F. 29179910V, Departamento/Instituto: Patología Centro: Facultad de Medicina

2.- Apellidos y nombre: Di Blasio, Anna Maria D.N.I. CA75199AB, Departamento/Instituto: Istituto Auxologico Italiano Centro: de Investigación y Tecnologías Biomédicas

3.- Apellidos y nombre: González Marrachelli, Vannina N.I.F. 29185198S, Departamento/Instituto: Fisiología Centro: Facultad de Medicina

Tutor o tutora (si procede)

Apellidos y nombre: Borrás Blasco, Consuelo N.I.F. 22571468G, Departamento/Instituto: Fisiología Centro: Facultad de Medicina

Directores/as y tutor/a, respectivamente, de la tesis doctoral: "THE INTERPLAY BETWEEN METABOLOME, EPIGENOME AND METABOLIC SYNDROME IN SEVERE OBESITY: THE INFLUENCE OF SEX AND AGE"

de D/Dña. Serena Pisoni,

estudiante del Programa de Doctorado 3139 Medicina (RD99/2011) en Medicina de la Universitat de València, emiten informe favorable (*favorable/desfavorable*) para la realización del depósito y la defensa de la tesis doctoral.

Fecha: 12 de diciembre de 2022

Fdo.: Daniel Monleón Salvadó

DANIEL|
MONLEO|
N|
SALVADO|
Firmado digitalmente por DANIEL| MONLEON| SALVADO
Fecha: 2022.12.14 19:17:33 +01'00'

Director/a

Fdo.: Anna Maria Di Blasio



Director/a

Fdo.: Vannina González Marrachelli

VANNINA|
ELENA|
GONZALEZ|
MARRACHE|
LI|
Firmado digitalmente por VANNINA ELENA GONZALEZ| MARRACHELI
Fecha: 2022.12.13 09:53:23 +01'00'

Director/a

Fdo.: Consuelo Borrás Blasco

CONSUE|
LO|
BORRAS|
BLASCO|
Firmado digitalmente por CONSUELO| BORRAS|BLASCO
Fecha: 2022.12.12 11:09:43 +01'00'

Tutor/a

ESCUELA DOCTORAL
UNIVERSITAT DE VALÈNCIA

This Doctoral Thesis has been funded by the following grants:

- European Project Joint Programming Initiative ‘A Healthy Diet for a Healthy Life’ (JPI HDHL) **GUTMOM Maternal obesity and cognitive dysfunction in the offspring: cause-effect role of the GUT MicrobiOME and early dietary prevention.** 2018-2020. 150,000 euros. IP Consuelo Borrás; collaborating researchers: Daniel Monleón Salvadó and Vannina González Marrachelli.
- Project n. **43C003_2020: Gender difference in Adipose Tissue Biology** funded by the Italian Ministry of Health.

“Scientific research is still an adventure.”

Louis De Broglie

Ai miei genitori.

ACKNOWLEDGES

“Si el destino es importante, el viaje lo es aún más”. Ha sido un camino largo e intenso en el que he aprendido mucho y he crecido a nivel formativo y emocional, tropezando, cayendo y levantándome, más fuerte y enriquecida de un preciado bagaje de conocimientos y recuerdos. Ahora que estoy casi en la meta de esta aventura con mi trabajo de tesis y palabras más sentidas quiero agradecer a todas las personas que han creído en mí y me han permitido llegar a poner estos puntos finales.

En primer lugar, quiero agradecer inmensamente a mis directores de tesis, Daniel Monleón, Vannina González y Anna Maria Di Blasio por apostar por mí. Vuestra importante guía, cada uno en su papel de competencia, ha sido fundamental para el desarrollo de esta tesis doctoral. Gracias por la cordialidad y calidez con que me acogiste en el laboratorio dándome la posibilidad de vivir un período de aprendizaje y crecimiento profesional y personal, fundamental para mi futuro. Me habéis alentado a confiar siempre más en mí y en mis capacidades, viendo en mis reflexiones y ideas potencialidades que, a mí misma, a veces me costaba ver. A Daniel agradezco sincera y cordialmente tus preciosos conocimientos y consejos, también la abultada deuda intelectual contraída contigo más allá de los límites de este trabajo. Un agradecimiento especial a ti, Vannina, por haberme ayudado a ver la luz del sol cuando las nubes la desdibujaban y darme el empujón para llegar hasta aquí. La dedicación y el entusiasmo que tienes por la investigación y la enseñanza han sido contagiosos y motivadores para mí, incluso durante los momentos difíciles. Infine, grazie Anna per incoraggiarmi a esplorare nuove realtà e per il costante sostegno lavorativo e non durante questi anni.

Un gracias también a mi tutora, Consuelo Borrás, por su disponibilidad y

atención, recibíendome siempre con con afecto.

Con la misma importancia quiero agradecer a José Manuel Morales tu disponibilidad, cariño, consejos, apoyo y paciencia, así como tu inmensa ayuda personal y científica desde el primer momento.

Gracias a todas las personas del grupo LABIMM por ser fuente de colaboración y buenos consejos, así como amistades, contribuyendo enormemente a mi tiempo profesional y personal en Valencia. A Mercedes, Itziar, María, Antonio, Musta, Pilar, Patricia y todos los que habéis cruzado mi camino, gracias por haberme acompañado y sosteniendo en el desarrollo de esta tesis, compartiendo experimentos, congresos, celebraciones y momentos divertidos.

Gracias también a los compañeros y profes de los Departamentos de Patología y Fisiología por el tiempo compartido y por vuestro interés por mí y apoyo. Especialmente a Javier Megías por tu ayuda desinteresada y compromiso con el desarrollo de los experimentos de cultivo celular. A pesar de las dudas y dificultades encontradas, gracias a tu experiencia, en nuestra lucha personal contra unos adipocitos particularmente hostiles, ¡al final salimos ganando!

Un ringraziamento speciale va inoltre al Dott. Davide Gentilini per le sue preziose conoscenze e al suo gruppo di ricerca per avermi dato la possibilità di sviluppare una parte importante di questa tesi. In particolare a Luciano, con cui ho collaborato maggiormente, per la sua disponibilità e attenzione.

Pero “no todo en la vida es trabajo”, así que gracias también a todos los amigos valencianos y no valencianos que he conocido en estos años por haberme brindado vuestro apoyo moral especialmente en las últimas etapas de este camino. Vivir lejos de casa no es siempre fácil, pero sin vosotros lo

habría sido aún menos. ¡Un baile celebrativo no podrá faltar!

Grazie ai miei ex colleghi italiani, Antonio, le “ziette” Ema e Ale, AleNa, Monica, Claudina, Ester, Marghe e Teo, e tutti (siete tantissimi e di ognuno ho un ricordo speciale) per avermi incoraggiato e sostenuto nel mio trasferimento a Valencia che doveva durare un anno e sono diventati 5; per non “esserci persi” nonostante tutto e per avere sempre un pensiero e una parola di affetto per me. É sempre una gioia venirvi a trovare!!

Un immenso grazie agli amici di una vita per esserci sempre con tutto il vostro affetto e incoraggiamento come se il tempo e le distanze non contassero. Ognuno di voi sa quanto sia importante per me!

Infine, il ringraziamento più grande va ai miei genitori, Norma e Umberto, che mi hanno cresciuto con infinito amore e hanno contribuito a formare la persona che sono oggi supportandomi sempre nelle mie scelte, anche se difficili, fino al raggiungimento di questo importante traguardo. In particolare, dedico questa tesi a te mia cara mamma, per esserci sempre stata e per continuare ad esserci sempre.

Un pensiero finale a me, per aver avuto il coraggio di intraprendere questo cammino che a volte mi é sembrato più una corsa ad ostacoli che una tranquilla passeggiata, per non aver mollato e, nonostante qualche livido, essere arrivata fino alla fine più allenata e forte, pronta per le nuove sfide che la vita mi riserverá.

LIST OF CONTENTS

ABBREVIATIONS	i
LIST OF TABLES	vii
LIST OF FIGURES	ix
ABSTRACT	xiii
RESUMEN	xix
1. INTRODUCTION	3
1.1. Adult overweight and obesity.....	3
1.1.1. Obesity measurement and classification.....	6
1.1.1a. Clinically severe (Class III) obesity.....	7
1.1.2. Metabolism in clinically severe obesity.....	8
1.1.2a. Metabolic healthy and unhealthy obesity.....	10
1.1.2b. Metabolic alterations: the role of adipose tissue....	13
1.1.3. The Metabolic Syndrome.....	15
1.1.3a. MetS clinical definition: characteristics and implications.....	16
1.1.3b. Synergistic effects of MetS components.....	17
1.1.3c. The relationship between sex and age and the role of sex hormones.....	20
1.1.4. Multifactorial causation of obesity and metabolic disorders: genetics, epigenetics and lifestyle.....	23
1.2. The metabolome and its metabolic pathways.....	25
1.2.1. Regulation and deregulation of metabolic pathways.....	27
1.3. The epigenetic landscape and concept.....	28
1.3.1. The chromatin fibre and main epigenetic mechanisms.....	30
1.3.1a. The modification of histones.....	32
1.3.1b. DNA methylation.....	34
1.3.1c. RNA-based mechanisms.....	36
1.3.2. The CpG islands.....	37
1.3.3. Stochastic epigenetic mutations and epigenetic drift.....	38
1.3.4. The epigenetic clock.....	40
1.3.5. Biological role in MetS.....	42
1.4. Metabolomics and epigenomics: “-omic” sciences in comparison.....	43
1.4.1. The metabolomics.....	45

1.4.2. The epigenomics.....	48
1.5. The need for MetS better understanding and the unsolved problems about the lack of common diagnostic criteria and biomarkers, sex and gender difference and social and scientific perception.....	50
2. HYPOTHESIS AND AIMS OF THE STUDY.....	57
2.1. Hypothesis.....	57
2.2. Aims of the study.....	58
3. EXPERIMENTAL DESIGN.....	63
3.1. Study design and experimental workflow.....	63
3.2. Characterization of the Piancavallo cohort.....	66
3.2.1. Recruitment of the Piancavallo cohort.....	66
3.2.1a. Inclusion/exclusion parameters collection and measurement.....	67
3.3. Mechanistic hints in experimental animal models fed with High Fat Diet.....	68
3.3.1. Cell assay on adipose tissue obtained from an HFD-fed rats model.....	70
4. MATERIAL AND METHODS.....	73
4.1. Methodological approaches applied to the Piancavallo cohort....	74
4.1.1. Collection of phenotypic data.....	74
4.1.1a. Phenotypic data processing and quality control....	75
4.1.2. Collection and storage of blood samples.....	76
4.1.3. NMR spectroscopy and serum metabolomics analysis.....	76
4.1.3a. Serum samples preparation for NMR measurement and pre-analytical quality control.....	78
4.1.3b. Serum spectra acquisition.....	78
4.1.3c. NMR spectra processing and quality control.....	79
4.1.3d. Metabolites and spectral regions assignment.....	79
4.1.3e. Metabolites and spectral regions quantification....	83
4.1.4. DNA methylation. Epigenetics.....	83
4.1.4a. Whole blood samples preparation for methylation assay.....	84
4.1.4b. Epigenome-wide methylation assay.....	86

4.1.4c.	Post-array quality control and data pre-processing.....	87
4.1.4d.	Estimation of lymphocyte subpopulations and biological (epigenetic) age.....	91
4.1.4e.	Analysis of stochastic epigenetic mutations.....	91
4.2.	Methodological approaches applied to the HFD-fed animal model.....	93
4.2.1.	Collection of rat body measurements.....	93
4.2.2.	Rat perigonadal fat tissue collection and processing for cell or organ cultures.....	94
4.2.3.	Cell and tissue culture techniques.....	96
4.2.3a.	Maintenance of cells and organ crops and D-mannose treatment.....	96
4.2.3b.	Collection and storage of samples of blank culture medium and culture medium after cell incubation.....	97
4.2.3c.	Collection and freezing of organ culture fragments and adherent differentiated adipocytes.....	98
4.2.4.	NMR spectroscopy and metabolic profile of culture media obtained from adipocytes and adipose tissue organ cultures.....	98
4.2.4a.	Adipocytes and adipose tissues culture media samples preparation for NMR measurement and pre-analytical quality control.....	99
4.2.4b.	Adipocytes and adipose tissues culture media spectra acquisition and processing for calculation of uptake or excretion.....	99
4.3.	Statistical analysis.....	101
4.3.1.	Analysis of phenotypic variables.....	104
4.3.2.	Metabolomics statistical analysis.....	106
4.3.2a.	NMR data processing and multivariate analysis.....	106
4.3.2b.	Metabolites pathways enrichment analysis.....	108
4.3.3.	Epigenetics statistical analysis.....	108
4.3.3a.	Logistic regression analysis.....	108

4.3.3b. Analysis of the epigenetic differences between MHO and MetS.5 subgroups of subjects over 54 years.....	109
4.3.3c. Prioritization analysis and gene ontology.....	110
4.4. Solutions composition.....	111
5. RESULTS.....	115
5.1. Characterization of MetS in clinically severe obesity.....	115
5.1.1. Anthropometric characterization of the Piancavallo cohort and analysis of MetS prevalence.....	115
5.1.1a. Comparison of the anthropometric measures used to assess weight-related risk between MHO and MetS subjects by sex and age ranges.....	117
5.1.1b. Comparison of metabolic characteristics.....	117
5.1.2. Metabolomics characterization of MetS in severe obesity: general view of metabolic profile in Piancavallo cohort.....	121
5.2. Piancavallo cohort metabolomic analysis: focus on MetS extreme case.....	127
5.2.1. The influence of age on metabolomic features in the extreme case of MetS.....	130
5.3. Age-related sexual dimorphism of metabolic traits in extreme MetS in severe obesity.....	135
5.4. Metabolomic-epigenetic interplay on MetS in severe obesity: the epigenetic study.....	144
5.4.1. Group level: differential methylation analysis.....	144
5.4.2. Single case level: SEM analysis and hyper- and hypomethylation levels of SEMs.....	148
5.4.2a. Association between SEMs and metabolomic, clinical and pathological characteristics.....	148
5.4.2b. Sex influence on the burden of SEMs.....	151
5.4.3. Biological age estimation in healthy and pathological severe obesity.....	152
5.5. Metabolic characterization of the HFD-fed Wistar rats animal model.....	154
5.5.1. The effect of diet on the body weight: comparison of CTL and HFD rats by sex.....	154

5.5.2. CTL vs HFD rats' perigonadal fat pads: differences in morphology, structure and metabolism.....	155
5.5.3. The potential role of the metabolome of adipocytes and adipose tissue on MetS in severe obesity.....	158
5.5.3a. The influence of diet on the metabolism of rat adipocytes and adipose tissue.....	159
5.5.3b. The influence of diet on metabolic sexual dimorphism in rat adipocytes.....	162
5.5.4. The effect of mannose on rat adipocytes and adipose tissue metabolism.....	166
6. DISCUSSION.....	171
6.1. The analysis of the metabolic profile of MHO and MUHO individuals can be supportive for a better and earlier classification of the MetS.....	171
6.2. The metabolome characterization may help to understand and manage the age-dependent sexual dimorphism on MetS prevalence in clinically severe human obesity.....	177
6.3. The role of metabolome-epigenome interaction in age- and sex-dependent incidence of MetS in clinically severe obesity.....	184
6.4. Adipocytes from animals under different diets show metabolic changes similar to those observed in MetS in human severe obesity.....	192
6.5. Our findings may be relevant in providing the basis for the introduction of specific preventive and therapeutic interventions to improve the prognosis and quality of life of severely obese patients.....	199
6.6. Limitations of the study.....	204
7. CONCLUSIONS.....	209
8. REFERENCES.....	215
9. ANNEXES.....	253
ANNEX I: Ethics Review Committee approval.....	253
ANNEX II: Experimental rat's diets composition sheets.....	257

ABBREVIATIONS (in alphabetic order)

AHC, Agglomerative Hierarchical Clustering;

ANOVA, One-way Analysis of Variance;

ApoB, apolipoprotein B albumin;

ATGL, adipose tissue triglyceride lipase;

ATMs, adipose tissue macrophages;

ATP, adenosine triphosphate;

ATP III, Adult Treatment Panel III;

AUC, area under the ROC curve;

BCAAs, branched-chain amino acids;

BMI, body mass index;

BMIQ, Beta MIxture Quantile;

cc, calorimetric calculation;

CCC, choline-containing compounds;

chAge, chronological ages;

ChAMP, Chip Analysis Methylation Pipeline;

CpG, dimer of cytosine (C) followed by guanine (G);

CR, caloric restriction;

CRP, C-reactive protein;

CTL, control;

CVD, cardiovascular disease;

D₂O, deuterium oxide;

DBP, diastolic blood pressure;

DEXA, dual-energy x-ray absorptiometry;

DM1, type 1 diabetes;

DM2, type 2 diabetes;

DMEM, Dulbecco's Modified Eagle Medium;

DNAm, methylation of DNA;

DNMTs, DNA methyltransferases;
EDTA, ethylenediaminetetraacetic acid;
EGIR, European Group for the Study of Insulin Resistance;
EWAS, epigenome-wide association study;
F, female;
FA, fatty acid;
FACO1, carbonyls in fatty acids 1;
FACO2, carbonyls in fatty acids 2;
FDR, False Discovery Rate;
FFA, free fatty acid;
FFM, fat-free mass;
FM, fat mass;
FTO, fat mass and obesity-associated protein;
glm, generalized linear regression model;
GO, Gene Ontology;
GWAS, genome-wide association study
HAT, histone acetyltransferase;
HDAC, histone deacetylase;
HDL, high-density lipoprotein cholesterol;
HFD, high-fat diet;
HIF-1 α , hypoxia-inducible factor 1-alpha;
HMDB, Human Metabolome Database;
HMP, Human Metabolome Project;
HMTs, histone methyltransferases;
HOMA-IR, homeostasis model of assessment for insulin resistance;
HRMS, high-resolution mass spectrometry;
HSL, hormone-sensitive lipase;
IBW, ideal body weight;

IDF, International Diabetes Federation;

IDOL, inducible degrader of the LDL receptor;

IEAA, Intrinsic Epigenetic Age Acceleration;

IQR, interquartile ranges;

KEGG, Kyoto Encyclopedia of Genes and Genomes;

LDL, low-density lipoprotein cholesterol;

LDL2, low-density lipoprotein cholesterol 2;

LINEs, long interspersed nuclear elements;

SINEs, short interspersed nuclear elements;

LPL, adipose tissue lipoprotein lipase;

LPS, lipopolysaccharide;

LV, latent variable;

M, men (humans); male (rats);

MDS, multidimensional scaling;

MetPA, metabolic pathway analysis;

MetS, metabolic syndrome status;

MetS.3, MetS subgroup manifesting three of MetS components, including visceral obesity;

MetS.4, MetS subgroup manifesting four of MetS components, including visceral obesity;

MetS.5, extreme MetS subgroup manifesting all five MetS components;

MHO, metabolically healthy obese status;

MUH-NW, metabolically unhealthy normal weight status;

MUHO, metabolically unhealthy obese status;

MYLIP, myosin regulatory light chain interacting protein;

NAC1, acetyls in glycoproteins 1;

NAC2, acetyls in glycoproteins 2;

NCDs, non-communicable diseases;

NCEP, National Cholesterol Education Program;
NEFAs, no-esterified fatty acids;
NIH, National Institutes of Health;
NMR, nuclear magnetic resonance;
PAI-1, plasminogen activator inhibitor 1;
PBS, phosphate-buffered saline;
PCA, principal component analysis;
PLS-DA, partial least-squares discriminant analysis;
ppm, parts per million;
PUFAs, polyunsaturated fatty acids;
REE, resting energy expenditure;
ROC, receiver operating characteristic;
s, serum;
SAM, S-adenosylmethionine;
SatO₂, oxygen saturation;
SBP, systolic blood pressure;
SD, standard deviation;
SEMs, stochastic epigenetic mutations;
SNP, single-nucleotide polymorphism;
ST, skinfold thickness;
SWAN, subset-quantile within array normalization;
T4, thyroxine;
TE, tris-EDTA;
TGL, triglyceride;
TMAO, trimethylamine oxide;
TNF α , tumour necrosis factor α ;
TSH, thyroid stimulating hormone;
TSP, trimethylsilyl propionate;

TXNIP, thioredoxin interacting protein;
UFA1, unsaturated fatty acids 1;
UFA2, unsaturated fatty acids 2;
W, women;
WC, waist circumference;
WHO, World Health Organization;
WHR, waist-to-hip ratio;
VIP, Variable Importance in Projection;
VLDL, very-low-density lipoprotein cholesterol;
VLDL2, very-low-density lipoprotein cholesterol 2;
Vs, versus.

LIST OF TABLES

Table MM1. List of the 55 metabolites spectral regions detected in the Piancavallo cohort serum samples.....	80
Table MM2. List of the 15 spectral regions detected in the culture samples in which adipocytes or adipose tissue were grown.....	100
Table R1. Anthropometric characteristics of the Piancavallo cohort in total and separated by sex.....	116
Table R2. Characterization of the Piancavallo cohort by anthropometric measures for weight-related risk prediction.....	118
Table R3. Cardiometabolic characterization and composition of the Piancavallo cohort	120
Table R4. Anthropometric characterization of Wistar rats' animal model.....	156

LIST OF FIGURES

Figure I1. Overweight and obesity global distribution in 2016.....	4
Figure I2. “World Obesity Day: March 4, 2021”: an informative panel of matters to take home.	5
Figure I3. Synergistic effects of MetS parameters.	17
Figure I4. Possible interrelationships between the features of MetS.....	18
Figure I5. Fat distribution by sex, age and hormone interactions. Android versus gynoid fat deposition and its consequences.....	21
Figure I6. Multidimensional perspective illustrating the complex interaction of diverse factors and networks underlying the development of obesity.....	24
Figure I7. The metabolic pathway: metabolism and catabolism.....	27
Figure I8. The developmental potential and epigenetic states of cells at different stages of development.	29
Figure I9. The three basic mechanisms of epigenetic gene regulation acting on chromatin fibre	32
Figure I10. Cytosine methylation in position 5'.....	34
Figure I11. The differential activation of human DNMTs isoforms in embryonic stem cells and somatic cells.....	36
Figure I12. The conventional schematic representation of epigenetic drift effects: causes and consequences.....	40
Figure I13. The advantages of metabolomics over other omics.....	45
Figure I14. Schematic overview of the analytical approaches mainly used for metabolomics studies.....	47
Figure I15. Tools for studying epigenomics.....	49
Figure ED1. Experimental workflow of the thesis.....	65
Figure ED2. Distribution of fat tissues in humans and rodents.....	69
Figure MM1. Summary of spectral processing and post-processing steps on NMR data.....	77
Figure MM2. Representative ¹ H NMR spectrum of serum samples from the Piancavallo subjects.....	82
Figure MM3. Outline of the EZ DNA Methylation™Kit procedure.....	85
Figure MM4. Schematic overview of the methylation essay’s data pre-processing and quality control steps.....	88
Figure MM5. Measuring of rat body weight and perigonadal fat pad weight.....	93
Figure MM6. Illustrative scheme of the tissue preparation process for	

primary cultures of adult rat adipocytes and adipose tissue.....	96
Figure R1. PLS-DA model for discrimination between MHO and MetS.....	122
Figure R2. Metabolic pathways altered in MetS.....	123
Figure R3. Cross-validation analysis of the PLS-DA model including the control subgroup (MHO) and the three pathological subgroups (Mets.3, MetS.4 and MetS.5).....	124
Figure R4. PLS-DA model for discrimination between MHO and MetS criteria subgroups.....	125
Figure R5. Significant metabolites in PLS-DA model for discrimination between MHO and MetS criteria subgroups.....	126
Figure R6. PLS-DA model for discrimination between MHO and MetS.5.....	128
Figure R7. Significant metabolites in PLS-DA model for discrimination between MHO and MetS.5.....	129
Figure R8. Metabolic pathways involved and affected in the extreme case of MetS.	130
Figure R9. PLS-DA model for discrimination between MHO and MetS.5 by age range.....	132
Figure R10. Significant metabolites in PLS-DA model for discrimination between MHO and MetS.5 by age range.....	133
Figure R11. Metabolic pathways affected in MetS.5 independently of age.....	134
Figure R12. Mean differences and 90% confidence intervals between MHO and MetS expressed in SD units for men and women for all the metabolic features measured in the study.....	137
Figure R13. PLS-DA model for discrimination between MHO and MetS.5 by age range in women.....	138
Figure R14. Significant metabolites in PLS-DA model for discrimination between MHO and MetS.5 by age range in women.....	139
Figure R15. PLS-DA model for discrimination between MHO and MetS.5 by age range in men.....	140
Figure R16. Significant metabolites in PLS-DA model for discrimination between MHO and MetS.5 by age range in men.....	141
Figure R17. Metabolic pathways affected in MetS.5 in all age and sex groups.....	143
Figure R18. RnBeads differential methylation analysis of CpG sites.....	145

Figure R19. Boxplots of beta-values of methylation in cg19693031 in TXNIP locus (A) and cg10474793 in MYLIP locus (B) in MHO and MetS.5 patients.....	146
Figure R20. REVIGO tree map of GO Enrichment Analysis.....	147
Figure R21. SEM analysis and hyper- and hypomethylation levels of SEMs.....	149
Figure R22. Boxplot graphical representations of the total scores obtained from the prioritization analysis of the unique lists of the epilepsions' related genes in MHO and MetS.5 patient groups.....	150
Figure R23. Correlation analysis between log (SEMs) and metabolic variables in MHO and MetS.5.....	151
Figure R24. Analysis of SEMs in men and women subgroups.....	152
Figure R25. Analysis of chronological and epigenetic ages in MHO and MetS.5 patients.....	153
Figure R26. Analysis of Grimage Acceleration in men and women subgroups.....	154
Figure R27. CTL and HFD perigonadal fat pad's visual aspect from extraction to cell culture.....	157
Figure R28. Wistar rats group prediction: CTL vs HFD.....	158
Figure R29. PLS-DA models for discrimination between adipocytes' culture media of HFD and control rats.....	160
Figure R30. PLS-DA models for discrimination between adipose tissues' culture media of HFD and control rats.....	161
Figure R31. Metabolic pathways altered by HFD in fat cells.....	162
Figure R32. PLS-DA models for discrimination between HFD and control female and male rats, separately.....	163
Figure R33. Significant metabolites in PLS-DA models for discrimination between HFD and control female and male rats, separately.....	164
Figure R34. Comparison of the mean concentration of metabolic regions between HFD and control female and male rats.....	165
Figure D1. Graphic representation of the Falconer threshold effect applied on the epigenetic drift in obesity.....	202
Figure A1. Composition of the standard diet. Teklad 2014 (Harlan).....	257
Figure A2. Composition of the HFD. Teklad Custom Diet TD08811 from Harlan.....	258

ABSTRACT

Background: obesity in adults is defined as an abnormal or excessive fat accumulation that presents a significant risk factor for health and contributes to increased morbidity and mortality. Although underlying health conditions and genetics could be in some cases the principal causes of obesity, it is predominantly the result of long-term unhealthy lifestyles. In its clinically most severe form (or Class III obesity) adipose tissue becomes the largest metabolic endocrine organ that strongly interacts with the endocrine system and contributes to the development of metabolic syndrome (MetS). MetS is considered the most common metabolic health problem related to obesity nowadays and it involves signs (central obesity, low high-density lipoprotein cholesterol (HDL), hypertriglyceridemia, hypertension, hyperglycemia) that could be related to the presence of abnormal metabolism and metabolome alterations. The metabolome is directly influenced by the diet and is the output of genes-environment interaction, of which epigenetics regulations represent their linker. So, a possible interconnection between metabolomics and epigenetics is reasonable, with repercussions on the epigenetic age, the functional state of the whole organism and its lifespan. Although MetS affects both men and women indistinctly, the prevalence of each MetS risk factor is reported to be sex- and age-dependent and it is affected by hormonal and endocrine processes. In particular, MetS is a significant health problem in postmenopausal women. This could be related to sex hormone levels and adipose tissue's disposition, metabolism and endocrine action that cause cardiovascular complications and accelerated ageing of multiple organs and their malfunction, especially in the elderly.

Aims: 1) to investigate the influence of sex and age on the metabolic

profile of subject with clinically severe obesity and metabolically healthy status (MHO) and patients with MetS through the study of differences in their metabolome and epigenome under the hormonal and endocrine influence in conjunction to sex and age; 2) to investigate the metabolome-epigenome-MetS interaction, its effects and the potential role of adipose tissue metabolism in the pathology; 3) to analyse specifically the metabolic profile of women of fertile age and postmenopausal and their comparison with men of the same age groups, focusing on extreme MetS (MetS.5); 4) to investigate the interactions between metabolome and epigenome in subjects over 54 years with MHO or MetS.5 to obtain a pathophysiological characterization patients at greater risk; 5) to use a high-fat diet (HFD) rat experimental model as a source of adipocytes for the *in vitro* validation of the hypotheses derived from the studies on the human cohort and to investigate the effect of a HFD diet on the metabolome of adipose tissue and adipocytes in MetS in severe obesity; 6) to evaluate by *in vitro* experiments the potential role of metabolomic and epigenetic modification induced by metabolites most significantly changed in subjects with MetS.

Design and methods: a case-control study was conducted with 1350 subjects of the Piancavallo cohort (women 65 %, men 35 %; age 19-85) with extreme obesity (body mass index (BMI) ≥ 40 kg/m² or between 35.0 and 39.9 kg/m² with one or more obesity-related comorbid conditions) was extensively characterized for clinical and anthropometrical profiles. The subjects were then divided into a total of four big subgroups for age and sex (women < 46 years, women > 54 years, men < 46 years and men > 54 years) and classified into controls MHO and cases MetS. Cases were further classified into MetS subgroups (MetS.3, MetS.4 and MetS.5) according to the International Diabetes Federation (IDF) Criteria (2005). Serum global metabolomic profiles were measured using nuclear magnetic

resonance (NMR). Ninety-six subjects (48 cases MetS.5, 48 controls MHO; aged between 55-85 years for both groups) were selected for the epigenetic analysis and global methylation levels were measured in serum using the Infinium MethylationEPIC BeadChip kit. Perigonadal fat pads were obtained from male and female Wistar rats fed with a modified HFD (45 % of fat) or fed with a control diet (4% fat) and sacrificed after 20 weeks of treatment. Cultures of adipocytes and adipose tissues were performed to collect metabolized culture media. Global metabolomic profiles of culture media were measured using NMR. Specific statistical analyses were developed.

Results: according to the anthropometric and clinical characterization, the global metabolic profile of MetS resulted uniformly different from MHO in the entire cohort, with a visible, constant and progressive change of the metabolites' levels according to the worsening of MetS gravity. MetS.5 showed the most significant difference in the metabolic profile and altered metabolic pathways. Moreover, PLS-DA scores plots revealed specific metabolic changes in control and MetS.5 groups of men and women related to sex and age. The differential profiles differed in the variety and the number of significant metabolites, especially between fertile and postmenopausal ages. Acetone was the preeminent metabolite in MetS.5 women's group of fertile age. Instead, postmenopausal women showed a raise in carbonyls in fatty acid 2 (FACO2) and low-density lipoprotein 2 (LDL2) cholesterol signals, which were the metabolites most significantly related to MetS.5. On the contrary, in men, leucine and choline-containing compounds (CCC) showed the main involvement in MetS.5 until 45 and after 55 years, respectively. Therefore, the metabolic pathways involved in MetS and MetS.5 were different between men and women of different ages, even though the

disease had a common basis regardless of sex. At the epigenetic level, the global methylation levels were comparable between cases and controls. However, differential methylation analysis identified two statistically significant probes belonging to TXNIP (thioredoxin interacting protein) and MYLIP (myosin regulatory light chain interacting protein) genes related to hyperglycemia and hypercholesterolemia. The epigenetic drift revealed in MetS.5 the decrease in the average number of stochastic epigenetic mutations (SEMs), which appeared more pronounced in the cohort of males. The biological age, reflected by the predictor of lifespan (DNAm GrimAge), resulted significantly higher in MetS.5 cohort. The GrimAge also appeared to be higher, on average, in men than in women of similar chronological age, regardless of disease status, although the diagnosis of MetS was related to a worse epigenetic scenario. Finally, the metabolomic analysis of the adipocytes' growth medium extracted from the perigonadal fat pads of control and HFD rats also showed significant differences related to the diet and sex of the animals. Nevertheless, the causes and contributors were non-identical between our human cohort and the rat model under study. Methionine/isoleucine, jointly, constituted the metabolites primarily associated with HFD in adipocyte cell cultures and the most significant metabolites in female HFD rats. Differently, 3methyl2oxovalerate was the most significant metabolite in males. Glutamine showed the highest VIP score value in adipose tissue organ cultures probably because of the presence of macrophages that play a critical role in initiating, maintaining, and resolving inflammation caused by the hypertrophy of adipocytes.

Conclusions: the study of clinically severe obesity both at the clinical, anthropometric and above all at the metabolomic-epigenetic level represents an aid to the discovery of risk biomarkers for the development

of metabolically unhealthy obese status (MUHO) and MetS. Combined with the epigenetics data, the metabolomic results may provide new insights into the pathophysiological mechanisms in severe healthy or unhealthy obesity and MetS, with a particular focus on the reciprocal relationship between the epigenome and the metabolome under the influence of sex, age and endocrine function of adipose tissue. MUHO women and men have a different age-related risk factor that is highlighted and reflected between metabolic and epigenetic profiles, manifested by the difference between chronological and biological (epigenetic) age between men and women. The latter may have some protection provided by estrogens until menopause which allows them to remain "metabolically and physiologically younger" even when the influence of estrogens decreases. Studying these biomarkers involved in the development and characterization of the disease in different stages of life and sex could help to provide new targets for preventive and therapeutic strategies and therapies. Moreover, cell models could be used to provide further evidence *in vitro* on the results of the studies on human samples. Based on patients' specific biological and clinical characteristics, this evidence could provide new insight for pharmacological, behavioural and nutritional strategies on host/microbiota co-metabolism and metabolic pathways, and progress towards personalized medicine.

Keywords: Metabolic syndrome, age, sex, hormonal and endocrine influence, metabolomic and methylation profile, epigenetic drift, biomarkers, animal models, adipocyte cell culture.

RESUMEN

Antecedentes: la obesidad en adultos se define como una acumulación anormal o excesiva de grasa que representa un importante factor de riesgo para la salud, contribuyendo a aumentar la morbilidad y la mortalidad. Aunque las condiciones de salud subyacentes y la genética podrían ser en algunos casos las principales causas de la obesidad, en la mayoría de los casos es el resultado de estilos de vida poco saludables a largo plazo. En su forma más severa clínicamente (obesidad de Clase III), el tejido adiposo se convierte en el órgano endocrino metabólico más grande que interactúa fuertemente con el sistema endocrino y contribuye al desarrollo del síndrome metabólico (MetS). El MetS es considerado el problema de salud metabólico más comunemente relacionado con la obesidad en la actualidad y presenta signos (obesidad central, colesterol unido a lipoproteínas de alta densidad (HDL) bajo, hipertrigliceridemia, hipertensión, hiperglucemia) que podrían estar relacionados con la presencia de un metabolismo anormal y alteraciones del metaboloma. El metaboloma está directamente influenciado por la dieta y es el resultado de la interacción genes-ambiente, de la que las regulaciones epigenéticas representan su nexo de unión. Por tanto, es lógico pensar que exista una posible interconexión entre la metabolómica y la epigenética, que repercuta en la edad epigenética, el estado funcional de todo el organismo y su esperanza de vida. Aunque MetS afecte tanto a hombres como a mujeres indistintamente, la prevalencia de cada factor de riesgo de MetS aparece depender del sexo y la edad y se ve afectada por procesos hormonales y endocrinos. En particular, MetS es un problema de salud importante en mujeres posmenopáusicas. Esto podría estar relacionado con los niveles de hormonas sexuales y la disposición, metabolismo y acción endocrina del tejido adiposo que provocan complicaciones

cardiovasculares y el envejecimiento acelerado de múltiples órganos y su mal funcionamiento, especialmente en los ancianos.

Objetivos: 1) investigar la influencia del sexo y la edad en el perfil metabólico de sujetos con obesidad clínicamente severa y estado metabólicamente saludable (MHO) y pacientes con MetS a través del estudio de las diferencias en su metaboloma y epigenoma bajo la influencia hormonal y endocrina en relación con el sexo y años; 2) investigar la interacción metaboloma-epigenoma-MetS, sus efectos y el papel potencial del metabolismo del tejido adiposo en la patología; 3) analizar específicamente el perfil metabólico de las mujeres en edad fértil y posmenopáusicas y su comparación con los hombres de los mismos grupos de edad, centrándose en el MetS extremo (MetS.5); 4) investigar las interacciones entre metaboloma y epigenoma en sujetos mayores de 54 años con MHO o MetS.5 para obtener una caracterización fisiopatológica de los pacientes de mayor riesgo; 5) utilizar un modelo experimental de rata con dieta alta en grasas (HFD) como fuente de adipocitos para la validación *in vitro* de las hipótesis derivadas de los estudios en la cohorte humana y la investigación dirigida al efecto de la dieta en el metaboloma del tejido adiposo y adipocitos en MetS en obesidad severa; 6) evaluar mediante experimentos *in vitro* el papel potencial de la modificación metabólica y epigenética inducida por los metabolitos más significativamente modificados en sujetos con MetS.

Diseño y métodos: se realizó un estudio caso-control con 1350 sujetos de la cohorte de Piacavallo (mujeres 65 %, hombres 35 %; edad 19-85) con obesidad extrema (índice de masa corporal (IMC) ≥ 40 kg/m² o entre 35,0 y 39,9 kg/m² con una o más condiciones comórbidas relacionadas con la obesidad) fueron ampliamente caracterizados por

perfiles clínicos y antropométricos. A continuación, los sujetos se dividieron en un total de cuatro grandes subgrupos por edad y sexo (mujeres < 46 años, mujeres > 54 años, hombres < 46 años y hombres > 54 años) y clasificados en controles MHO y casos MetS. Los casos se clasificaron además en subgrupos de MetS (MetS.3, MetS.4 y MetS.5) de acuerdo con los Criterios de la Federación Internacional de Diabetes (IDF) (2005). Los perfiles metabólicos globales séricos se midieron mediante resonancia magnética nuclear (RMN). Se seleccionaron 96 sujetos (48 casos MetS.5, 48 controles MHO; con edades comprendidas entre 55 y 85 años para ambos grupos) para el análisis epigenético y los niveles de metilación global se midieron en suero utilizando el kit Infinium MethylationEPIC BeadChip. Los acúmulos de grasa perigonadal se obtuvieron de ratas Wistar machos y hembras alimentadas con una dieta modificada enriquecida en grasas HFD (45 % de grasa) o alimentadas con una dieta de control (4 % de grasa) y sacrificadas después de 20 semanas de tratamiento. Se realizaron cultivos de adipocitos y tejidos adiposos para recoger los medios de cultivo metabolizados. Los perfiles metabólicos globales de los medios de cultivo se midieron mediante RMN. Se desarrollaron análisis estadísticos específicos.

Resultados: en línea con la caracterización antropométrica y clínica, el perfil metabólico global de MetS resultó uniformemente diferente de MHO en toda la cohorte, con un cambio visible, constante y progresivo de los niveles de metabolitos de acuerdo con el empeoramiento de la gravedad de MetS. MetS.5 mostró la diferencia más significativa en el perfil metabólico y rutas metabólicas alteradas. Además, los diagramas de dispersión tipo PLS-DA a partir de los espectros de RMN revelaron cambios metabólicos específicos en grupos de control y MetS.5 de hombres y mujeres relacionados con el sexo y la edad. Los perfiles

diferenciales diferían en la variedad y el número de metabolitos significativos, especialmente entre la edad fértil y la posmenopáusica. La acetona fue el metabolito preeminente en el grupo de mujeres MetS.5 en edad fértil. En cambio, las mujeres posmenopáusicas mostraron un aumento en las señales de carbonilos en ácidos grasos 2 (FACO2) y de colesterol de lipoproteínas de baja densidad 2 (LDL2), que fueron los metabolitos más significativamente relacionados con MetS.5. Por el contrario, en los hombres, la leucina y los compuestos que contienen colina (CCC) mostraron una mayor repercusión en el MetS.5 hasta los 45 y después de los 55 años, respectivamente. Por lo tanto, aunque la enfermedad tenga una base común independientemente del sexo, las vías metabólicas involucradas en MetS y MetS.5 fueron diferentes entre hombres y mujeres de diferentes edades. El análisis epigenético mostró niveles globales de metilación fueron comparables entre casos y controles. Sin embargo, el análisis de metilación diferencial identificó dos sondas estadísticamente significativas pertenecientes a los genes TXNIP (proteína que interactúa con tiorredoxina) y MYLIP (proteína que interactúa con la cadena ligera reguladora de miosina) relacionados con la hiperglucemia y la hipercolesterolemia. La deriva epigenética reveló en MetS.5 la disminución, en el número promedio de mutaciones epigenéticas estocásticas (SEMs), que apareció más pronunciada en la cohorte de hombres. La edad biológica, reflejada por el predictor de esperanza de vida (DNAm GrimAge), resultó significativamente mayor en la cohorte MetS.5. El GrimAge también pareció ser mayor, en promedio, en hombres que mujeres de edad cronológica similar, independientemente del estado patológico, aunque el diagnóstico de MetS se relacionó con un peor escenario epigenético. Finalmente, el análisis metabolómico del medio de crecimiento de adipocitos extraídos de los acúmulos de grasa perigonadal

de ratas control y HFD también mostró diferencias significativas relacionadas con la dieta y el sexo de los animales. Sin embargo, las causas y los factores que contribuyen al síndrome metabólico no fueron idénticos entre nuestra cohorte humana y el modelo de estudio en rata. La metionina/isoleucina, combinadas, constituyeron los metabolitos principalmente asociados con HFD en cultivos celulares de adipocitos y los metabolitos más significativos en ratas HFD hembras. Por el contrario, el 3metil2oxovalerato fue el metabolito más significativo en los machos. La glutamina mostró el VIP score más alto en cultivos de tejido adiposo, probablemente por la presencia de macrófagos que juegan un papel fundamental en el inicio, mantenimiento y resolución de la inflamación causada por la hipertrofia de los adipocitos.

Conclusiones: el estudio de la obesidad clínicamente severa tanto a nivel clínico y antropométrico como sobre todo a nivel metabolómico-epigenético representa una ayuda para el descubrimiento de biomarcadores de riesgo para el desarrollo del estado de obesidad metabólicamente no saludable (MUHO) y el MetS. Combinados con los datos epigenéticos, los resultados metabolómicos pueden proporcionar nuevos conocimientos sobre los mecanismos fisiopatológicos en la obesidad grave saludable o no saludable y MetS, con un enfoque particular en la relación recíproca entre el epigenoma y el metaboloma bajo la influencia del sexo, la edad y la función endocrina del tejido adiposo. Las mujeres y los hombres de MUHO tienen diferentes factores de riesgo relacionados con la edad que se destacan y reflejan entre los perfiles metabólicos y epigenéticos, puestos de manifiesto por la diferencia entre la edad cronológica y la edad biológica (epigenética) entre hombres y mujeres. Estas últimas pueden tener cierta protección proporcionada por los estrógenos hasta la menopausia, lo que les permite permanecer "metabólica y fisiológicamente más jóvenes"

incluso cuando la influencia de los estrógenos disminuye. El estudio de estos biomarcadores implicados en el desarrollo y caracterización de la enfermedad en diferentes etapas de la vida y el sexo podría ayudar a proporcionar nuevas dianas para estrategias y terapias preventivas y terapéuticas. Además, los modelos celulares podrían utilizarse para proporcionar más pruebas *in vitro* sobre los resultados de los estudios en muestras humanas. En función de las características biológicas y clínicas específicas de los pacientes, esta evidencia podría proporcionar nuevos conocimientos para las estrategias farmacológicas, conductuales y nutricionales sobre el cometabolismo huésped/microbiota y las vías metabólicas, y el progreso hacia la medicina personalizada.

Palabras clave: síndrome metabólico, edad, sexo, influencia hormonal y endocrina, perfil metabolómico y de metilación, deriva epigenética, biomarcadores, modelos animales, cultivos celulares de adipocitos.



INTRODUCTION

1. INTRODUCTION

1.1. Adult overweight and obesity.

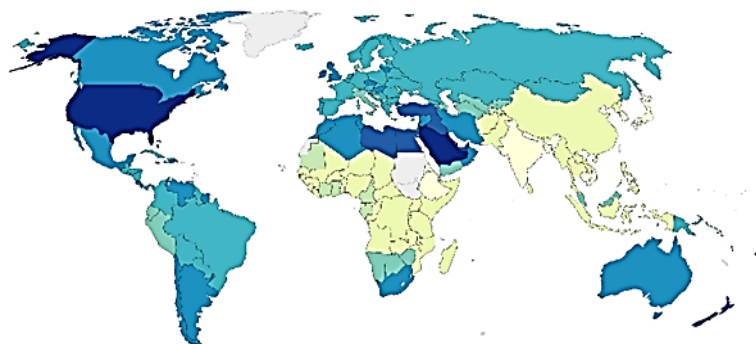
Obesity is a medical condition in which excess body fat has accumulated to an extent that it may negatively affect health [1]. The term derives from the Latin “*obesitas*”, which indicates the condition of someone who is “fat, big or chubby”, in turn, derived from “*esum*”, past participle of “*edere*” (“to eat”), with the addition of prefix “*ob*” (“for, due to”).

Rates of overweight and obesity continue to grow in adults and children, and most of the world's population lives in countries where overweight and obesity cause more deaths than underweight. Worldwide obesity has nearly tripled since 1975: 39 % (more than 1.9 billion) of adults aged 18 years and over were overweight in 2016, and 13 % (over 650 million) were obese (Figure I1). An estimated 38.2 million children under the age of 5 years were overweight or obese in 2019. Due to the severity of the problem, already in 1997, the World Health Organization (WHO) recognized obesity as a global epidemic [2] and estimates that by 2025, approximately 167 million people, including children, will become less healthy because they will be overweight or obese [3]. On current trends, by 2050, 60 % of man and 50 % of women will be obese.

Obesity is one difficult aspect of malnutrition and, even if it should be more easily preventable than undernourishment, today more people are obese than underweight in every region except sub-Saharan Africa and Asia.

Share of adults that are obese, 2016

Obesity is defined as having a body-mass index (BMI) equal to or greater than 30. BMI is a person's weight in kilograms divided by his or her height in metres squared.

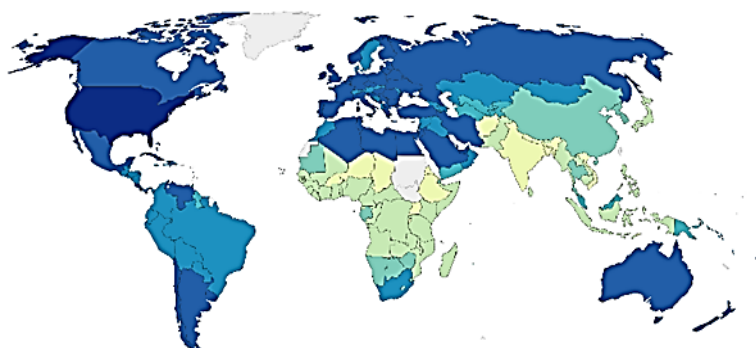


Source: WHO, Global Health Observatory

OurWorldInData.org/obesity • CC BY

Share of adults that are overweight or obese, 2016

Being overweight is defined as having a body-mass index (BMI) greater than or equal to 25. Obesity is defined by a BMI greater than or equal to 30. BMI is a person's weight in kilograms divided by his or her height in metres squared.



Source: WHO, Global Health Observatory

OurWorldInData.org/obesity • CC BY

Figure II. *Overweight and obesity global distribution in 2016 (WHO).*

Nowadays, overweight and obesity are dramatically on the rise in high-income and low- and middle-income countries, particularly in urban settings. The vast majority of overweight or obese children live in

developing countries, where the rate of increase has been more than 30 % higher than that of developed countries [4, 5]. Obesity is the leading cause of preventable death worldwide and is considered one of the most severe public health problems of the 21st century [6].

To support practical nutritional education actions and stimulate people to achieve and maintain a healthy weight and reverse the global obesity crisis, World Obesity Day was established in 2015 as an annual campaign that each year is based on a specific theme to increase awareness, encourage advocacy, improve policies, and share experiences. Figure 12 shows the summary panel created for the World Obesity Day of 2021.

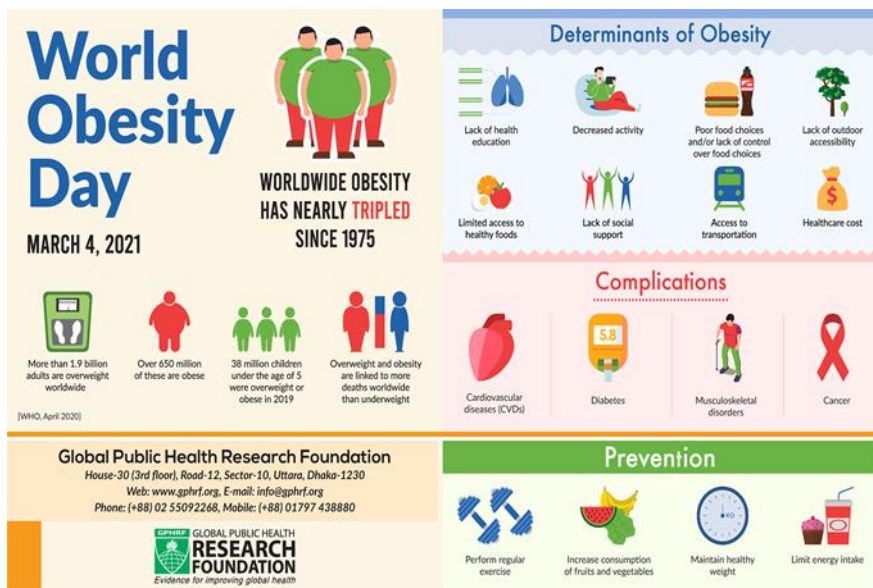


Figure 12. “World Obesity Day: March 4, 2021”: an informative panel of matters to take home (Global Public Research Foundation).

1.1.1. Obesity measurement and classification.

Body mass index (BMI) is the most widespread and used medical screening to establish the presence of adult obesity and to classify its type, for its simplicity, immediacy and non-invasiveness. To obtain the BMI, there is no need for other body parameters than the measurement of weight in kilograms divided by height in meters squared (kg/m^2). Due to the increasing doubts about the functionality of this method for defining abdominal obesity [7, 8], indirect measures such as waist circumference (WC) and body fat percentage estimated from skinfold thickness (ST) or waist-to-hip ratio (WHR) have been widely accepted and more used in recent years. Although body fat can be measured directly by methods such as dual-energy X-ray absorptiometry (DEXA) [9], currently this method still appears to be underutilized compared with indirect methods. Nevertheless, since the 1990s, the BMI remains the most widely used and universally recognized instrument, suggested as an ideal measure of adiposity and closely associated with obesity-related health risks.

The diseases of overweight and obesity are classified into gradually rising BMI levels that have increasingly higher levels of health consequences.

The following BMI ranges classify different weight types:

- Underweight: $\text{BMI} \leq 18.5 \text{ kg}/\text{m}^2$
- Optimum range: $\text{BMI} 18.5\text{-}24.9 \text{ kg}/\text{m}^2$
- **Overweight: BMI 25.0-29.9 kg/m^2**
- **Class I Obesity: BMI 30.0-34.9 kg/m^2**
- **Class II Obesity: BMI 35.0-39.9 kg/m^2**
- **Severe (Class III) Obesity: BMI $\geq 40.0 \text{ kg}/\text{m}^2$**

The higher the level of excess weight, the higher the risk of serious health problems, disability and risk of early death for the patients.

1.1.1a. Clinically severe (Class III) obesity.

Clinically severe (Class III) obesity is considered a disease associated with other chronic health conditions and, in common scientific language, was defined and known for years as morbid obesity. The Oxford English Dictionary defines “morbid” as “an abnormal and unhealthy interest in disturbing and unpleasant subjects”. In a medical setting, “morbidity” means illness or disease. Healthcare professionals also often use the term “comorbidity,” meaning that an individual has more than one co-occurring illness. Although the medical meaning of “morbid” is appropriate in describing this type of obesity, in the last years, according to the WHO, the term preferably usable in the interaction with the patient as psychologically more accepted is no longer morbid obesity but either class III obesity or clinically severe obesity. This precaution is part of the "People-first language" policy, the standard for respectfully addressing people with a chronic disease rather than labelling them by their illnesses, and the change is also spreading to scientific research.

The actual medical definition by the National Institutes of Health (NIH) of severe obesity is “a serious health condition that results from an abnormally high body mass” that is diagnosed by one of the following conditions:

- BMI of 40 or greater;
- or having a BMI of 35 or greater and one or more obesity-related comorbid conditions;
- or having a total body weight greater than 20 % or more than the

ideal body weight (IBW).

IBW is calculated as:

Sex	IBW (kg)
Male	$50 + (0.91 \times \text{height (cm)}) - 152.4$
Female	$45.5 + (0.91 \times \text{height (cm)}) - 152.4$

IBW: Ideal body weight

Clinically severe obesity is a common condition. Approximately 11.5 % of women have severe obesity compared to 6.9 % of men. Age and sex seem to have an important role in its onset [10]. Severe obesity affects 11.5 % of adults aged 40 to 59, 9.1 % of adults aged 20 to 39 and 5.8 % of adults aged 60 and over. Following the current trends, severe obesity will become about as common in 2030 as regular obesity was in the 1990s [11].

1.1.2. Metabolism in clinically severe obesity.

Adult severe obesity is predominantly the result of long-term unhealthy lifestyles. Many studies have attributed the increase in people affected by overweight and obesity to the rich lifestyle and the sedentary job, with excess consumption of highly processed, energy-dense food that has poor nutritional value. A lack of exercise and physical activity due to greater dependence on cars and mechanized production also concurs [12, 13]. Nevertheless, excess fat is not explained by these two variables alone. Today it seems clear that people who suffer from obesity have mainly imbalances in the cerebral hypothalamic mechanisms that regulate hunger and satiety, mainly due to genetics, health reasons or psychiatric illnesses [14, 15]. Polymorphisms in the different genes that control appetite and metabolism predispose to obesity; since 2006, over 41 of these genes have

been linked to the development of obesity when inserted in a supportive environment [16]. For example, people with two copies of the FTO gene (fat mass and obesity-associated protein) weigh 3-4 kilos more and have a 1.67 times greater risk of obesity than those without the risk allele [17]. Depending on the population examined, the differences in BMI between people due to genetics vary from 6 % to 85 % [18]. Hence, it is now clear that, as with many other medical conditions, obesity is the result of interactions between genetic and environmental factors. Therefore, studies on physiological, metabolic and hormonal processes are necessary.

Obesity is strongly associated with significant abnormalities in endocrine function since hormones are chemical messengers that regulate metabolic processes in our body and are one of the main factors in the cause of obesity. The hormones ghrelin and leptin, sex hormones, cortisol, insulin and growth hormone influence body composition, metabolism and distribution of body fat. Ghrelin and leptin are hormones that play key roles in regulating appetite, food intake, and energy metabolism [19]. The changes that occur with age in the levels of sex hormones in men and women are associated with changes in the distribution of body fat. Obesity is also associated with an increased cortisol production rate, which is compensated by increased clearance of cortisol, resulting in plasma-free cortisol levels that do not change with increased body weight [20]. Plasma insulin levels are positively correlated with body weight and adipose tissue. Finally, growth hormone, whose secretion decreases in obesity, has an important impact on body composition and fat distribution, due to its effect on energy metabolism, lipolytic and energy saving [21].

Other studies affirmed that obese and overweight people have a metabolism that cannot respond adequately during and after meals.

According to these studies, the defect affects the thermogenic function of the metabolism that, through the dissipation of energy introduced with food as heat, keeps body weight constant [18, 22]. The metabolic response following food intake or exposure to cold would be less important in the obese than in people of normal weight. This does not mean that obese individuals have an inherently low basal metabolic rate, even if the opposite is commonly believed. It has been repeatedly shown that the obese have a higher energy requirement under standard conditions than thin people, due to the greater mass of metabolically active tissues [23]. This happens because weight gain is borne by both fat and lean mass; the latter must adapt to support the greater body weight in the various daily activities. However, this increase is not linear, since the more weight is gained, the more the weight gain is mainly due to the fat component. Therefore, since the metabolic rate of adipose tissue is much lower than that of muscle, the basal metabolism increase is not proportional to the rise in body weight. This leads to a disequilibrium in energy requirement and consumption and the consequent appearance of diseases related to metabolism.

1.1.2a. Metabolic healthy and unhealthy obesity.

Most of the individuals affected by obesity present a condition of metabolically unhealthy obesity (MUHO). Nevertheless, a less common phenotype of obesity, the metabolically healthy obese status (MHO), is characterized by a favourable and protective metabolic profile, favoured by a lower inflammation state than MUHO. This condition is characterized by significantly lower levels of visceral fat, fasting insulin, plasma triglycerides, high-sensitivity C-reactive protein, and alpha-1 antitrypsin

levels and higher levels of high-density lipoprotein cholesterol (HDL) that may be associated metabolically with a lower risk for cardiovascular disease [24]. The prevalence fluctuates considerably from 6 % to 40 % in the obese population depending on the design of the study and the criteria used for its definition. The metabolic characteristics of these people are still largely unknown and related reports are often controversial. To date, MHO does not yet have a unique definition that garners consensus [25]. These subjects, despite obesity, are recognized to have normal metabolic clinical parameters, not presenting the typical bariatric complications (hypertension, hyperglycemia, dyslipidemia, hypertriglyceridemia). For this reason, some refer to MHO as patients without metabolic syndrome (MetS), the most common health problem related to MUHO.

Although the mechanisms that determine this "healthy" condition are not fully understood, previous studies have shown a reduced abdominal fat mass and a more peripheral fat distribution [26], if compared with MUHOs, as the biological mechanisms possibly associated with the MHO [27, 28]. The fat tends to remain subcutaneous just under the skin, where it appears to be fairly innocuous. A particular genetic predisposition, with socio-demographic (age, sex, ethnicity, etc) and environmental factors (physical activity, smoking, alcohol intake, etc) result also contributors [29]: the prevalence of MHO appeared higher in women and younger individuals, and in Asian populations compared to Caucasian or multi-ethnic origin ones. Although postmenopausal women are more exposed to develop MUHO, studies conducted on small selected samples of MHO postmenopausal obese women suggested more favourable inflammatory profiles, reduced visceral fat, and probably less hepatic fat than same-aged women with insulin resistance and other metabolic anomalies [30, 31].

Even if fat tissue is nowadays recognised as a complex, essential, and highly active metabolic and endocrine organ with a fundamental influence on metabolism, it remains to test how much genetics, exercise and environment determine MHO.

It is important to underline that, relying on the definitions of "overweight and obesity" and "health" provided by the WHO, the concept of MHO can be an example of "metabolically healthy" but does not necessarily mean "healthy" obese and that for one-third of these subjects MHO condition is not stable over time [32]. Despite this, obese MHO patients constitute a very interesting model of virtuous adaptability to obesity and the ability to develop less related cardiovascular complications. MHO subjects seem to be resistant to manifest the bad metabolic effects of small increases in body mass thanks to the capacity of adipose tissue to increase lipid synthesis, generating new cells to share fat as it accumulates.

As counterparts, MUHOs have impaired mitochondria, with reduced activity and production of adenosine triphosphate (ATP). This compromises their ability of stimuli to generate new fat cells and it could explain why the MUHOs have a limited number of fat cells. Without a renewal that allows the breakdown and mobilization of their fat stores, the existent adipocytes must store new fat, becoming larger and more swollen than those of MHOs. They are then surrounded by white blood cells, to their death. This malfunction is accompanied by inflammation and it leads to ectopic fat accumulation in organs like the heart, liver, and skeletal muscle, affecting them. A fatty liver frequently coincides with metabolic abnormalities, and studies suggest that it may be one of the causes of insulin resistance, the fundamental defect in type 2 diabetes (DM2).

1.1.2b. Metabolic alterations: the role of adipose tissue.

Regardless of the nature of the triggering factors, the resulting metabolic alterations reveal a disequilibrium in the energy balance, due to an excess in energy intake concerning energy expended. Consequently, this excess of nutrients and calories is stored in adipose tissue and cells, leading to hypertrophy (increase in size) and/or hyperplasia (increase in number) and finally, metabolic alterations.

Commonly named body fat, adipose tissue is a loose connective tissue derived from preadipocytes. It contains adipocytes, the principal component, and a stromal vascular fraction of fibroblasts, vascular endothelial cells, preadipocytes and immune cells, especially adipose tissue macrophages (ATMs). Although in the past adipose tissue was considered only for its main function as a reserve of lipids, today it appears as an important, complex, essential, and highly active metabolic and endocrine organ with a homeostatic role in maintaining health [33]. Mature adipocytes secrete numerous factors and hormones such as leptin, resistin, estrogens and cytokines (especially tumour necrosis factor α (TNF α)) involved in the regulation of energy balance, insulin sensitivity and cardiovascular disease (CVD).

Until reaching adulthood, adipose tissue growth is due to the combine increase in both size and the number of fat cells. In adults with stable body weight, an elevated process of cell turnover maintains fat cell numbers almost constant over time and allows tissue's correct functionality. A decrease in body weight reduces fat cell size, whereas an increase in body weight causes a rise in fat cell size and number but decreases cell turnover [34]. In individuals who suffer from obesity,

adipose tissue constitutes almost half the body weight, taking the role of the largest endocrine organ [35]. Adipocytes develop intrinsic inflammatory properties and this takes the health problems related to impaired turnover to the extreme. Low fat cell lipid turnover is associated with the most common metabolic problems such as insulin resistance, CVD, dyslipidemia and DM2, characteristic conditions observed in MUHO.

Fat mass (FM) reaches a peak by middle age or early old age, followed by a functional decline and a substantial change of fat deposition in advanced oldness. Ageing causes loss of subcutaneous fat (peripherally first and then centrally), accumulation of visceral fat, and ectopic fat deposition (in the liver, muscle, bone marrow, and elsewhere). Furthermore, the fats' metabolites lead to an increase in insulin resistance and therefore to DM2, but also affect muscle and cardio-circulatory function, causing hypertension, hypercholesterolemia and hypertriglyceridemia. These are all pro-thrombotic factors, which affect cardiovascular risk, elevating it. The accumulation of toxins within the inter-cellular exchange tissues, that the excretory organs (especially the liver and kidneys) struggle to dispose of, plumps, in turn, low-grade inflammation and, consequently, the risk factors for the development of the MetS and disorders rise, triggering a vicious circuit that feeds itself.

The number of adipose tissue macrophages increases in obesity with age due to factors derived from adipocytes that induce macrophage activation and infiltration. In turn, activated macrophages secrete cytokines that can stimulate further activation and infiltration of peripheral monocytes and macrophages into fat. Moreover, it was reported that preadipocytes could be converted to macrophages under certain conditions

[36]. The inflammatory pathways that are so activated in adipose tissue trigger the adipose tissue dysfunction characteristic of obesity [37]. This condition leads to chronic low-grade inflammation that rise the global inflammation level and induces insulin resistance through various molecular mechanisms. This state promotes oxidative stress, related to CVD and significant risk factor for the appearance of metabolic disease and DM2, which define the pathological state. Even cancer and other chronic diseases, including musculoskeletal disorders (especially osteoarthritis), liver and kidney disease, sleep apnea, and depression have been strongly related to obesity [38]. Considering all above, obesity causes a reduction in life expectancy [39].

1.1.3. The Metabolic Syndrome.

MetS is the most common health problem related to obesity and the accumulation of abdominal fat and it is a strong contributor to the exacerbation of morbidity and mortality [40].

Professor Gerald Reaven (USA, 1928–2018) mentioned the important role of insulin resistance and metabolic diseases for the first time in 1988, in his Banting conference of the American Diabetes Association. He showed the intimate relationships that existed between insulin resistance, hyperinsulinemia, glucose intolerance, hypertriglyceridemia, low levels of HDL, arterial hypertension and a variety of hormones and cytokines derived from adipocytes. He defined this group of factors “syndrome X”, a syndrome that would later be renamed MetS [41]. MetS is part of chronic non-communicable diseases (NCDs) and nowadays it can be considered a 21st-century epidemic, affecting both quality and life expectancy.

1.1.3a. MetS clinical definition: characteristics and implications.

The first definitions of MetS were developed by WHO and the European Group for the Study of Insulin Resistance (EGIR) in 1998 and 1999, respectively. Subsequently, in 2001, the National Cholesterol Education Program (NCEP) developed Adult Treatment Panel III (ATP III) for the detection, evaluation, and treatment of high blood cholesterol in adults. ATP III recognizes MetS as a secondary target of risk-reduction therapy targeted at LDL cholesterol levels. Finally, in 2005, the International Diabetes Foundation (IDF) published new criteria for MetS Worldwide's definition [42, 43], considering that different populations, ethnicities and nationalities have different distributions of norms for body weight and waist circumference. It also recognizes that the relationship between these values and the risk for DM2 or CVD differs in different populations. On these bases, IDF states that MetS includes the combination of central obesity (defined as WC with ethnicity-specific values: white women ≥ 80 cm, white men ≥ 94 cm, or BMI ≥ 40 kg/m²) plus at least any two of the following four factors:

1. Raised blood pressure: systolic blood pressure (SBP) ≥ 130 mmHg or diastolic blood pressure (DBP) ≥ 85 mmHg or treatment of previously diagnosed hypertension;
2. Raised concentration of serum triglycerides: ≥ 150 mg/dl (1.7 mmol/l) or specific treatment for this lipid abnormality;
3. Raised fasting plasma glucose concentration ≥ 100 mg/dl (5.6 mmol/l) or previously diagnosed DM2;
4. Low levels of serum HDL: < 40 mg/dl (1.03 mmol/l) in men and < 50 mg/dl (1.29 mmol/l) in women or specific treatment for this lipid abnormality.

For the diagnostic procedure, the use of WC is preferable to the BMI because visceral obesity is a crucial component of MetS and is the most frequently observed as involved in the pathological state [44]. In fact, in most cases, the typology of the adipose tissue and its body's fat distribution appears to be more important than the percentage of FM [45].

1.1.3b. Synergistic effects of MetS components.

The clinical consequences of MetS seem to reflect not the simple sum of the metabolic alteration involved, but their synergistic effects that aggravate the outcome [46]. Synergistic effects are the combined effects of at least two physiological processes, biological structures or chemical substances that jointly make a more significant impact than both could have obtained by themselves. The pathological threshold of MetS is between two and three parameters, and the disease can include all five (Figure I3).

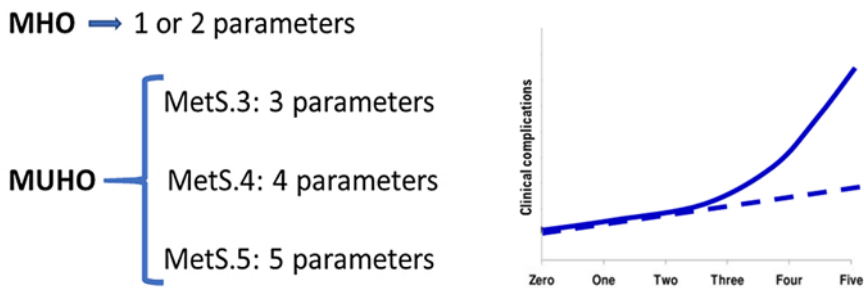


Figure I3. Synergistic effects of MetS parameters. Figure modified from Bonora et al., 2015.

Moreover, their association occurs more often than might be expected if it were due by chance and it is suggested that insulin resistance

INTRODUCTION

is the hallmark of these metabolic clusters, representing their common background. Therefore, the number of their combinations increases exponentially, generating as many different clinical conditions and causing pathological outcomes of different severity.

The knowledge of this feature is very important to define the clinical implication and severity of a diagnosis of MetS. Above all, it helps in identifying patients at high risk for CVD and DM2. It is known that some combinations of MetS components are associated with a significant synergic increase in the homeostasis model assessment-estimated insulin resistance (HOMA-IR) index, and some combinations of two MetS components entailed a synergistic risk of developing the pathology [47].

The possible interrelationship linking causal mechanisms of MetS are described below and depicted in Figure I4.

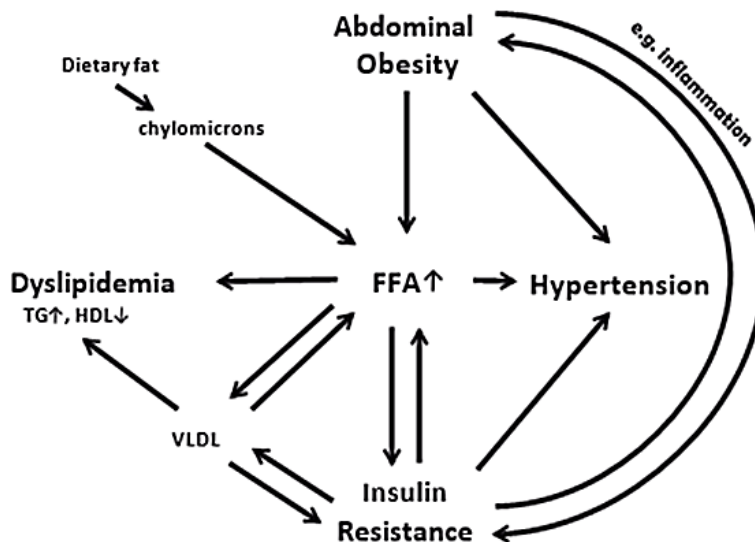


Figure I4. Possible interrelationships between the features of MetS (TG, triglycerides; HDL, high-density lipoprotein cholesterol; VLDL, very-low-density lipoprotein; FFA, free fatty acids) from Povel, 2012.

Adipose tissue dysfunction appears to play an essential role in grouping the characteristics of MetS. The balance between lipolysis and lipogenesis determines free fatty acid (FFA) efflux from the adipose tissue [48]. In clinically severely obese or insulin-resistant individuals, this balance is often disturbed. Endogenous lipolysis is higher because of defects in hormone-sensitive lipase (HSL) and adipose tissue triglyceride lipase (ATGL). FFA absorption by adipose tissue is reduced due to the defective regulation of lipoprotein lipase (LPL) in response to insulin. This, along with insufficient lipogenesis, leads to reduced absorption of chylomicrons in adipose tissue and an increased release of fatty acids (FAs) into the plasma FFA pool, whose levels are increased [49]. The adipose tissue's inability to trap FFA leads to an increased accumulation of lipids in the liver, muscle and β cells, resulting in metabolic abnormalities and specific organ dysfunctions. An increased flow of FFA to the liver can increase triglyceride levels and very low-density lipoprotein (VLDL) production. It can also stimulate insulin resistance in the liver, which can further exacerbate and worsen the overproduction of VLDL. Their increased hydrolysis can lead to higher FFA concentrations, increased LDL cholesterol levels, and reduced HDL cholesterol levels in the bloodstream, resulting in dyslipidemia. In addition, it can mediate vasoconstriction, thus causing hypertension. High absorption of FFA into muscle increases the content of intra-myocyte triglyceride with simultaneous insulin resistance. In β -cells, a chronic increase in the flow of FFA from adipose tissue decreases glucose-stimulated insulin secretion, resulting in insulin resistance. Insulin resistance may also explain the clustering and synergistic effect of MetS characteristics, regardless of plasma FFA levels.

The reduced insulin response can lead to diminishing some of its

metabolic consequences. First, hyperinsulinemia can increase sympathetic nervous system activity and sodium reabsorption, which contribute to hypertension development. Second, glucose uptake by the tissues decreases, resulting in hyperglycemia. Third, insulin resistance reduces endothelial nitric oxide (NO) production, leading to endothelial dysfunction and atherosclerosis [50]. Furthermore, obesity can lead to the activation of the renin-angiotensin system, resulting in the possible development of insulin resistance and hypertension. Finally, the production of adipokines, such as IL-6, TNF- α or leptin, increased in obese people due to the increased size of adipose tissue. Elevated levels of these adipokines can have various metabolic effects [51] including increased FFA levels and triglycerides, insulin resistance and blood pressure [52].

1.1.3c. The relationship between sex and age and the role of sex hormones.

Although the prevalence of obesity does not seem to be sex-related and MetS occurs at all ages, in the last years, sex-specific differences in its pathophysiology, diagnosis and treatment have received special attention. The numerous sex-specific differences of MetS are related especially to its components [53] and they have been attributed to variations in body fat metabolic patterns and endocrine profiles. In particular, sex hormones appear to play a predominant role. So, the diagnosis and treatment of MetS have aroused great interest in the development of sex-specific personalized medical strategies [54, 55].

It has been reported that the prevalence of each MetS individual risk factor is sex- [56] and age-dependent [57], representing an important health problem, especially in men and postmenopausal women. This is due to

significant differences in the distribution of body adipose tissue, clearly represented by android (or apple body shape) and gynoid (or pear body shape) phenotypes (Figure I5).

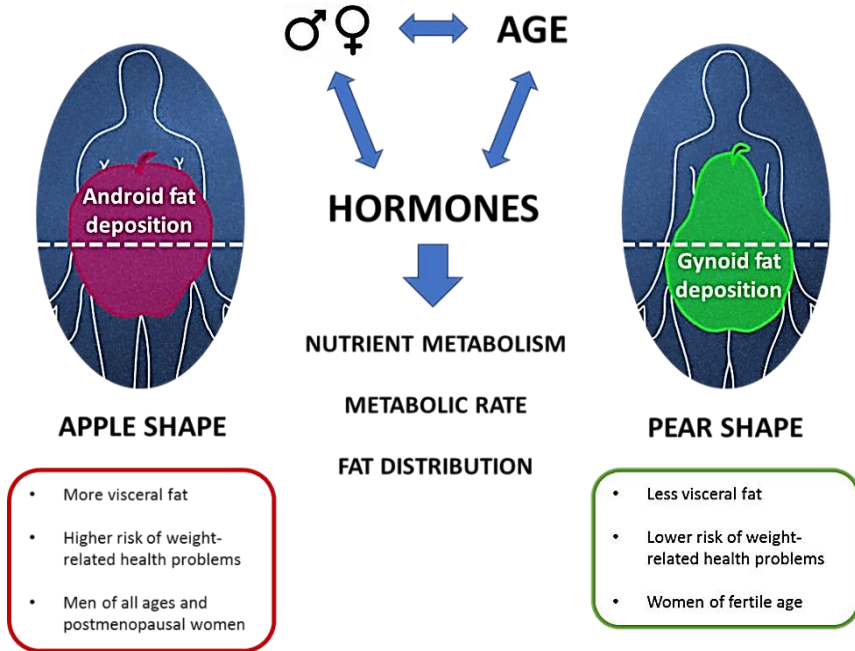


Figure I5. Fat distribution by sex, age and hormone interactions. Android versus gynoid fat deposition and its consequences.

Women have an overall and physiologically higher body fat content than men, but they also have different adipose tissue distribution and different energy metabolism. During exercise, for example, women burn a mixture in which the fat/glucose ratio is higher. Women have lower plasma levels of insulin, FFA and triglycerides that correlate with a lower visceral fat percentage and a lower presence of hepatic steatosis. Especially before menopause, in female subjects, the fat tends to be present mainly at the subcutaneous level, manifesting mostly gynoid fat deposition. On the contrary, fat tissue in males tends to accumulate more viscerally, especially in the android or abdominal region. Android fat cells are larger and have

high metabolic activity and they secrete hormones with direct access to the liver.

It is known that increased visceral adipose tissue deposition with age is particularly significant among men and postmenopausal women who, on average, have up to twice the amount of visceral adipose tissue compared with premenopausal women [58].

The formation of a lot of visceral fat and a protruding abdomen is surely partly caused by hormonal fluctuations or disorders, both in men and women [59]. Lower sex hormone levels might be particularly associated with insulin levels, insulin sensitivity, and obesity, which in turn are strongly related to MetS [60]. This result in different combination of risk factors and MetS component clusters in men and women of different ages [61]. In men, testosterone plays a key role in carbohydrate, fat and protein metabolism and significantly influences body fat composition and muscle mass [62]. In women, estrogens act on the energetic metabolism and influence the transition from a gynoid to an android phenotype, with an increase in cortisol, the so-called stress hormone. It tends to favour hyperglycemia, a greater release of sugar in the blood, and consequently, there is a greater propensity to metabolic diseases. This is because an excess of visceral fat, which lines the internal organs and is different from subcutaneous fat, increases the release of pro-inflammatory substances, adipocytokines. Adipocytokines, in turn, interact with sexual hormones and both have been implicated in the central control of appetite, energy homeostasis, maintenance of FM, and inflammation [63, 64].

Although women seem safer from strokes and heart attacks, they are, in fact, more predisposed to silent inflammation, due to estrogens that have

pro-inflammatory activity. In women who are overweight or suffer from obesity that increases the waistline, visceral fat acts on the aromatase enzyme, which can convert testosterone into estrogens, raising inflammation levels. In menopause, then, the physiological decline in estradiol, a type of estrogen with cardio-protective activity, contributes directly to the onset of CV risk factors. Understanding these differences and correlations may have important implications for interpreting the association between MetS and mortality risk.

1.1.4. Multifactorial causation of obesity and metabolic disorders: genetics, epigenetics and lifestyle.

The genetics of most diseases is complex and can range from rare monogenic forms to the more common polygenic and multifactorial forms. For obesity and its consequent metabolic disorders, including MetS, it is well known that in addition to the individual genetic load and ageing that predispose to their development, also environmental factors, behavioural habits and lifestyle contribute to defining the clinical outcome [65, 66]. Among them stand out food and diet, physical activity, health care, education and socioeconomic status, among others (Figure I6).

Both metabolic pathways and epigenetic processes are characterized by their ability to respond dynamically to intracellular and extracellular stimuli, suggesting that their changes are variable and reversible [67]. Several pieces of evidence suggest that epigenetics affects the organism's homeostatic metabolism and pathological conditions [68]. Consequently, the alteration of the metabolic pathways and the epigenetic modifications may assume important roles, potentially contributing to health and disease.

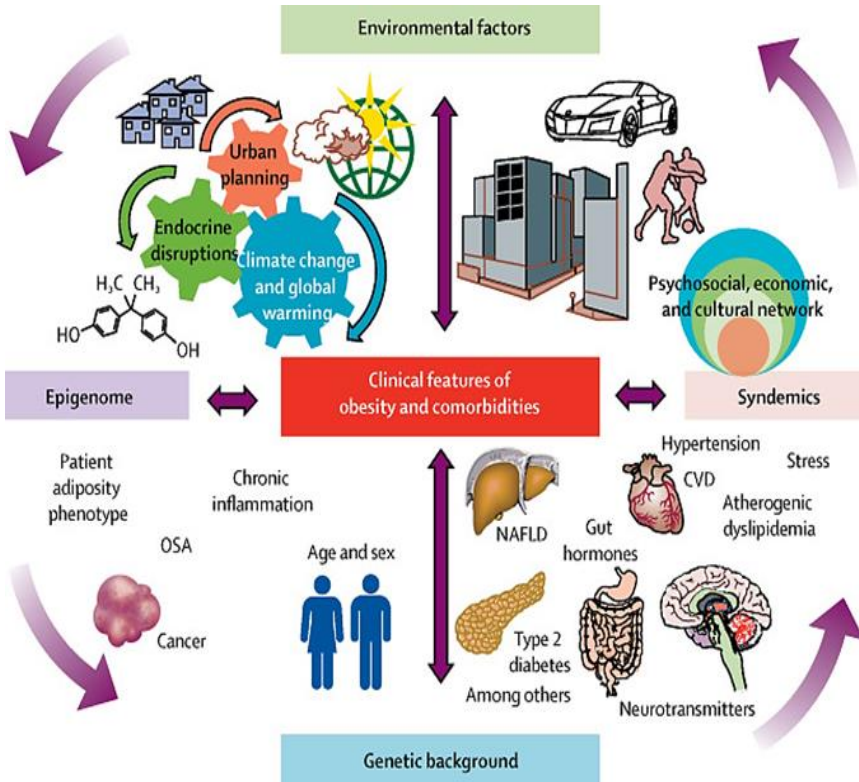


Figure 16. Multidimensional perspective illustrating the complex interaction of diverse factors and networks underlying the development of obesity. CVD, cardiovascular disease; NAFLD, non-alcoholic fatty liver disease; OSA, obstructive sleep apnoea from Frühbeck et al., 2018.

This evidence strengthens the idea that metabolic pathways deregulation and epigenetic modifications can be used as clinical biomarkers for diseases such as metabolic disorders. Epigenetic modifications, in particular, participate in the regulation of gene expression and are relevant to the health of the individual from conception to adulthood, and their offspring.

1.2. The metabolome and its metabolic pathways.

Oliver and colleagues first coined the term ‘metabolome’ in 1998 in analogy with transcriptomics and proteomics [69]. The metabolome is defined as the entire set of metabolites, that is, of all the small molecules that can participate in the processes of an organism and that can be found in a biological sample.

Concerning the human metabolome, although the individual variations make it difficult to obtain the complete metabolic profiling of a population, in the past decade estimation suggests that in humans more than 10^6 metabolites are present [70, 71]. Metabolites have a molecular weight ranging from 50 to 1500 kilodaltons (kDa) and include molecules such as glucose, organic acids, cholesterol, lipids, amine neurotransmitters, ATP, amino acids, and steroids that are synthesized during metabolism and act both as metabolic intermediates (substrates necessary for biochemical reactions and products derived from them), as well as hormones and other signal molecules, and secondary metabolites.

The concentrations of metabolites, which define the metabolome at any given time point, strictly depend on metabolic reactions driven by endogenous factors. Exogenous chemicals arising from organism-environmental interactions and dietary resources can also considerably participate and influence the metabolome composition and the concentrations of metabolites [72]. The metabolites are active participants in metabolic reactions that are essential for normal physiological functions and compose the metabolic network. It is substantially the complete set of metabolic pathways and includes processes for cell growth, reproduction, environmental responses, survival mechanisms, sustenance, and

maintenance of the cell structure and integrity. Metabolic pathways are essentially series of chemical reactions, catalysed by enzymes, whereby the product of one reaction becomes the substrate for the next reaction. These reactions can be divided into anabolism (production of new cell components, usually through processes that require energy) and catabolism (production of energy and reducing power breaking down molecules and nutrients).

There is a very large number of metabolic pathways. In humans, as shown in Figure I7, the most important metabolic pathways are:

- glycolysis: glucose oxidation to obtain ATP;
- citric acid cycle (Krebs' cycle): acetyl-CoA oxidation to obtain GTP and valuable intermediates;
- oxidative phosphorylation: disposal of the electrons released by glycolysis and citric acid cycle. Much of the energy released in this process can be stored as ATP;
- pentose phosphate pathway: synthesis of pentoses and release of the reducing power needed for anabolic reactions;
- urea cycle: disposal of NH_4^+ in less toxic forms;
- fatty acid biosynthesis: from acetyl-CoA and NADPH through the action of enzymes called fatty acid synthases;
- fatty acid β -oxidation: FAs break down into acetyl-CoA, to be used by the Krebs' cycle;
- gluconeogenesis: glucose synthesis from smaller precursors used by the brain.

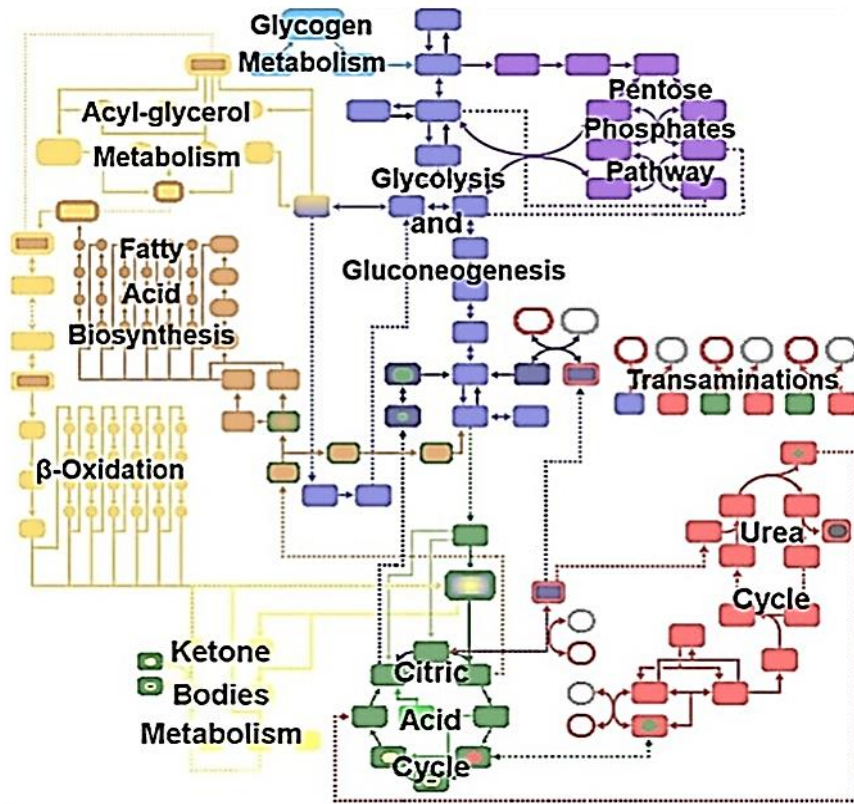


Figure 17. The metabolic pathway: metabolism and catabolism. (www.metabolicpathways.teithe.gr)

1.2.1. Regulation and deregulation of metabolic pathways.

Metabolic reactions and pathways must be finely regulated to maintain cellular homeostasis, a constant set of conditions that allows the correct function of the organisms. Particularly, the control of metabolic pathways allows organisms to respond to internal and external signals and interact actively with their environments.

Regulation of metabolic pathways includes regulation of one or more enzymes in a pathway by increasing or decreasing its response to signals, with effects on the overall rate of the pathway. Metabolic pathways interact in a complex way to allow adequate regulation. Thus, both the tissue and the microenvironment will determine the metabolic phenotype of the cells and influence how regulatory events affect normal and pathological states [73]. While the main metabolic pathways used to adapt to these conditions are fairly constant, how cells detect and respond to endogenous and exogenous signals is different. Therefore, alterations in cellular metabolism must be considered in relevant contexts.

Metabolic deregulation is an emergent hallmark of many homeostasis alterations and pathological conditions. Altered patterns of metabolic pathways result in the intensified synthesis of macromolecules, increased proliferation, and resistance to treatment [74]. Alterations in endogenous metabolite levels may result from disease processes, incorrect nutrient intake, addictions and unhealthy lifestyles, drug toxicity, or gene function and epigenetic modifications. This huge fluctuation in molecular metabolism represents a source of diagnostic and prognostic challenges and an opportunity for novel care options and therapeutic interventions [75].

1.3. The epigenetic landscape and concept.

The term epigenetic (from the Greek, *epì* = “above” and *genetikòs* = “relating to family inheritance”) indicates the dynamic actions that lead from the genotype to the phenotype as “a gradual coming into being of organs and tissues on a newly formed mass initially undifferentiated” (Figure I8). The epigenetic landscape underlies the organism’s

development thanks to a complex network of genetic feedback and feed-forward interactions between DNA, proteins and other endogenous and exogenous biochemical compounds [76].

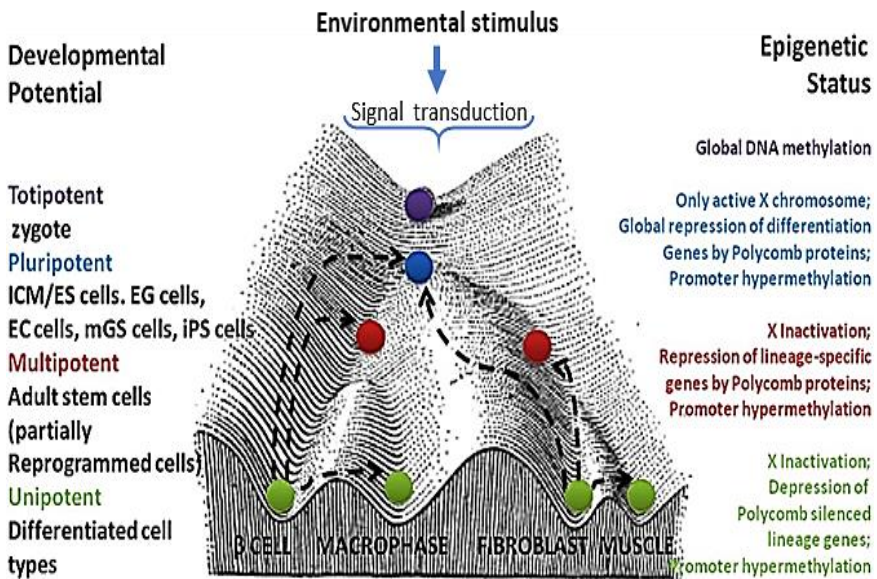


Figure 18. The developmental potential and epigenetic states of cells at different stages of development. Figure modified from Helai et al., 2010.

The epigenetic processes include any activity of regulating gene expression through chemical processes that do not involve modifications in the DNA code but that affect its functionality [77], involving heritable and “*de novo*” stable changes in the genome that may modify the phenotype of the individual or progeny. This occurs by adding chemical groups covalently linked to the DNA or the proteins around which the DNA is wrapped [78] the chromatin fibre together. These stable but potentially reversible structural changes in DNA can modify the transcriptional potential of the cell. It is important to emphasize that epigenetics represents a fundamental process for the survival of every

individual and is precisely the basis of cellular variability. The alteration of the physical accessibility to the genome of molecular complexes responsible for gene expression allows the activation of different genes. The result is the consequent regulation of cell differentiation in hundreds of types and tissues with characteristics and functions that are also very different, despite having the same genetic code.

1.3.1. The chromatin fibre and main epigenetic mechanisms.

The chromatin fibre is constituted by nucleosomes, its fundamental units, which follow each other to form a sort of string of pearls linked using a DNA linker strand about ten nucleotides long. Each nucleosome consists of a DNA segment of 146 pairs of nucleotides wrapped around a histone core composed of 4 types of histone proteins, basic proteins ($\text{pH} > 7$ as they are rich in Arginine and Lysine) with a net positive charge that facilitates their binding to DNA. A globular domain and an N-terminal tail that extends outside the globular domains compose each histone.

Nucleosomal histones (H2A - H2B - H3 - H4) are linked in dimers and heterotetramers to form a histone octamer called histone core; H1 histones bind the DNA linker and the sequence wrapped around the histone core to allow further stabilization and compaction of the chromatin fibre. These histones are larger than the nucleosomal ones and are found in a 1:1 ratio with the nucleosomes. Each histone H1 has a central body and two tails that adhere to both the octamer and the incoming and outgoing DNA strands. Its interaction with the DNA linker allows and contributes to solenoid folding. However, the functions of H1 in the supercoiling of chromatin are not fully known.

The chromatin fibre represents the DNA morphology normally present in cells with different levels of organization depending on the cellular state. In fact, in addition to a “packaging” function, it is intimately linked to cellular processes such as DNA replication, repair, recombination, chromosomal segregation and transcription regulation.

Chromatin-mediated regulation of transcription involves several mechanisms such as positioning of nucleosomes and chromatin remodelling due to DNA methylation and post-transcriptional modification of histones [79], and RNA-based mechanisms (Figure I9). Following these mechanisms is possible to distinguish the active chromatin, or euchromatin, with a more relaxed and open conformation, from the inactive chromatin, or heterochromatin, more condensed. The remodelling of chromatin in the two different forms respectively determines the activation or repression, temporary or permanent, of the transcription and it is largely due to epigenetic modifications.

Specific enzymatic chemical signals indicate whether the corresponding genes need to be transcribed and how much chromatin needs to be thickened, allowing the creation of epigenetic markings. Physiological and pathological conditions and the environment can affect gene activity by regulating the behaviour of that enzymes. The ensuing marking and restructuring of chromatin can last for a short time, for example, to allow the cell to respond quickly to intense stimulation, but most of the time, these chemical signals remain linked for months, years, or even for the entire life of the organism.

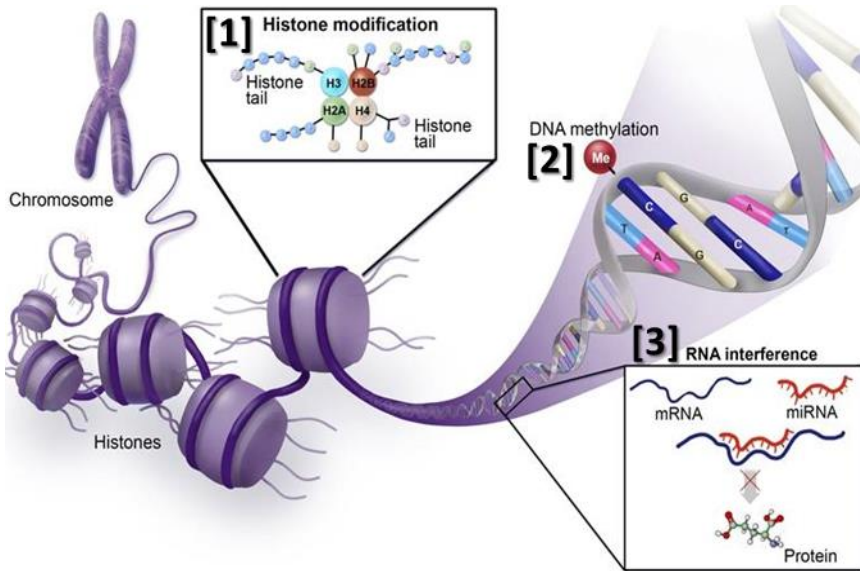


Figure 19. The three basic mechanisms of epigenetic gene regulation acting on chromatin fibre (American Society of Hematology).

Chemical modifications of histones proteins and DNA methylation, along with RNA-based mechanisms, are the most important types of epigenetic mechanisms. These processes act separately and in close correlation to remodel chromatin, altering the physical accessibility to the regions of the genome on which bound proteins and enzymes are responsible for regulating gene expression.

1.3.1a. The modification of histones.

Some of the histones' modifications occur immediately after their synthesis, before their assembly into nucleosomes. However, the modifications of main interest (methylation, acetylation, phosphorylation, ubiquitination, glycosylation, butyration, sumoylation, ADP-ribosylation, proline isomerization, citrullination, propionylation, biotinylation) take

place after the nucleosome assemblage and appear on at least 30 sites of N-terminal tails of the histones. These post-translational modifications of histones were intensively studied to propose a model for the complex relationships that bind them to DNA metabolism. In fact, in response to environmental signals, the different modifying enzymes can work sequentially or conditionally to create specific combinations that constitute the so-called “histone code” [80]. This code is directly involved in the modulation of cellular processes because it is read and interpreted by different cellular factors that lead to transcriptional activation or repression [81].

The main manipulators of the histone code are acetylation/deacetylation and methylation:

- In acetylation, the Histone Acetyltransferases (HAT) provide an acetyl group to the amino acid residues of Lysine and Arginine on the tails and central residues of all the histones of the nucleosome. The reversible and dynamic reduction in the positive charge leads to a lower affinity of the histone for DNA. Consequently, the DNA chain has a more relaxed and accessible conformation, allowing the activation of transcription. On the contrary, in deacetylation, the Histone Deacetylase (HDAC) leads the chromatin to be more condensed and transcriptionally inactive.
- Methylation consists of the transfer of one or more methyl groups to a lysine or arginine of nucleosomal histones H3 and H4. Their (mono, di, tri) methylation, incompatible with their acetylation, is performed by a series of three Histone Methyltransferases (HMTs). Depending on the number of methyl groups transferred, the histone and the position of the lysine in the tails, the methylation can be associated with both activation and repression

of gene expression and specific histone methylation patterns are related to an increase or decrease in the expression of the associated gene. Nevertheless, this modification mainly causes a transcriptional block in the heterochromatin regions.

1.3.1b. DNA methylation.

DNA methylation consists of the covalent addition of a methyl group to specific cytosines with the formation of 5-methylcytosine (Figure I10).

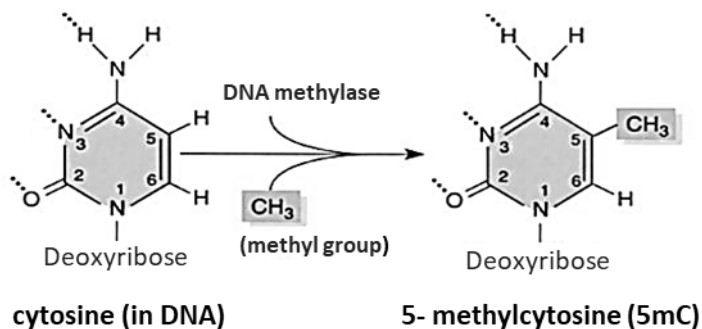


Figure I10. Cytosine methylation in position 5'.

The process is carried out by a family of enzymes, the DNA methyltransferases (DNMTs) and it is controlled at different levels in the cells. S-adenosylmethionine (SAM), involved in the methionine and folate cycle, is the main donor of methyl groups in DNA and histone methylation reactions [82]. DNA methylation allows fixing and transmitting a specific and localized chromatin state from cell to cell, which involves gene inactivation and consequent transcriptional repression. Generally, the target of methylation is the cytosine of the CpG site, a dimer of cytosine (C) followed by guanine (G). Methylation of these sites can suppress

transcription and regulate gene expression directly, by preventing the binding of transcription factors to the gene, and indirectly, by modifying the chromatin conformation more extensively. Interestingly, only 3% of the cytosines of the human genome are methylated.

Four specific DNA methyltransferases are:

- DNMT1, with the role of maintaining the methylation state of DNA. At every cell replication cycle, the enzyme can recognize the newly synthesized helix and copy the methylation pattern present on the template helix. This is the main mechanism of epigenetic memory; it allows the methylation pattern of CpGs to remain intact through DNA replication and transmitted to daughter cells through mitosis.
- DNMT3A1,2 and DNMT3B1,2 are particularly important in the early stages of embryonic development. They act *de novo*, establishing the specific methylation pattern for the various tissues.
- DNMT3L, without enzymatic activity. It binds to a specific position of the unmethylated cytosine and increases the affinity of other DNMTs for DNA, stimulating their activity in the *de novo* methylation process [83].
- DNMTs are expressed differentially in embryonic stem cells and somatic cells, as resumed in Figure I11. Consequently, the isoforms involved in the processes of *de novo* DNA methylation or its maintenance are specifically active or not [84].

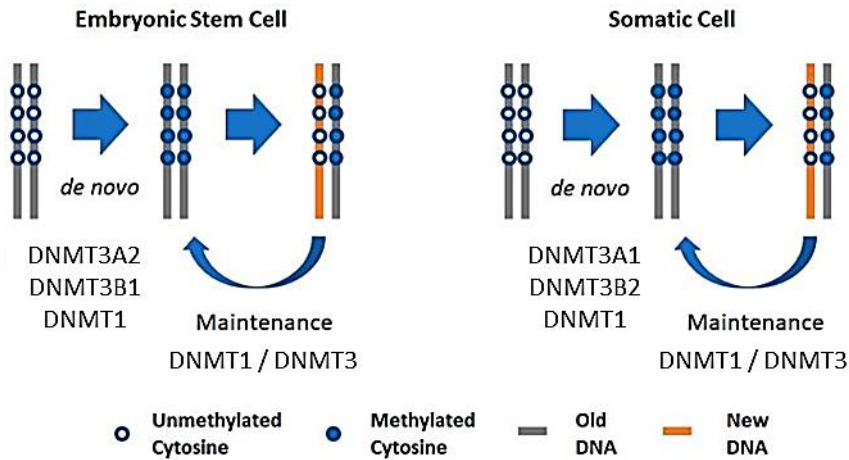


Figure III. The differential activation of human DNMTs isoforms in embryonic stem cells and somatic cells. Modified figure from Gujar et al., 2019.

1.3.1c. RNA-based mechanisms.

A non-coding RNA (ncRNA)-associated gene silencing is a functional RNA molecule that is transcribed but not translated into proteins. The most significant ncRNA molecules include microRNAs (miRNAs) and short interfering RNAs (siRNAs), with less than 30 nucleotides, and long non-coding RNAs (lncRNAs), with 200 nucleotides or longer. Despite the full extent of their role in epigenetics is still being determined, recently ncRNA molecules' crucial role in epigenetic gene expression has been suggested [85]. There is evidence suggesting that ncRNAs participate in DNA methylation and histone modifications in addition to gene silencing. Moreover, siRNAs and lncRNAs regulate both gene expressions by the formation of heterochromatin [86].

1.3.2. The CpG islands.

CpG sites are theoretically expected to make up about 4 % of the genome but their experimentally determined frequency is only about 1 %. This phenomenon of “suppression of CpG” prevents and reduces the spontaneous deamination of the methylated Cs, which tends to convert them into thymine, generating a hotspot for pathological mutation in the human genome [87]. The suppression of CG dimers causes these dinucleotides to be quite rare in the genome, symmetrical concerning the two DNA strands and usually methylated on both sides of the double helix. They are concentrated within highly repeated DNA regions upstream of the gene promoters, generally defined as CpG repeats or islands. These regions can be further classified, based on the specific localization and methylation levels. About 40-70 % of the genes are estimated to have CpG islands in proximity to the promoter. Typically, these islands are long between 300 and 3,000 base pairs and, according to the criteria set by Takai and Jones [88, 89], have a CG content of at least 55 % and an observed CpG / expected CpG ratio of at least 65 %. The CpG island regions are generally demethylated, with methylation levels around 10-15 %. However, an increase in methyl groups’ percentage plays an important role in the control of gene transcription. CpG islands are among the main regulatory regions in humans, with functional roles in normal and disease-related gene expression [90].

Besides the CpG islands, other types of CpG repeats, commonly classified as “non-CpG islands”, comprise an extremely heterogeneous set of sequences, including the long and short interspersed nuclear elements (LINEs and SINEs, respectively), and the satellite DNA, characteristic of the telomeric and centromeric regions [91, 92]. Contrary to the previous

ones, the non-CpG islands are in a state of extensive methylation and the levels can reach 40-60 % [93] allowing the maintenance of the heterochromatin state of numerous regions of the genome. It indirectly contributed to the regulation of the genes found within these territories, blocking the transposition ability of numerous transposable elements [94]. The result is fundamentally the stability of the genome over time.

1.3.3. Stochastic epigenetic mutations and epigenetic drift.

Epigenetic drift, defined by stochastic patterns of gene expression not dependent on dynamic changes in coding DNA, is a genome-wide mechanism, suggesting global dysregulation of DNA methylation patterns with age [95], even if the biological, evolutionary, functional and clinical significance remains unclear. Substantially, stochastic DNA methylation drift reflects imperfect maintenance of epigenetic marks. Two critical aspects of epigenetic drift are chromatin deterioration during ageing and genomic instability, which lead to stochastic epigenetic mutations (SEMs) accumulation. SEMs have been encoded as CpG methylation sites with extremely aberrant methylation states if compared with the reference values and remain as such also after the enrichment analysis. This aberrant process leads to changes in gene activity not involving DNA mutations but rather the gain or loss of DNA methyl groups, which are conserved in cells during mitosis. SEMs are stochastic due to their rare and inconsistent incidences, as they tend to be different from one individual to another [96]. Their study is interesting because SEMs have been recently defined as a potential measure of the accumulation of DNA damage due to exposure to a pathological state or altered physiological state, in this case, represented

by MetS. However, they can be influenced by genetic factors and can find a common basis in environmental or pathological factors. Moreover, SEMs seem to be strongly correlated with age. The number of SEMs is low in childhood and increases exponentially during ageing, even if they remain very variable among individuals. Two main components of the drift have been identified. One is tissue-specific and allows for the construction of extraordinarily accurate predictive models of age. The other is tissue independent and affects stem cells by targeting their differentiation pathways, which may explain the decline in stem cell function with age (Figure I12). Epigenetic drift is conserved across species, and the drift rate correlates with lifespan when comparing mice, rhesus monkeys, and humans [97]. The drift rate appears inversely proportional to longevity and the greater the degree of epigenetic drift, and the faster it occurs, the shorter the species' lifespan. The increase in DNA methylation associated with age affects developmental genes, adding to the effects on genes associated with environmental risk factors and the disease itself. A clear example is cancer precursor lesions and tumours showing signs of aggravated age-related DNA methylation. Moreover, obesity, ageing, fitness, diet, addictions and smoking habits are examples of environmental factors that have been proposed to have a long-term influence on epigenetic changes [98].

Associations between an epigenetic score for BMI and variables related to poor physical health and MetS have been observed and replicated, indicating independent and additive effects of epigenetic and phenotypic BMI scores. This suggests that alterations in DNA methylation are a downstream effect of obesity [99]. The relationship between obesity and adverse "epigenetic health" appears well established and the DNA methylation sites associated with obesity seem to predict future risk of DM2 [100]. Nevertheless, it is not yet well known what all the clinical

consequences of accumulated SEMs are and whether clinically severely obese individuals with a high burden of SEMs are more prone to develop pathological conditions.

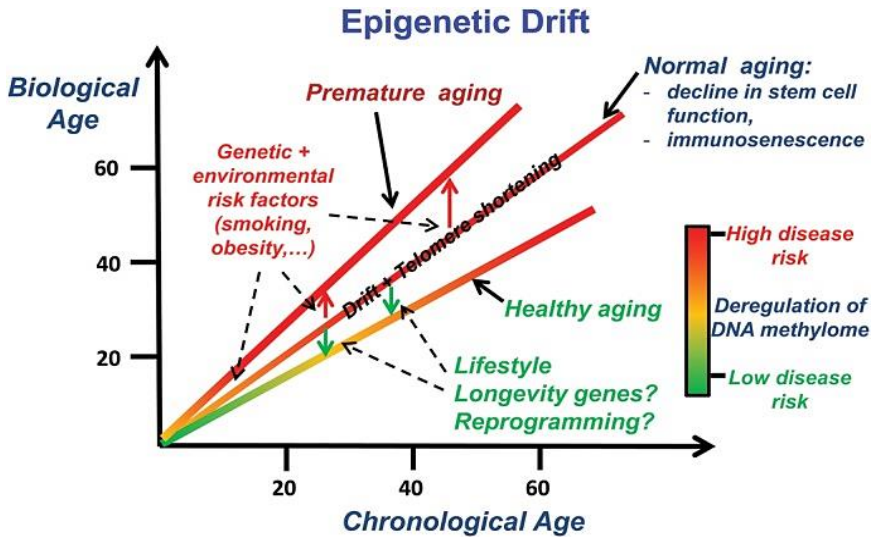


Figure I12. The conventional schematic representation of epigenetic drift effects: causes and consequences. Teschendorff et al., 2018.

1.3.4. The epigenetic clock.

Organisms' biological (epigenetic) and chronological ages (chAge) do not always correspond. The biological age, strictly linked to the methylation of DNA (DNAm), can undergo acceleration in association with various conditions, endogenous or environmental, related to it. On this basis, by tracing how DNA methylation levels changes with age throughout life, scientists have developed a scientific tool called the "epigenetic clock" to explore the acceleration of age, that is, how biological clocks can be accelerated by disease [101] or by the environment and even how this could be related to the risk of death.

The epigenetic clock could be defined as a predictor of DNAm age since it tries to inform about organisms' lifespan and how much they are prone to old age diseases, with a special focus on humans. Epigenetic markers control the extent to which genes are turned on and off across the different types of blood cells and tissues that make up a human body and DNAm has emerged as one of the most efficient biomarkers for predicting biological age. Changes in specific epigenetic signs over time can be used to accurately predict biological age from a DNA sample. In detail, the epigenetic clock refers to specific CpG sites at which DNA methylation levels steadily increase or decrease with age and thus can be used to predict chronologic age with high accuracy [102]. The most commonly used version is the multi-tissue epigenetic clock hypothesized and developed by Horvath in 2013 [103]. The Horvath's clock and its deviation Intrinsic Epigenetic Age Acceleration (IEAA) are based on 353 CpGs and the cellular composition of the blood, respectively. Their basic approach is to form a weighted average of the 353 clocks CpGs, which is then transformed to DNAm age using a calibration function. This property allows one to compare the ages of different human body areas using the same ageing clock.

In addition to Horvath's clock, "new generation clocks" have improved in age estimation focusing not only on epigenetic variants but also on a complex set of biomarkers and environmental components which in turn are associated with individual health, diseases and mortality [104]. The objective is a better characterization of the predisposing aspects to accelerated biological ageing. Among the newest clocks, the DNAmGrimAge [105] stands out. It is a biomarker composed of DNAm-based risk factors estimators of plasma proteins including those of plasminogen activator inhibitor 1 (PAI-1) and growth differentiation factor

15 and a DNAm-based estimator of smoking pack-years. Adjusting DNAm GrimAge for chronological age generated a novel measure of epigenetic age acceleration, AgeAccelGrim. Taking a huge and variant pool of risk factors into account allows GrimAge to outperform any other epigenetic clock in the "prediction of death". The variation in epigenetic ageing rates varies greatly according to sex and ethnic origin and its acceleration is also linked to physical and cognitive fitness. Patients with obesity, Huntington's disease, Down syndrome, and Werner and Sotos syndromes tend to show a greater acceleration of age.

Focusing on obesity, very strong associations have been proposed between higher WC, BMI and WHR with accelerated epigenetic clocks [106]. With regards to MetS components, a weak but statistically significant correlation ($r = 0.09$) has been observed between BMI and intrinsic age acceleration of blood, reaching a greater significant correlation ($r = 0.42$) in the liver [107]. Also, various biomarkers of MetS (WHR, triglyceride, insulin and glucose levels, C-reactive protein) were found associated with epigenetic age acceleration in blood, whether high levels of the good cholesterol HDL were associated with a lower epigenetic ageing rate of blood [108].

1.3.5. Biological role in MetS.

The combined action of DNA methylation and histone modifications affects the organism's homeostatic metabolism and pathological conditions. Besides the constant control of gene expression, both epigenetic processes are involved in important and complex biological phenomena such as imprinting, X chromosome inactivation, cell differentiation and embryonic development. They regulate the immune

system and ageing processes. Recent evidence indicates the importance of epigenetic regulation in the differentiation and function of adipocytes [109], due to the association between specific methylation sites measured in blood and adipose tissue. Moreover, several fundamental aspects of adipose tissue biology, including the regulation of different transcription factors, are directed by epigenetic events [110]. Studies about the association between BMI and DNA methylation levels seem to confirm this theory [111, 112]. On these bases, the effects of epigenetic markers and modifications have been proposed as an underlying factor in the development of obesity and the evolution of MetS [113]. They play also an important role in the predisposition to certain pathological symptoms related to MetS [114], especially DM2 and CVD. Consequently, the identification of epigenetic alterations in adipose-type disorders should allow the development of new therapies for metabolic diseases.

1.4. Metabolomics and epigenomics: “-omic” sciences in comparison.

Metabolomics and epigenomics are part of the "-omics" sciences along with genomics, transcriptomics and proteomics. The term "-omics" identifies the disciplines that study the characterization and quantification of pools of biological molecules to delineate an organism's structure, functions and dynamics [115]. On the contrary, traditional biological sciences deal with studying biological processes individually. Moreover, if combined, omics sciences allow studying the interaction networks created between the components that mainly characterize the physiology of everyone: DNA, RNA, proteins, and metabolites.

Genomics, transcriptomics and proteomics, which study DNA,

RNA, and proteins respectively, can only tell us what may happen in organisms. Transcriptomics and proteomics are very inadequate to monitor cell function because there is no simple relationship between mRNA or protein level and metabolism due to RNA splicing or post-translation. On the contrary, metabolomics, studying the metabolites, can directly and accurately reflect the current status of organisms and tell us what has precisely happened in the organisms. Moreover, the metabolome is much smaller than the proteome and the genome, making it relatively simple for data analysis. As illustrated in Figure I13, there are only about 3000 commonly used metabolites in the key metabolic pathways, while more than 40,000 genes are in the genome [116].

Furthermore, because environmental influences, such as diet, habits and exposure to pollutants, can affect not only the metabolites pool but all these networks, knowledge is further expanded by epigenomics which studies the outside's effects on internal processes of DNA modifications and their consequences. The final aim is to have an "all-around vision" of the body's functional condition and allow increasingly targeted and specific interventions.

One of the goals of the omics sciences is to provide the basis for increasingly personalized therapy. The omics sciences allow us to move from a generalized approach to an individualized approach, responding specifically to the needs of the patient. For this purpose, metabolomics and epigenomics appear to be one of the best tools to study metabolism and metabolic alterations, like Mets [117]. Metabolism is the general term used to describe all biochemical reactions that occurred in the body under the regulation of genes and proteins by epigenetic actions. Metabolites are important in maintaining the normal physiological function of cells and

organs and are the key components for intercellular signal transduction. Epigenetic regulation of metabolic processes via DNA methylation and gene expression may play a major role in this system [118]. So, methylome-metabolome associations could provide an all-around vision of the causes and consequences of obesity and MetS on the biological processes implicated and allow a better understanding of their pathophysiology.

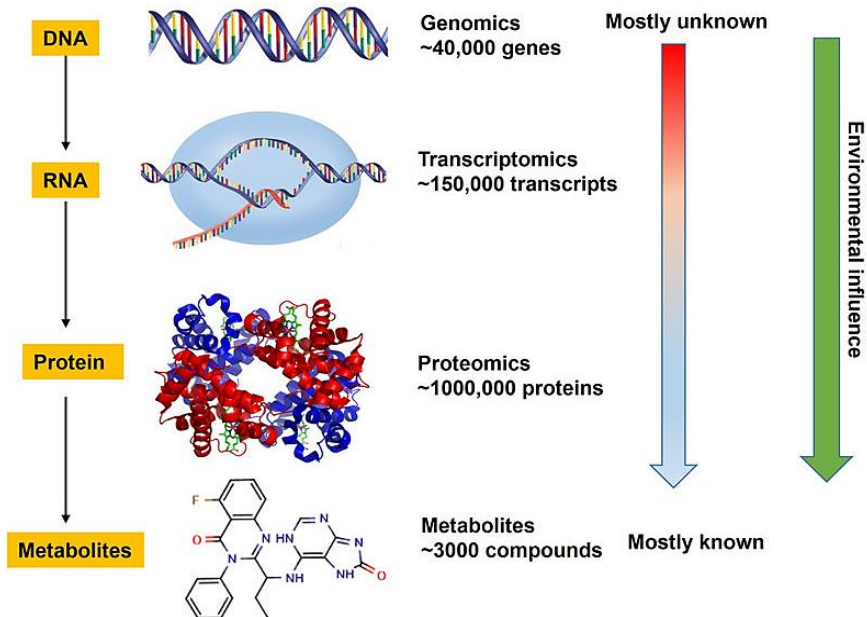


Figure 113. The advantages of metabolomics over other omics. Yu et al., *Oncotarget*. 2017.

1.4.1. The metabolomics.

Metabolomics (or metabonomics) systematically studies the unique chemical footprints represented by small-molecule metabolic profiles left by specific cellular processes. The origin of the word is from the Greek

μεταβολή which means change and *nomos* which means set of rules or laws [119]. In detail, metabonomics has been defined as "the quantitative measurement of the dynamic and multiparametric metabolic response of living systems to pathophysiological stimuli or genetic modification" [120].

Metabolomics is focused on the metabolome (the total number of metabolites present in an organism) that is the output of gene-environment interaction and reflects the environmental influence [121]. So, it reveals directly the current status of organisms and their alterations. The purpose of metabolomics is to determine all small molecule metabolites in organisms. The idea that each individual is characterized by a metabolic fingerprint was first introduced by Roger Williams in 1940, who hypothesized the existence of a metabolic signature in schizophrenia, following the chromatographic analysis of saliva and urine samples. However, only in 1971 the concepts of metabolomics and metabolic profile were introduced by Horning and colleagues, who began to apply methods of diagnosing metabolic diseases and their causes in the general population [122]. In the same years, Seeley and collaborators [123] demonstrated the use of the nuclear magnetic resonance (NMR) technique for the identification of metabolites present in untreated biological samples. The increased sensitivity of this technique, combined with high-resolution mass spectrometry (HRMS), makes it one of the most used to identify a metabolomic signature in a huge variety of biological samples [124].

Figure I14 summarizes the analytical approaches mainly used for metabolomics studies and their specific applications for a more accurate metabolite measurement.

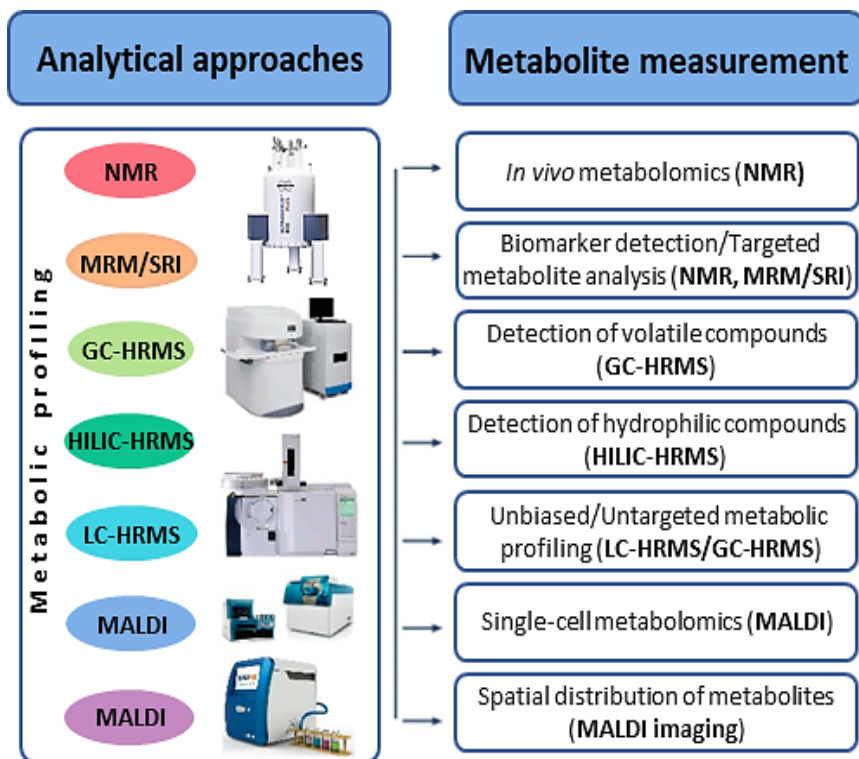


Figure I14. Schematic overview of the analytical approaches mainly used for metabolomics studies.

Thanks to NMR and HRMS techniques, in 2007 the Human Metabolome Project (HMP) created the Human Metabolome Database (HMDB) [125] to complete the first draft of the human metabolome. The HMDB contains approximately 11422 metabolites in all. Consequently, metabolomics allows for detailed characterization of metabolic phenotypes and can enable precision medicine at different levels, including the characterization of the metabolic alterations underlying the disease, the discovery of new therapeutic targets, and the discovery of biomarkers that can be used to diagnose a disease or monitor therapeutic activity [126].

Metabolomics based on NMR spectroscopy, if compared with Mass spectrometry, is a rapid and low-cost metabolic profiling technique for high throughput analysis of the complement of low-molecular-weight metabolites and their intermediates. They reflect the dynamic response to genetic modification and physiological and pathophysiological stimuli, helping to explore and investigate pathological metabolic processes and to identify their alterations [127].

1.4.2. The epigenomics.

Epigenomics is based on epigenetics and is the study of all the epigenetic changes and modifications that occur throughout an individual's entire genome, thanks to the exploration of heritable and reversible modifications of DNA and chromatin that do not change primary nucleotide sequences. Epigenomics joined with epigenetics has greatly contributed to elucidate the molecular mechanisms that give rise to the development of many illnesses, analysing and describing epigenetic changes across many genes in a cell or throughout an entire organism, as well as the processes that regulate how and when specific genes are turned on and turned off.

Epigenetics was defined as “the branch of biology that studies the causal interactions between genes and their cellular product and puts in place the phenotype” by Conrad Waddington in 1942 [128].

The study of epigenetics on a global level has only recently been made possible through the adaptation of high-throughput genomic assays. The high-yield data obtained thus allowed the discovery of the abundance of epigenetic modifications and their relationship with the functioning of

chromatin. On this basis, the Human Epigenome Project (HEP) [129] was developed as a multinational scientific project that aimed to identify, catalogue and interpret the DNA methylation patterns of the entire genome of all human genes in all major tissues. This has motivated the build-up of new theoretical models for the appearance, maintenance and modification of these patterns. Epigenetic modifications and variants including DNA methylation, chromatin architecture, histone modifications and non-coding RNA can be investigated using multi-skilled detection methods. These methods are specific to each modification, such as antibody-based affinity methods in detecting DNA methylation or histone modification. However, these methods' results are often analysed and processed with routine analysis technologies: sequencing, PCR and microarray [130] (Figure I15).

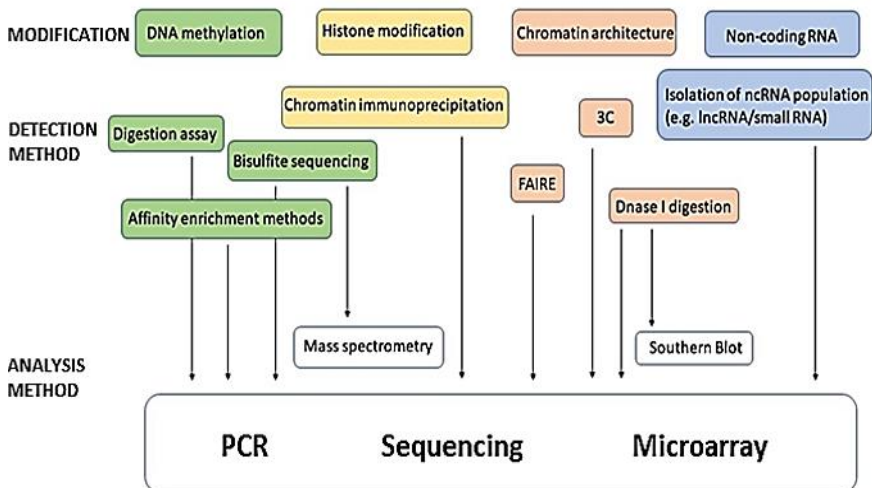


Figure I15. Tools for studying epigenomics. Turunen et al., 2018.

Next-generation sequencing platforms (NGS) and microarray-based technologies, producing a huge amount of data, make epigenomics studies as fundamental as metabolomics. The latest computational tools are

necessary to reveal any biological significance present in their experimental result.

Epigenomics, like metabolomics, contributes to explore and investigate a huge variety of pathological processes, including metabolic ones. DNA methylation analysis supplies valuable insight into gene regulation and helps in the identification of potential biomarkers. Until today, it has also been proved that aberrant DNA methylation is implicated in many disease processes, including obesity, cancer, and addiction. Thus, EWAS offer new ways to understand the significance of DNA methylation, providing novel insights into the functional consequences of genes' functional variations, with the hope that epigenetic risk may be modifiable or even reversible [131].

1.5. The need for MetS better understanding and the unsolved problems about the lack of common diagnostic criteria and biomarkers, sex and gender difference and social and scientific perception.

In the last decade, MetS has been recognized as a specific pathology and the scientific community has increased awareness of its extension in the population and severity. Nevertheless, its global definition is still unsettled because not all the disorders associated with MetS have obvious signs or symptoms and many biomarkers remain uncertain. Moreover, its knowledge, perception and acceptance by society are still low, as well as the implementation of preventive and protective lifestyles and health behaviours. For this reason, health screening campaigns to identify potential risk groups and the development of educational and therapeutic programs for lifestyle modification, focused on those metabolic

biomarkers strongly linked to education [132], are seen to be more and more necessary to prevent future increases in cardiovascular complications and to decrease health care costs. Various international studies have shown that the association of this disorder with the onset of CVD, DM2 and cancer, as well as the occurrence of death from heart disease and all-cause mortality, represented one of the major health challenges of the century that has attracted the attention of many scientists. Nevertheless, MetS' complex nature, characterized by the number and variability of the factors, makes its study and treatment difficult globally.

For years the concept of MetS as a distinct disease in itself characterized by a unifying pathophysiological factor had been questioned since several studies demonstrated that the diagnosis of MetS by traditional criteria did not provide additional prediction on the pathological gravity beyond that highlighted already by its components individually [133]. It could be a weakly associated cluster of components and risk factors for metabolic diseases. Among the components of the MetS, dyslipidemia appeared to have been the major contributor to the natural development of MetS. Furthermore, in the succession of metabolic alterations, people's future pathological status appeared to be most likely determined by the combination of dyslipidemia with obesity or hyperglycemia. So, most scientific studies and medicine continue to focus more on researching and treating the individual components. On the one hand, deepening their investigation separately and implementing increasingly effective treatments is certainly positive and allows for better patient health and living conditions. On the other hand, there is a lack of in-depth knowledge of the interrelationships generated between various metabolic components and the metabolic and epigenetic biomarkers that characterize the Mets. If MetS is a clinical entity, characterized by a unifying pathophysiological

factor, the characterizing symptoms are most likely highly correlated and represent a statistical entity. This may explain the clustering of its features and the fact that two distinct pathophysiological factors cause a similar disease symptom.

Not only the clinical definition but also the diagnosis criteria and parameters of MetS are debated issues and several changes to the current diagnosis parameters of MetS have been suggested in the scientific literature. First, besides the different criteria for diagnosing MetS that are mainly based on having at least several components of central obesity, hypertension, hyperglycemia, high triglyceride, and low HDL cholesterol concurrently, it has been proposed to add more parameters to the diagnosis of MetS. These include FFA, increased apolipoprotein B (ApoB), albumin and C-reactive protein (CRP) altered levels, as well as fatty liver [134]. They are flanked by proinflammatory adipocytokines such as tumour necrosis factor (TNF), leptin, circulating adiponectin, plasminogen activator inhibitor (PAI), and resistin, bioactive substances produced and released in a dysregulated form by the enlarged adipose tissue [135]. Given that a crux of the development of MetS is the buildup of adipose tissue and tissue dysfunction that in turn leads to insulin resistance, the list of these dysregulated adipokines and cytokines is constantly growing and reflects the heterogeneity of adipose tissue due to the number of resident cell types, the diet, the lack of physical activity and the genetic predisposition. This would allow a better characterization and classification of the developmental stages of the disease depending on the greatest number and combinations of components a person manifests at each point in time [136]. However, it is unclear whether MetS remains a statistical entity after adding one or more of these characteristics. A continuous characterisation has been proposed as even more distant from the current bivariate MetS

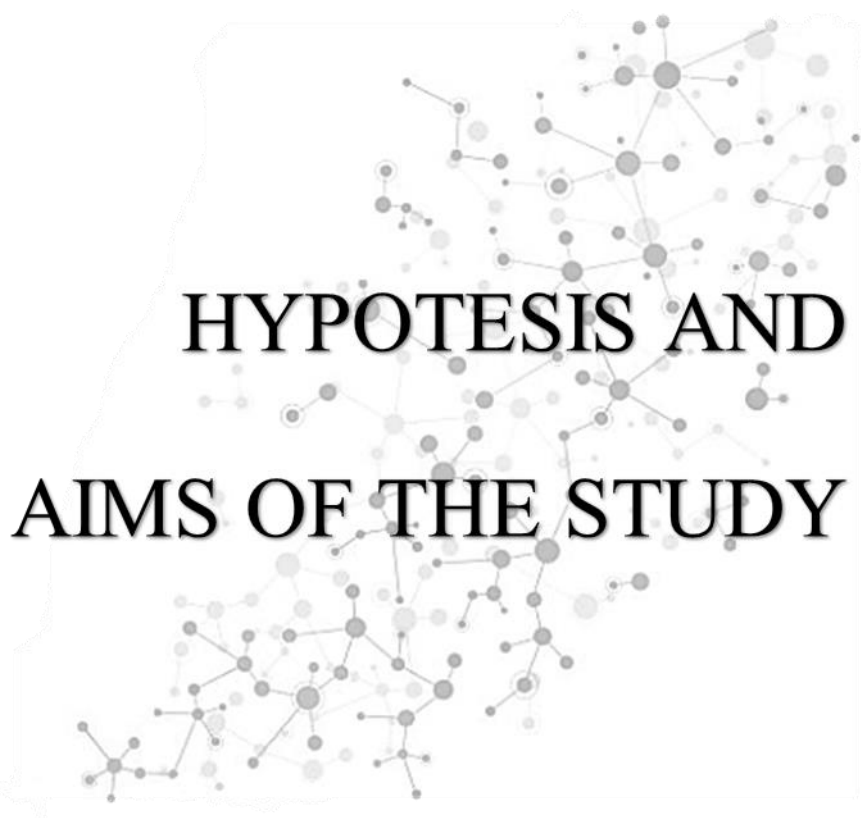
characterization, resulting in the loss of some pathological information due to the presence of a cut-off value of each component [137]. A small change in the levels of any of the components of the MetS near the cutoff level could result in the misclassification of an individual as having or not having MetS. Although, these changes would only have a minor effect on his metabolic profile and clinical risk. Furthermore, when compared with the number of positive characteristics, the cardiovascular risk increases continuously, with no suggestion of a threshold effect. However, there is still little information for a possible continuous definition of MetS.

Besides the paucity of globally recognized diagnostic criteria and biomarkers resulting in limited and incomplete specific approaches to MetS, the lack of information increases by focusing on sex and gender differences [138, 139], and their relation to age. These differences are both biological and social and interconnected to each other. In detail, if gender heterogeneity may be influenced by environment and/or behavioural habits, biological sex differences are surely more remarkably affected by age differences and environmental effects during ageing [140]. Consequently, sex differences in MetS prevalence are due to physiological differences such as hormones, differences in social and psychological stressors, and differences in lifestyle. In some studies, for example, alcohol drinking was identified as the leading risk factor associated with MetS and hypertension in men. In women, the main risk factors were household income and education level, showing different patterns in different age groups and indicating that the vulnerable groups at high risk of MetS are middle-aged men and women, with strong repercussions in old age, especially for the latter [141]. Unfortunately, even if it is well known that women have physiological and metabolism differences from men, they have always suffered from reduced consideration and inclusion in clinical

studies.

Nevertheless, the increasing evidence that in a complex pathology such as MetS, in which the sex hormone interactions appear crucial, an individual's sex is one of the most important modulators of disease risk and response to treatment, is inverting this tendency. In the last decades, women have been included more and more in clinical trials, even if there is still a substantial discrepancy with men.

In this landscape, in which further factors such as the different racial/ethnic characteristics may come into play [142], additional research is needed and compulsory on various aspects of MetS to better define its underlying causes, its development and its clinical importance to identify treatments specific to the syndrome itself as a cluster of joint causative elements rather than treat its distinct components. This could also provide a better and more complete understanding of factors already considered to be involved, or possibly involved, in the cause or pathogenesis of atherosclerosis such as inflammation, insulin resistance, or central obesity. The growing awareness that overweight and obesity are important precursors of CVD and implicated in many metabolic alterations must therefore be accompanied by greater attention to prevention and treatment interventions customized for sex, gender and age. This result is possible only by promoting research on the pathophysiology of obesity and MetS to give a useful answer to the questions which have still to be solved.



2. HYPOTHESIS AND AIMS OF THE STUDY

2.1. Hypothesis.

Adult severe obesity is mainly the result of long-term unhealthy lifestyles and represents a significant risk factor that increases morbidity and mortality. The connection between diet, metabolism and epigenetics is rather complex. Diet modulates metabolism and metabolome composition. On the one hand, metabolites are the substrates used to generate chromatin modifications. On the other hand, changes in metabolism and metabolic pathways can induce changes in gene expression programs and therefore impact epigenetics profiles. As epigenetics may represent the link between environmental and genetic factors, changes in epigenetics profiles can have a feedback effect on gene expression and protein production, modifying metabolic pathways with loop effects on the metabolome and the body's metabolism, which can be detected by NMR. In addition, hormones have also an important regulatory function. For this reason, the different hormone profiles between men and women and their changes during the various stages of life are important factors to consider for interaction with metabolism and epigenetic changes. The alterations of the epigenetic profile influence and modify disease predisposition during all life and may help to understand human metabolic diseases and obesity.

The hypothesis of this thesis is that the identification of metabolic biomarkers by NMR of the MetS and epigenetic signatures involved in the development of the disease and for the different clinical conditions related to MetS considering sex specificities could be useful for identifying people at risk. Moreover, adipocyte cell culture experiments should allow us to

better understand the role of adipose tissue in MetS' pathophysiology by determining potential cause-effect relationships between the products of adipose tissue metabolism and the metabolome alteration in severe obesity and MetS.

2.2. Aims of the study.

The general objective of the project is twofold, firstly, to investigate the influence of sex and age on the metabolic profile of subjects MHO and patients with MetS in a context of clinically severe obesity by studying differences in their metabolome and epigenome under the hormonal and endocrine influence in different sexes and ages. Secondly, better characterization of MetS patients by the analysis of the potential role of adipose tissue metabolism in the pathology using a rat model with a high-fat diet (HFD) as a source of adipocytes for *in vitro* validation of the hypotheses arising from the studies on the human cohort.

The specific objectives are the following:

Human samples analysis-related objectives:

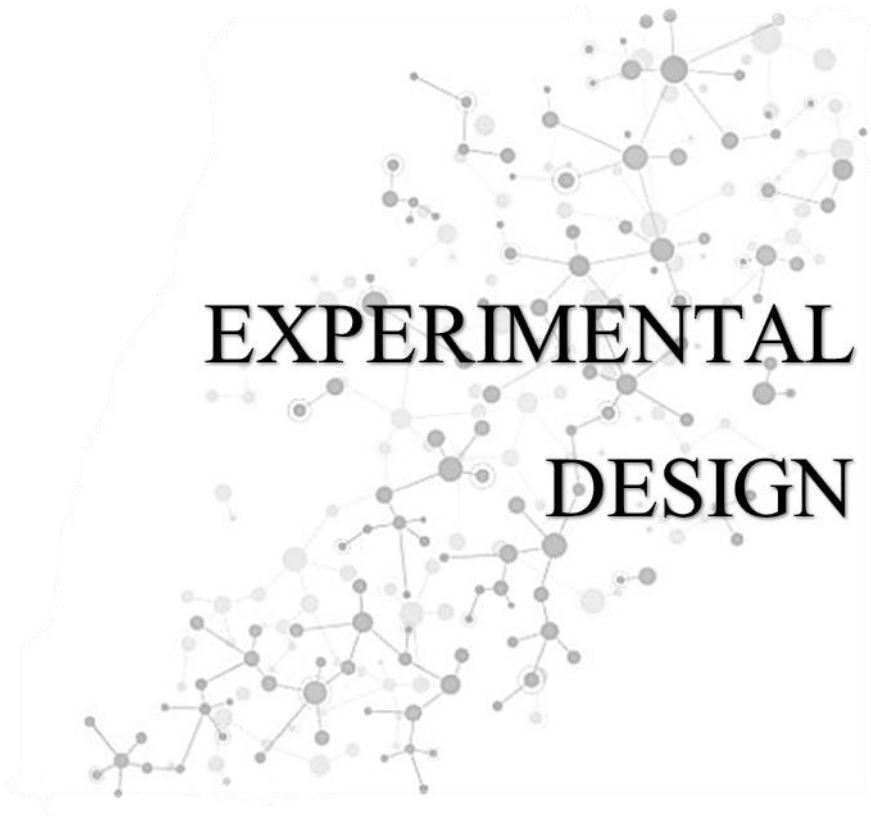
1. Evaluation of the influence of sex and age on anthropometric parameters through analysing the prevalence of MetS and its components, their interactions and clinical consequences.
2. Definition of the metabolic parameters of the MetS and its pathological stages in the context of MHO and MUHO.
3. Examination of the differences between men and women with extreme MetS in metabolomic traits and adipose tissue metabolism in clinically severe obesity at different ages.
4. Identification of epigenetic differences in DNA methylation and

epigenetic drift in severely obese elder adults with and without Mets and the effects on epigenetic age.

5. Understanding the role of methylated metabolites and epigenetic modifications in the mutual regulation between epigenome and metabolome and the impact on metabolic risk and disease.
6. Identification of specific and early biomarkers in metabolic diseases, with a particular focus on patterns by sex and age based on statistical models and data mining.

Cell culture experiments-related objectives:

1. Analysis of the influence of a HFD on the metabolism of rat adipocytes and adipose tissue.
2. Determine the sex-related changes in the metabolome and in the adipose tissue induced by HFD.
3. Study the mannose's effect on rat adipocytes and adipose tissue metabolism.
4. Detection of the metabolic profile induced by HFD in highly controlled models of MetS based on experimental cell cultures of adipocytes and adipose tissue to be validated in the Piancavallo cohort.



3. EXPERIMENTAL DESIGN

3.1. Study design and experimental workflow.

This retrospective and observational study was schemed (figure ED1) to compare and analyse clinical, metabolomics and methylation data of a cohort composed of adult individuals MUHO, affected by MetS, and MHO to investigate their differences in the development of MetS and its effects in terms of the interplay among metabolome, epigenome and the endocrine role of adipose tissue under the influences of sex and age and environmental aspects as diet.

After an extended anthropometric measurement and complete metabolic characterization, all the MHO and MUHO subjects and all the MetS case subgroups were statistically analysed. The study focused on comparing the extreme MetS.5 case subgroup and MHO. Furthermore, according to the literature and due to a lack of the age at which women went through menopause, we divided women into three big subgroups and applied the same criteria for men: fertile age, from 19 to 45 years, menopausal transitional age, from 46 to 54 years, and postmenopausal age, from 55 to 85 years. We focused our analyses on the study of the effects of sex, age and hormonal interactions on MetS.5 comparing men and women at fertile and postmenopausal ages.

According to the results obtained in the metabolomics analysis and considering the elderlies as the most affected by MetS and by its consequences also on the epigenome, we conducted a pilot epigenetics analysis focused on the comparison of methylation changes of a representative sample of 96 subjects (48 cases MetS.5 and 48 controls MHO; age range 55-85 years). Men and women samples were carefully

selected using integrated quality control procedures, respecting their percentage proportion over the entire cohort and matching the subjects of two groups MetS.5 and MHO as much as possible for age and sex.

Finally, an experimental model of obesity and metabolic alterations represented by HFD and control Wistar rats was used to investigate the influence of the diet on the metabolome of adipose tissue and adipocytes in controlled conditions. We performed a cellular study to analyse the metabolomics profile and morphological and functional characteristics of adipose tissue and adipocytes obtained from the animal model. Moreover, we conducted specific treatments on the tissue and cell cultures based on the results obtained by analysing the Piancavallo human cohort. This mechanistic and functional approach was applied to test the potential correspondence with the human condition of MetS in severe obesity and to investigate the biological processes related the diet to severe obesity and MetS.

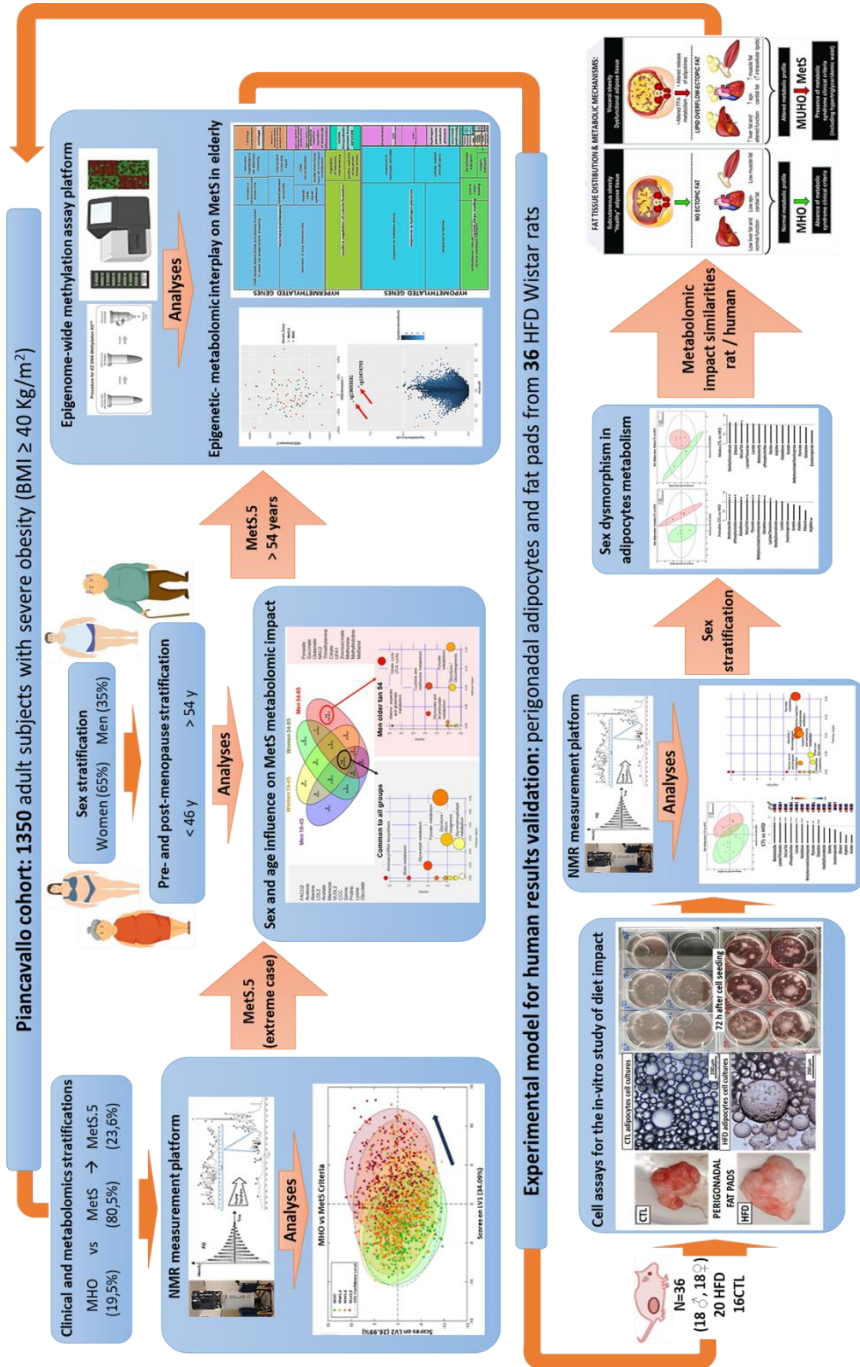


Figure ED1. Experimental workflow of the thesis.

3.2. Characterization of the Piancavallo cohort.

This cohort was composed of 1463 (resulting in the final effective number of 1350 samples after the quality control of clinical and experimental data) adult subjects. All of them were between the ages of 19 and 85 and had clinically severe (Class III) obesity: BMI ≥ 40 kg/m² or between 35.0 and 39.9 kg/m² with one or more obesity-related comorbid conditions, WC ≥ 80 cm in women and ≥ 94 cm in men, and moderate to high WHR. According to the IDF MetS Worldwide definition (2005), the cohort was divided into people with MHO, as controls, and people with MUHO, as cases affected by MetS. The MUHO group was divided into subgroups based on the numbers of MetS parameters, from 3 to 5 (MetS.3, MetS.4, MetS.5), where MetS.5 represented the extreme case of the disease.

3.2.1. Recruitment of the Piancavallo cohort.

All the voluntary participants in the study were recruited for diagnostic or therapeutic characteristics related to clinically severe obesity or its morbidity problems among the patients who attended the Division of General Medicine of the obesity clinical centre of Istituto Auxologico Italiano (Ospedale San Giuseppe, Piancavallo) between years 2006-2017. During this period, all adult patients who presented the parameters of inclusion (see section 3.2.1a.) in the study received an informed consent document with all the detailed information about the study's aims and the procedure of sample collection and data management before taking part in it. Of these, all those who gave their written informed consent to participate and to sample their blood samples to be used for research studies became members of the Piancavallo cohort. The Italian Ministry of Health funded

the study which was conducted by the Declaration of Helsinki and was approved by the Ethics Review Committee of Istituto Auxologico Italiano (Milano) in the session on 10 December 2008 (document attached in Annex I). Regulations were Decreto Legislativo 24 Giugno 2003, n. 211 "Attuazione della direttiva 2001/20/CE relativa all'applicazione della buona pratica clinica nell'esecuzione delle sperimentazioni cliniche di medicinali per uso clinico". Treatment of personal data (decreto legislativo 30 giugno 2003, n. 196), and following integrations, and deliberazione del 24 Luglio 2008 (Linee guida per i trattamenti di dati personali nell'ambito delle sperimentazioni cliniche di medicinali. Deliberazione n. 52).

3.2.1a. Inclusion/exclusion parameters collection and measurement.

The anthropometric variables collected and measured included: age, sex, height, body weight, and waist and hip circumference. Body composition, in terms of the percentage of FM and fat-free mass (FFM), was determined using a bioelectrical impedance analysis (BIA101/S model; Akern, Florence, Italy) in the morning following an overnight fast and less than 2 days later the execution of the indirect calorimetry. The presence of hypertension, hyperglycemia and DM2, dyslipidemia (hypertriglyceridemia and low HDL) were evaluated using routine laboratory measurements. Resting oxygen uptake and resting carbon dioxide production were measured from a ventilated canopy at 1-minute intervals for 30 minutes and expressed as a 24-hour value. Resting energy expenditure (REE) (kcal / 24 h) was measured between 8 and 9 a.m. after a fasting period and physical inactivity of 12 h in a thermoneutral conditions room (22–24 °C) using indirect computerized calorimetry (Vmax 29, Sensor Medics, Yorba Linda, CA, USA) by an open-circuit and

was calculated using the Weir equation, as published previously [143]. Subjects were awake and supine with the head placed in a rigid, transparent ventilated canopy. Average daily caloric intake was assessed using a standardized 7-day booster technique. Diet and weight histories were assessed according to standardized methodologies during interviews carried out by two trained dietitians.

After the data collection, patients who did not achieve waist circumference ≥ 80 cm in women and ≥ 94 cm in men and fluid overload patients, according to vector analysis, were excluded to minimize errors in estimating FM and FFM in severe obesity. All obese patients who showed a negative difference between reported food intake and REE multiplied by 1.2 (as a conservative estimate of total energy expenditure) were also excluded as considered underestimated. Therefore, their medical history has been classified as unreliable. MetS severe concomitant disease, type 1 diabetes (DM1) or psychiatric disorders, illnesses unrelated to the MetS or an unreliable medical history were also considered exclusion criteria. Finally, the failure to fill in a Data Collection Form and/or the informed consent document resulted in the exclusion.

3.3. Mechanistic hints in experimental animal models fed with High Fat Diet.

The use of animal models to obtain tissues and cells for specific analyses and controlled cultures is very useful for testing the results from integrated analyses of multiple omics data and environmental response phenotypes. These experimental models represent a sort of mechanistic and functional validation study to understand the structural and functional relationships of cells and tissues by monitoring conditions and key

components such as cell viability and proliferation, cell signalling pathways and complex biological interaction networks, cell cycle and cell structure analysis. Various diet-induced-obesity animal models have been proposed to better understand the physiopathology of abnormalities associated with obesity. For example, overconsumption of a high-energy diet has been proposed to promote a positive energy balance and can reproduce many features of human overweight and obesity [144]. The use of HFD-fed rats is particularly indicated because both humans and rodents tend to gain weight with high caloric intake. Moreover, while humans have large abdominal viscera including omental, perirenal and retroperitoneal fat pads in addition to mesenteric, gonadal and epicardial fat tissues, mice and rats have large perigonadal fat pads [145], which, besides perirenal and retroperitoneal fat, can be considered comparable with humans' visceral adipose tissue as shown in figure ED2.

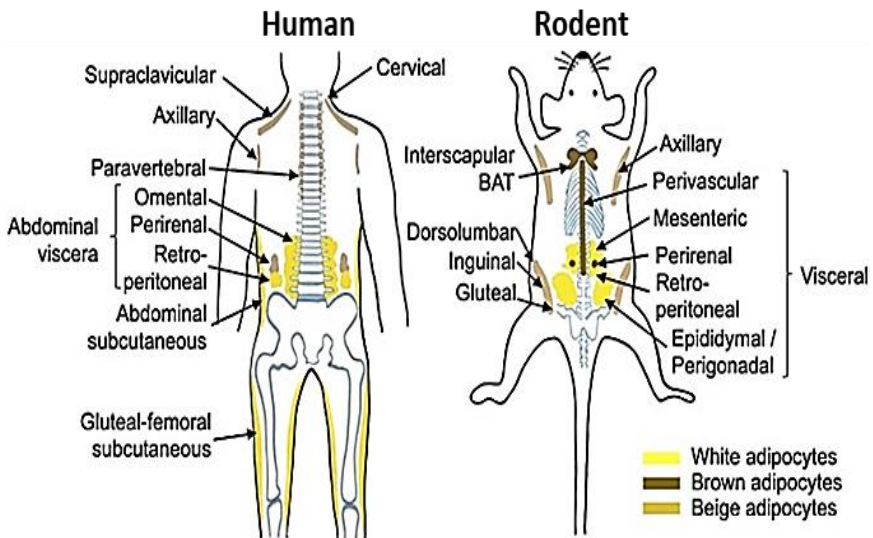


Figure ED2. Distribution of fat tissues in humans and rodents. Modified figure from Cheong et al., 2021.

3.3.1. Cell assay on adipose tissue obtained from an HFD-fed rats model.

Perigonadal fat pads were supplied by a laboratory colleague after an HFD feed experimental protocol on 36 Wistar rats (18 males and 18 females, 39 weeks of age, weighing 600-860 g (males) and 290-350 g (females)). The rats were part of the project "Longitudinal study of the development of non-alcoholic fatty liver disease (NAFLD). Interaction of diet - intestinal microbiota - adipose tissue - liver". The project protocol was subjected to the Ethics Committee of the University of Valencia with the following code: A1538561308126, evaluated and approved (approved proceeding number: 2019/VSC/PEA/0129) and the experimentation on the animals was performed in our laboratory simultaneously with the development of this thesis. Both male and female rats were randomly separated into the control (CTL) groups (8 animals per sex), fed with an ordinary chow diet Teklad Global 2014 (diet sheet attached in Annex II, Figure A1), and the HFD groups (10 animals per sex), fed with Teklad Custom Diet TD.08811 (45 % kcal Fat Diet) from Harlan (diet sheet attached in Annex II, Figure A2). The access to water and food was *ad libitum* and all the animals were sacrificed after 20 weeks of treatment. Perigonadal fat tissues were extracted just after the sacrifice procedure. Specifically, epididymal fat pads were obtained from male rats. Periovarian fat bodies were obtained from female rats.



4. MATERIAL AND METHODS

This thesis's general methodology involved applying omic technologies such as metabolomics and epigenetics for the analysis of serum samples from the study cohort and all the cell culture media samples from rat adipose cells and tissue cultures. The correct collection, quality control and processing of biometric and anthropometric data and biological samples, as well as cell culture techniques, represented a critical step to optimize high-throughput technologies. The development of adequate statistical analyses constituted a fundamental point for the correct visualization, validation and biological interpretation of the results. All procedures and analyses listed are extensively described and detailed below.

Methodological approaches applied to the Piacavallo cohort:

- Collection and quality control analysis of phenotypic data;
- Collection and specific preparation of serum samples for processing;
- Metabolomic analysis through NMR spectroscopy;
- Epigenetic analyses through DNA methylation quantification and related assays;
- Statistical analyses and biological interpretation.

Methodological approaches applied to the HFD animal model:

- Collection of rat body measurements;
- Rat perigonadal fat tissue collection and preparation for processing;
- Cell and organ cultures maintenance and treatment;
- Collection and processing of adipocytes and adipose tissues culture

media samples, organ culture fragments and adherent differentiated freezing adipocytes;

- Metabolomic analysis through NMR spectroscopy;
- Statistical analyses and biological interpretation.

4.1. Methodological approaches applied to the Piancavallo cohort.

4.1.1. Collection of phenotypic data.

The patients enrolled in the study were asked to fill in a Data Collection Form. Together with the biometric characteristics and clinical data, information related to habits and lifestyle was reported to identify any risk factors related to MetS or influencing the DNA methylation status. The compilation of this questionnaire took place at the same hospital. In particular:

Clinical and biometric and anthropometric data:

- Sex and age
- Weight and height
- Waist and hip circumference
- BMI and WHR
- Hyperglycemia
- DM2
- Low HDL
- Hypercholesterolemia
- Hypertriglyceridemia
- HOMA-IR

- SatO₂, oxygen saturation
- REE
- Altered levels of thyroxine (T₄) and thyroid stimulating hormone (TSH); Thyroids disorders
- Other disorders or complications
- Pharmacological treatments

Habits and lifestyle:

- Consumption of alcohol and smoking
- Consumption of coffee
- Diet
- Physical activity

4.1.1a. Phenotypic data processing and quality control.

The quality control of phenotypic and clinical data was a fundamental process for correctly carrying out the experimental part of the study and subsequent statistical analyses. The human Piancavallo cohort data collected during clinical analysis and provided by the patients (1463 subjects) were verified. First, the correspondence between the biological samples collected and the information obtained through the Data Collection Form was checked. In case of uncertainty or mismatch between these data, the samples were excluded from the experiment. This led to the exclusion of 59 samples. Even in the case of correct correspondence, further screening was carried out to exclude from the analysis samples that could not be compared with the others due to the lack or incompleteness of clinical, biometric and/or anthropometric data information (33 samples). Lamentably, it was deemed necessary not to consider the data relating to habits and lifestyle due to the impossibility of verifying their reliability and

the lack of information for many patients. Hence, the final number of serum samples suitable for the experimental part of the study and subsequent statistical analyses was 1371.

4.1.2. Collection and storage of blood samples.

Blood samples were obtained in the early morning after eight to twelve hours of fasting before their drawing. During the sampling, the blood samples were collected in different tubes to allow their subsequent specific use: in a covered test tube to obtain serum samples or in an ethylenediaminetetraacetic acid (EDTA)-treated tube that prevents the coagulation of whole blood samples for the further extraction of genomic DNA.

The covered test tube was left undisturbed at room temperature from 30 minutes to 1 hour to allow the blood to clot. The serum was then separated from the clot by centrifuging at 1,000-2,000 x g for 10 minutes and immediately transferred with a pipette into a sterile 1.5 mL Eppendorf tube and was frozen immediately at -80 °C until the experimental measurements were made.

4.1.3. NMR spectroscopy and serum metabolomics analysis.

The metabolomic approach on serum samples of the Piancavallo cohort and culture medium samples was done by the use of ¹H-NMR to study the metabolic features of the MetS and obesity. NMR provides precise and useful information on the structure and composition of low-molecular-mass metabolites in biological fluids thanks to its unbiased

metabolite detection, quantitative nature, and high reproducibility [146]. The metabolomic analysis routine is summarized in Figure MM1.

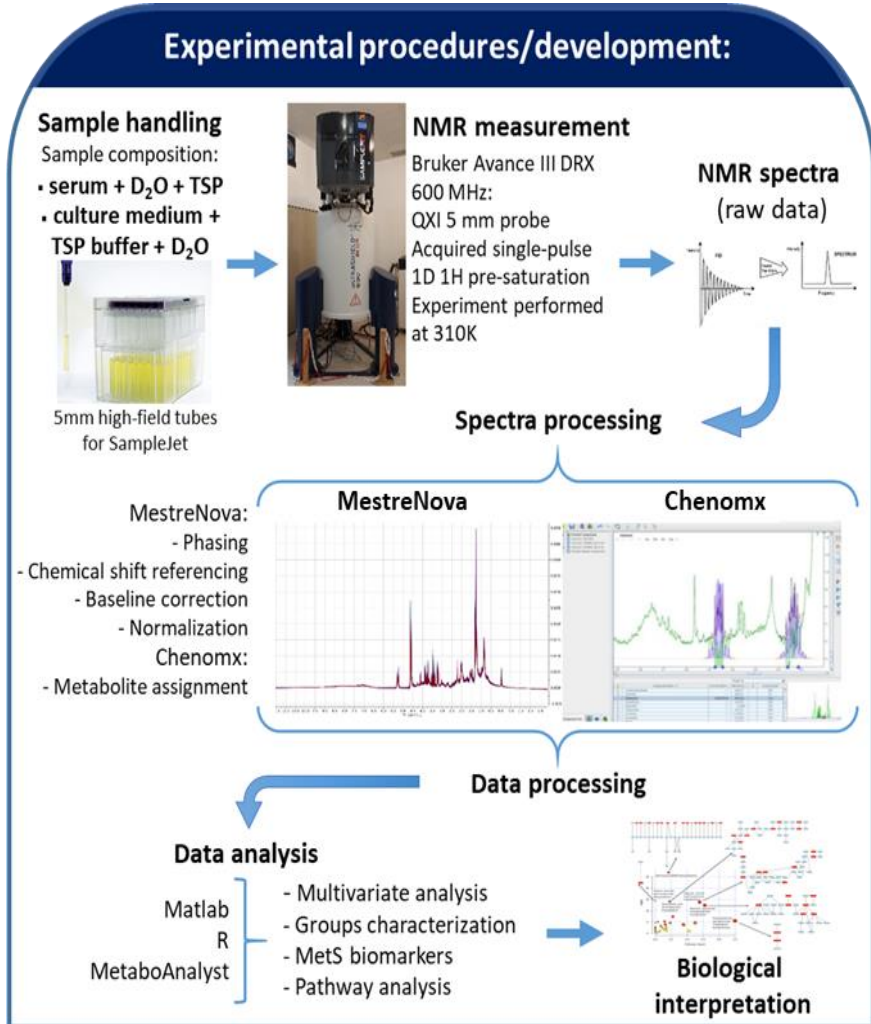


Figure MM1. Summary of spectral processing and post-processing steps on NMR data (TSP, trimethylsilyl propionate; D₂O, deuterium oxide).

4.1.3a. Serum samples preparation for NMR measurement and pre-analytical quality control.

All samples were thawed at room temperature before metabolites were measured by NMR spectrometry. The sample handling was performed in the Molecular and Metabolomic Imaging Laboratory (UCIM-University of Valencia, Spain) following the NMR technician's directions and support. The manual sample handling is detailed below.

A volume of 470 μL of serum was mixed with 30 μL of deuterium oxide (D_2O) with internal reference to trimethylsilyl propionate (TSP) 2.5 mM (final concentration) and placed in a 5 mm high-resolution NMR tube for SampleJet. Pre-analytical quality control was performed to verify the quantity and quality of the serum samples. A total of 21 samples with a serum volume of less than 200 μl were excluded.

4.1.3b. Serum spectra acquisition.

A final number of 1350 of human serum spectra from the Piancavallo cohort were processed individually. NMR spectra were acquired using a standard one-dimensional pulse sequence ^1H ZGPR with water suppression (pre-saturation) using a Bruker Avance III DRX 600 MHz spectrometer (Bruker GmbH, Rheinstetten, Germany) operating at a ^1H frequency of 600.13 MHz. The instrument was equipped with a QXI 5 mm quadruple resonance $^1\text{H}/^{13}\text{C}/^{15}\text{N}/^31\text{P}$ probe and a SampleJet automated sample changer thermostatted at 277 K. For each serum sample, a volume of 500 μL was measured using a 5 mm probe. Pre-saturation were acquired using a 3.95 s acquisition time, 32 transients, 14 parts per million (ppm) (8417 Hz) spectral width, and a relaxation delay of 2 s. Water pre-

saturation was used for 1 second throughout the recycle time for solvent signal suppression. The total acquisition time was 4 min 47 sec per sample and the experiments were recorded at 310 K. The measurement was carried out randomly between the samples of the different sample groups.

4.1.3c. NMR spectra processing and quality control.

The raw data obtained were initially manipulated by the technician and Fourier-transformed to allow the following analysis. Then, all spectra were processed using MestReNova 14.1.1 software (Mestrelab Research S.L., Santiago de Compostela, Spain). Each spectrum was phased and baseline corrected, focalizing on the chemical shift region including resonances between 0.50-4.50 ppm and 5.00-9.50 ppm of spectrometer frequency. The two intervals of ppm include the aliphatic region and the aromatic region, respectively. The spectral region of water (4.50-5.00 ppm) was excluded. The spectra were referenced using the chemical shift of the second peak of the Alanine's doublet at 1.478 ppm and were normalized to the aliphatic area (0.50-4.50 ppm) of the spectra. The reproducibility of NMR spectroscopy was verified by the superposition of normalized spectra. No samples were removed after having performed the quality control of the processed spectra samples. Quality control on experimental data was necessary to verify the success of the manual and automatic parts of the experiment (protocol, reagents, instruments and equipment calibration, internal bias).

4.1.3d. Metabolites and spectral regions assignment.

Metabolite spin systems and resonances were identified by literature data, ^1H , ^1H -TOCSY NMR spectra, and the Chenomx resonances database

MATERIAL AND METHODS

(Chenomx NRM Suite 8.1, Chenomx Inc. Edmonton, Canada). In addition, when the software was not able to identify a metabolite, specialized NMR databases such as HMDB were consulted together with the currently available literature on NMR-based metabolomics. This strategy allowed us to obtain a more complete list of identified metabolites.

Our metabolic profiling approach provided information on 55 well-defined spectral metabolic characteristics, listed in Table MM1 and illustrated in the spectra in Figure MM2. All of the metabolites were assigned to unique metabolic components, although five of them, namely proline, glycolate, 2-oxosuccinate, creatinine and threonine were not confirmed by the spectra due to the low signal-to-noise in the 2D spectra.

Table MM1. List of the 55 metabolites' spectral regions detected in Piancavallo cohort serum samples.

PIANCAVALLO METABOLIC SYNDROME SAMPLES		
	SERUM METABOLITES REGIONS	ppm
1	Cholesterol	0,6 - 0,72
2	FA1	0,78 - 0,9
3	Leucine	0,945 - 0,97
4	Isoleucine	0,992 - 1,015
5	Valine	1,022 - 1,075
6	2oxobutyrate	1,055 - 1,075
7	Ethanol	1,155 - 1,17
8	3hydroxybutyrate	1,18 - 1,21
9	FA2	1,21 - 1,24
10	VLDL2	1,24 - 1,28
11	LDL2	1,28 - 1,31
12	Alanine	1,46 - 1,485
13	FACO1	1,49 - 1,6
14	Acetate	1,905 - 1,925
15	UFA1	1,93 - 2,02
16	NAC1	2,02 - 2,06
17	NAC2	2,06 - 2,09
18	Proline	2,092 - 2,113
19	FACO2	2,2 - 2,215
20	Acetone	2,215 - 2,23
21	Glutamate	2,33 - 2,358

PIANCAVALLO METABOLIC SYNDROME SAMPLES		
	SERUM METABOLITES REGIONS	ppm
22	Pyruvate	2,358 - 2,37
23	Succinate	2,392 - 2,405
24	Glutamine	2,417 - 2,5
25	Citrate	2,507 - 2,56
26	Methionine	2,635 - 2,645
27	Dimethylamine	2,7 - 2,723
28	Sarcosine	2,728 - 2,733
29	Trimethylamine	2,885 - 2,888
30	Dimethylglycine	2,9 - 2,92
31	PUFAs	2,94 - 2,99
32	Lysine	3,01 - 3,02
33	Creatine	3,03 - 3,052
34	Choline	3,185 - 3,195
35	CCC	3,195 - 3,225
36	Arginine (+ Glucose)	3,225 - 3,238
37	TMAO (+ Glucose)	3,238 - 3,252
38	2oxosuccinate	3,34 - 3,352
39	Methanol	3,352 - 3,37
40	Glucose	3,38 - 3,5
41	Glycine (+ Glucose)	3,545 - 3,559
42	Threonine (+ α -Phosphocholine)	3,574 - 3,59
43	myoinositol	3,608 - 3,62
44	Methylhistidine	3,68 - 3,69
45	Glycolate	3,92 - 3,935
46	Serine	3,957 - 3,985
47	Creatinine	4,038 - 4,085
48	Lactate	4,085 - 4,135
49	Threonine	4,24 - 4,29
50	Mannose (+ Glycogen fragments)	5,17 - 5,21
51	α -Glucose	5,22 - 5,25
52	UFA2	5,25 - 5,37
53	Tyrosine	6,88 - 6,905
54	Phenylalanine	7,39 - 7,44
55	Formate	8,445 - 8,455

List of detected metabolites and chemical shift assignment in the NMR spectra of serum. The resonance's relative position in the NMR spectrum is indicated by its ppm values. Key for NMR moieties: FA: fatty acids; FA1: CH₃-; FA2: -CH₂-; FACO1: -CH₂CO; FACO2: -CH₂CH₂CO; UFA1: =CHCH₂CH₂-; UFA2 =CHCH₂-; PUFAs: =CHCH₂CH=; CCC: choline-containing compounds; TMAO: trimethylamine oxide; NAC1: acetyls in glycoproteins 1; NAC2: acetyls in glycoproteins 2.

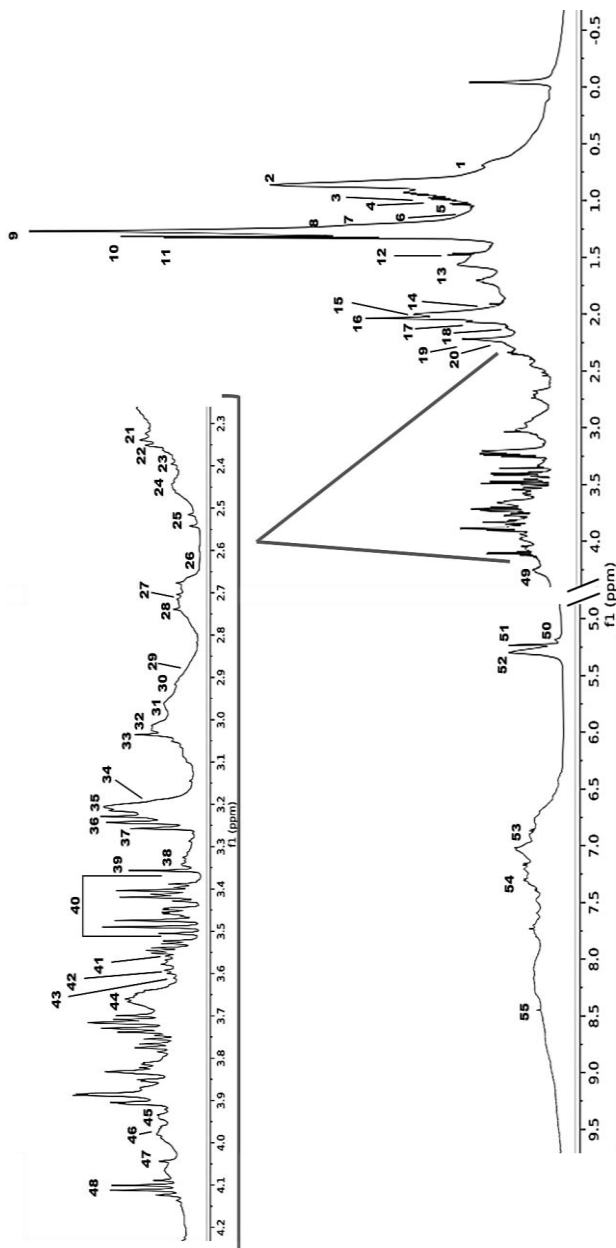


Figure MM2. Representative ^1H NMR spectrum of serum samples from the Piancavallo subjects. 1, cholesterol; 2, FA1; 3, leucine; 4, isoleucine; 5, valine; 6, 2-oxobutyrate; 7, ethanol; 8, 3-hydroxybutyrate; 9, FA2; 10, VLDL2; 11, LDL2; 12, alanine; 13, FACO1; 14, acetate; 15, PUFAs; 16, NAC1; 17, NAC2; 18, Proline; 19, FACO2; 20, acetone; 21, glutamate; 22, pyruvate; 23, succinate; 24, glutamine; 25, citrate; 26, methionine; 27, dimethylamine; 28, sarcosine; 29, trimethylamine; 30, dimethylglycine; 31, ufa1; 32, lysine; 33, creatine; 34, choline; 35, ccc; 36, arginine + glucose; 37, TMAO; 38, 2-oxosuccinate; 39, methanol; 40, glucose; 41, glycine + glucose; 42, *o*-phosphocholine; 43, *myo*-inositol; 44, π -methylhistidine; 45, glycolate; 46, serine; 47, creatinine; 48, lactate; 49, threonine; 50, mannose + glycogen fragments; 51, α -glucose; 52, UFA2; 53, tyrosine; 54, phenylalanine; 55, formate. Key for NMR moieties: FA: fatty acids; FA1: CH3-; FA2: -CH2-; FACO1: -CH2CO; FACO2: -CH2CH2CO; UFA1: =CHCH2CH2-; UFA2 =CHCH2-; PUFAs: =CHCH2CH=; CCC: choline-containing compounds; TMAO: trimethylamine oxide; NAC1: acetyls in glycoproteins 1; NAC2: acetyls in glycoproteins 2.

4.1.3e. Metabolites and spectral regions quantification.

The quantification of every listed metabolite per sample was obtained as the area under the metabolite or spectral region curve. Chenomx NRM Suite 8.1 profiler (Chenomx Inc. Edmonton, Canada) was used to perform the assignment. The data were then imported into the semi-automated in-house Matlab R2019b software (The MathWorks Inc., Natick, MA, USA) for additional processing and routine laboratory analysis, like integration and peak-fitting procedures. The final metabolite relative spectral abundance was calculated in arbitrary units as the peak area was normalized to the total aliphatic spectral area, lipid excluded, to eliminate any differences in the metabolite total concentration. Good quality of the sample and its management, the NMR setup and processing parameters can have a significant impact on the quality of NMR spectra and their subsequent interpretation. The choice of an appropriate number of acquisitions also significantly impacts the quality of NMR spectra and the presence of peak distortions or anomalies in pulse sequence for data acquisition. In parallel, also spectral processing choices including the accuracy of the phasing, and the quality of baseline correction, affect the results [147, 148].

4.1.4. DNA methylation. Epigenetics.

Genome-wide methylation assay is part of epigenome-wide association studies (EWAS) and consists of quantitative interrogation of selected methylation sites across the genome, offering high-throughput research capabilities at a minimal cost per sample.

4.1.4a. Whole blood samples preparation for methylation assay.

All the 96 selected samples (48 controls MHO and 48 cases MetS.5) (see section 3.1. for details) were thawed at room temperature before starting the process to measure the methylation levels. The samples handling was performed in the Molecular Biology Laboratory of the Department of Molecular Genetics (I.R.C.C.S. Istituto Auxologico Italiano, Cusano Milanino, Italy) thanks to the supervision of Prof. Davide Gentilini and the directions and support of his unit of research. The manual sample handling is detailed below.

- DNA extraction: genomic DNA was obtained using an automated system and a commercial kit capable of extracting DNA from whole blood samples using magnetic beads for separation; some samples, due to their small quantities or the presence of blood clots, required manual DNA extraction using the Wizard genomic DNA purification kit (PROMEGA, Madison WI, USA). In this case, a volume equal to 3-5 ml of blood was treated with a lysis solution provided in the kit and then digested at 37 ° C for 1 hour with Protease K in a buffer containing sodium dodecyl sulfate (SDS). The DNA was subsequently extracted by salting-out method and resuspended in a buffer containing Tris-EDTA (TE).
- DNA quality control and dilution after extraction: for each sample, a volume of 1.5 µl of total genomic DNA was quantized using an N60 NANOPhotometer PEARL IMPLIN (NanoDrop Products Thermo Scientific Wilmington, DE) to verify its concentration and quality. DNA was then diluted with a TE buffer at pH 8.0 to obtain a normalization to a theoretical concentration of 20 ng/µl and re-quantified to ensure the correct

sample concentration. No samples showed aberrant protein (260 / 280) as well as organic compounds (230 / 260) ratio that would have entailed discarding or purification.

- Conversion with bisulphite: for each sample, 900 ng of DNA were treated with sodium-bisulfite to convert the unmethylated cytosines (C) presented in the genome into uracils (U), replaced by thymines (T) after amplification, leaving 5-methylcytosine residues unaffected, to make them identifiable and quantifiable. The addition of sodium-bisulfite makes unmethylated cytosine susceptible to hydrolytic deamination. The deaminated cytosines were then converted to U in an alkaline pH and replicated as T during PCR. The procedure was performed using the commercial EZ DNA Methylation Kit (Ref: D5001, Zymo Research Corporation, Orange, CA), following the manufacturer's directions. The basic steps are summarized in Figure MM3. Specific incubation conditions (Illumina Protocol) were applied to improve conversion efficiency.

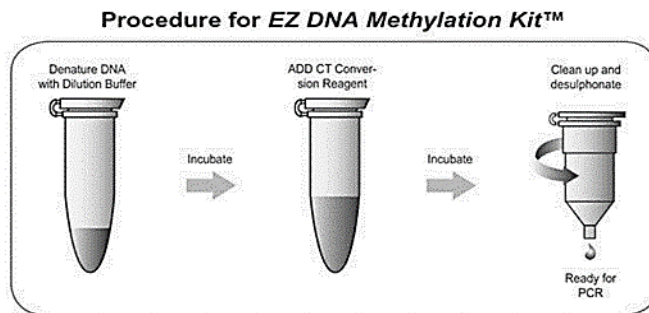


Figure MM3. Outline of the EZ DNA Methylation™ Kit procedure.

- DNA quality control after conversion: for each sample, the single-strand DNA quantity after conversion (ssDNA) was verified for the subsequent phase of the experiment as previously reported for total

genomic DNA. The quality was assessed by direct visualization after an electrophoretic run in 1 % agarose gel. All ssDNAs, following bisulfite conversion, were found to be non-fragmented and with a concentration greater than 50 ng/ μ l. So, no DNA samples were discarded or reprocessed for resulting fragmented or diluted, and all 96 samples were subsequently processed.

4.1.4b. Epigenome-wide methylation assay.

Epigenome-wide methylation profile analysis of the samples was directed to the quantitative measurement of over 850,000 methylation sites at single-nucleotide resolution using the Infinium MethylationEPIC BeadChip kit (Illumina San Diego, CA). The samples were processed according to the manufacturer's protocols and using reagents and conditions provided by Illumina in a semi-automatic procedure. Specifically, 250 μ g of converted DNA was suitably treated through a whole genome amplification phase (WGA) followed by enzymatic fragmentation, precipitation and resuspension. The resuspended samples were then hybridized on the chips at 48° C for 16 h. During hybridization, the DNA-WGA molecules were bound to locus-specific DNA oligomers, differentiated in the terminal part as they were designed to be complementary to the methylated or non-methylated site, and linked to individual beads. Non-specifically hybridized DNA was eliminated. After hybridization, an allele-specific single base extension phase provided an additional level of specificity by inserting a sort of label for analysis. The incorporated nucleotides were labelled with biotin (ddCTP and ddGTP) and 2,4-dinitrophenol (DNP) (ddATP and ddTTP). After the extension, a staining phase with different fluorophores was followed. Finally, the

BeadChips were washed and protected for scanning through the Illumina iScan scanner. It is a two-colour fluorescent laser scanner (532 nm / 660 nm) with a spatial resolution of 0.375 microns able to excite the fluorophores introduced during the staining step of the protocol. The methylation levels were determined for each locus thanks to the intensity level of the two possible fluorescent signals, specific for the methylated or non-methylated allele. The methylation level for each CpG site was represented by beta (β) values obtained from the ratio of fluorescence intensity between methylated and unmethylated probes, according to the formula: $\beta = (\text{methylated fluorescence intensity}) / (\text{fluorescence intensity (methylated + unmethylated)})$. The β values can range between 0 (unmethylated) and 1 (fully methylated). This method ensured a wide coverage of CpG sites at the level of the gene regions: transcription start site (TSS), 5'UTR, first exon, gene (gene body), 3'UTR, as well as at the level of the CpG islands including regions flanking (shelves and shores). The fluorescence intensities were stored as intensity data files (*.idat) which can be used as input for most of the available software packages. Quality control steps were carried out to identify and correct technical biases typical of this type of method, including batch effect, sampling errors and technical analysis errors.

4.1.4c. Post-array quality control and data pre-processing.

Post-array quality control of the raw data obtained after scanning the methylation chips was carried out using the RnBeads [149, 150] software package to identify and correct both biological and technical biases typical of this type of method, including batch effect, sampling errors and technical analysis errors. Figure MM4 presents the different points to

MATERIAL AND METHODS

check during processing to ensure accurate analysis and correct interpretation of the data.

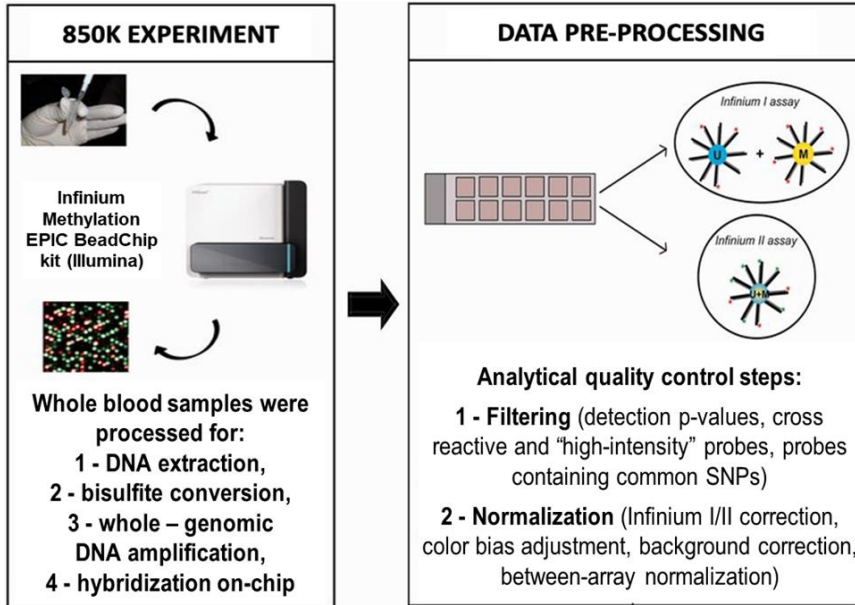


Figure MM4. Schematic overview of the methylation assay's data pre-processing and quality control steps.

Specifically, data pre-processing included two quality control steps: filtering and normalization.

Filtering:

- For each sample, a further check of the conversion efficiency index with bisulfite was carried out for the possible rejection of samples with a low index. This parameter is indicated by the presence of internal control on the chip which must necessarily have a fluorescence intensity greater than 4000. No sample was rejected in this step.
- Probes with too high or too low fluorescence ($n = 4217$) were removed

from the dataset using the Greedycut algorithm. This algorithm allowed the evaluation of the specificity (false positive rate) and the sensitivity considering the measurements as predictive of each other.

- All β values corresponding to a p-value that exceeded the T threshold of 0.05 ($p \geq T = 0.05$) were considered non-measurable. Furthermore, from all the CpG sites analysed, only the significant ones in at least 95 % of the samples were used for the subsequent analyses. Only the samples reaching 99.5 % of CpG sites determined successfully were included. A total number of 823446 CpG Sites, including 253821 Tiling, 34997 Genes, 44902 Promoters and 26529 CpG Islands (n = 21861 probes removed).
- All sites containing SNPs, and natural C / T polymorphisms (n = 17371) were filtered and removed from the analysis; their presence can significantly influence subsequent methylation analyses as it reflects the genotype and is not an actual measurement of the level of methylation.
- Probes that hybridized at the sex chromosome level (n = 18924) were eliminated. The methylation differences associated with the X and Y chromosomes are not comparable in the entire population because it is composed of individuals of both sexes and would require specific analyses.
- Finally, the correspondence between phenotypic and genotypic sex was checked and, if present, the samples classified incorrectly at the time of collection were excluded. Genotypic sex was obtained by calculating the methylation levels of the sex chromosomes. In women, following the inactivation process of one of the two X chromosomes, higher methylation levels are measured than in males. Therefore, it is possible to classify individuals based on their sex.

Normalization:

The data were normalized following different strategies to minimize the variability due to methodological factors. The Beta Mixture Quantile (BMIQ) normalization method [151] let normalize the signal intensities.

- Background correction: it is exclusively a procedure for removing the background noise introduced by the different measurements of the red and green probes [152]. The background signal was subtracted from the analysed samples from the raw fluorescence data measured during the experiment. For this correction was used the “noob” (normal-exponential convolution using out-of-band probes) method of the methylumi package.
- Quantile normalization: assuming that the identifying fluorescence signals of methylated and unmethylated DNA should not be globally different between the samples analysed, it represents a more sophisticated and robust data normalization technique. The values were divided based on percentiles and a scaling factor was calculated for each percentile. This normalization technique, carried out using the SWAN (Subset-quantile Within Array Normalization) method present in the RnBeads minfi package, took better account of the fact that the different samples might have not only global differences in the measured fluorescence but also a different trend [153].

No samples were excluded after the quality control step by filtering and normalization because all satisfied the quality requirements. It was thus possible to define the number of subjects and probes to carry out the statistical analysis to identify possible differences in methylation (differences between β values) between subjects and among enrolled groups.

4.1.4d. Estimation of lymphocyte subpopulations and biological (epigenetic) age.

Lymphocyte cellular composition was inferred from methylation data through the presence of some specific epigenetic markers. Using the method developed by Houseman *et al.* [154] and the AdvancedAnalysisBlood option of DNA Methylation Age Calculator analysis software (<https://dnamage.genetics.ucla.edu/>) [103] was, therefore, possible to obtain estimates of the proportions of CD8 cells (naive and differentiated into CD8T), CD4 cells (naive and differentiated into CD4T), natural killer (NK) cells, B cells, monocytes and granulocytes. Subtypes' estimates were conveniently evaluated as PCs in the differential methylation analysis. Using the same software, DNA methylation measurements were also used to predict biological (epigenetic) age using several approaches developed by Horvath including the pan tissue DNAmAge epigenetic clock and the DNAm-based mortality biomarker "DNAm GrimAge" [105] (see section 1.3.4.). Positive high values of accelerated DNAmAge and accelerated GrimAge indicated faster biological ageing, based on chronological age, while lower or negative values indicated decelerated ageing.

4.1.4e. Analysis of stochastic epigenetic mutations.

SEMs have been recently defined as a potential measure of the accumulation of DNA damage due to exposure to a pathological condition or altered physiological state [155]. The complementary methylation analysis strategy developed by Prof. Gentilini and his team [156, 157] was applied to single (individual) methylation profiles to pick out aberrant beta values (extreme outliers) according to a reference methylation range

(obtained from the same reference subjects), through a non-parametric statistical approach. We specifically defined SEMs as extreme outliers within a population. Extreme outliers do not fall within a reference methylation range obtained from the methylation profiles of a reference population and calculated as follows: upper value = $Q3 + (k * IQR)$; lower value = $Q1 - (k * IQR)$; where $Q1$ is the first quartile, $Q3$ the third quartile, IQR (interquartile range) = $Q3 - Q1$ and $k = 3$. For each case, the extreme outliers of the individual methylation profiles were noted and classified as hypomethylated or hypermethylated concerning the median values of the relative probe of the controls. To estimate epigenetic drift, SEM analysis at a single individual level was employed as a correlative approach and the number of SEMs was compared between the two groups to identify potential differences in epigenetic drift. In addition, potential relationships between SEMs and clinical outcomes of MetS were investigated. Overrepresentation analysis of all identified SEMs was conducted to detect the SEM-enriched regions, for each individual without any cut-off on methylation differences. We evaluated the enrichment of SEMs in a window of a predefined size (eg 11 CpG sites) and generated a p-value associated with the window, using a sliding window algorithm based on a cumulative hypergeometric test on the annotated genome, as extensively explained previously [158]. Quality control, pre-processing and generation of β values dataset were performed using the Chip Analysis Methylation Pipeline (ChAMP) R package [159], a BMIQ normalization method. Sites with a detection p-value greater than 0.01 (6803 probes) and a bead count less than 3 in at least 5 % of the samples (10521 probes), non-CpG probes (2933 probes), and probes potentially affected by SNP (95584 probes), aligned to multiple positions (11 probes) and related to sex chromosomes (16587 probes) have been removed from the analysis. After doing all

filterings, 733479 probes and 96 samples resulted suitable for the following steps of analysis. SEMs were therefore annotated using wANNOVAR software [160] obtaining the lists of epilepsions' related genes for each group. Finally, the development and application of specific statistical analyses (see section 4.3.) were aimed at allowing their possible and useful biological interpretation.

4.2. Methodological approaches applied to the HFD-fed animal model.

4.2.1. Collection of rat body measurements.

The measures of the body weight of every rat were taken individually before the HFD treatment and before the sacrifice (Figure MM5 A) to obtain the initial and final body weights. The measure of weight of every perigonadal fat pad was taken individually just after the extraction from the animal (Figure MM5 B).

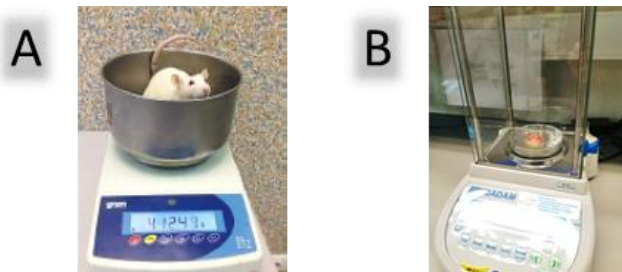


Figure MM5. *Measuring of rat body weight and perigonadal fat pad weight.*

4.2.2. Rat perigonadal fat tissue collection and processing for cell or organ cultures.

The veterinary staff obtained the tissues under aseptic conditions from euthanized animals (HFD-fed Wistar rats model, see section 3.3 for more information) using isoflurane overdose. The following procedure was applied both to male (18 animals) and female (18 animals) rats. Both perigonadal fat pads (epididymal for males, periovarian for females) for each animal were removed. One pad of each animal was then frozen at -80 °C in an unaltered state or a solid matrix constituted of Tissue-Tek resin (O.C.T. compound, Labtech International Ltd Mytogen House, Heathfield, East Sussex), for subsequent cryo-sectioning for histological and immunohistochemical processing (experimental part not included in this thesis). The other pad was collected in a Petri dish and quickly moved to the laboratory for further processing. Every perigonadal fat pad was weighted and properly processed for extraction of adipocytes (9 samples, 4 CTL and 5 HFD) or organ culture (9 samples, 4 CTL and 5 HFD) as shown in Figure MM6.

- Adult adipose cell extraction: perigonadal fat pads were washed with Wash buffer and adequately minced with sterile scissors after the removal of blood vessels. Every tissue sample was transferred immediately in a 15-ml falcon tube and an adequate volume of Digestion buffer (2-3 ml per 1 g of tissue) was added for the digestion process. The tissues were digested at 37 °C for 30-60 minutes in a shaking bath until a smooth and uniform consistency was obtained. Then, smoothed tissues were filtered using a sterile nylon mesh and transferred to a new 15-ml falcon tube. A double volume of wash buffer was added to stop the digestion and cells could float to the surface for 5 minutes. Then, cells were separated via centrifugation

(500 x g, 3 minutes). The fat cells floated to the surface whereas the stromal-vascular cells were sedimented and removed by aspiration. The floating infranatant was washed 3 times with Phosphate-buffered saline (PBS) and, finally, was aspirated and transferred to an Eppendorf tube to quantify the volume. Four cell culture replicates were obtained from every Eppendorf containing perigonadal mature adipose cells from one animal. An adequate volume of Standard Medium or D-mannose Treatment Medium was added to every plate and cells were plated in 6-well cell culture plates with a surface of 9.5 cm² (see section 4.4. for buffers and cell media composition details).

- Organ culture procedure: immediately after weighing, the tissue was divided into four equal parts and minced finely into 5-10 mg fragments with sterile scissors into Petri dishes. Minced tissues were accurately transferred into 6-well cell culture plates with a surface of 9.5 cm² and filled with Standard Medium or D-mannose Treatment Medium.

From each sample were obtained four replicates. The total number was 72 wells for cell culture: 8 from CTL rats (4 females and 4 males), and 10 from HFD rats (5 females and 5 males). The same procedure was applied to organ culture. All the solutions necessary for the experiment were prepared before the animals' sacrifice

Male and female Wistar rats fed with HFD and control diet

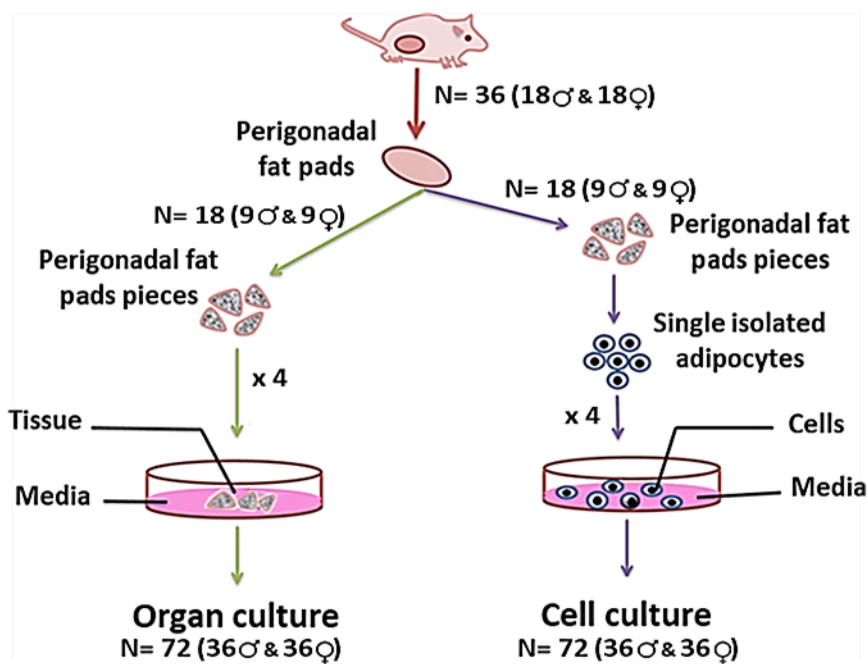


Figure MM6. Illustrative scheme of the tissue preparation process for primary cultures of adult rat adipocytes and adipose tissue. For organ culture, the fragmented perigonadal adipose tissue is grown in an artificial environment (green arrows). For cell culture, adipocytes are enzymatically isolated from the shredded perigonadal adipose tissue and cultured in an artificial environment (purple arrows) ♀, females; ♂, males; N, samples number.

4.2.3. Cell and tissue culture techniques.

4.2.3a. Maintenance of cells and organ crops and D-mannose treatment.

The cultures of adipose cells and tissues were routinely maintained under stable physiologic conditions in the incubator in 6-well cell culture plates with a surface of 9.5 cm² and filled with 1,5 ml of Standard Medium

or D-mannose Treatment Medium. The procedure was the same for samples obtained from both male and female rats. D-mannose treatment was performed on a total number of 18 wells of adipocytes (10 from HFD rats, 8 from CTL rats, 2 replicates per rat) and 18 wells of organ culture fragment (10 from HFD rats, 8 from CTL rats, 2 replicates per rat). After seeding, samples were cultured in 1,5 ml of D-mannose Treatment Medium (Standard Medium supplemented with 25 nM D-mannose; see section 4.4. for solution composition details and D-mannose reference) to investigate if mannose took part in adipocytes and adipose tissue metabolism in our experimental rats. The first replacement culture media was done after 72 h for adipocytes cell culture and after 48 h for adipose tissue fragments culture, simultaneously with the collection and storage of metabolized Standard Medium or Treatment Medium. The cultures' maintenance involved a partial change or replacement of culture medium 2-3 times a week for the following steps of collection and freezing of organ culture fragments and adherent differentiated adipocytes.

4.2.3b. Collection and storage of samples of blank culture medium and culture medium after cell incubation.

Before the culture, aliquots of 1 mL of blank Standard Medium and D-mannose Treatment Medium were collected in Eppendorf, immediately frozen and stored at -80° C until NMR measurement to obtain the “reference” values of analytes contained in the culture media.

After culture, aliquots of 1 mL of cell incubation Standard Medium and D-mannose Treatment Medium were collected from all the wells (after 48 h of culture from adipose tissue wells; after 72 h of culture from adipocytes wells). All cultured medium samples were immediately frozen

and stored in Eppendorf at -80°C until NMR measurement.

4.2.3c. Collection and freezing of organ culture fragments and adherent differentiated adipocytes.

After 9 days from seeding, all fragments of adipose tissue CTL and HFD (treated with D-mannose or not) were collected and stored frozen at -80°C in different ways for further experiments. In detail, in three different ways:

- Included in Tissue-Tek O.C.T. solid matrix on specific holders for further cryosectioning.
- In Eppendorf tubes, immersed in RNeasyTM Solution (AM7020, Invitrogen by Thermo Fisher Scientific, Waltham, Massachusetts, US) for the subsequent RNA extraction.
- In Eppendorf tubes, dried for the following extraction of the proteins.

4.2.4. NMR spectroscopy and metabolic profile of culture media obtained from adipocytes and adipose tissue organ cultures.

The metabolomic approach on culture medium samples followed the same steps and parameters previously described for human serum samples (see section 4.1.3. for details and metabolomic analysis routine summarized in Figure MM1). At the end of this experimental procedure, the metabolomic data obtained were subjected to the same statistical analyses as the human samples (see section 4.3.) for the biological interpretation and the validation of the results obtained on the cohort.

The specific steps for processing the culture media samples obtained from adipocytes and adipose tissue organ culture are explained below.

4.2.4a. Adipocytes and adipose tissues culture media samples preparation for NMR measurement and pre-analytical quality control.

A volume of 480 μL of culture medium was mixed with 20 μL of buffer mix. The tampon mix contained Phosphate buffer solution pH 7.4 (see section 4.4. for buffer composition details) with internal reference to TSP 1.1 mM (final concentration) This buffer was added because pH variations can influence metabolomic spectra in culture medium samples. The final mix (sample + tampon mix) was placed in a 5 mm high-resolution NMR tube for SampleJet. No samples were excluded following the pre-analytical quality control

4.2.4b. Adipocytes and adipose tissues culture media spectra acquisition and processing for calculation of uptake or excretion.

A total number of 144 samples of culture media obtained from adipocytes (72 samples: 8 from CTL rats (4 females and 4 males), and 10 from HFD rats (5 females and 5 males); 4 replicates per rat of which 2 treated with D-mannose) and adipose tissue organ cultures (72 samples: 8 from CTL rats (4 females and 4 males), and 10 from HFD rats (5 females and 5 males); 4 replicates per rat of which 2 treated with D-mannose) were processed individually. Different from the usual metabolite assay in cell lysates, the spectra profiling results of the cell culture medium need to be recalculated. So, blank Standard Medium and D-mannose Treatment

MATERIAL AND METHODS

Medium samples were also measured and processed to obtain the "standard" spectral area values of the analyte component. These were used to obtain the net values of cellular metabolism, accordingly to the target approach [161]. This metabolic profiling approach provided information on 15 well-defined spectral metabolic characteristics (Table MM2).

Table MM2. List of the 15 spectral regions detected in the culture samples in which adipocytes or adipose tissue were grown.

ADIPOCYTES AND ADIPOSE TISSUES CULTURE MEDIUM SAMPLES		
	SPECTRAL REGIONS	ppm
1	Ile/Leu/Val	0,9 - 1,02
2	Methyl-succinate/2-oxobutyrate	1,05 - 1,10
3	3-methyl-2-oxovalerate	1,10 - 1,12
4	Ethanol	1,15 - 1,19
5	Lactate/Threonine	1,31 - 1,33
6	Alanine	1,46 - 1,48
7	Arginine	1,64 - 1,66
8	Acetate	1,905 - 1,915
9	Glutathione	2,10 - 2,15
10	Pyruvate	2,36 - 2,37
11	Glutamine	2,42 - 2,44
12	2-oxo-isocaproate	2,59 - 2,61
13	o-phosphocholine	3,56 - 3,58
14	Methionine/Ile	3,63 - 3,66
15	Lactate	4,08 - 4,12

List of detected spectra regions and chemical shift assignment in the NMR spectra of metabolized culture medium. The resonance's relative position in the NMR spectrum is indicated by its ppm values. Ile, isoleucine; Leu, leucine; Val, valine.

Only the regions of most significant interest were selected for the study. The selection was made based on the main differences between the spectrum profiles of blank and culture media after the incubation of CTL and HFD adipose cell or tissue cultures, by subtracting the area under the metabolite or spectral region curve of the components of the culture medium collected after the incubation from the blank one. To observe the uptake or excretion of the metabolite's derivatives by the cultured adipocytes cells or adipose tissue organ culture, their mean residual

concentrations were further recalculated, considering the individual values of the medium samples from the cells/organ culture medium minus the mean value of the blank medium samples. A parametric method (t-test) was used to check if the concentration of a particular metabolite significantly differed between the investigated groups and a multiple testing adjustment was considered to control false positive results. The final data of uptake or excretion were given in positive values representing excretion and negative for uptake.

4.3. Statistical analysis.

The statistical analysis was developed and conducted at multiple levels with several package software, including R version 3.5.0 with RnBeads package, Genome Studio, MetaboAnalyst 5.0, Matlab R2019b with the PLS Toolbox 8.8 (Eigenvector Research, Inc., Wenatchee, WA, USA), IBM SPSS Statistics 19, and Excel Office 2019. The clinical parameters (physiological and biochemical) and inflammation analysis were checked with different statistical tests including Agglomerative Hierarchical Clustering (AHC), according to the necessity of the groups and the values obtained. R, SPSS and Excel were used to perform these statistical analyses. AHC is a clustering method that aims to build a cluster hierarchy with a “bottom-up” approach, in which we start by inserting each element in a different cluster and proceed then to the gradual unification of clusters two by two to obtain a representative dendrogram of the result [162, 163].

The evaluation of groups' normality was calculated with Shapiro-Wilk and Kolmogorov-Smirnov tests, according to the sample size. Moreover, the evaluation of groups' homogeneity was calculated with the Levene test.

Data groups were presented as the mean \pm standard deviation (SD). All data results from tests were regarded as statistically significant when the p-value < 0.05 .

The differences in measured variables between groups were analysed with the t-Student test or One-way Analysis of Variance (ANOVA) followed by the *post hoc* analysis based on the Bonferroni multiple comparison tests, according to the group analyses. When the groups' distribution was not normal, the non-parametric Kruskal-Wallis test or Mann-Whitney U-test was used.

Multivariate analyses of metabolome and methylation levels were performed with multidimensional scaling (MDS), and its particular case of Principal Component Analysis (PCA), and Partial Least-Squares Discriminant Analysis (PLS-DA) using Matlab R2019b (The MathWorks Inc., Natick, Massachusetts) and R version 3.5.0 [164]. MDS and PCA are unsupervised multivariate analyses for low-dimensional visualization of multivariate data, which optimally conserves the organization of the data. This technique aims to capture common information and summarize it with good approximation into a small number of dimensions or principal components (PCs) orthogonal (independent) between them, each of which expresses a linear combination of the original variables. Hence, MDS is a means of visualizing the level of similarity of individual cases of a dataset and PCA produces a conversion of the variables in a data set into new latent variables. Their purpose is to detect outliers and to evaluate samples' aggrupation spontaneously. PLS-DA is a supervised method of classification, with the discrimination power of discriminant analysis [165], that uses multivariate regression techniques to decide a linear connection between a data matrix (metabolomic and methylation data) and a response matrix (pathological status: case-control). PLS-DA produces a

conversion of the variables in a data set into new latent variables (LVs) and it is commonly used to build a statistical model that adjusts the separation between two or more groups of interest. The main advantage of these multivariate models is allowing the visualization and understanding of different patterns and relations in the data, through the associated scores and loadings.

Receiver operating characteristic (ROC) curve analyses were performed to evaluate the model's accuracy and to discriminate between the case and control groups, and the case subgroups when present. Each point on the ROC curve represents a sensitivity/specificity pair corresponding to a particular decision threshold. ROC is a probability curve and the value of the “area under the curve” (AUC) ROC represents the degree or measure of separability. The higher the AUC, the better the model is [166].

Variable Importance in the Projection (VIP) scores were useful to detect the variables considered relevant for the discrimination between groups. The variables with values $VIP > 1$ were considered good markers of discrimination.

Relative Fold Change measure reflected how much a variable changed in quantity between two measurements, one in the control and one in the case group. The ratio of the changes of every variable has been calculated as (variable mean concentration of case group - variable mean concentration of control group) / variable mean concentration of control group.

ANOVA or multiple t-tests enabled us to carry out the determination of the statistical significance between the metabolites or methylation levels of the different groups.

Bonferroni and False Discovery Rate (FDR) methods were used as an adjustment for the multiplicity of tests often necessary to restrict the total number of false discoveries. FDR, formally described by Benjamini and

Hochberg in 1995, is a statistical approach used in multiple hypothesis testing to correct for multiple comparisons. It is generally used in high-throughput experiments to correct for random events that falsely appear significant. The FDR must correspond to a maximum of 10 %. This correction reduces the probability of incurring a first-type error without losing small, potentially significant differences between cases and controls. Logistic Regression is a specific case of a generalized linear model (glm) having the logit function as a link function. This is a regression model applied in cases in which the dependent variable y is of a dichotomous type (es case-control) attributable to the values 0 and 1.

Correlation Heatmaps were used to study pattern discovery and pattern recognition, to visualize in a graphical form the data association representation of different variables.

Finally, Logistic Regression Analysis and multivariable analyses based on multiple t-tests were applied, using R and SPSS, to visualize the changes in the general variables related to case-control status under the influence of sex and age among different groups.

4.3.1. Analysis of phenotypic variables.

To characterize the study population through phenotypic variables (clinical, biometric and anthropometrics, demographic and lifestyle characteristics, and lymphocyte subpopulations) these were analysed individually for cases and controls. In particular, the mean and SD were calculated for the continuous variables while the percentage of subjects showing the phenotype of interest was calculated for the dichotomous variables. A non-parametric hypothesis was applied to test the hypothesis that two samples were drawn from the same distribution. This allowed us

to evaluate whether the observed differences between case and control groups were compatible with the null hypothesis H_0 (difference due to chance) or whether the observed difference was real. Once the statistical test was applied, a p-value < 0.05 indicated the significance of the result, with the consequent rejection of the null hypothesis. The Wilcoxon test and the Fisher test were used for variables with continuous distribution and dichotomous variables, respectively. Then, two clustering techniques were used to group the subjects under study according to similar relations between individual subjects and between case/control groups:

- Agglomerative hierarchical clustering (AHC): The metric distance of the samples was evaluated using Average-Linkage for the case/control status and the clinical and phenotypic variables related. It is used to check the presence or absence of clustering due to these factors, i.e. to verify whether one or more variables could be responsible for a clear distinction between the two investigated groups from an epigenetic point of view.
- Analysis of the main components and analysis of the multiple correspondences (MDS and PCA): considering the number of phenotypic traits analysed and the presence of collinearity, MDS, and its particular case PCA, are used to reduce the complexity of the variables analysed. The data examined were: weight, height, age and sex, WHR, WC, BMI, hypertension, hypertriglyceridemia, hyperglycaemia, DM2 and thyroid problems, etc. To obtain a better classification of the samples, anthropometric and clinical variables were complemented with the estimation of white blood cell proportions (CD8.naive, CD4.naive, CD8T, CD4T, NK, Bcell, Monocytes, Granulocytes, Plasmablasts) obtained using Horvath's DNA-methylation-based online calculator (see section 4.1.4d).

4.3.2. Metabolomics statistical analysis.

Metabolite levels obtained from the NMR spectra raw (untransformed) data, computed and normalized to the SD in all the samples to obtain z-scores (see section 4.3.1.), were used for the following statistical analysis.

4.3.2a. NMR data processing and multivariate analysis.

Chemometric statistical analyses were developed using in-house Matlab scripts, the PLS Toolbox 8.8, R and MetaboAnalyst, and the statistical associations were adjusted for relevant variables and potential covariates. The categorical variables were analysed by percentages. The analysis routine included previous mean-centring and auto-scaling of the data. PLS-DAs were applied to the NMR metabolomic vectors of each sample. The results of the cross-validation were evaluated by the RMSECV, R² and the AUC; FDR filtered the endpoint predictive biomarkers. Permutation tests were used for evaluating the significance of the models. All calculated models were significant at the 95 % confidence level. The accomplishments of PLS-DA analyses were useful to visualize the metabolic variations between groups in a multivariate analysis, showing the group classification and the main metabolites involved. The analyses were performed separately for human serum and rat adipocytes and adipose tissues culture media samples. In detail:

Human serum samples data: the purpose of PLS-DA models was to identify class, age and sex differences from a multivariate dataset where each class was referred to as a specific MetS component number group. Results were cross-validated by performing a 10-fold Venetian blind technical replication to evaluate the accuracy of each classification model.

Then, VIP scores and respective Relative Fold Changes between MetS and its subclass MetS.5, and MHO were calculated for each variable (metabolite). These values specify the impact of each variable on the group classification (see section 4.3 for details). *Post hoc* multivariable analyses based on multiple t-tests corrected by the Bonferroni method were performed to estimate the statistically significant differences between case-control status and the extreme case MetS.5 and age categories based on the main metabolites acquired from VIP scores. A chi-squared was used for relative and comparative proportions. Finally, the same analysis method was adopted to determine the statistical significance of means differences between MetS.5 cases and control groups in the women and men groups, separately. The significance levels were (*) $p < 0.05$; (**) $p < 0.01$; (***) $p < 0.001$. Corresponding adjusted p-values (Student's t-test corrected by Bonferroni method) were (*) $p < 0.00091$; (**) $p < 0.00018$; (***) $p < 0.000018$.

Cell culture media of rat adipocytes or adipose tissue growth: PLS-DA models were done to identify HFD- and sex-induced metabolomic differences. A cross-validation model was applied as quality control to validate the experimental procedure and protocol and evaluate the correspondence between experimental data and metabolomic profiles. Then, VIP scores and respective Relative Fold Changes between HFDs and controls were calculated for each variable (metabolite). *Post hoc* multivariable analyses based on multiple t-tests corrected by the Bonferroni method were performed to estimate the statistically significant differences between case-control status for all the animals and for female and male groups separately based on VIP scores. A chi-squared test was used for relative and comparative proportions. The significance levels were (*) $p < 0.05$; (**) $p < 0.01$; (***) $p < 0.001$. Corresponding adjusted p-

values (Student's t-test corrected by Bonferroni method) were (*) $p < 0.003$; (**) $p < 0.00067$; (***) $p < 0.000067$.

4.3.2b. Metabolites pathways enrichment analysis.

Pathway analysis helps to understand which biological pathways, representing collections of molecules performing a particular function, may be involved in response to MetS. The construction, interaction, and pathway analyses of metabolic networks that involved selected metabolites (VIP score > 1) were performed with MetaboAnalyst 5.0 [167] and Cytoscape [168]. The result of the Metabolomic Pathway Analysis (MetPA) and Pathway Topology Analysis based on the Kyoto Encyclopedia of Genes and Genomes (KEGG) database (<http://www.genome.jp/kegg/>) were properly validated using standard validation protocols. The KEGG database helped to identify pathways that were the most significantly altered.

4.3.3. Epigenetics statistical analysis.

The proper detection and processing of specific probes within promoters, genes, CpG islands and tiling (regions of 5,000 base pairs consecutively selected along the genome) through the EWAS procedure (see section 4.3.2.) allowed obtaining the data for statistical analysis of the differences in methylation.

4.3.3a. Logistic regression analysis.

To evaluate a correlation between epigenetic and phenotypic differences characterizing MetS status, multivariate regression was

performed using the previously calculated phenotypic dimensions (PCs) as independent variables x (or predictors). The phenotypic dimensions that were significantly associated with the case/control status were then used as covariates in the differential analysis of methylation levels. The last was particularly suitable because one of the assumptions of this type of analysis is that the predictive variables must be linearly independent, i.e. it must not be possible to express any predictor as a linear combination of the others. The PCs fully satisfy this assumption. The `glm` or the `"wilcox.test"` function provided in the R `"class"` package was used to evaluate the differences in variables between cases and controls. The evaluation of groups' normality was calculated with the Shapiro-Wilk test according to the sample size.

4.3.3b. Analysis of the epigenetic differences between MHO and MetS.5 subgroups of subjects over 54 years.

An average methylation value and a relative SD were generated for each locus analysed (~ 850,000). The exploratory analysis of the raw data allowed us to avoid potential confounding factors (e.g. age, sex, cellular composition and lot). Using MDS and correlation analysis, the associations of these factors with dependent (degree of disease severity) and independent (methylation values) variables were evaluated; the associations were then used as covariates in the differential methylation module. Differential methylation analyses were conducted based on the paired sample groups both at the site level, with the calculation of p-values by the `limma` method, and at the level of predefined regions (genes, promoters, CpG island, tiling), where a combined p-value was calculated from the p-values of the individual sites. Finally, an evaluation of the differential methylation between the group of cases and controls was

carried out; the values obtained were corrected using the FDR approach and the respective q-values were produced (analysis conducted using the RnBeads package in R), considered significant for values $p < 0.05$.

4.3.3c. Prioritization analysis and gene ontology.

Gene ontology (GO) enrichment analysis was performed to identify significantly enriched or depleted classes of genes or proteins. All data resulting from tests were regarded as statistically significant when the p-value < 0.05 unless otherwise indicated. Firstly, we linked the huge differentially methylated gene lists to biological functions using RnBeads (GOstats) [169], an algorithm based on a hypergeometric test that uses the hierarchical structure relationships among GO terms. This allows for recovering the functional profile of that set of genes, understanding the underlying biological processes better and identifying a possible association with the pathological event. Once the differently methylated between case and control groups were selected, they were prioritized using the online tool Phenolyzer (phenotype-based gene analyzer) which uses input phenotype description terms to prioritize complex disease genes according to the combined rank score until reaching the cut-off established with the previously described method. The genes that passed this further selection were used for the GO analysis using DAVID [170] and summarised, clusterized as tree maps and classified into macro-categories using the ReviGO (Reduce + Visualize Gene Ontology) tool [171]. The tree maps contained significant GO terms based on the methylation scores for the combined rank among the 100 best-ranking sites based on variance across samples. To understand the cellular processes involved in the MetS condition and its consequences groups of genes linked and correlated with

each other in certain biological pathways were therefore searched. As a biological pathway reproduces the biological relationships between the macromolecules of a cell, the KEGG database, which contains the pathways of genes with known regulatory and metabolic functions, was used to deepen their knowledge.

4.4. Solutions composition.

Cell and Organ culture:

- Phosphate buffer: 1X PBS (Sigma-Aldrich, St.Louis, MO, USA), containing 137 mM NaCl, 2.7 mM KCl, 10 mM Na₂HPO₄, and 1.8 mM KH₂PO₄.
- Wash buffer: PBS (Sigma-Aldrich, St.Louis, MO, USA), supplemented with 1% Bovine serum albumin (BSA).
- Digestion buffer: Wash buffer containing Collagenase type II (Sigma-Aldrich, St.Louis, MO, USA), 1 mM final concentration.
- Standard Medium: DMEM 1X (4,5 g/L D-Glucose, L-Glutamine, 25 mM HEPES; Gibco by life technology) supplemented with all the substances necessary for mature adipocyte cell growth and maintenance. Specifically: 5 % Fetal bovine serum (FBS), 2,5 µg/ml of Amphotericin-B and antibiotics Penicillin / Streptomycin at concentrations 100 U/ml and 100 µg/ml respectively, 50 nM of Adenosine (it seems to help cells to survive longer, break less, and release fewer lipids into the medium (Fried, S.K.)).
- D-mannose solution: D-mannose powder (3458-28-4, TCI Europe NV) in Standard Medium, concentration 1 M. Sterilized by filtration with 0,22 µm membrane filter.

MATERIAL AND METHODS

- D-mannose Treatment Medium: Standard Medium supplemented with D-mannose solution at a final concentration of 25 mM.

NMR sample preparation:

- Phosphate buffer solution pH 7,4: sodium hydrogen phosphate ((NaH_2PO_4) • H_2O (1,5 M)), potassium dihydrogen phosphate (K_2HPO_4 (1,5 M)), 27,47 mM TSP, 10 % of D_2O .



5. RESULTS

5.1. Characterization of MetS in clinically severe obesity.

5.1.1. Anthropometric characterization of the Piancavallo cohort and analysis of MetS prevalence.

Our study population included 1350 individuals. All of them had extreme obesity: BMI ≥ 40 kg/m², WC ≥ 80 cm in women and ≥ 94 cm in men, and moderate to high WHR. The cohort was composed of 65.5 % of women and 34.5 % of men with ages between 19 and 85 years. The mean age was 53 ± 14 years with a significantly higher mean for females (55 ± 13 years) and lower in men (50 ± 14 years). The anthropometric parameters of weight, WC, WHR and DBP also showed statistically significant differences between men and women. As expected, body composition (FM, FFM and correlated parameters) and RRE parameters significantly differed statistically. Finally, clinical biochemistry also indicated sexual dimorphism in cholesterol, triglycerides, and insulin metabolisms (Table R1).

RESULTS

Table R1. Anthropometric characteristics of the Piancavallo cohort in total and separated by sex.

Variables	All cohort (n = 1350)	Males (n = 465)	Females (n = 885)	P- value
Age (years)	53 ± 14	50 ± 14	55 ± 13	***
Height (cm)	162,5 ± 10,5	173 ± 7,7	157,1 ± 7,1	***
Weight (kg)	126,5 ± 23,9	142,9 ± 24,1	118 ± 18,7	***
BMI (kg/m²)	47,7 ± 6,54	47,63 ± 6,6	47,7 ± 6,5	
WC (cm)	133,3 ± 14,6	142,8 ± 13,1	128,3 ± 12,7	***
Hip Circ (cm)	140,7 ± 14,4	139,3 ± 15,5	141,4 ± 13,8	
WHR (cm/cm)	0,95 ± 0,1	1,03 ± 0,07	0,91 ± 0,08	***
SBP (mm Hg)	139 ± 18	141 ± 17	137 ± 18	
DBP (mm Hg)	83 ± 9	84 ± 9	82 ± 9	***
SatO₂	93,5 ± 2,8	93,2 ± 2,5	93,7 ± 3	
HOMA-IR	4,4 ± 3,3	4,9 ± 2,9	4,1 ± 3,4	
s-Glucose (mg/dL)	112,3 ± 35,7	112,9 ± 34	112 ± 36,6	
s-LDL Chol (mg/dL)	120,2 ± 34,9	119,5 ± 35,9	120,5 ± 34,3	
s-HDL Chol (mg/dL)	42,7 ± 12,4	36,9 ± 9,7	45,7 ± 12,6	***
s-TGL (mg/dL)	144,1 ± 62,1	157 ± 60,9	137,3 ± 61,7	***
s-Insulin (mU/L)	15,8 ± 9,4	17,9 ± 9	14,6 ± 9,4	***
cc_H₂O tot	39,1 ± 15,7	43,6 ± 4,4	36,8 ± 18,8	***
cc_FM	49,5 ± 19,8	41,52 ± 5,7	53,7 ± 23	***
cc_FFM	51,6 ± 18,1	58,21 ± 6	48,2 ± 21,1	***
cc_muscular mass	29,6 ± 11,5	33,6 ± 6,5	27,59 ± 12,9	***
Basal metabolic rate	1995,8 ± 460,2	2376,7 ± 439,6	1777,4 ± 302,6	***
REE x day	2074,9 ± 457,1	2540,6 ± 395,5	1807,6 ± 207,8	***
REE %	96,5 ± 11,1	93,7 ± 10,7	98,2 ± 11,1	***

*Comparison and analysis to assess MetS in people who suffer from severe obesity. Numbers data are reported as means ± SD. p-values are given for the difference in values between the sexes: (***) p < 0.001. Abbreviations: BMI, body mass index; WC, waist circumference, WHR, waist-to-hip ratio; SBP, systolic blood pressure; DBP, diastolic blood pressure; SatO₂, oxygen saturation; HOMA-IR, homeostasis model of assessment for insulin resistance; s-, serum; TGL, triglyceride; cc-, calorimetric calculation; FM, fat mass; FFM, fat-free mass; REE, resting energy expenditure.*

5.1.1a. Comparison of the anthropometric measures used to assess weight-related risk between MHO and MetS subjects by sex and age ranges.

WC and WHR indicated a strong relationship between fat tissue and its distribution and MUHO related to MetS. WC and WHR were raised in the MUHO group, showing higher significance in the Total population and the Women subgroup, regardless of age. Whereas maintained its statistical significance in young Men until 45 years old but not in the elderly subgroup over 54 years old. On the contrary, BMI lacked significance or appeared only slightly related to MUHO in both men and women (Table R2).

5.1.1b. Comparison of metabolic characteristics.

The anthropometric and clinical characterization of our cohort showed a prevalence of MetS of 80.5 % (Table R3). We also analysed the prevalence of MetS.5 to explore extreme effects and better differentiate between MHO and the disease of obesity in the context of extreme BMI. MetS.5 was observed in 23.6 % of the entire cohort with an increasing prevalence with age in both women and men. The analysis of the different components of MetS was stratified by sex and age. This, along with the prevalence of MetS.5 and MHO, demonstrated a higher prevalence of MetS after 54 years in both sexes. However, the increase in prevalence with age was much sharper in women, whereas it was almost neglectable in men. This increase in the prevalence of MetS after the age of 54 was parallel to changes in anthropometric parameters such as WC, WHR, and BMI (Table R2).

Table R2. Characterization of the Piancavallo cohort by anthropometric measures for weight-related risk prediction.

Anthropometric Measures (mean \pm SD)	Total			Women			Men			
	MHO	MetS.5	p-value	MHO	MetS.5	p-value	MHO	MetS.5	p-value	
WC (cm)	all ages	128,9 \pm 15,3	137,1 \pm 18,9	1,4E-15***	123,7 \pm 11,4	132,1 \pm 11,5	7,6E-11***	144 \pm 15,4	144,4 \pm 13,8	0,87
	range 19-45 y	130,9 \pm 18,1	143,8 \pm 14,1	4,1E-05***	122,9 \pm 13,9	137,5 \pm 13,5	4,5E-04***	145 \pm 16,1	146,8 \pm 13,6	0,63
	range 55-85 y	127,3 \pm 11,4	134,1 \pm 12,3	8,6E-06***	124,7 \pm 10,2	131,1 \pm 1,2	2,7E-05***	139,9 \pm 12,4	141 \pm 13,1	0,56
WHR	all ages	0,92 \pm 0,1	0,98 \pm 0,1	1,4E-15***	0,89 \pm 0,1	0,94 \pm 0,1	9,4E-12***	1 \pm 0,1	1,04 \pm 0,1	0,0022**
	range 19-45 y	0,92 \pm 0,1	1,02 \pm 0,1	8,9E-08***	0,88 \pm 0,1	0,92 \pm 0	0,0231*	1 \pm 0,1	1,06 \pm 0,1	0,0015**
	range 55-85 y	0,92 \pm 0,1	0,97 \pm 0,1	6,6E-08***	0,9 \pm 0,1	0,94 \pm 0,1	8,7E-06***	1 \pm 0,1	1,03 \pm 0,1	0,087
BMI (kg/m ²)	all ages	47 \pm 6,2	48,1 \pm 6,5	0,036*	46,5 \pm 5,6	48,4 \pm 6,5	0,0038**	48,4 \pm 7,4	47,8 \pm 6,5	0,59
	range 19-45 y	47,9 \pm 7,3	50,4 \pm 6,8	0,054	46,6 \pm 6,5	51,7 \pm 7,2	0,010*	50,1 \pm 8	49,7 \pm 6,5	0,83
	range 55-85 y	45,6 \pm 4,6	46,7 \pm 5,9	0,086	46 \pm 4,8	47,6 \pm 5,7	0,025*	44,8 \pm 5,4	45,7 \pm 6,3	0,56

Comparison of anthropometric measures for weight-related risk prediction between MHO and MUHO subjects of all ages and in the 2 age groups (range 19–45 y and range 55–85 y) in the Total (entire cohort) and subsets of Women and Men. Mean values and SD of WC, WHR and BMI were calculated for each group. t-tests were used to test the significance of the differences in subjects MHO and MUHO in different sexes and age ranges. Significance: (*) p < 0.05, (**) p < 0.01, (***) p < 0.001. Abbreviations: = MHO, metabolically healthy obese status; MUHO, metabolically unhealthy obese status; BMI, Body mass index; range 19-45 y, fertile age; range 55-85 y, postmenopausal status.

A percentage of 69.4 % of women in the younger group (18–45 y) and 79.6 % of women in the older group (55–85 y) displayed MetS, corresponding to an odds ratio of 1.72. Men belonging to the same

ages displayed MetS with a prevalence of 79.6 % and 89.7 %, respectively, with an odds ratio of 2.22. Conversely, focusing on MetS.5 was possible to appreciate a difference more related to sex than to age. Whereas in men the prevalence of MetS.5 was similar in both age groups with values around 25 %, in women, the older age group showed more than double the prevalence of the younger age group, rising from 11 % to 23.2 % (Table R3).

The analysis of individual metabolic components also showed changes in their contribution to the MetS pathological state strongly related to sex and age ranges. In detail, the percentage of individuals with hypertension and hyperglycemia and/or DM2 changed significantly between age groups. These differences also proved to be statistically relevant when comparing men and women. The percentage of individuals with low HDL was significantly different by age but its prevalence was comparable in both sexes. On the contrary, hypertriglyceridemia percentage did not change relevantly between the two age ranges, but it did change notably with sex, indicating a strong influence of sex but not of age on the prevalence of this metabolic component (Table R3). Notably, older women showed an increasing tendency to have raised SBP and/or DBP compared with women in the younger age group; instead, the percentage of men with hypertension was high and stable for both ages. Interestingly, the prevalence of low HDL parameters decreases with age in both sexes, showing differences strongly related to sex and age ranges in their contribution to the MetS pathological state.

Table R3. *Cardiometabolic characterization and composition of the Piacavallo cohort.*

Piacavallo cohort composition n(%)	Total				Women				Men				p-value Women VS Men (by age ranges)	
	all ages	range 19-45 y	range 55-85 y	p-value age ranges	all ages	range 19-45 y	range 55-85 y	all ages	range 19-45 y	range 55-85 y	all ages	range 19-45 y		range 55-85 y
		1350	363 (26,9%)			723 (53,6%)	196 (22,1%)		520 (58,8%)	465 (34,8%)		167 (35,9%)		203 (43,7%)
Metabolic Profile	MHO (control)	264 (19,5%)	94 (25,9%)	127 (17,6%)		196 (22,1%)	60 (30,6%)	68 (14,6%)	34 (20,6%)	21 (10,3%)		167 (35,9%)	182 (89,7%)	
	Mets (case)	1086 (80,5%)	269 (74,1%)	596 (82,4%)		689 (77,8%)	136 (69,4%)	397 (85,4%)	133 (79,6%)	182 (89,7%)		133 (79,6%)	182 (89,7%)	
	Mets.5 (extreme Mets)	256 (23,6%)	46 (17,1%)	144 (24,2%)		153 (22,2%)	15 (11%)	103 (25,9%)	31 (23,3%)	48 (26,4%)		31 (23,3%)	48 (26,4%)	
Metabolic Components	Hypertension	1100 (81,5%)	267 (73,6%)	611 (84,5%)	5,8E-07***	698 (78,9%)	124 (63,5%)	402 (86,5%)	143 (85,6%)	177 (87,2%)	3,4E-05***	143 (85,6%)	177 (87,2%)	
	Hyperglycemia / DM2	804 (59,6%)	134 (36,9%)	496 (68,6%)	2,2E-16***	517 (58,4%)	67 (34,2%)	287 (61,7%)	67 (40,1%)	153 (75,4%)	0,01*	67 (40,1%)	153 (75,4%)	
	Low-HDL	905 (67%)	275 (75,6%)	452 (62,5%)	9,1E-06***	601 (67,9%)	153 (78,1%)	304 (65,4%)	122 (73%)	123 (60,6%)	0,27	122 (73%)	123 (60,6%)	
	Hypertriglyceridemia	522 (38,7%)	140 (38,6%)	264 (36,5%)	0,97	308 (34,8%)	62 (31,6%)	214 (46%)	78 (46,7%)	92 (45,3%)	3,1E-05***	78 (46,7%)	92 (45,3%)	

Cohort comparison of metabolic characteristics (profile and components) in the Total (entire cohort), and in subsets of Women and Men patients. In Total numbers are shown with the respective % of subjects of all ages and in the 2 age groups (range 19-45 y and range 55-85 y). The same representation is shown in subsets based on sex (Women and Men). By the same cohort stratification, the number and respective % of subjects MHO, Mets and its subset Mets.5 and the number and respective % of subjects affected by each metabolic component are shown in all ages and specific age ranges. The % of each subset Mets.5 were calculated about the corresponding Mets group. Mantel-Haenszel tests were used to test the differences in % of subjects affected by metabolic components: between age ranges net of sex (p-value age ranges), between men and women adjusted for age ranges (p-value Women VS Men (by age ranges)). As an example: % of subjects who present hypertriglyceridemia does not change significantly between the 2 age ranges but it changes significantly with sex, indicating a strong influence of sex but not of age for this metabolic component (underlined values). Significance: (**p* < 0.05, (***) *p* < 0.001. Abbreviations: = MHO, metabolically healthy obese status; Mets, metabolically syndrome status; Mets.5, a subset of Mets status which presents all 5 Mets components; range 19-45 y, fertile age; range 55-85 y, postmenopausal status; VS, versus.

5.1.2. Metabolomics characterization of MetS in severe obesity: general view of metabolic profile in Piancavallo cohort.

Exploratory PLS-DA analyses between MHO and MetS in the entire Piancavallo cohort of 1350 subjects revealed that the global metabolic profiles differed in healthy and pathological conditions in the entire population (Figure R1 A). Moreover, combined criteria of VIP scores and Relative Fold Change in the entire population (Figure R1 B) identified differential profiles that contrasted in variety and number of significant metabolites (VIP scores values ≥ 1). As shown, choline-containing compounds (CCC) constituted the metabolite most significantly associated with MetS in the entire population. Whereas, mannose with glycogen fragments showed the highest fold change value, resulting in the metabolite whose concentration changes more between MHO and MetS.

The significant metabolites were analysed using MetPA in MetaboAnalyst (Figure R2) to counteract the problem of multiple comparisons due to large-scale data analysis and to obtain information about the metabolic mechanism of MetS. Eight metabolic pathways were statistically significant for the 16 metabolites that differentiate MetS from MHO, including alanine, aspartate and glutamate metabolism; pyruvate metabolism; glycolysis/gluconeogenesis; cysteine and methionine metabolism; glycerolipid metabolism; fatty acid degradation; biotin metabolism; glycerophospholipid metabolism.

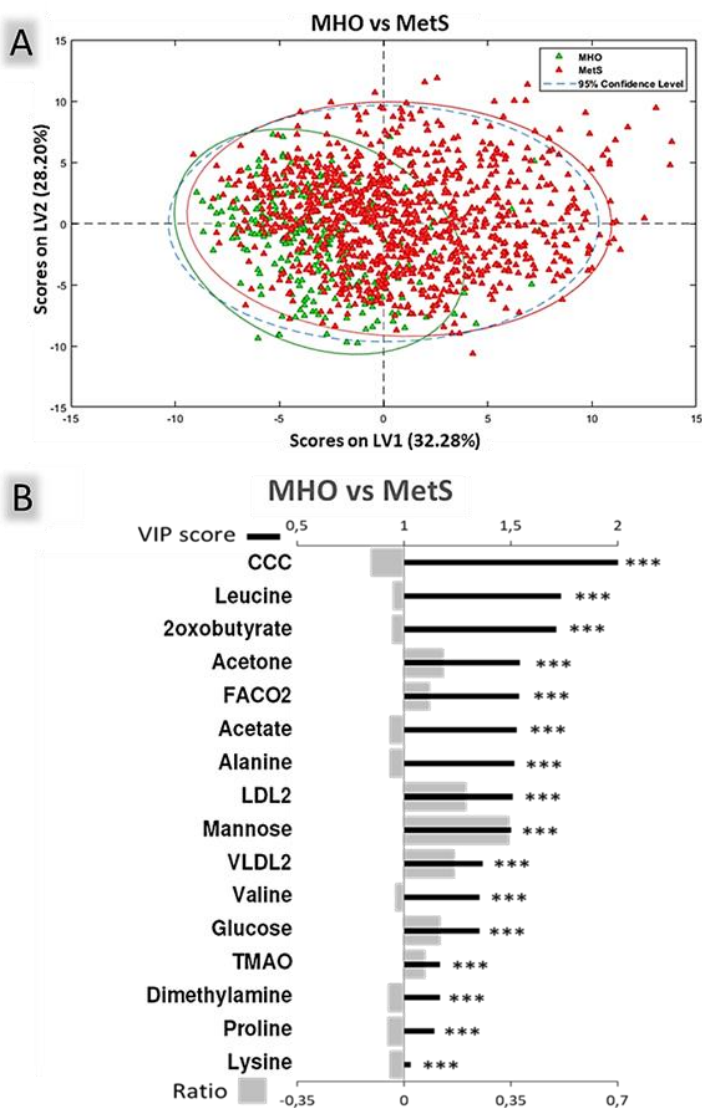


Figure R1. PLS-DA model for discrimination between MHO and MetS. The model was built using 2 LVs. Cross-validation parameters: RMSECV: 0.365, R2CV: 0.155; ROC Curve AUC: 0.82. (A) The score plot shows MetS samples in red and MHO samples in green with a 95% confidence ellipse in the same colours. (B) VIP score and Relative Fold Change bar plots show the metabolites with $VIP \geq 1$ as black thick lines (scale on the top) and Relative Fold Change values represented by grey bars (scale on the bottom). Significant alterations are indicated by *. Adjusted *p*-values (Student's *t*-test corrected by Bonferroni method) to 0.000018 (***).

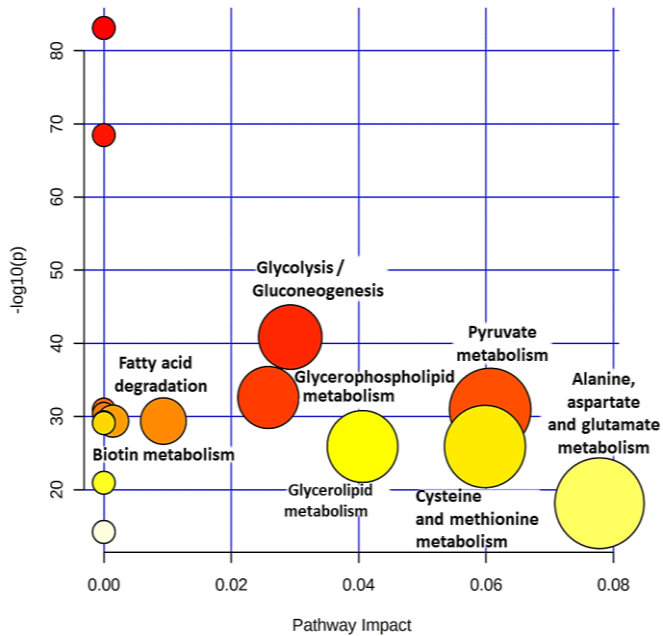


Figure R2. Metabolic pathways altered in MetS. In the scatterplot, the x-axis indicates the impact on the route, while the y-axis indicates significant changes to a route. The pathways are represented as circles: the colour indicates the significance level, from highest (red) to lowest (white) in MetPA; the size is proportional to the impact value of each road from the topology analysis. Metabolic pathways whose name is indicated are significant (p -value < 0.05 after the adjustment using the Holm-Bonferroni method and FDR) and have a pathway impact value over 0.

After the global comparison between MHO and MUHO, as patients affected by MetS, we focused our attention on a deeper characterisation of MetS based on the clinical severity of MetS. The aim was to study the effects of the rising number of MetS criteria from 3 to 5 on the metabolic profile of patients. A cross-validation model was applied to validate the classification model and evaluate the correspondence between clinical data and metabolomic profiles as shown in Figure R3. The results showed a better fit of the model for MHO (RMSECV: 0.366, R2CV: 0.150; ROC Curve AUC: 0.81) and MetS.5 (RMSECV: 0.339, R2CV: 0.258; ROC Curve AUC: 0.87) subgroups. This corresponds to a better ability in the

RESULTS

metabolomic characterization of the two clinical extreme conditions if compared to the intermediate conditions, represented by MetS.3 (RMSECV: 0.446, R2CV: 0.065; ROC Curve AUC: 0.66) and MetS.4 (RMSECV: 0.456, R2CV: 0.025; ROC Curve AUC: 0.63) subgroups.

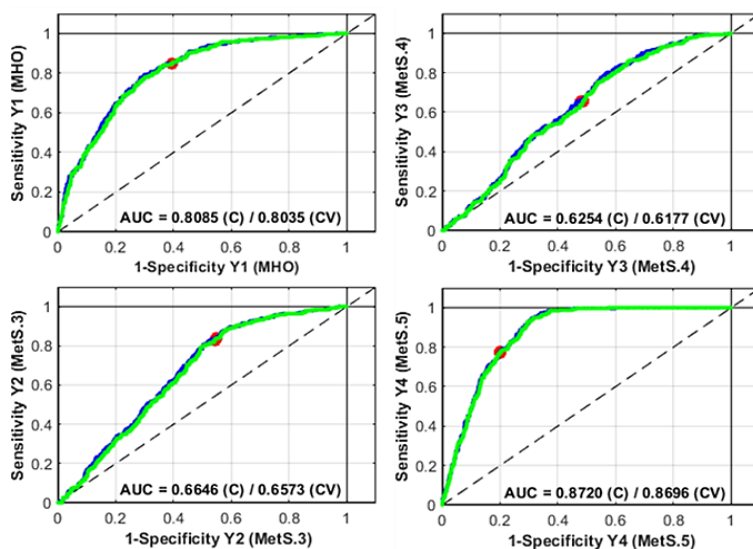


Figure R3. Cross-validation analysis of the PLS-DA model including the control subgroup (MHO) and the three pathological subgroups (Mets.3, MetS.4 and MetS.5). Estimated and cross-validated ROC are represented by blue and green lines, respectively. The value of AUC is indicated for each subgroup.

The results of the PLS-DA (Figure R4) between the control subgroup (MHO) and the three pathological subgroups (Mets.3, MetS.4 and MetS.5) showed the distribution of MHO, MetS.3, MetS.4 and MetS.5 in order along the LV1, which summarizes the highest percentage of variability. This indicated a progressive and constant change in the metabolic profile from the MHO condition to the extreme pathological case. This evidence seemed to be confirmed by the representation of the 26 metabolites with correlation scores (VIP scores) higher than 1, of which

LDL2 was the metabolite with a higher VIP score value in MetS (Figure R5 A). The mean intensities of all of them followed a progression from higher to lower or lower to higher with the same order MHO, MetS.3, MetS.4 and MetS.5 (Metaboanalyst, Figure R5 B). Concretely, the general tendency pushed to a reduction of most of the 26 metabolites from MHO to MetS.5. Only 5 of them (LDL2, acetone, carbonyls in fatty acids 2 (FACO2), very-low-density lipoprotein 2 (VLDL2) and mannose + glycogen fragments) showed the opposite trend. Interestingly, the metabolites appearing in the plot included all the metabolites that described the MetS in the general picture except glucose and TMAO which did not show a statistical significance in the subgroups' characterization.

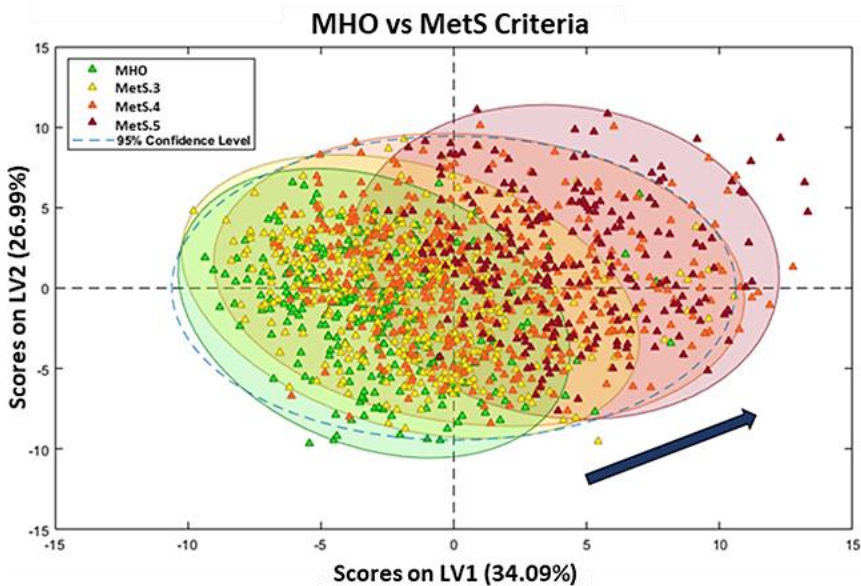


Figure R4. PLS-DA model for discrimination between MHO and MetS criteria subgroups. The model of discrimination and comparison between the group control MHO and the 3 MetS subgroups in metabolic terms was built using 2 LVs on MHO and MetS.5 groups and including the other two groups as projection. The score plot shows MHO samples in green, MetS.3 samples in yellow, MetS.5 samples in orange and MetS.5 samples in dark red with 95a % confidence ellipse in the same colours.

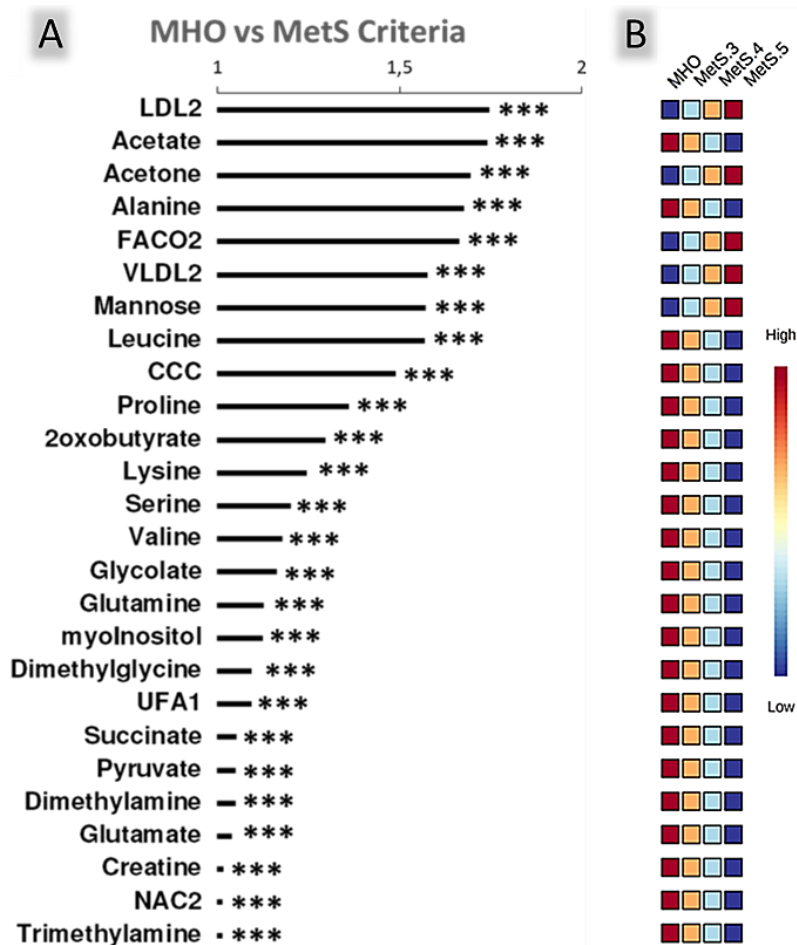


Figure R5. Significant metabolites in PLS-DA model for discrimination between MHO and MetS criteria subgroups. Representation of metabolites based on VIP scores (A) and correlation scores intensity (B) resulting from PLS-DA for the MHO group and all MetS groups (3, 4 and 5 parameters). The coloured boxes show the mean intensity of the variable in the respective group after the comparison with the other three groups. Blue and red boxes indicate metabolite levels that are lower or higher, respectively, between the four groups, whereas orange and light blue indicate intermediary levels. Significant alterations are indicated by *. Adjusted p-values (one-way ANOVA by using Fisher's Least Significant Difference (LSD) test method) to 0.000018 (***).

5.2. Piancavallo cohort metabolomic analysis: focus on MetS extreme case.

Based on the results obtained from the metabolomic characterization of the MetS by groups, it would seem that MetS.3 and MetS.4 can be considered intermediate and probably temporary situations leading to MetS.5. By the evidence that MetS.5 represents the worst clinical picture of MUHO patients and based on the results obtained from the metabolomic characterization of the MetS for groups and the relative quality control of the study model, we decided to focus our attention on the extreme conditions of MHO and MetS.5 for a better characterization of both conditions. PLS-DA analyses emphasised the specific global metabolic profile changes in MetS.5, most of them already predicted by the analysis by subgroups (Figure R6). The VIP score plot appeared similar to that obtained from the analysis of MetS criteria in the number of significant metabolites with slight changes in the order of statistical importance of the metabolite, indicating that the MetS.5 condition was already prevalently represented (Figure R7). In detail, MetS.5 showed a rise in FACO₂ signal, which became, with LDL2 in the first position, the second most significant metabolite. Acetone and acetate followed them, remaining among the most involved components. Interestingly, the CCC climbed up in order, returning to the top positions. As expected, also the Relative Fold Change value of each metabolite remained similar, indicating a shared metabolic trait of MetS. Among them, the mannose joint with glycogen fragments maintains the highest value, resulting in the metabolite whose concentration changes more between MHO and MetS extreme case.

The significant metabolites were analysed using MetPA (MetaboAnalyst, Figure R8) to counteract the problem of multiple

RESULTS

comparisons due to large-scale data analysis and to obtain information about the metabolic mechanism of the extreme MetS.

Thirteen metabolic pathways were statistically significant for the 26 MetS.5 metabolites, including alanine, aspartate and glutamate metabolism; pyruvate metabolism; glycolysis/gluconeogenesis; cysteine and methionine metabolism; glycerolipid metabolism; fatty acid degradation; biotin metabolism; glycerophospholipid metabolism; glycine, serine and threonine metabolism; inositol phosphate metabolism; aminoacyl-tRNA biosynthesis; arginine and proline metabolism and citrate cycle (TCA cycle).

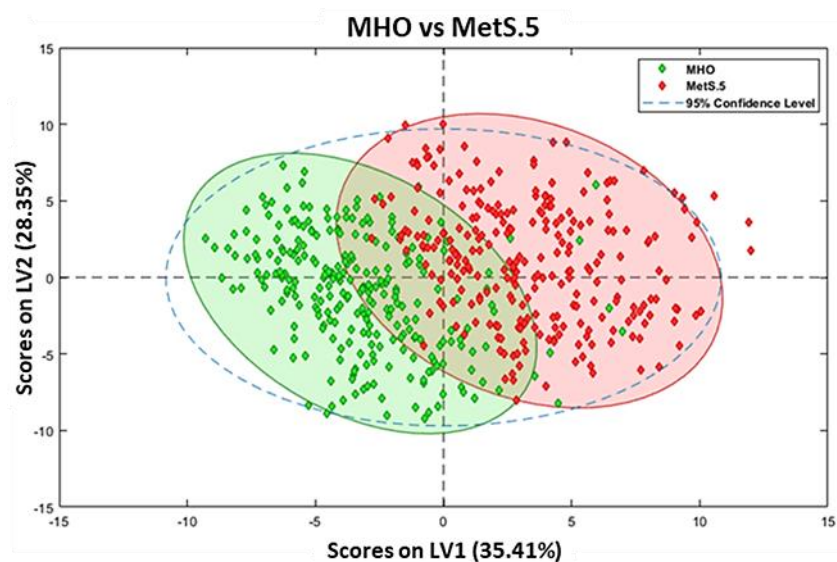


Figure R6. PLS-DA model for discrimination between MetS.5 and MHO. The model was built using 2 LVs. The score plot shows MetS.5 samples in red and MHO samples in green with a 95% confidence ellipse in the same colours. Cross-validation parameters: RMSECV 0.305, R2CV: 0.628; ROC Curve AUC: 0.97.

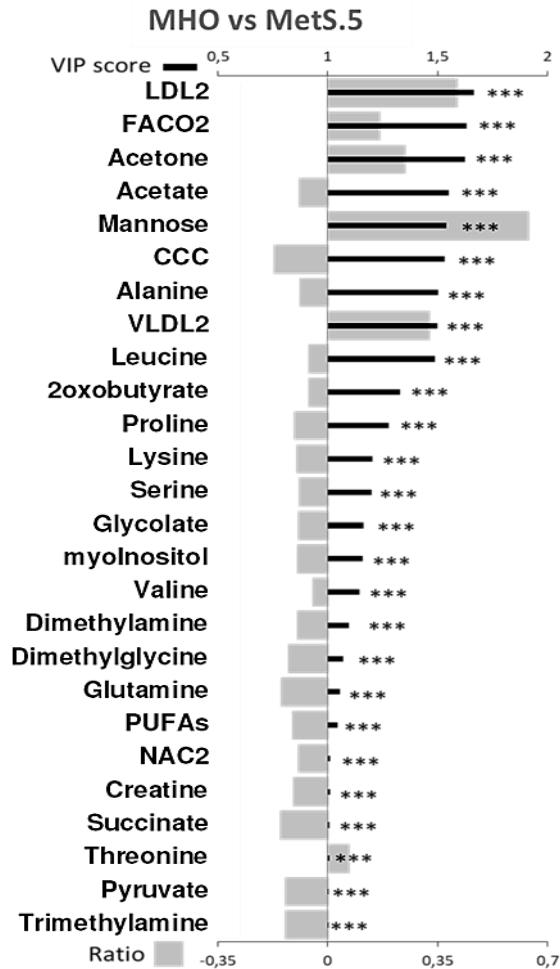


Figure R7. Significant metabolites in PLS-DA model for discrimination between MHO and MetS.5. VIP score and Relative Fold Change bar plots show the metabolites with $VIP \geq 1$ represented in decreasing order as black thick lines (scale on the top) and Relative Fold Change values represented by grey bars (scale on the bottom). Significant alterations are indicated by *. Adjusted *p*-values (Student's *t*-test corrected by Bonferroni method) to 0.000018 (***).

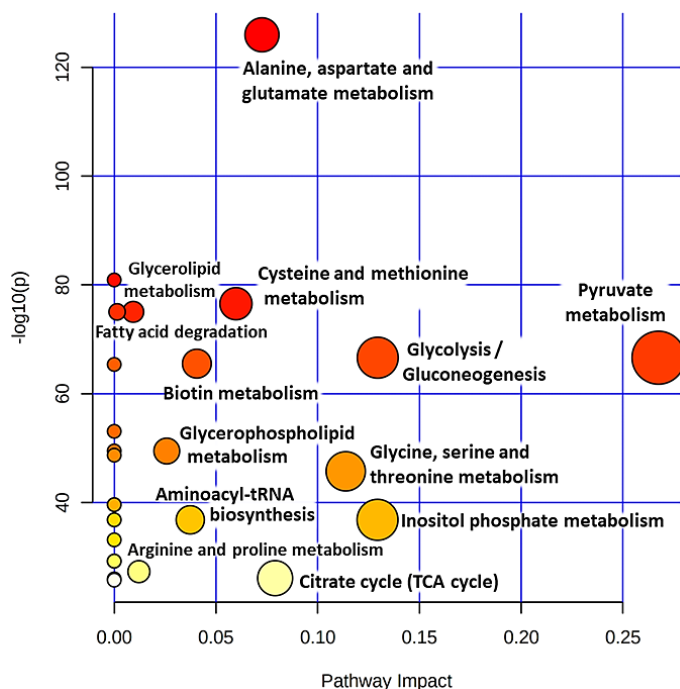


Figure R8. Metabolic pathways involved and affected in the extreme case of MetS. In the scatterplot, the x-axis indicates the impact on the route, while the y-axis indicates significant changes to a route. The pathways are represented as circles: the colour indicates the significance level, from highest (red) to lowest (white) in the enrichment analysis; the size is proportional to the impact value of each road from the topology analysis. Metabolic pathways whose name is indicated are significant (p -value lower than 0.05 after the adjustment using the Holm-Bonferroni method and FDR) and have a pathway impact value over 0.

5.2.1. The influence of age on metabolomic features in the extreme case of MetS.

We detected that MetS prevalence increases with age in our cohort. To maximize the differences associated with age and to further select relevant metabolic components, we calculated PLS-DA models to discriminate between MHO and MetS.5 conditions for both the age range 19–45 y and the age range 55–85 y. The analyses revealed specific

metabolic changes in MetS.5. The global metabolic profiles showed differences between MHO and MetS.5 at both age ranges (Figure R9 A and B). Moreover, the combined criteria of VIP scores and Relative Fold Change (Figure R10 A, B) revealed common trends regardless of age in the impact of MetS.5, including FACO₂, LDL particles, acetone, acetate and derivatives. Although most of the metabolites were selected as relevant for MetS.5 in both age groups and the number of metabolites with a VIP greater than one were comparable, their scores revealed different contributions to the models. Acetone, a dicarboxylic molecule, along with FACO₂, was the metabolite most significantly associated with MetS.5 in younger ages in the entire population (Figure R10 A), whereas in older ages FACO₂ showed the most important contribution to the model (Figure R10 B). Interestingly, polyunsaturated FAs (PUFAs) only contributed significantly to the model in the younger age group, whereas pyruvate and succinate, involved in the Krebs cycle, were only selected in the older age group. Mannose joint with glycogen fragments was the metabolite with a higher Relative Fold Change value in both age ranges resulting in the metabolite whose concentration changes more between MHO and extreme MetS, regardless of age.

Based on the results obtained, the metabolites significantly altered in MetS.5 as compared to MHO independently of age were studied using MetPA (MetaboAnalyst, Figure R11) to obtain information about the metabolic mechanisms of the extreme MetS that was not related to age and were not influenced by it. From the 17 common metabolites, ten metabolic pathways statistically significant were detected. These include glyoxylate and dicarboxylate metabolism; alanine, aspartate and glutamate metabolism; fatty acid degradation; pyruvate metabolism; inositol phosphate metabolism; glycolysis/gluconeogenesis; arginine and proline

RESULTS

metabolism; phosphatidylinositol signalling system; glycerolipid metabolism and glycerophospholipid metabolism.

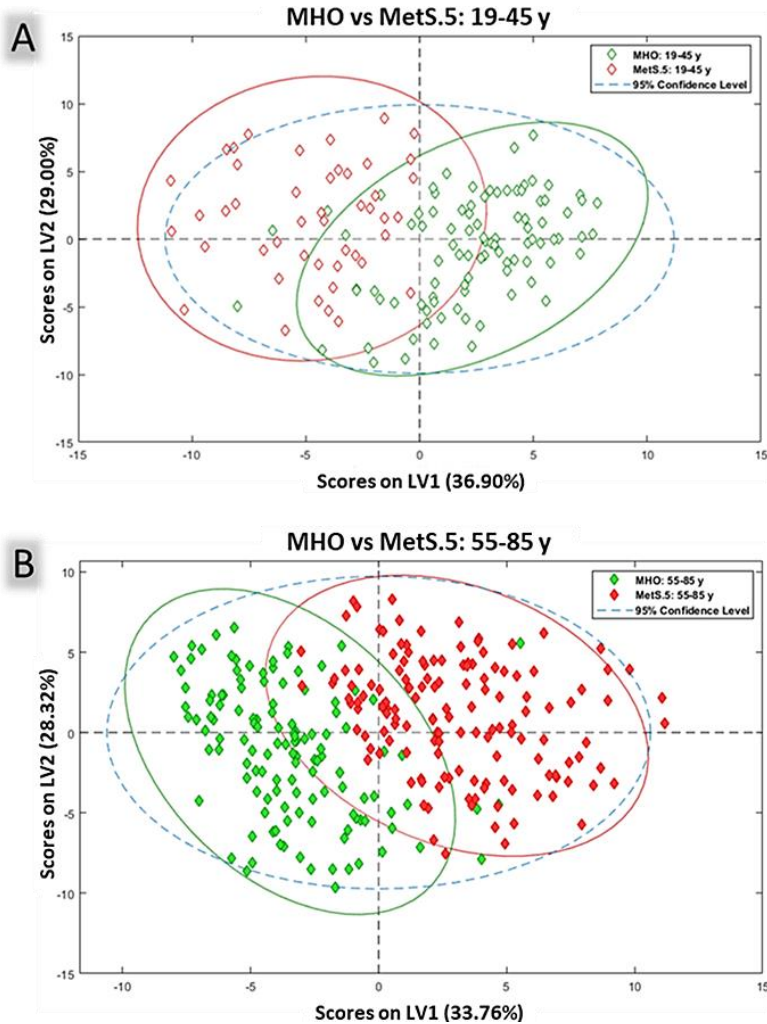


Figure R9. PLS-DA model for discrimination between MHO and MetS.5 by age range. All models were built using 2 LVs. The scores plots show MetS.5 samples in red and MHO samples in green with a 95% confidence ellipse in the same colours. (A) Scores plot for the age range 19 to 45 years model. Cross-validation parameters: RMSECV 0.304, R2CV: 0.582; ROC Curve AUC: 0.96. (B) Scores plot for the age range 55 to 85 years model. Cross-validation parameters: RMSECV 0.300, R2CV: 0.640; ROC Curve AUC: 0.97

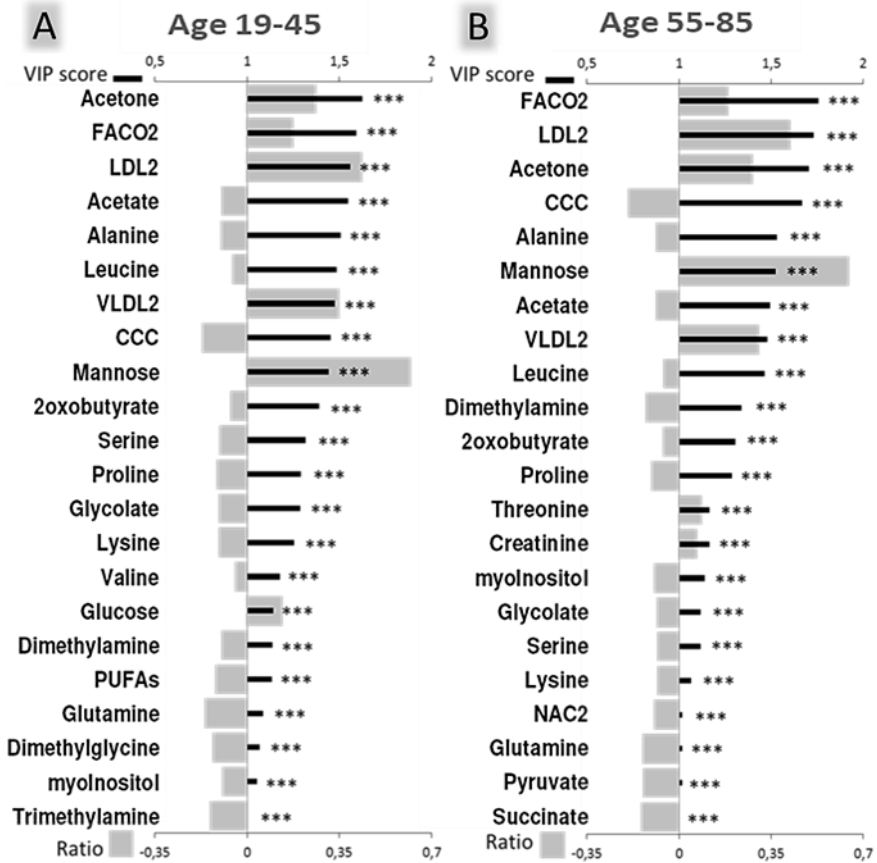


Figure R10. Significant metabolites in PLS-DA model for discrimination between MHO and MetS.5 by age range. VIP score and Relative Fold Change bar plots show the metabolites with $VIP \geq 1$ represented in decreasing order as black thick lines (scale on the top) and Relative Fold Change values represented by grey bars (scale on the bottom). Significant alterations are indicated by *. Adjusted *p*-values (Student's *t*-test corrected by Bonferroni method) to 0.000018 (***). (A) VIP score and Relative Fold Change bar plot for the age range 19 to 45 years model. (B) VIP score and Relative Fold Change bar plot for the age range 55 to 85 years model.

RESULTS

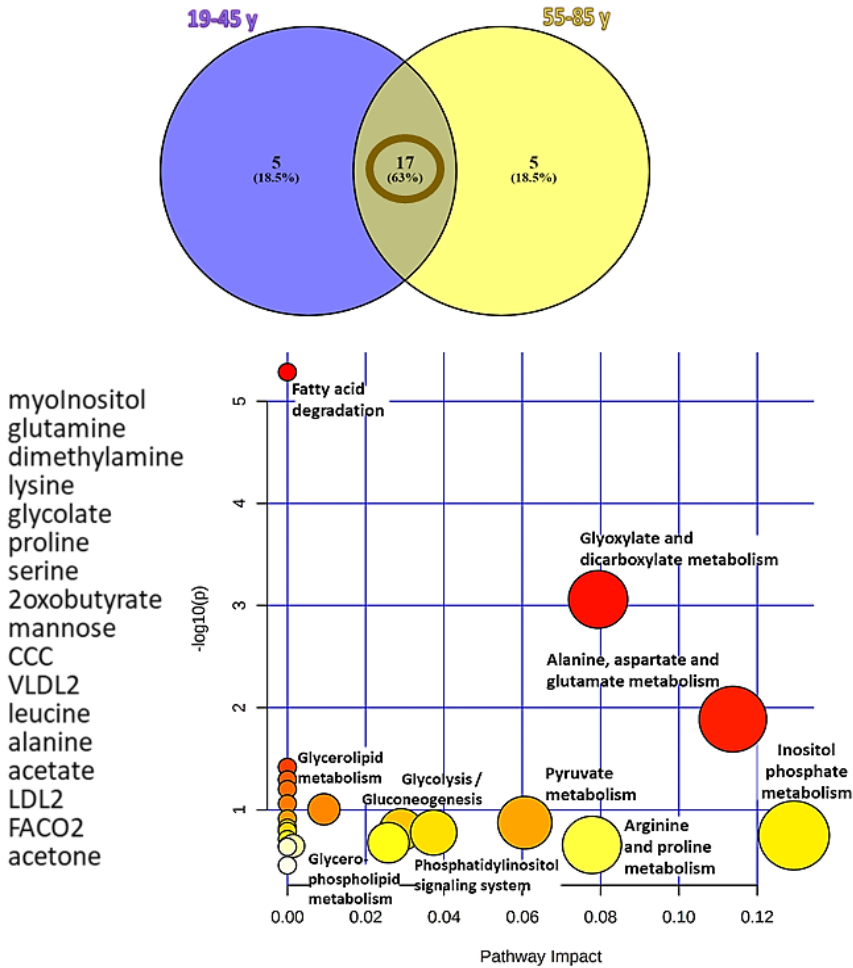


Figure R11. Metabolic pathways affected in MetS.5 independently of age. Two dimensions Venn diagram of the metabolites significantly altered in MetS.5 as compared to MHO in the two different age groups, and MetPA of groups' intersections. For the subgroups (represented by circles of different colours) is shown the number of the metabolites that are common (overlapping zone) or those that are exclusive to the group (outer circles). Metabolic pathways whose name is indicated are significant (p -value < 0.05 after the adjustment using the Holm-Bonferroni method and FDR) and have a pathway impact value, calculated from pathway topology analysis, over 0. In the scatterplots, the x-axis indicates the impact on the route, while the y-axis indicates significant changes to a route. The pathways are represented as circles. The circle colour indicates the significance level, from highest (red) to lowest (white) in the enrichment analysis. The circle size is proportional to the impact value of each road from the topology analysis.

5.3. Age-related sexual dimorphism of metabolic traits in extreme MetS in severe obesity.

We analysed the metabolic differences associated with MetS in different sex and age groups to identify sex-specific mechanistic clues and the impact of age on them. We evaluated the association of MetS with all 55 metabolic components. Figure R12 shows the mean difference and confidence intervals between MetS and MHO for the four different groups, based on sex and age. Sixteen metabolic components showed a statistically significant association with MetS in all four groups.

Overall, men in both age groups showed increasingly intense metabolomic differences between MHO and MetS. Women in the older group showed different and more intense changes closer to men's changes than the younger group. Since most of the clinical parameters of MetS showed statistically significant differences between men and women in both age groups, we applied the same strategy for analyzing the metabolomic profiles in the four sex and age subgroups (Figures R13, R14, R15 and R16). The comparison of the global metabolomes at younger and older ages for women (Figures R13 and R14) and men (Figures R15 and R16) showed discrimination and global differences (scores plots in Figure R13 A and B for women and Figure R15 A and B for men). The MetS.5 metabolomic impact at younger ages was different between women (Figures R14 A) and men (Figure R16 A).

Moreover, the combined criteria of VIP scores and Relative Fold Change refined even more the associations identified by the mean differences (Figure R12) since the number of metabolites with a VIP greater than one differed in the sex-stratified analysis. Women showed fewer metabolites with a VIP greater than one in the older group and men

show the opposite trend. Acetone and acetate, both dicarboxylic molecules, were the metabolites most significantly associated with MetS.5 only in younger women, whereas appeared less important in the other subgroups. Although in all the comparisons FACO2 were among the top four VIP scores, the change in this metabolic component contribution with age was much sharper in women (from the fourth to the first position) than in men (from the second to the third position). Host-microbiota co-metabolites also showed different trends between men and women with CCC as the top contributor in the model for older men but as a medium contributor (fourth and fifth position for younger and older ages respectively) in the women models.

Although changes in the contributions to the models showed interesting age-related trends and MetS.5 differences between men and women, most of the Relative Fold Change of each metabolite remained similar in all the MetS.5 analyses for the different groups, indicating a common metabolic impact of MetS. Among them, mannose showed the highest fold change and was statistically significant in all the comparisons. Other metabolites that also showed a VIP greater than one and statistically significant differences between MHO and MetS.5 in severe obesity included alanine, LDL2, VLDL2, mannose, serine, proline, lysine, and glycolate. Interestingly, the Relative Fold Change value of each metabolite remained similar in all the analyses between the different groups, indicating a shared metabolic trait of MetS. Among them, the mannose joint with glycogen fragments showed the highest value, resulting in the metabolite whose concentration changes more between MHO and MetS.5.

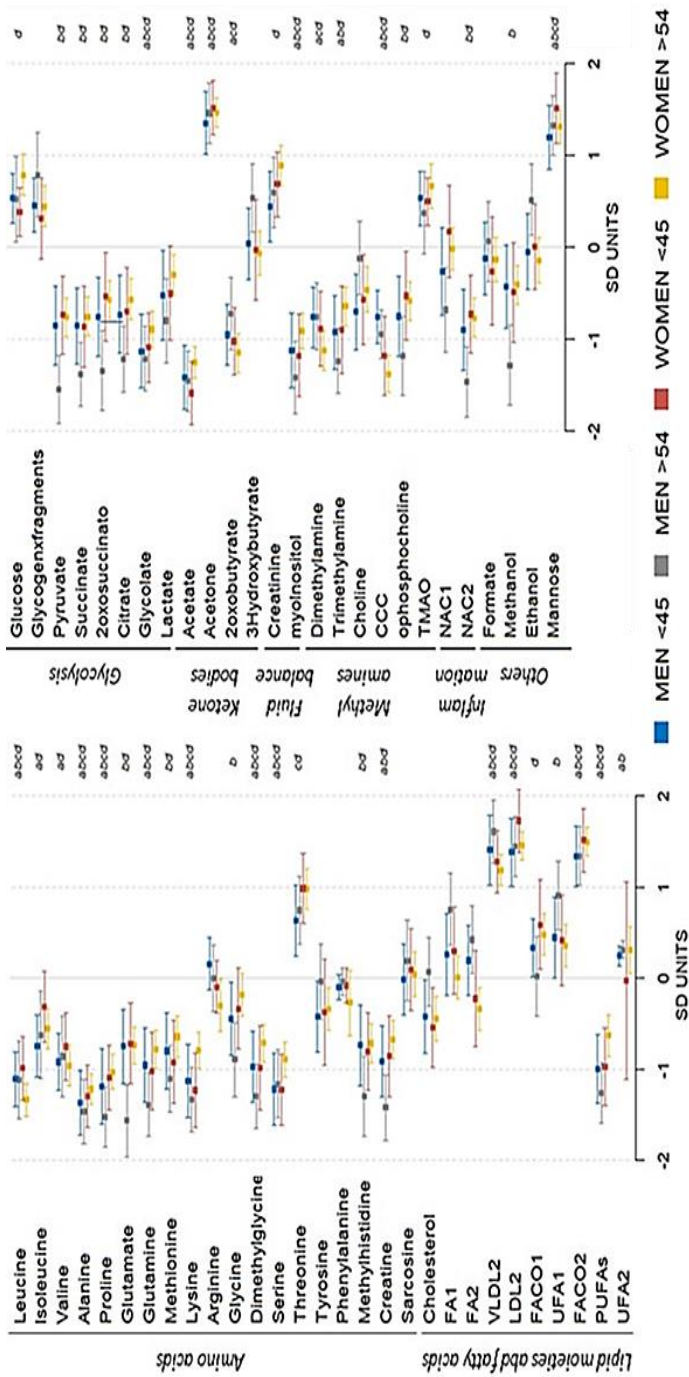


Figure R12. Mean differences and 90 % confidence intervals between MHO and MetS expressed in SD units for men and women for all the metabolic features measured in the study. Men (age < 45y in blue, age > 54y in grey), women (age < 45y in red, age > 54y in yellow). Multiple tests corrected statistical significance for the comparison between MHO and MetS (p-value below 0.00091) is marked with a (men < 45 y), b (men > 54 y), c (women < 45 y) and d (women > 54 y) in the last column. Key for NMR moieties: FA: fatty acids; FA1: CH3-; FA2: -CH2-; FACO1: -CH2CO; FACO2: -CH2CH2CO; UFA1: =CHCH2CH2-; UFA2: =CHCH2CH2-; PUFA: =CHCH2CH=; CCC: choline-containing compounds; TMAO: trimethylamine oxide; NAC1/2: acetyl in glycoproteins.

RESULTS

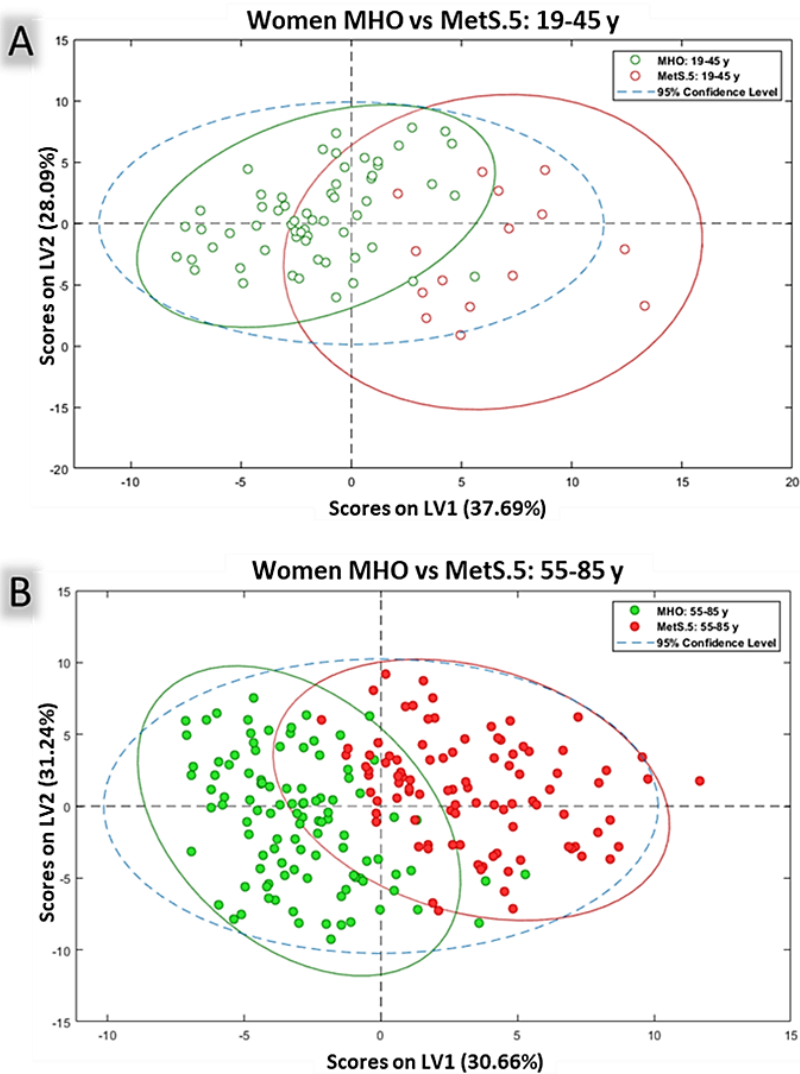


Figure R13. PLS-DA model for discrimination between MHO and MetS.5 by age range in women. All models were built using 2 LVs. All scores plots show MetS.5 samples in red and MHO samples in green with a 95% confidence ellipse in the same colours. (A) Scores plot for the age range 19 to 45 years model. Cross-validation parameters: RMSECV 0.273, R2CV: 0.534; ROC Curve AUC: 0.97. (B) Scores plot for the age range 55 to 85 years model. Cross-validation parameters: RMSECV 0.298 R2CV: 0.642; ROC Curve AUC: 0.98.

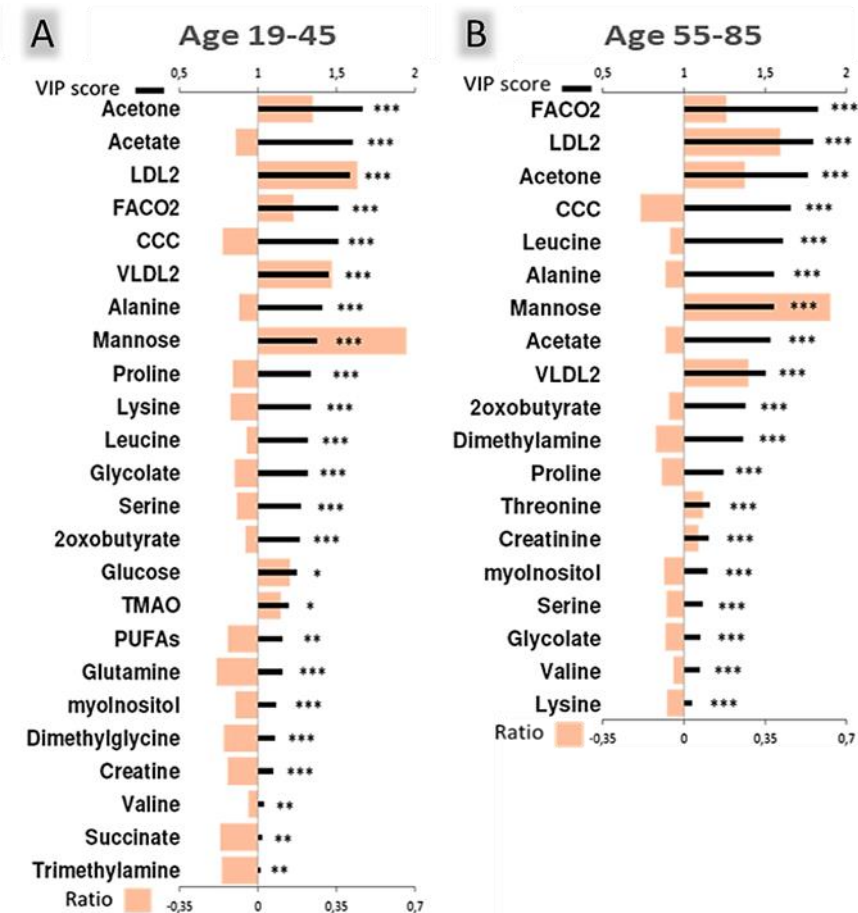


Figure R14. Significant metabolites in PLS-DA model for discrimination between MHO and MetS.5 by age range in women. VIP score and Relative Fold Change bar plots show the metabolites with $VIP \geq 1$ as black thick lines (scale on the top) and Relative Fold Change values represented by pink bars (scale on the bottom). Significant alterations are indicated by *. Adjusted p-values (Student's t-test corrected by Bonferroni method) to 0.00091 (*), 0.00018 (**), 0.000018 (***). (A) VIP score and Relative Fold Change bar plot for the age range 19 to 45 years model. (B) VIP score and Relative Fold Change bar plot for the age range 55 to 85 years model.

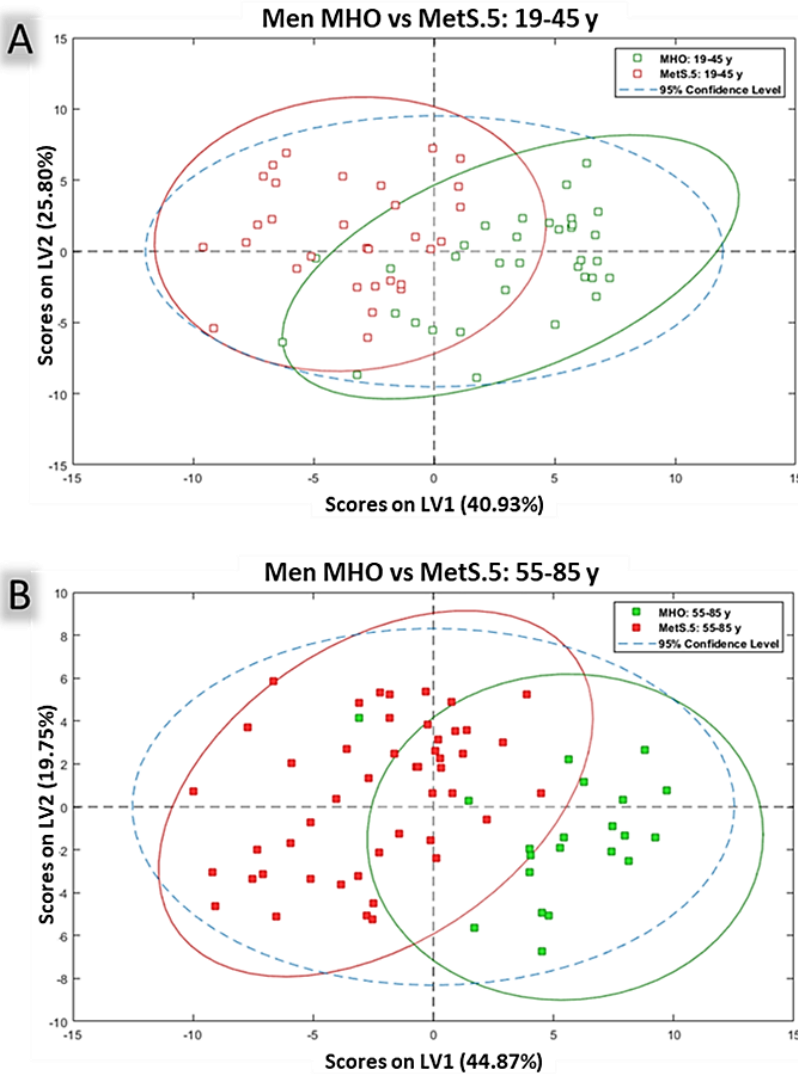


Figure R15. PLS-DA model for discrimination between MHO and MetS.5 by age range in men. All models were built using 2 LVs. All scores plots show MetS.5 samples in red and MHO samples in green with a 95% confidence ellipse in the same colours. (A) Scores plot for the age range 19 to 45 years model. Cross-validation parameters: RMSECV 0.341, R2CV: 0.534; ROC Curve AUC: 0.95. (B) Scores plot for the age range 55 to 85 years model. Cross-validation parameters: RMSECV 0.304, R2CV: 0.566; ROC Curve AUC: 0.95.

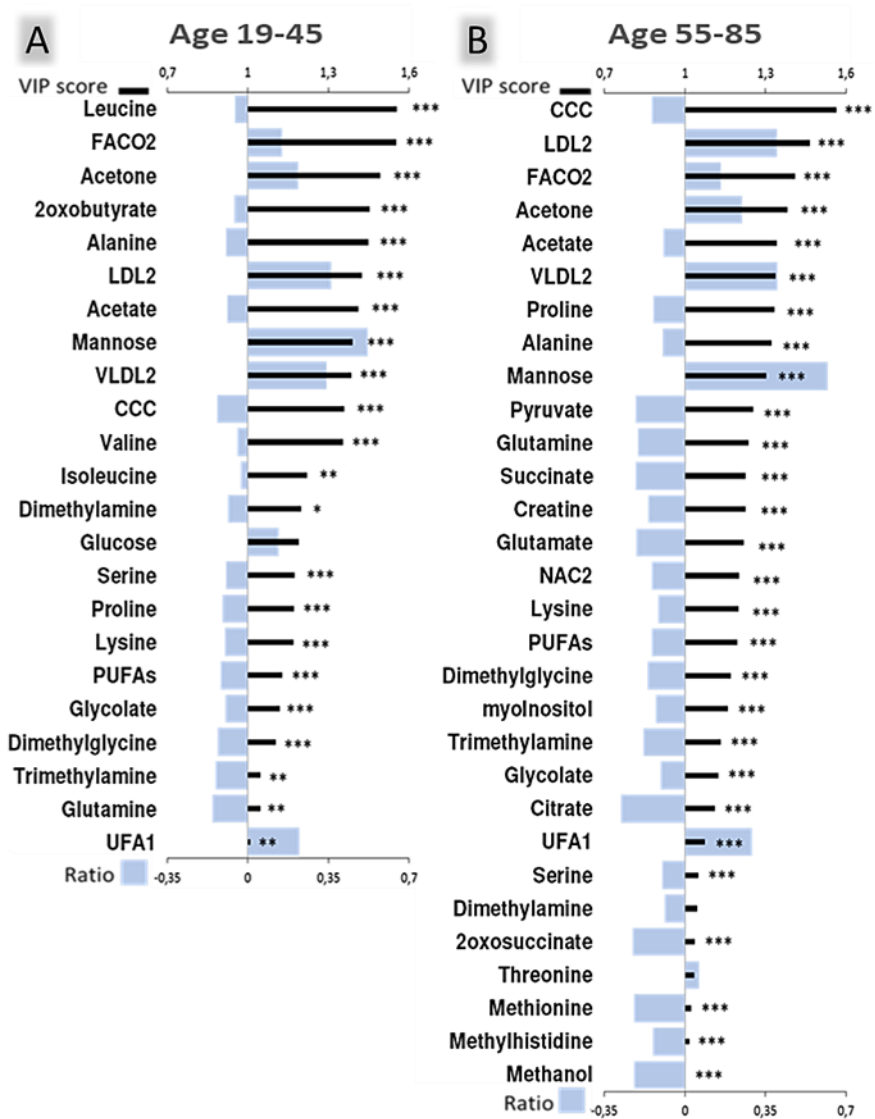


Figure R16. Significant metabolites in PLS-DA model for discrimination between MHO and MetS.5 by age range in men. VIP score and Relative Fold Change bar plots show the metabolites with $VIP \geq 1$ as black thick lines (scale on the top) and Relative Fold Change values represented by light blue bars (scale on the bottom). Significant alterations are indicated by *. Adjusted *p*-values (Student's *t*-test corrected by Bonferroni method) to 0.00091 (*), 0.00018 (**), 0.000018 (***). (A) VIP score and Relative Fold Change bar plot for the age range 19 to 45 years model. (B) VIP score and Relative Fold Change bar plot for the age range 55 to 85 years model.

The comparison of the specific profiles of MetS.5 in each age and sex subgroup by the Venn diagram (Figure R17) revealed minor differences concerning age and sex, with variations in only up to two metabolites, except for men over 54 years where the variations included more metabolites. Twelve metabolites (35.3 % of the total) resulted in common among all the subgroups and eleven metabolites (32.4 % of the total) appeared specific for the subgroup of men over 54 years old (Figure R17). The impact of MetS.5 in this subgroup specifically affected up to 11 metabolites, including pyruvate, succinate, glutamate, acetyls in glycoproteins (NAC2), trimethylamine, citrate, unsaturated FA (UFA1), 2-oxosuccinate, methylhistidine, and methanol.

To gain insights into the metabolic mechanism of MetS in the context of severe obesity and the specific pathways affected differentially in older men, these selected metabolites were analysed using MetPA (MetaboAnalyst, Figure R17). Seven metabolic pathways were statistically significant for the MetS.5 metabolites common to all group comparisons, including pyruvate metabolism; glycolysis/gluconeogenesis; glycerophospholipid metabolism; glycerolipid metabolism; fatty acid degradation, biotin metabolism and aminoacyl-tRNA biosynthesis. MetPA of the 11 metabolites (exclusively for the comparisons in men older than 54) included four additional pathways, namely, citrate cycle (TCA cycle), cysteine and methionine metabolism, alanine, aspartate and glutamate metabolism and glyoxylate and dicarboxylate metabolism, and it further confirmed the pathways identified in the common metabolomic profile.

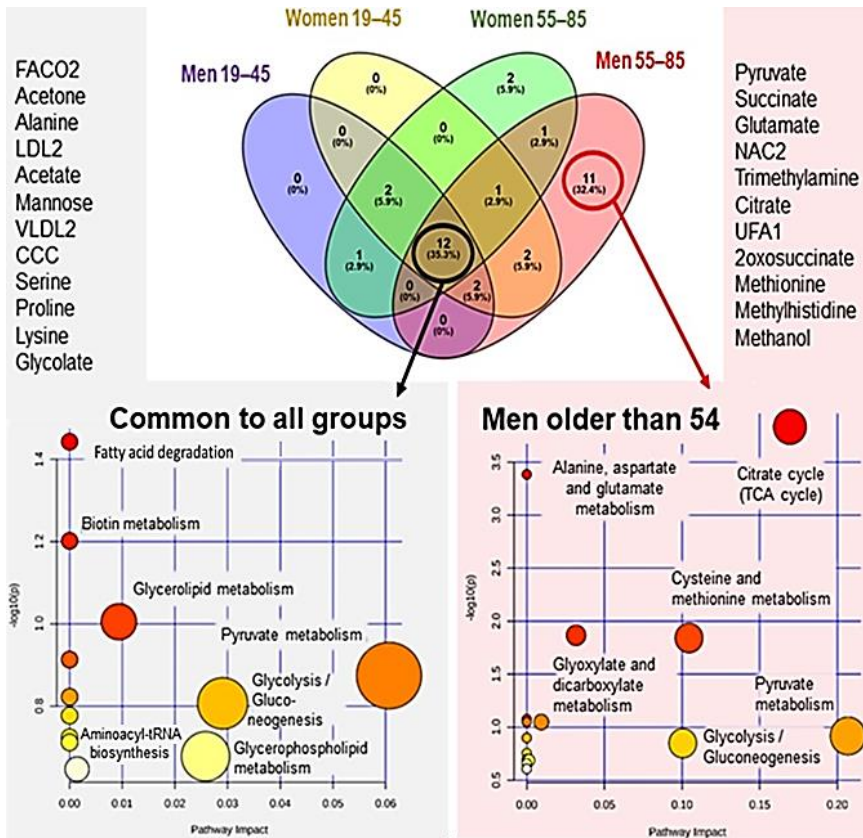


Figure R17. Metabolic pathways affected in MetS.5 in all age and sex groups. Four dimensions Venn diagram of the metabolites significantly altered in MetS.5 as compared to MHO in the different age and sex groups, and MetPA of all groups' intersections and the metabolic specific for men older than 54. For each subgroup (represented by ovals of different colours) is shown the number of the metabolites that are common to two, three or all the four groups (where ovals overlap) or those that are exclusive to each group (outer ovals). MetPA for metabolites common to all groups (left, grey background) and exclusive for men over 54 years old (right, pink background) are also represented. Metabolic pathways whose name is indicated are significant (p -value < 0.05 after the adjustment using the Holm-Bonferroni method and FDR) and have a pathway impact value, calculated from pathway topology analysis, over 0. In the scatterplots, the x-axis indicates the impact on the route, while the y-axis indicates significant changes to a route. The pathways are represented as circles. The circle colour indicates the significance level, from highest (red) to lowest (white) in the enrichment analysis. The circle size is proportional to the impact value of each road from the topology analysis.

5.4. Metabolomic-epigenetic interplay on MetS in severe obesity: the epigenetic study.

The results of the applied multi-approach made it possible to obtain an exhaustive epigenetic characterization of the subjects studied both at the group level, through differential methylation analysis to measure global average methylation levels, and at single-case on individual methylation profiles for the analysis of SEMs.

5.4.1. Group level: differential methylation analysis.

MDS was used to evaluate variations in the methylation profiles, reduce data complexity and visually inspect the dataset for strong signals in the methylation values. Differential methylation analysis was computed at the group level both at the sites and at specific regions (genes, promoters and CpG islands). After FDR adjustment of the p-values considering multiple testing, the results obtained failed to detect significant methylation differences between MetS.5 and MHO groups since no separation was observed along the first and the second dimensions, revealing that global average methylation levels were comparable (Figure R18 A). Nevertheless, two sites, belonging to TXNIP (thioredoxin interacting protein) and MYLIP (myosin regulatory light chain interacting protein) genes, turn out to be significantly differently methylated (Figure R18 B). At the site level, we found two statistically significant deregulated positions (cg19693031 and cg10474793 probes), belonging to TXNIP and MYLIP genes, respectively (Figure R19). The cg19693031 probe appeared hypomethylated in the MetS.5 group with a mean methylation value 7 % lower than the MHO control group (Figure R19 A). On the contrary, the cg10474793 probe appeared hypermethylated in the MetS.5 group with a

mean methylation value 3 % higher than the MHO control group (Figure R19 B).

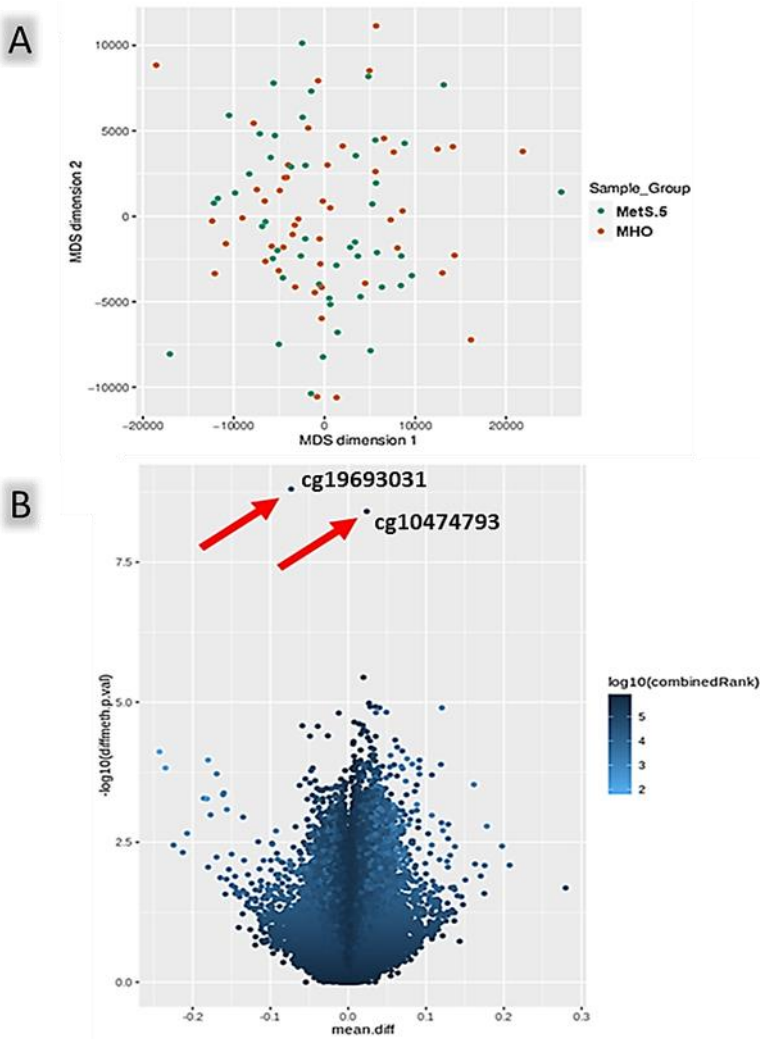


Figure R18. RnBeads differential methylation analysis of CpG sites. (A) The scatter plot shows the samples' coordinates on MDS dimensions based on methylation scores of CpG sites in cases MetS.5 (green) and controls MHO (orange). (B) Volcano plot of pairwise comparison for differential methylation. The colour range quantifies the mean methylation score difference between whole blood (x-axis) and the combined adjusted p-value of a given site (y-axis). Red arrows indicate the significantly differently methylated sites. The analysis was performed using the R package RnBeads.

RESULTS

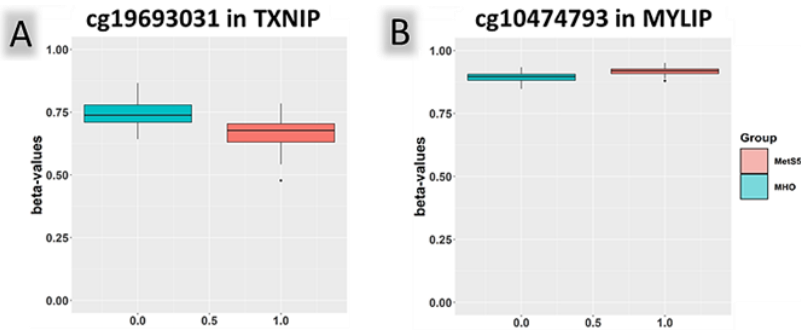


Figure R19. Boxplots of beta-values of methylation in *cg19693031* in *TXNIP* locus (A) and *cg10474793* in *MYLIP* locus (B) in MHO and MetS.5 patients. *cg19693031* site p -value = 0.0013 **; *cg10474793* site p -value = 0.0016 **. The p -value was adjusted for FDR correction.

At the regional level (genes, promoters and CpG islands), according to our previous findings, no significant enriched regions emerged (data not shown).

A gene ontology analysis was performed on the 100 best-ranked genes. The result of the gene ontology analysis was presented as TreeMaps (Figure R20) which summarize and represent the significant enrichment in the biological processes mainly involved. GO-terms resulted enriched for hypermethylated gene regions, that are subject to no or reduced activity, had been clustered semantically and divided into few main categories such as the telomeric D-loop disassembly, positive regulation of t-circle formation, lactate biosynthetic process from pyruvate, cartilage homeostasis and negative regulation of interleukin-6-methylated signalling pathway. On the contrary, the clustering of enriched GO-terms for hypomethylated genes, potentially more active, revealed a very heterogeneous pattern of biological processes and metabolic processes, highlighting pathways related to hydrogen peroxide, vesicular transport and oxidative stress

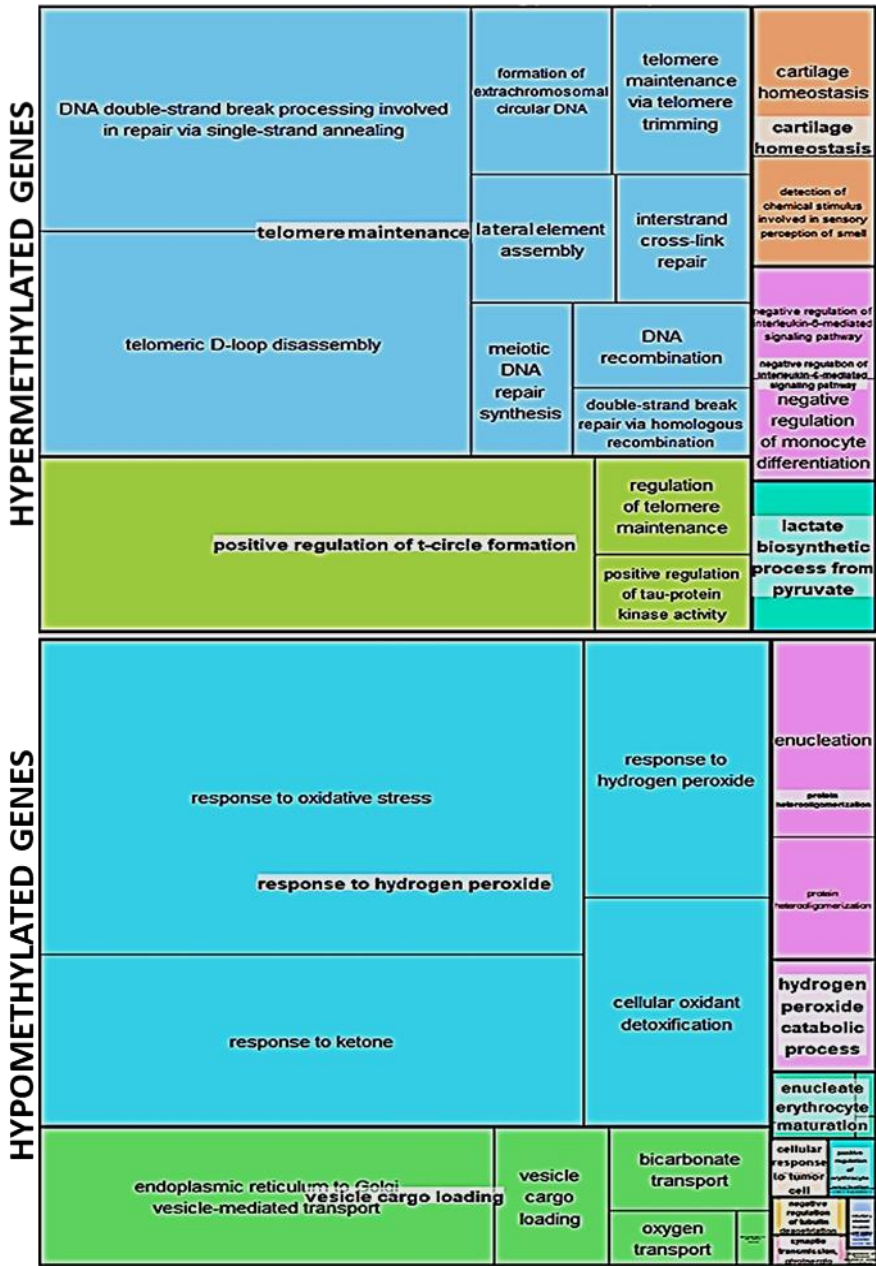


Figure R20. REVIGO tree map of GO Enrichment Analysis. The treemap shows biological processes enriched related to differential hypermethylated and hypomethylated sites in the MetS.5 case group. Only the best-ranked enriched terms are reported due to space constraints.

5.4.2. Single case level: SEM analysis and hyper- and hypomethylation levels of SEMs.

As described in the Methods section we carried out a single case analysis for the identification of SEMs. The calculated burden of SEMs in the MetS.5 group was compared to that observed in controls MHO and reported on a logarithmic scale. SEMs analysis highlighted, in MetS.5, a significant decrease in the median number of total log (SEMs) when compared to MHO controls (Figure R21 A) revealing that hypomethylations ($p = 0.0185^*$), rather than hypermethylations ($p = 0.0388^*$), mainly contribute to the epigenetic drift (Figure R21 B and C).

5.4.2a. Association between SEMs and metabolomic, clinical and pathological characteristics.

We wanted to test the association between SEMs and MetS clinical and pathological characteristics. After the annotation of SEMs to obtain the epilepsions' related genes using wANNOVAR software, we identified the unique lists of these genes for MHO ($n = 142$) and MetS.5 ($n = 121$). We then carried out a literature-based prioritization of genes through the computational tool Phenolyzer. As shown in Figure R22, the prioritization analysis using terms related to MetS and its pathological characteristics of MetS such as abdominal obesity, diabetes mellitus type 2, hyperglycemia, hypertension and hypertriglyceridemia showed no statistically significant association between SEMs and clinical and pathological characteristics.

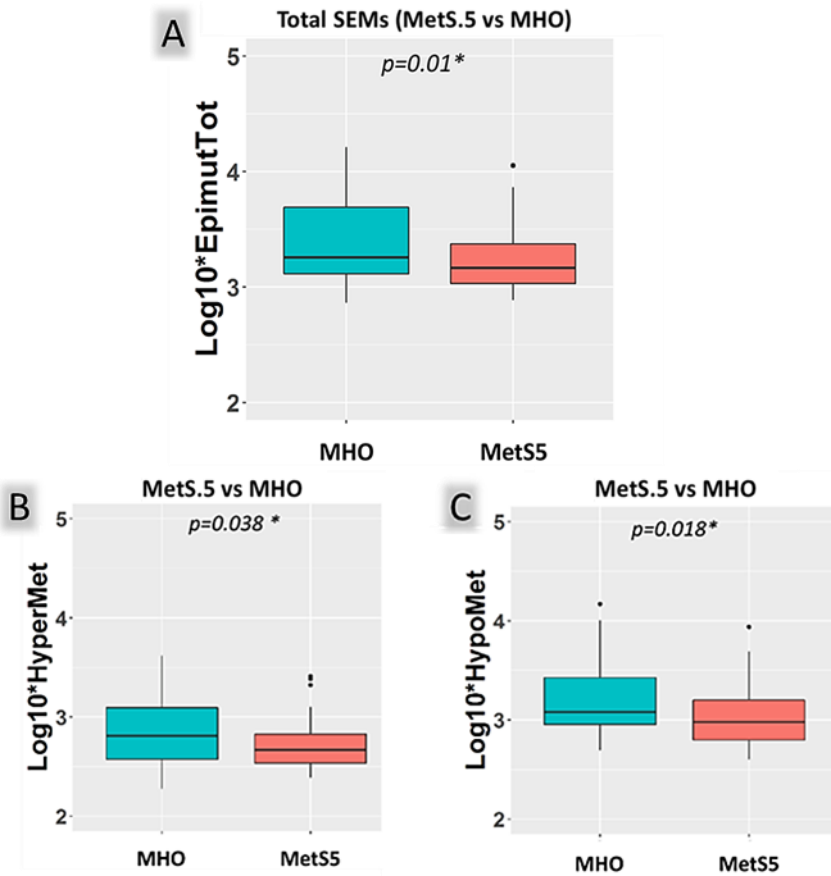


Figure R21. SEM analysis and hyper- and hypomethylation levels of SEMs. In (A) boxplots describe the quantity of total SEMs in MHO and MetS.5 patient groups. SEMs were expressed as \log (SEMs). P-value of the difference = 0.01 *. (B, C) Boxplot of β values of the means of total differential hypermethylation (B) and hypomethylation (C) levels of SEMs in MHO and MetS.5 patients. Hypermethylation means levels showed a p-value = 0.0388 *; hypomethylation means levels showed a p-value = 0.0185 *. The analysis was conducted by separating the SEMs by direction of deregulation and correcting for sex and age.

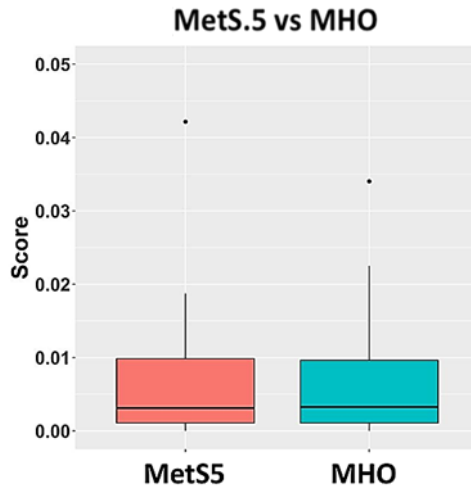


Figure R22. Boxplot graphical representations of the total scores obtained from the prioritization analysis of the unique lists of the epilepsions' related genes in MHO and MetS.5 patient groups.

To investigate the interplay between epigenetic and metabolomic alterations we carried out a correlation analysis. The aim was to identify candidate variables to be implicated in this cause-effect interplay. We tested the possible association between the decrease in epimutations in cases, represented by the variable EpimutTot (SEMs) and the 22 metabolic variables significant resulting from the metabolomic analysis of MetS.5 in the elderly. Statistically significant associations with the metabolites such as mannose, VLDL2, LDL2, FACO2, myoinositol and creatinine were identified, although very weak in some cases (Figure R23). Since there is a decrease in SEMs in cases, a significant variation of these variables concerning case/control will also be associated with this decrease (negatively if it increases in cases, positively if it decreases in cases).

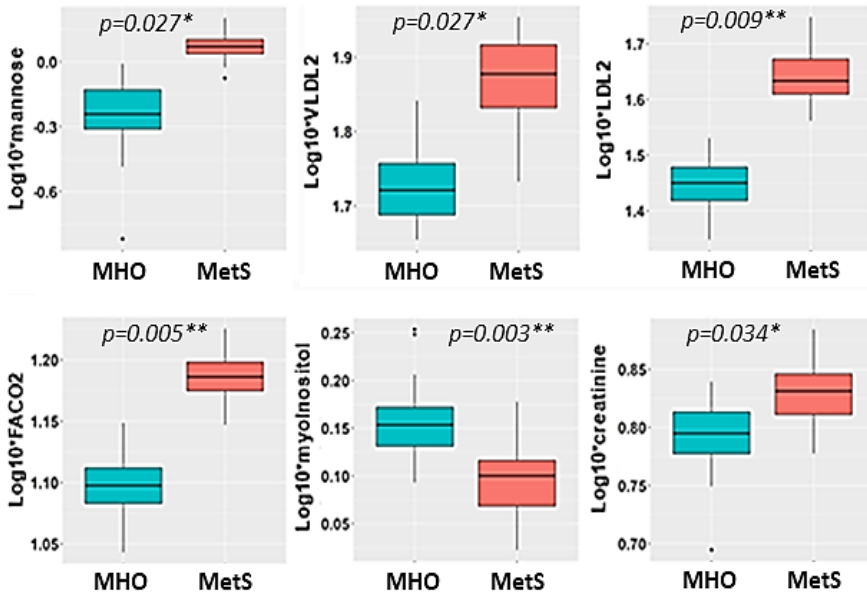


Figure R23. Correlation analysis between \log (SEMs) and metabolic variables in MHO and MetS.5. Boxplots describe the association levels of total SEMs and metabolites in MHO and MetS.5 patient groups. SEMs were expressed as \log (SEMs). In the figure are represented only the statistically significant correlations. The p-value (adjusted for FDR correction): (*) $p < 0.5$; (**) $p < 0.1$. Abbreviations and keys for NMR moieties: VLDL2, very-low-density lipoprotein; LDL2, LDL cholesterol; FA: fatty acids; FACO2: $-CH_2CH_2CO$.

5.4.2b. Sex influence on the burden of SEMs.

We also investigated the relationship between sex and SEMs through a single case analysis aimed at evaluating the rate of decreased stochastic SEMs in MetS.5 case groups in men and women, separately. Unexpectedly, the decrease in SEMs in MetS.5 groups seemed to be much more pronounced in the cohort of men only, while in women, the trend remained even if not significant (Figure R24 A and B).

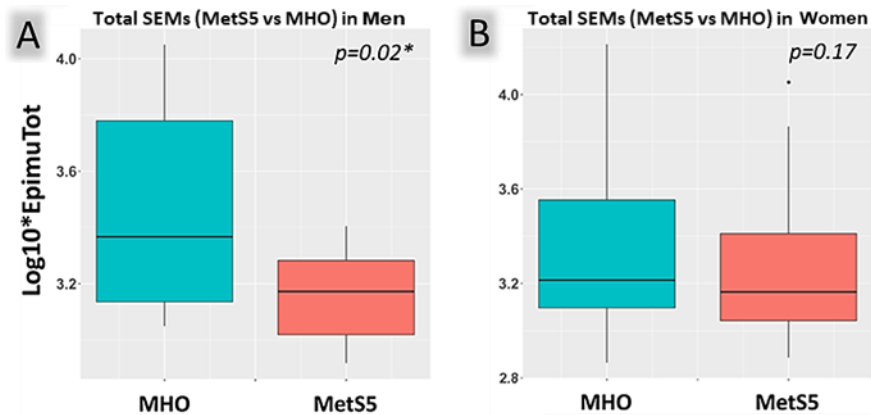


Figure R24. Analysis of SEMs in men and women subgroups. Boxplots describe the quantity of total SEMs in MHO and MetS.5 patients in the men (A) and women (B) subgroups, respectively. SEMs were expressed as $\log(\text{SEMs})$. p -value of the difference in men = 0.02*; p -value of the difference in women = 0.17.

5.4.3. Biological age estimation in healthy and pathological severe obesity.

To verify the presence of a correlation between the corrected biological age and chronological age and to individuate differences in the rate of ageing and susceptibility to MetS not accounted for by chronological age alone, we applied the DNA methylation measurements to predict biological age using several epigenetic clocks. Neither differences in chronological age nor differences in the ratio between chronological age and Horvath's DNAmAge were noticed neither in the case nor in control groups (Figure R25 A and B). By considering another age estimate (Grimage Acceleration - AgeAccelGrim) (Figure R25 C), able to predict the expected lifespan of individuals concerning the presence of diseases or pathological conditions, a significant variation (Mann Whitney $p = 0.025$) was observed. MetS.5 cohort showed increased values, indicating higher biological ageing than MHO.

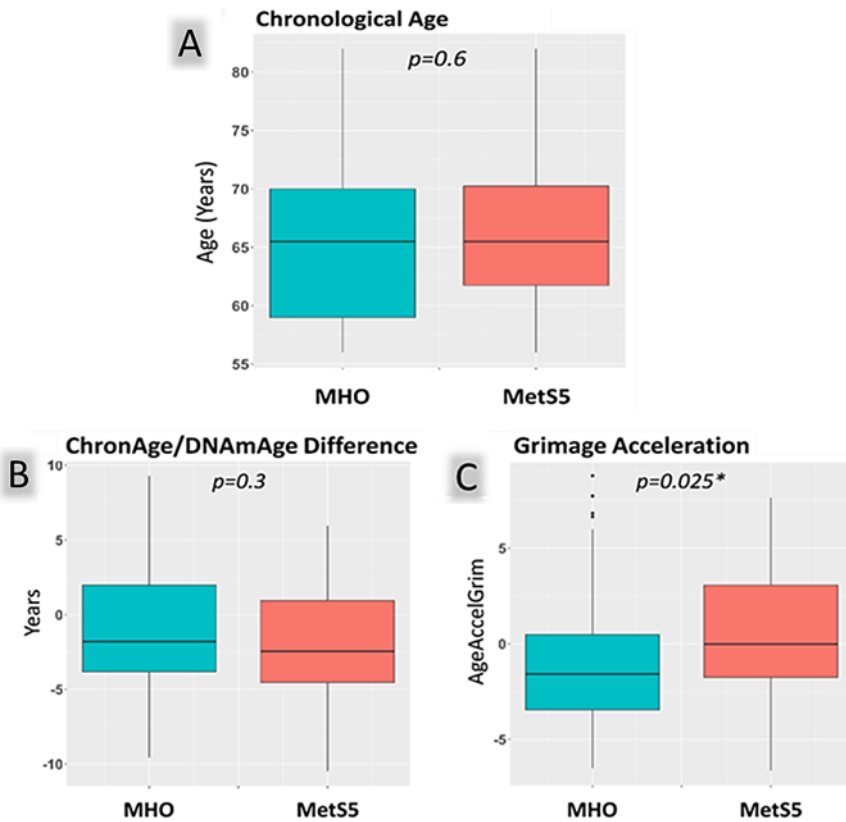


Figure R25. Analysis of chronological and epigenetic ages in MHO and MetS.5 patients. Boxplots describe the differences, and their Mann Whitney p-value, between MHO and MetS.5 patient groups in terms of Chronological Age (A), ChronAge/DNAAge Difference (B) and Grimage Acceleration (C), respectively. P-value of the difference (A) = 0.6; p-value of the difference in (B) = 0.3; p-value of the difference in (C) = 0.025*

We also studied the Grimage Acceleration related to sex between MHO and MetS.5 groups in men and women, separately. Interestingly, the increased values of Grimage Acceleration in MetS.5 groups seemed to be much more pronounced and statistically significant (Mann-Whitney $p = 0.009$) in the cohort of women only, while in males, the trend remained even if not significant (Mann-Whitney $p = 0.982$) (Figure R26 A and B).

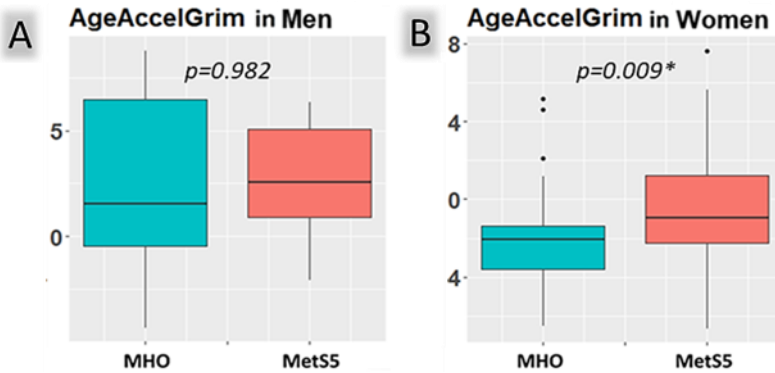


Figure R26. Analysis of Grimage Acceleration in men and women subgroups. Boxplots describe the differences, and their Mann-Whitney p -value, between MHO and MetS.5 patient groups in terms of Grimage Acceleration. Men (A) and women (B) were analysed separately. P -value of the difference in men = 0.982; p -value of the difference in women = 0.009*.

5.5. Metabolic characterization of the HFD-fed Wistar rats animal model.

HFD obese and thin Wistar rats represented a good experimental model for the metabolic characterization of MetS, allowing the development of a mechanistic and functional approach to analyse the effects of HFD on adipose tissue. A special focus was put on its body distribution, composition, and metabolism to study and validate the potential role of adipose tissue and adipocyte metabolomes in the MetS observed in severe obesity in the Piancavallo cohort.

5.5.1. The effect of diet on the body weight: comparison of CTL and HFD rats by sex.

The body weight of the rats and the weight of their perigonadal fat pads (epididymal for males, periovarian for females) were affected by 20

weeks of HFD intake. Body weight increased in both CTL and HFD groups, but the rise was higher in the latter. However, BMI did not show statistical significance in diet and body weight change. As in humans, HFD induced an increase in weight both in male and female rats, being this increase statistically greater in male than in female rats. The difference in body weight was more significant considering male and female rats separately. On the contrary, perigonadal fat pad weight at sacrifice between CTL and HFD lacked statistical relevance in the males' subgroup, whereas a slight significance was present in the females' subgroup. It is interesting to note that, in the control situation, the females already appeared to have much more perigonadal fat than the males (3.02 vs. 1.82) and the fat diet brought a similar fat gain (1.30) in both groups. (Table R4).

5.5.2. CTL vs HFD rats' perigonadal fat pads: differences in morphology, structure and metabolism.

The perigonadal fat pads showed differences related to their provenance: CTL or HFD rats (Figure R27). On average, the pads obtained from HFD animals had bigger dimensions, a more compact consistency and a lighter colour due to increased cell hypertrophy and a lower density of the blood capillaries (Figure R27 A). After their isolation and seeding in cell culture wells, the fat cells of CTL rats, fed with a standard diet, appeared in general smaller and morphologically more uniform in size and aspect than swollen cells of HFD rats when observed through the optic microscope as shown in Figure R27 B. In fact, among the HFD adipocytes, it was possible to note the presence of cells with a surface that was not smooth, or "curled" at many points, probably due to lymphocytic infiltration by macrophages, suggesting more inflammation status. Moreover, also the naked-eye observation of adipocyte cultures found diet-

RESULTS

induced differences between CTL and HFD related to the different types of cellular contents released in the culture medium during cellular lysis (Figure R27 C). The constant accumulation of lipids makes the wall of mature adipocytes fragile and in hypertrophic HFD cells, the increased instability led to a greater probability of rupture, especially in culture.

Table R4. Anthropometric characterization of Wistar rats' animal model.

Anthropometric Measures (mean ± SD)	Total			Females			Males		
	CTL	HFD	p-value	CTL	HFD	p-value	CTL	HFD	p-value
	Body Weight (g)	402,9 ± 139,8 503,2 ± 186,8 +100,3 ± 52,7	382,7 ± 131 529,8 ± 212,6 +147,1 ± 83,3	0,66 0,7 0,06	269,1 ± 15,7 325,1 ± 20,2 +56 ± 11,6	257,3 ± 7,9 328,2 ± 10 +70,9 ± 10,9	0,05 0,67 0,01†	536,7 ± 27,2 508,2 ± 34,4 +144,6 ± 36,5	681,3 ± 42,8 731,4 ± 70,7 +223,2 ± 40,5
BMI (g/cm ²)	0,74 ± 0,18 0,75 ± 0,19 +0,01 ± 0,11	0,73 ± 0,16 0,79 ± 0,24 +0,06 ± 0,11	0,86 0,58 0,19	0,58 ± 0,04 0,58 ± 0,03 +0 ± 0,06	0,58 ± 0,04 0,56 ± 0,04 +70,9 ± 10,9	0,85 0,43 0,57	0,91 ± 0,09 0,92 ± 0,1 +0,01 ± 0,1	0,88 ± 0,07 1,02 ± 0,09 -0,02 ± 0,07	0,52 0,056 0,7
Perigonadal fat pads weight at sacrifice (g)	2,42 ± 1,08	3,44 ± 1,56	0,03*	3,02 ± 1,19	4,34 ± 1,30	0,04†	1,82 ± 0,49	2,53 ± 1	0,09

Comparison of body weight, BMI and perigonadal fat pads weight at the sacrifice of CTL and HFD rats in the Total and in females and males, separately. Mean values and SD of initial and final Body weight and BMI, and perigonadal fat pad weight at the sacrifice were calculated for each group. t-tests were used to test the significance of the differences in CTL and HFD animals of different sexes. Significance (t-tests): (†, ‡, *) p < 0,05; (***) p < 0,001, where # represents the Total, † the females and * the males. Abbreviations: = CTL, animals fed with standard diet; HFD, animals fed with HFD; BMI, body mass index (body weight/body length²); initial, measures before the HFD treatment of 20 weeks; final, measures after the HFD treatment of 20 weeks; diff, the body weight difference between the initial and the final stages.

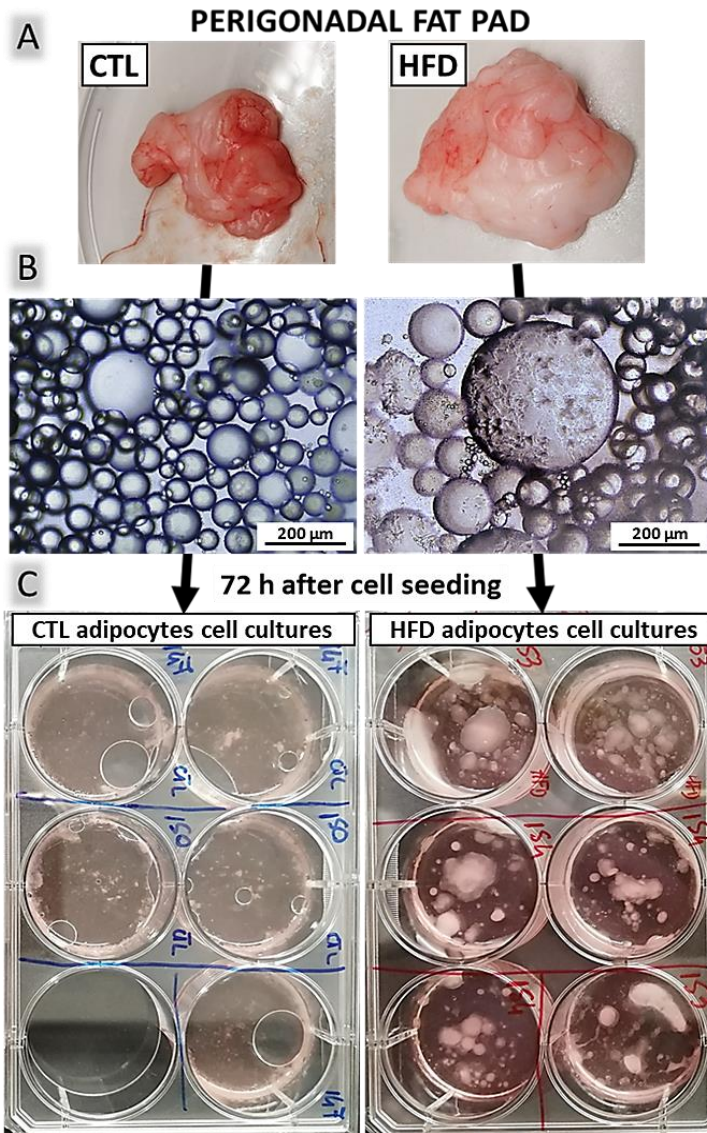


Figure R27. CTL and HFD perigonadal fat pad's visual aspect from extraction to cell culture. (A) Perigonadal fat pad samples before processing. On the left side, a perigonadal fat pad extracted from a CTL rat; on the right side, a perigonadal fat pad extracted from an HFD rat. (B) Optic Microscopy Image of mature adipocyte culture after 72 h from seeding. CTL mature adipocytes on the left; HFD mature adipocytes on the right. Scale bar, 200 μ m. (C) Top view of 6-well cell culture plates after 72 h from seeding. The plate containing CTL mature adipocytes is on the left; the plate containing HFD mature adipocytes is on the right.

5.5.3. The potential role of the metabolome of adipocytes and adipose tissue on MetS in severe obesity.

The Scores plot in Figure R28 showed the probability that a sample belonged to its group of cases HFD or controls analysing the relationship among the samples. The result indicated that the metabolomic profiles of two female HFD rats did not correspond to their experimental profile, on the contrary matching better with the experimental profile of the controls. For this reason, despite the small number of samples, to avoid analytical errors, the two outlier samples were excluded from the metabolomic PLS-DA analysis models.

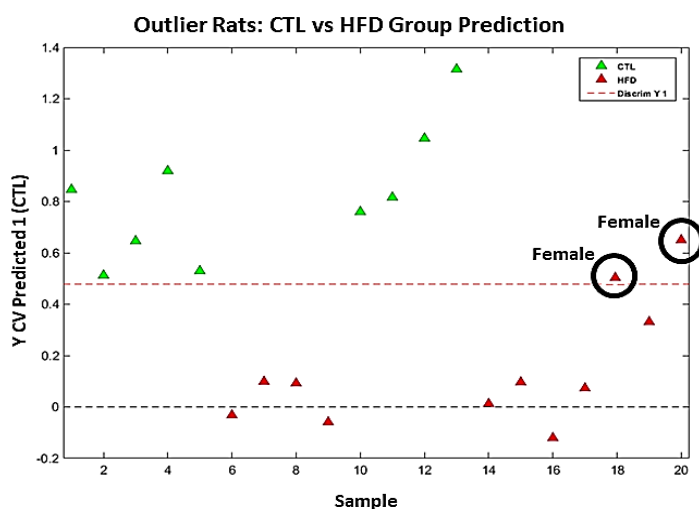


Figure R28. Wistar rats group prediction: CTL vs HFD. Wistar rats group prediction: CTL vs HFD. The scores plot shows the binary classification of predicted y values for "CTL" versus "HFD" listed along the axis as "Y CV Predicted 1 (CTL)", plotted against "Sample", distributed along the X axis. Red triangles indicate HFD rats, green triangles indicate CTL rats. Samples of both sexes are included. The dashed red line represents the discriminant threshold value for Y1, corresponding to 0,5. To be well classified, CTL samples must remain above the threshold line, while HFD samples must remain below. The black circles highlight the outlier samples.

5.5.3a. The influence of diet on the metabolism of rat adipocytes and adipose tissue.

Exploratory PLS-DA analyses between CTL and HFD Wistar rats revealed differences in the global metabolic profiles of culture media both in adipocyte cell cultures and adipose tissue organ cultures (Figures R29 A and R30 A).

Moreover, combined criteria of VIP scores in both adipocytes cell cultures and adipose tissue organ cultures (Figures R29 B and R30 B) identified differential profiles that contrasted in variety and number of significant metabolites (VIP scores ≥ 1). As shown, Methionine/Isoleucine constitute the metabolomic spectral area most significantly associated with HFD in adipocyte cell cultures. Whereas, in adipose tissue culture media, Glutamine showed the highest value in adipose tissue organ cultures, resulting in the metabolite whose concentration changes more between CTL and HFD. However, none of the metabolites was statistically significant after correction for multiple tests.

The metabolites and metabolic areas with VIP scores ≥ 1 from the PLS-DA model for discrimination between adipocytes' culture media of HFD and control rats were analysed using MetPA (MetaboAnalyst, Figure R31) to obtain information about how HFD influences the metabolic pathways of fat cells. Seven metabolic pathways resulted statistically significant, including pyruvate metabolism; glycolysis/gluconeogenesis; alanine, aspartate and glutamate metabolism; cysteine and methionine metabolism; glycine, serine and threonine metabolism; citrate cycle (TCA cycle); and glutathione metabolism.

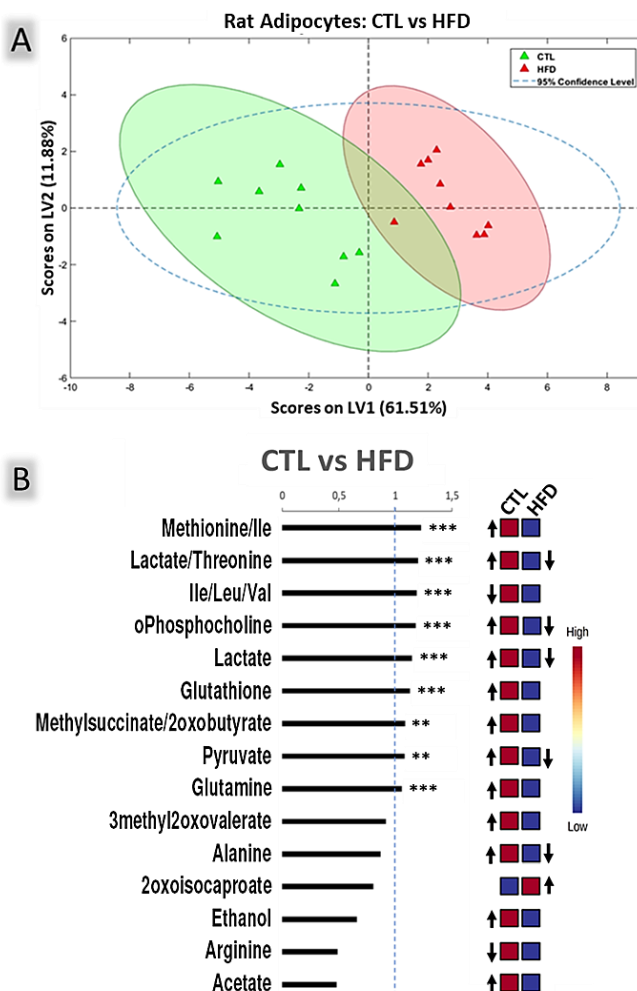


Figure R29. PLS-DA model for discrimination between adipocytes' culture media of HFD and control rats. (A) Score plot. The model was built using 2 LVs. The score plot shows HFD in red and CTL in green with a 95% confidence ellipse in the same colours. Cross-validation parameters: RMSECV 0.253, R2CV: 0.762; ROC Curve AUC: 1,000. (B) VIP score bar plot. Significant alterations are indicated by *. Adjusted *p*-values (Student's *t*-test corrected by Bonferroni method) to 0.00067 (**), 0.000067 (***). On the right, the coloured boxes show the mean concentration of the metabolites in the respective group net of their baseline levels. Blue and red boxes indicate metabolite levels that are lower or higher, respectively, between the two groups. Down arrows indicate metabolites uptake compared to their baseline value in culture media; Up arrows indicate their excretion by cells.

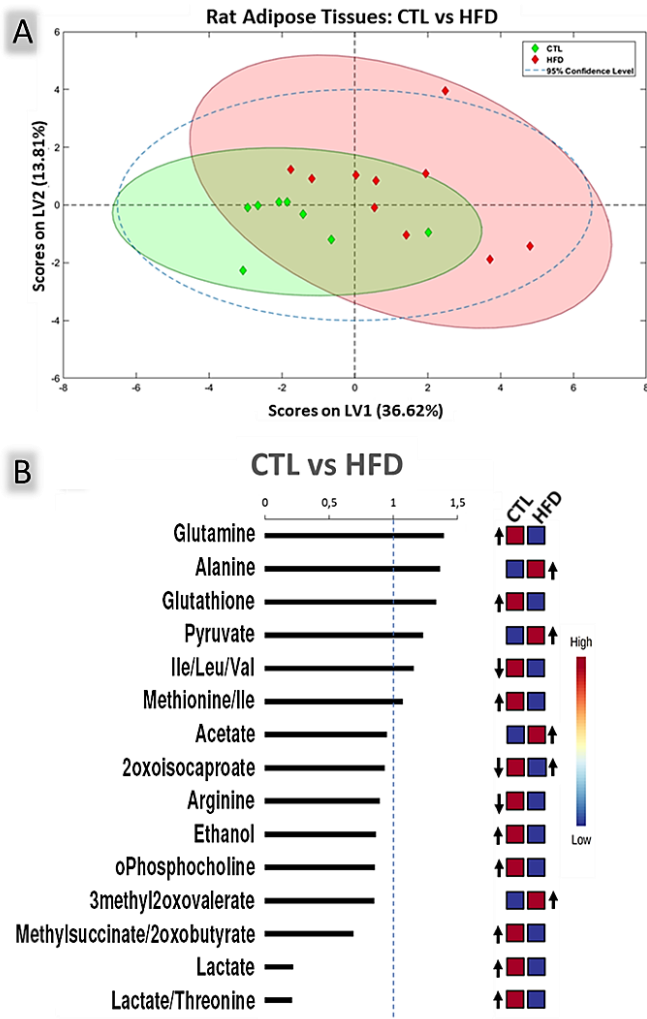


Figure R30. PLS-DA model for discrimination between adipose tissues' culture media of HFD and control rats. (A) Score plot. The model was built using 2 LVs. The score plot shows HFD in red and CTL in green with a 95% confidence ellipse in the same colours. Cross-validation parameters: RMSECV 0.584, R2CV: 0.487; ROC Curve AUC: 0.937. (B) VIP score bar plot. On the right, the coloured boxes show the mean concentration of the metabolites in the respective group net of their baseline levels. Blue and red boxes indicate metabolite levels that are lower or higher, respectively, between the two groups. Down arrows indicate metabolites uptake compared to their baseline value in culture media; Up arrows indicate their excretion by cells.

RESULTS

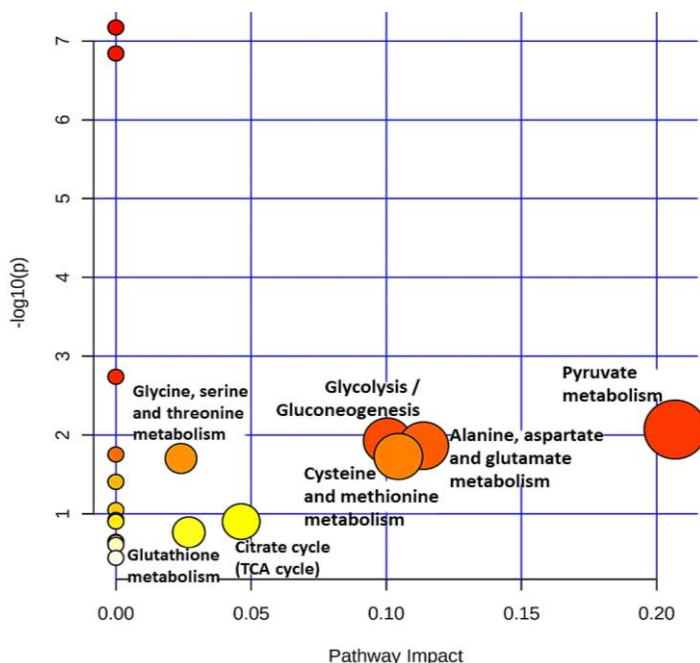


Figure R31. Metabolic pathways altered by HFD in fat cells. In the scatterplot, the x-axis indicates the impact on the route, while the y-axis indicates significant changes to a route. The pathways are represented as circles: the colour indicates the significance level, from highest (red) to lowest (white) in MetPA; the size is proportional to the impact value of each road from the topology analysis. Metabolic pathways whose names are indicated are statistically significant (p -value < 0.05 after the adjustment using the Holm-Bonferroni method and FDR) and have a pathway impact value over 0.

5.5.3b. The influence of diet on metabolic sexual dimorphism in rat adipocytes.

Since the metabolomic and epigenetic results on MetS in Piancavallo human cohort showed statistically significant differences between men and women groups, we evaluated HFD impact on adipose metabolism separately by sex (Figures R32, R33 and R34). This allowed us to further maximise the differences associated with sex and to find relevant metabolic components through the characterization of the cell

culture media. The results of the PLS-DA we performed exhibited clear discrimination between the medium samples of adipocytes culture obtained from control and HFD rats, in both female and male rats. Similarly to what was observed in humans, this separation was stronger in the female rats (as highlighted by VIP score plots in Figure R32 A for females and B for males).

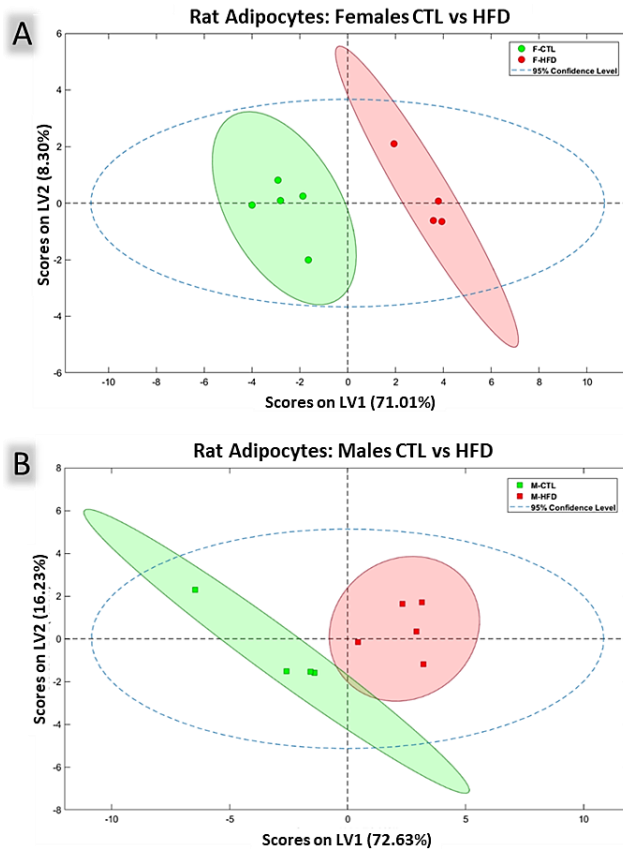


Figure R32. PLS-DA models for discrimination between HFD and control female and male rats, separately. All models were built using 2 LVs. All scores plots show HFD samples in red and control samples in green with a 95% confidence ellipse in the same colours. (A) Scores plot for female rats. Cross-validation parameters: RMSECV 0.364, R2CV: 0.595; ROC Curve AUC: 1.000. (B) Scores plot for male rats. Cross-validation parameters: RMSECV 0.355, R2CV: 0.670; ROC Curve AUC: 0.98.

RESULTS

The HFD metabolomic impact was different between the female and male rats (Figure R33 A and B). Eight analytes (methionine/ile, O-phosphocholine, glutathione, ile/leu/val, pyruvate, lactate/threonine, methylsuccinate/2oxobutyrate, glutamine) of excretion or uptake were dysregulated ($p < 0.05$) in the culture media of adipocyte cells extracted from female rats fed with HFD, compared to the ones in the culture media of adipocyte cells from control diet-fed female rats, using the student's t-test (Figure R33 A). In the culture media of adipocyte cells extracted from male rats, only BCAAs (ile/leu/val) were significantly dysregulated by the HFD, showing reduced uptake of these metabolites concerning the adipocytes from control rats (Figure R33 B).

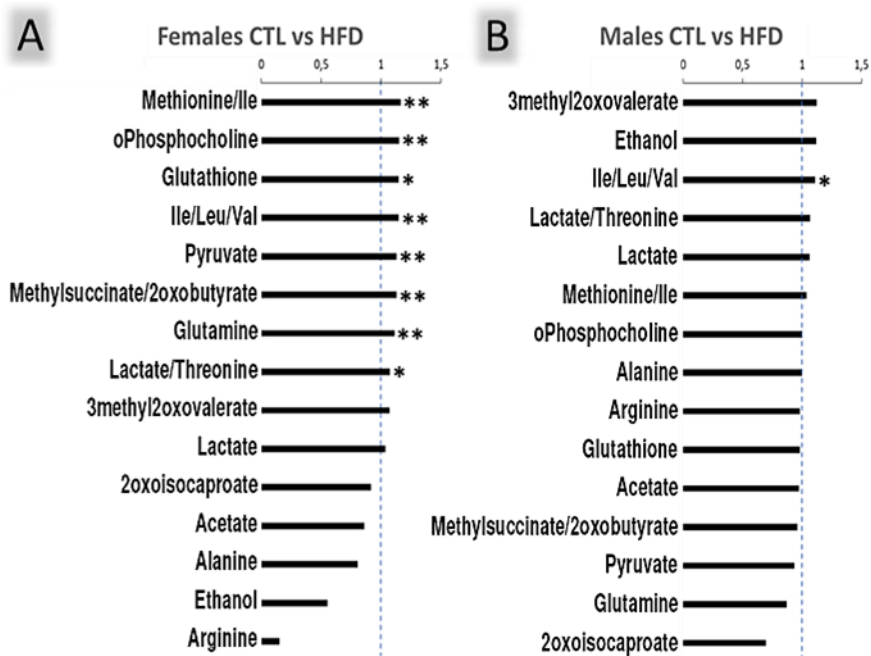


Figure R33. Significant metabolites in PLS-DA models for discrimination between HFD and control female and male rats, separately. VIP score bar plots for female rats (A) and male rats (B) show all the metabolites represented in decreasing order. Significant alterations are indicated by *. Adjusted p -values (Student's t -test corrected by Bonferroni method) to 0.003 (*), 0.00067 (**), 0.000067 (***).

In general, there is an overall alteration in the metabolism of adipocytes extracted from HFD rats compared with those extracted from CTL rats of both excretion and uptake of metabolites in the culture medium, as appreciable by observing the coloured boxes in Figure R34.

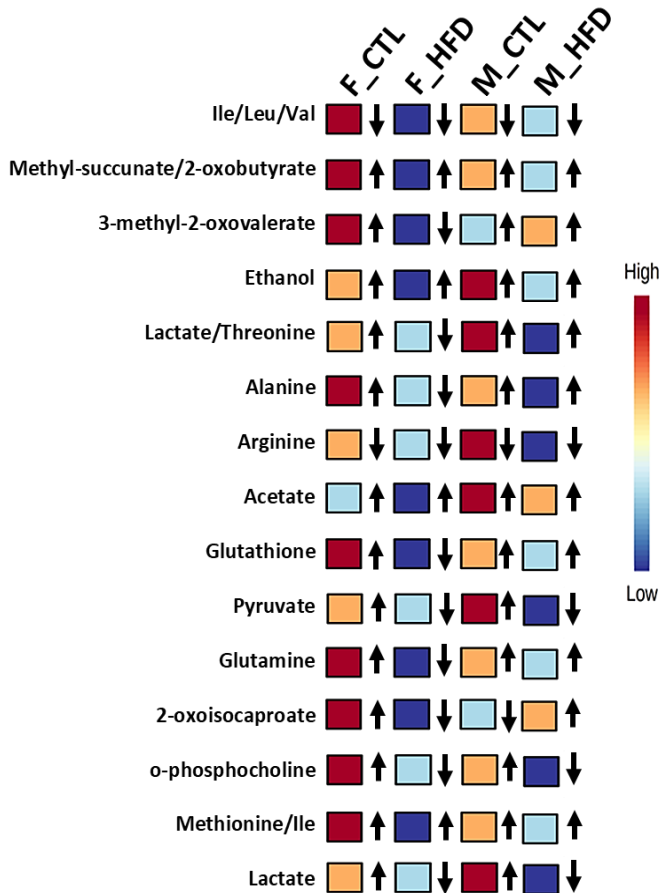


Figure R34. Comparison of the mean concentration of metabolic regions between HFD and control female and male rats. The coloured boxes show the mean concentration of the metabolites in the respective group net of their baseline levels. Blue and red boxes indicate metabolite levels that are lower or higher, respectively, between the four groups, whereas orange and light blue indicate intermediary levels. Down arrows indicate metabolites uptake compared to their baseline value in culture media; Up arrows indicate their excretion by cells. Abbreviations: F, females; M, males.

Focusing on the individual metabolites, it was possible to note differences in uptake/excretion related to diet and sex-specific. Concretely, in females, oPhosphocholine, glutathione, pyruvate, glutamine and lactate/threonine were the metabolites whose uptake/excretion was shifted, with a significant uptake from the medium by the adipocytes of the rats fed with a HFD, which is in contrast to their increased excretion in CTL. Differently, in males, O-phosphocholine, pyruvate, lactate (higher uptake) and 2-oxoisocaproate (higher excretion) levels were shifted from the medium by the adipocytes of the rats fed with a HFD, although no statistical significance was observed.

5.5.4. The effect of mannose on rat adipocytes and adipose tissue metabolism.

Mannose was the metabolite whose metabolomic concentration showed the most consistent change and resulted significantly positively associated with SEMs epigenetics alteration in the pathological condition in the Piancavallo cohort. High levels were positively related to diabetes and insulin resistance and were particularly involved in the metabolic syndrome and its clinical complications, probably representing a MetS common ground in severe obesity.

On this basis, we wanted to investigate if mannose could be related to the shift of the metabolism in adipose tissue and/or adipocytes in a well-controlled experimental MetS induced by a HFD rat model. Supplementation of the culture medium with the D-mannose Treatment Medium did not alter the metabolism of adipocytes either in cells or in tissue culture. The comparison of the spectra of blank D-mannose Treatment Medium and after the appropriate period of adipocytes and

adipose tissues treatment highlighted the lack of use of the metabolite by the adipocytes since the mannose concentration peaks appeared unaltered (data not shown).

Identifying the cell population capable of metabolizing and using mannose as occurs in human metabolism would be required different and more specific analytical strategies, showing that mannose may be probably metabolized by other cells than adipocytes.



6. DISCUSSION

6.1. The analysis of the metabolic profile of MHO and MUHO individuals can be supportive for a better and earlier classification of the MetS.

MetS has been widely reported around the world as being mainly related to central obesity, which is on the steep rise, and a sedentary lifestyle [172], both of which are modifiable. MetS is also directly related to an increased risk of developing coronary artery disease and related conditions [173]. For these reasons, individuals with MetS should be identified early to implement lifestyle modification strategies to reduce their metabolic alterations and cardiovascular risk factors [174].

In the Piancavallo population, we found a prevalence of MetS of 80.5 % in severely obese patients (77.8 % in W and 85.4 % in M) with an average increase of 10 % with age. These values seem very high if compared with previous studies conducted in Italy, where the prevalence of MetS among Italian adults in a general population study defined by ATP III was 18 % in women and 15 % in men and increased from 3% among subjects aged 20-29 years to 25 % in subjects aged 70 years and older [175]. In our cohort, the prevalence of MetS is abnormally high due to the clinically severe obesity context but in line with other studies on the prevalence of MetS in overweighted and obese subjects. In a study on Palestinian refugees, MetS prevalence among obese and overweight was 69.4 % according to IDF definition [176], whereas in Vietnam it was 41.6 % among overweight adults [177]. This strong heterogeneity in prevalence could be due to the different criteria used for MetS, ethnic variations,

genetics, environmental and cultural differences, study settings, and other risk factors. For these reasons, due to the multifactoriality of MetS and the synergy among its components, it is fundamental to stratify MUHO in MetS subgroups based on the number of parameters for a better characterization of the pathological state and to better understand its effects. For example, in our study, most patients were diabetic and hypertensive, two of the diagnostic components of MetS. Interestingly, the relationship between MetS and DM2 appears to be very strong, as found by Ahmed *et al.* who reported a 91.9 % prevalence of MetS in DM2 patients [178].

Therefore, we have investigated associations between MHO and MUHO, characterized by the absence or presence of MetS, and their clinical and metabolic parameters. We have determined an association between the development and progression of the disease and differences in the anthropometric parameters WC, WHR and BMI indicating a proportional relationship between the increase of MetS criteria and the growth of abdominal adipose tissue, exacerbated in presence of severe obesity. Interestingly, WC and WHR appear to correlate more significantly with the increase and fluctuations of adiposity due to age and represent better the differences between MHO and MetS.5 groups than BMI. BMI, although considered a valid tool for assessing overweight and obesity, it does not directly measure body fat composition [7] and it is influenced by the component of FFM, especially bone and muscle which are denser than fat. Therefore, BMI cannot always assess individual risk for endocrine and metabolic complications. Our results corroborate the importance of WC as a commonly used parameter to define central obesity and its vital role in diagnosing MetS. When confounders such as temperature, interday variations, age and sex and also ethnicity, which may significantly

influence WC measurement, are avoided, this parameter can correctly estimate the amount of abdominal fat, providing both independent and additive information to BMI for morbidity and mortality prediction [179]. Moreover, normally, elder people suffer a decrease in FFM, losing muscle mass and having low bone density, which leads to sarcopenia and frailty [180, 181] with a consequent reduction of body weight. On this basis, changes in BMI are related to progressive variations in weight, fibre consumption, physical activity and the presence of chronic diseases and their number, but do not directly reflect a change in abdominal fat. In these cases, BMI can underestimate FM [182], which can constitute the most relevant physiological metabolic and endocrine component, and its importance in the pathological state.

MetS is characterized as a progressive condition encompassing a wide range of disorders with specific metabolic abnormalities occurring at different times [183]. The relationships and mutual influences among the factors that characterize MetS are still not well known. In our cohort, the gradual, progressive, and steady change in the metabolic profile from the MHO condition to the extreme case of MetS.5 disease, and from youth to old age, evidenced by multivariate PLS-DA analyses, suggests that the metabolic status reflects the clinical progression. It thus helps to explain changes in the prevalence of clinical criteria identifying MetS and their involvement in the disease state of obesity, the condition generally most shared by MetS patients. MetS and its extreme case of MetS.5 disease appeared to primarily reflect variations in 13 metabolic pathways including aminoacyl-tRNA biosynthesis; fatty acid degradation; glycerolipid and glycerophospholipid metabolism; biotin metabolism; inositol phosphate metabolism and citrate cycle. Predictably, lipid metabolism prevails as a shared characteristic between MetS contributors in severe obesity. Besides

them, other studies have reported that the associations of MetS with BCAAs levels are the most biologically relevant [184]. This is because evidence suggests that BCAAs, aromatic amino acids and acylcarnitines may play an early role in insulin resistance, exposing defects in amino acid metabolism, the tricarboxylic acid cycle and β -oxidation [185]. In reality, in the context of severe obesity distinctive of our cohort, these amino acids maintain a solid statistical association with MetS but appear to be less significant than lipid markers and related metabolic pathways [186]. Interestingly, among the metabolites associated to extreme MetS, FACO, acetone and acetate, LDL, VLDL, leucine, alanine, proline, myo-inositol, glutamate, lysine, dimethylamine, glycolate, serine, 2-oxobutyrate, CCC and mannose have shown a significant or elevated VIP score in the model independently by age and constitute a common signature of MetS in severe obesity.

High levels of mannose, the metabolite whose concentration shows the most consistent change in the disease condition in all the Piacavallo cohort analyzed subgroups, were positively correlated with DM2 and insulin resistance and were significantly involved in the syndrome and its clinical complications [187]. Plasma mannose levels have been reported to be elevated in subjects with insulin resistance, although they appear independent of obesity [188]. Thus, mannose is a biomarker of insulin resistance which may be useful for the early identification of diabetic individuals with insulin resistance and increased risk of its complications such as chronic diseases including DM2, CVD and albuminuria [188, 189].

MetPA of age-independent extreme MetS' metabolites showed that most of them belonged to 10 metabolic pathways statistically significant which include glyoxylate and dicarboxylate metabolism; alanine, aspartate

and glutamate metabolism; fatty acid degradation; pyruvate metabolism; inositol phosphate metabolism; arginine and proline metabolism; glycolysis/gluconeogenesis; phosphatidylinositol signalling system; glycerophospholipid metabolism and glycerolipid metabolism. Many of these are probably related to abnormal metabolism of the three major nutrients of carbohydrates, lipids and proteins [190] and the well-known effect of the diet on the gut microbiome variety and functionality that can modify the nutrient intake from the diet in terms of quality and quantity, altering the metabolic pathways and influencing the susceptibility to obesity [191].

Pyruvate metabolism and glyoxylate and dicarboxylate metabolism are metabolic pathways related to carbohydrate metabolism; fatty acid degradation, glycerophospholipid metabolism, glycerolipid metabolism and phosphatidylinositol signalling system are metabolic pathways related to lipid metabolism; whereas alanine, aspartate, and glutamate metabolism is related to amino acid metabolism. Disruption of glyoxylate and dicarboxylate metabolism, strongly associated to altered gut microbiota and influenced by the metabolites glutamine, glutamate, and threonine, has been linked to mitochondrial dysfunction [192], which adversely affects the ability to detoxify reactive oxygen species (ROS), causing cellular damage and further leading to oxidative stress, strongly related to MetS and CVD [193]. Glycerophospholipid metabolism, along with primary bile acid biosynthesis, amino acid metabolism, and purine and pyrimidine metabolism, was found in a recent experimental study to be one of the targets of the treatment with *Lactobacillus* FRT10, being *Lactobacillus plantarum* a significant constituent of the health gut microbiota, to alleviate obesity in an obese mice animal model [194]. Moreover, in previous studies, decreased circulating levels of α -ketoglutarate and increased levels

of glutamate have suggested that glutamate accumulation increases the transamination of pyruvate into alanine, leading to the development of insulin resistance associated with obesity [195]. In fact, the increase in alanine, a highly gluconeogenic amino acid, contributes to the development of glucose intolerance in obesity, as circulating levels of alanine are elevated in obese subjects [196]. Finally, metabolites with a potential bacterial origin, specifically bile acids, short-chain fatty acids, branched-chain amino acids, trimethylamine N-oxide, tryptophan and indole derivatives are among the most significantly associated with metabolic disorders and MetS [197] and many studies suggest that metabolites that belong to the choline to trimethylamine pathways indicate the gut microbiome's state and the host/microbiota co-metabolism [198]. Our analysis revealed that the levels of choline- and methylamine-containing compounds were significantly reduced in severely obese individuals with MetS, compared with MHO.

On the other hand, although the issue continues to be debated, obesity itself would seem to have a "feedback effect" that alters the gut bacterial ecosystem and the corresponding host/microbiota co-metabolism [199]. The analyses of gut microbial pathways and gene families suggest that obesity is associated with a decreased capacity for transferring genetic material between bacteria through directional conjugation, important not only for bacterial evolution, but also for human health, and a reduction in superoxide reductase, potentially leading to intestinal oxidative stress [200], promoting low-grade inflammation, metabolic diseases and consequently CVD. The involvement of pathways such as metabolisms of pyruvate, metabolisms of arginine and proline, and metabolisms of methionine and cysteine in MetS in our analysis reflects this evidence. It is noteworthy that methionine, being an essential precursor of the primary

methyl donor SAM, is important for the methylation epigenetic processes [201], whereas cysteine is the limiting precursor of the major intracellular antioxidant glutathione [202].

This generalized characterization allows us to understand the complexity of the factors involved in the pathological state due to the strong interrelation between the external environment and internal metabolism, in which epigenetics also participates, and it points out the most involved processes, to focus on for prevention and treatments. It also shows the strong implication of adipose tissue at the metabolic level and its different distribution with age between men and women, highlighting the necessity of a better description of the specific influences of age-related sexual dimorphism in the disease state. To understand its role and effects, the results of its analysis will be thoroughly discussed in section 6.2.

6.2. The metabolome characterization may help to understand and manage the age-dependent sexual dimorphism on MetS prevalence in clinically severe human obesity.

The anthropometric, cardiometabolic and metabolomic profiles of MetS in the entire obese cohort have shown highly consistent age and sex differential effect patterns between MHO individuals and individuals MetS.5, who met all five criteria for MetS as extreme cases of MetS. To our knowledge, there is no previous literature directly focused on the identification of sex and age influences and differences in MetS profile in a cohort entirely composed of clinically severe obesity subjects metabolically healthy and diseased.

So, to explore the sexual dimorphism in the prevalence and the metabolic impact of MetS and its components in severe obesity, we focused our attention on MHO and MetS.5 groups. Men and women were analyzed in two age subgroups, equivalent to pre- and post-menopause, separately. Overall, according to the results obtained, the prevalence of MetS in severe obesity seemed to increase after age 54 in both sexes.

However, the proportion of women with MetS.5 increased sharply after this age, juxtaposing the modest increase seen in the same proportion of men. The increasing prevalence of hypertension in women with the age, reaching the men one, in which instead it is almost stable, shows the same prevalence profile of MetS.5. This may be associated with the reduction in sex hormone levels with menopause and ageing, facilitating alterations in blood pressure regulation and promoting hypertension and vascular ageing [203]. Women in fertile age are partially protected against vascular diseases as their ovaries produce sex hormones, principally estrogen that show direct effects on blood vessels inducing endothelium-dependent vascular relaxation [204] and maintaining a healthy cholesterol profile which counteracts the development of hypertension. Sex steroid receptors have been identified in vascular endothelium and smooth muscle. Moreover, recent literature suggests that LDL cholesterol, residual cholesterol, acetate and apolipoprotein B are positively associated with SBP change over time, whereas HDL particle size is negatively associated. Furthermore, serum lipids, particularly LDL- and VLDL-derived cholesterol as well as abnormalities in glucose metabolism are associated with the onset of hypertension [205].

Variations in fat accumulation and metabolism, strongly related to sex and age ranges and influenced by hormonal changes, are probably the

common cause for both. The variations in abdominal adipose cells structure and quantity, which can double in the elderly, but especially the worsening of fat tissue metabolism due to the change in sexual hormones actions, seem to be directly correlated with the doubling of the prevalence of MetS.5 in postmenopausal women. While in men the accumulation of visceral adiposity does not show to be related to sex hormonal changes during their entire life, in women it is known that estrogens level changes have an impact on energy metabolism and are related to worsening clinical outcomes with age [206]. Their influence, when reduced, would result in the transition from a gynoid to an android phenotype, closer to men's and related to a higher risk of weight-related health problems, especially CVD.

In particular, estradiol seems to prevent lipolysis in subcutaneous adipose tissue with subsequent reduction in visceral fat mass and accumulation of subcutaneous fat. It is unclear whether this effect on fat distribution is sufficiently supported and effective in severe obesity, especially due to the dangerous effects of a fat-enriched diet on metabolism and 'hypothalamic pituitary ovarian axis' perturbations [207]. However, also in this case, unequivocally, hormonal influences lead to a change in fat accumulation between fertile and postmenopausal ages. Whether in fertile age estrogens prevent the transformation of subcutaneous adipose tissue into visceral fat, this preventive role seems to be much less effective with menopause. Moreover, the age-related increase in visceral adiposity is an essential component of alterations in lipoprotein-lipid metabolism and plasma glucose homeostasis in middle-aged premenopausal women compared with young women [208]. These pathophysiological processes partly explain the changes in the prevalence of metabolic criteria and their contribution to the pathological state.

Remarkably, when the criteria were analysed one by one, we observed parallel rises with age for both sexes in all criteria except hyperglycemia. Men with severe obesity showed higher rates of hyperglycemia than women of equivalent age, with a sharp increase after age 54. The age-related decline in sex hormone function, in addition to a myriad of alterations, leads to changes in the quantity and structure of adipocytes, metabolism of adipose tissue and insulin sensitivity [209], which may be directly associated with the doubling of the prevalence of MetS.5 in postmenopausal women, reaching that of men, in whom it remains relatively constant. Interestingly, although some of these differences between men and women with MetS have been reported previously [210], this is the first time they have been observed in the context of severe obesity.

Not only the anthropometric characteristics but also the metabolomic traits reveal the strong relationship between adipose tissue, hormones, sex and age showing a different regulation of the metabolism in MHO and MetS.5 conditions between men and women. The comparison between these differences, in divergent sexes and age groups, allows us to understand better how the disease develops in women and men. In fact, in this study, we observed variations in how MetS affects the metabolome of severely obese men and women, focusing on mean differences, multivariate PLS-DA patterns, VIP scores, and Relative Fold Change between MHO and MetS.5 individuals by separating the analyses for sex. Most metabolites with a significant association with MetS and with a high contribution to multivariate models persist in all comparisons, suggesting common ground for the development of extreme MetS regardless of sex and age. However, we noticed higher differences between controls and MetS in men in both age groups and older individuals of both sexes.

Overall, our discoveries agree with previous studies, in which the principal components of the MetS in women and men have been characterized in different populations, such as Chinese and Indian [211, 212], although we have identified interesting new trends related to sex and hormonal changes. For a better comprehension of the role of estrogens in the metabolic impact of MetS in severe obesity, we separately analyzed women and men in age groups associated with the passage to menopause status. Since changes associated with menopause can persist for several years after the last ovulation, menopause is not a well-defined event in terms of physiology and overall metabolism. The status of menopause should be examined using accurate and precise criteria that are not easily applied in some patient groups. For this motivation, we have delineated two age groups, excluding the grey zone between the ages of 45 and 54, to include the larger majority of pre-menopausal and post-menopausal women. We noticed a sharp increase in the prevalence of MetS in the postmenopausal group, probably due to body composition and associated structural changes including fat distribution and decreased protective effects of estrogens. Related to this increased prevalence of MetS, the changes in MetS-related metabolites also showed a stronger intensity.

Interestingly, the lipid profiles of women and men with MetS showed similar elements but with different significance. We also observed that MetS affects acetone and acetate levels in premenopausal women, but not in postmenopausal, proposing that also the production of ketone bodies is affected by changes in fatty acid metabolism associated with menopause or MetS. It is known that FAs in the blood are transformed into ketone bodies when the concentration of FAs is high and insulin is low [213, 214]. The energy metabolism normally includes ketone bodies between its substrates both in the liver and in peripheral tissues. However, the

immoderate production of ketone bodies brings to their accumulation in the circulation and the acidosis of ketoacidosis and the development of ketosis, as it appears in diabetes. On the other side, women in the postmenopausal age group with MetS showed higher levels of carbonyls in FAs and low-density lipoprotein cholesterol, further supporting alterations in lipid metabolism and hormonal implications, and proposing the potential role of oxidative stress.

During fertile age, estrogens, produced in the ovaries using LDL cholesterol as substrate, have antioxidant properties that protect mitochondrial integrity and function [215]. However, in postmenopause, when the ovaries no longer possess oocytes and reach their functional exhaustion, the demand for estrogen decreases, to the point of cessation. Circulatory LDL cholesterol did not long be utilized to synthesize estrogens with a consequent decrease in estrogens production [216]. Hence, postmenopause is associated both with a rise in blood LDL cholesterol levels that leads to the switch to a clinical picture more related to the rising risk of cardiovascular problems. The metabolomic profile of obese women in a probably postmenopausal age group seems to represent a sort of intermediate position between younger and older obese men. Altogether, these results suggest that the protection against MetS provided by estrogens, and prolonged after menopause, is also accompanied by less severe modifications in the metabolome.

Our study establishes that the prevalence of MetS is higher in men than in women regardless of age and menopause. The impact on the distinct components of the MetS was different between men and women based on age. Young men (under 45 years) with MetS displayed similar but more intense metabolomic changes than those seen in women in both age groups,

which may likely be associated with different natures in individual MetS components. For instance, there was an increase in the percentage of men suffering from DM2 and/or hyperglycemia among the younger and older groups.

Our MetPA determined that in this subgroup the TCA cycle appears to be specifically affected and emerges as the most significant pathway at the expense of other pathways relevant in the context of severe obesity, such as metabolism of glycerophospholipids or fatty acid metabolism. The TCA cycle is a set of biochemical reactions used by all aerobic organisms to produce energy and it is robustly associated with mitochondrial function. The results also indicate that the age-related decrease in muscle mitochondrial function correlated neither with adiposity nor with insulin sensitivity. Interestingly, it has been reported a greater capacity for mitochondrial ATP production in men, while women are more sensitive to insulin, demonstrating a further dissociation between insulin sensitivity and muscle mitochondrial function [217]. We also noticed in the discrimination models that, in this subgroup of elderly men, the comparison of MHO and MetS.5 disclosed CCC as the major contributor to the models, leading to a more severe unfavourable cardiometabolic pathological profile. This is in line with the PREDIMED study in which plasma metabolites from the choline pathway have been associated with an increased risk of CVD [218]. These compounds have been proposed as proatherogenic by altering sterol metabolism, affecting platelet activation and thrombosis risk [219] and inhibiting reverse cholesterol transport, which is also sustained by cholesterol profiles [198]. Finally, BCAAs, metabolites related to metabolic disease and MetS in several studies, result among the most contributing metabolites only in the model for younger men, suggesting an early predisposition to CVD and a more dramatic effect

of metabolic disease in severe obesity on the metabolic core [220] and other pathways.

In summary, we analyzed the metabolome in well-phenotyped severely obese individuals and demonstrated that there is a strong sex-dependent association between MetS and circulating metabolites. Importantly, we have shown that metabolic dysregulation in women and men with severe obesity and MetS is age-dependent. Estrogens have a significant influence on adipose tissue function and metabolism and may be closely involved in determining the sexual dimorphism in both body composition and body fat distribution during fertile age. This sexual dimorphism in energy metabolism results to be maintained also in menopause, even if the action of estrogens ends, giving a temporal advantage that delays and slows the course of MetS. Moreover, the metabolic profiles of our study showed age-dependent sex differences in the impact of MetS that are consistent with cardiometabolic characterization. Although there is a common landscape for MetS in the metabolome of severe obesity, men over the age of 54 have been affected more extensively and intensively. These findings strongly support the need for further studies aimed at unravelling the mechanisms underlying this sex-specific metabolic dysregulation in severe obesity.

6.3. The role of metabolome-epigenome interaction in age- and sex-dependent incidence of MetS in clinically severe obesity.

Genetic predisposition, ageing, and sex contribute to epigenetic variability, and several environmental factors, including exercise and diet, further interact with the human epigenome. Since epigenetics is one of the

mechanisms that explain the influence of environmental factors on gene activity, there has been a growing interest in the past decade in the possible role of epigenetic mechanisms as a link between nutritional imbalances and the development of NCDs [221]. Among these conditions, great interest has been aroused by the link between the rapid change in dietary habits and the observed obesity and MetS phenotypes, since the alteration of epigenetic mechanisms can result in oxidative stress, insulin resistance, DM2, and vascular dysfunction in animals and humans [222].

Because DNA methylation is a key part of epigenome regulation, genome-wide (array-based) DNA methylation analysis is critical to better define the factors linking obesity to clinical MetS conditions and to characterize them. We have denoted the importance of the effect of old age in relation to sex on the interaction between the external environment and body metabolism, thus the epigenetic analysis could provide critical information for a complete view of the mechanism of action of the MetS. Methylation profiles and the epigenetic state of a sample of elder extreme MetS patients MetS.5, the most vulnerable to comorbidities, were compared through specific epigenetic analyses with those of MHO subjects matched for sex and age. The results suggested that the DNA global methylation levels between extreme cases MetS.5 and controls MHO are comparable. Although the differences at site levels were slight, the differential methylation analysis identified two statistically significant probes, hypomethylated cg19693031, belonging to the gene TXNIP, resulting in potential gene activation, and hypermethylated cg10474793 belonging to the genes MYLIP, resulting in potential gene inactivation.

The TXNIP gene has been associated with metabolic diseases such as hyperglycemia, hyperlipidemia, and diabetes in several studies [223-

225]. Moreover, TXNIP methylation was inversely and intensely associated with glycosylated haemoglobin (HbA1c) levels, particularly in diabetic patients with poor glucose control, underlying an association between the gene TXNIP and DM2 through epigenetic mechanisms [226]. Interestingly, our highlighted site cg19693031 is the top diabetes-linked methylation site and its hypomethylation significantly increases the risk of DM2 development, as suggested in EWAS [227]. This site has also been related to fasting blood glucose regulation [228]. As a component of the family of α -arrestins implied in regulating oxidative stress-sensitive signalling pathways related to insulin resistance, hypomethylated TXNIP, upregulates the expression of its coding protein forbids insulin transcription activity and stimulates the apoptosis of beta-cell.

On the other hand, MYLIP, the E3 ubiquitin-protein ligase also known as IDOL (inducible degrader of the LDL receptor) for its involvement in LDL cholesterol receptor regulation [229] and degradation, which in turn produces an elevation of plasma LDL-C and lead to hypercholesterolemia [230]. MYLIP correlates with familial hypercholesterolemia and the pathway of lipid metabolism and, although the hypermethylation of the cg10474793 probe has never been directly associated with them, MYLIP is reported among the genes that manifest a differential methylation profile associated with lipid traits in EWAS [231]. This gene seems to have also a clear biological and clinical importance in hypertriglyceridemia, plasma lipid metabolism regulation and alterations and atherosclerosis [232] being contained in one of at least ninety-five loci across the human genome that bear common variants associated with inter-individual variation in serum lipid concentration [233, 234]. Elevated methylation of MYLIP could decrease its gene expression and consequently increase the availability of LDL receptors. The

downregulation of MYLIP has also been associated with an increased risk of DM2, thus suggesting that increased LDL receptor-mediated intracellular cholesterol accumulation could be one of the first epigenetic changes to contribute to the pathogenesis of DM2 [235]. Finally, in some GWAS, both TXNIP and MYLIP seem to have a clear biological and clinical concurrently importance in hypertriglyceridemia and lipid metabolism alterations since they harbour common variants associated with serum lipid levels, specifically increased levels of cholesterol LDL and triglycerides [236].

These data are consistent with the metabolomic changes observed in our patients, in which FACO and LDL were the MetS' preminent and distinctive metabolites and with either the clinical characteristics of Mets in our cohort, primarily represented by the presence of hypertriglyceridemia and hypercholesterolemia. All of these relationships with alterations in lipid metabolism and metabolic diseases seem very interesting, not only because they are closely associated with MetS, but more importantly because they emphasize that the results of metabolomics and epigenetics, combined, globally reflect the clinical outcome of our patients. However, in this study, we were no able to identify significantly enriched areas at the regional level (genes, promoters and CpG islands).

It is now accepted that obesity can drive methylation change [237] with significant rearrangements in obese methylation profiles [238], also in MHO, and that each region has a specific meaning and task for gene activation and repression. With these assumptions, we could indeed hypothesize that the current result is due to the presence of severe obesity in all the subjects in the study that masks the subtler differences. This hypothesis seems to be supported by SEMs analysis that unexpectedly

highlighted in MHO controls a higher number of SEMs when compared to MetS.5, revealing that hypomethylation, rather than hypermethylation, mainly contributed to the epigenetic drift.

This certainly interesting evidence seems to indicate that obesity not only alters the epigenetic landscape at the methylation level but is also the main cause of increased epigenetic drift. Extreme MetS does not seem to aggravate further in its totality the epigenome degeneration of people suffering from clinically severe obesity because this altered body condition already submits them to a higher number of SEMs and epigenetic drift. In reality, this result could be considered a sort of artifact explained by the fact that MetS patients, following the diagnosis of the disease, underwent previous behavioural, pharmacological or para-pharmacological treatments that have attenuated the existing epigenetic alterations and offset their effects, preventing the onset of new SEMs related to them. Despite this, thanks to the metabolomics characterization of MetS, was possible to identify which metabolic alterations of this pathological state influenced the epigenetic drift more, correlating with a higher number of SEMs, through the metabolome-epigenome interplay. It is about specific characteristics at the basis of MetS and closely related to adipose tissue typology and metabolism as alterations in lipid profile [239], oxidative stress [240, 241] and inflammatory state [242, 243]. Once again, sexual dimorphism analysis revealed significant differences between men and women, as the epigenetic drift between MetS.5 and MHO was significantly greater in men than in women. It is known that epigenetic drift affects most of the genome, prefiguring the onset of (epi)genomic instability [244] and suggesting global deregulation of DNAm patterns with age with potential implications for ageing, stem cell biology and disease risk prediction [95]. So, assuming that a reduced drift overall correlates with a protective or less

dangerous epigenetic status, we could speculate that in women of fertile age, estrogens act "preventing" the accumulation of SEMs [245] and delaying further the manifestation of MetS phenotype. It would explain the visible effects of the lower difference between women of MHO and MetS.5 groups and men at the level of epigenetic deregulations. MHO women would also undergo preventive treatment against increased epigenetic drift, while MHO men would not. Estrogens have, in fact, a significant influence on adipose tissue function and metabolism.

The epigenetic discrepancy between men and women could be justified by the different quantity and increase of abdominal fat at fertile age [58], which would lead men to develop severe abdominal obesity and related health problems at a younger age than women. If in young people fat accumulation is a risk factor for morbidity and mortality [246], an increase in a more advanced age would be less dangerous, if not nearly favourable as postulated by the "obesity paradox". It suggests that, in a phase of life in which the ability to assimilate nutrients from food is physiologically reduced, elderly individuals who have a greater reserve of fat are more protected than those who do not. This would allow them to have less physiological body wasting and, in case of a debilitating disease, to have a more favourable clinical outcome.

The evidence of a discrepancy in the age of onset of the disease between obese men and women and their different metabolomic profiles led us to evaluate the epigenetic markers to obtain an estimate of various biological age measures (DNAm) (Steve Horvath's epigenetic clock). No differences between chronological age and Horvath's DNAmAge were observed both in the case and control groups.

However, it is known that obese subjects have higher DNA damage and epigenetic drift compared to normal-weight subjects [238, 247, 248] and that the rate of drift appears inversely proportional to longevity. The greater the degree of epigenetic drift, and the faster it occurs the shorter the lifespan. This is because the altered physiological state of obesity, causing general malfunction of the organism with premature ageing of the organs [249] and a higher increase in epigenetic age [107], adds up and accentuates the physiological epigenetic age-related conditions like shortening of the telomeres [250].

Metabolic alterations and related morbidities must be considered as further aggravating factors. The age estimator Grimage was strongly related to an excessive visceral fat and was associated with a range of age-at-menopause-related conditions including comorbidity count [105], showed globally increased values in MetS.5 cohort, pointing out a significant variation in the expected lifespan. So, MetS appear to further accelerate the biological ageing already caused by obesity.

Analysis of the genetic pathways most involved in and in turn affected by DNA methylation deregulation may explain these results. MetS patients showed hypermethylation in many pathways related to telomere maintenance and DNA repair, contributing potentially to worsening the epigenetic drift and hypomethylation in pathways involved in response to hydrogen peroxide and the defence against oxidative damage. These phenomena appear particularly interesting and interconnected since it was demonstrated that a reduction in the normal length of telomeres can be caused by factors like stress, inflammation and oxidative stress, which increase the amount of telomere loss during cell division [251, 252]. Moreover, many studies have found that a variety of lifestyle factors

including diet, smoking, alcohol abuse and exercise [253] can negatively or positively influence telomere length.

These results further highlight the complexity in analyzing a multifactorial pathology such as the MetS, strongly influenced by sex and age, and which development and progression depend on the balance between all the internal and external contributors, modifiable or not, involved. Precisely about sex, we noticed a clear and highly interesting distinction in Grimage Acceleration. Men have shown, on average, values much higher than women of similar chronological age, especially in MHO conditions. Among MetS groups instead, the values remained different but more comparable.

Synthesizing, men seemed to have a biological age, reflected by epigenetic age, higher, on average, than women of similar chronological age, regardless of the pathological state, even if extreme MetS worsened the outcome. Once again, the presence of sexual dimorphism is appreciated. The longer lifespan of women could be partly due to the "protective effect" of sex hormones of fertile age, which, also acting at the epigenetic level, would appear to allow obese women to reach menopause epigenetically younger, benefiting them from the negative effects of MetS on the epigenome. Because of this evidence, we might consider the Grimage Acceleration results as an additional epigenetic warning, especially for obese, albeit healthy, men about the negative effects of the altered interaction between metabolome and epigenome through the concomitant influence of gender and age. In light of these results, lifestyle changes are fundamental and the sooner these happen, the better the outcome.

6.4. Adipocytes from animals under different diets show metabolic changes similar to those observed in MetS in human severe obesity.

Obesity and associated metabolic complications have been linked to inflammation of white adipose tissue [254], principally the visceral one. However, the causal factors and the diet relationship remain unclear. Due to adipose tissue's function as an endocrine organ, inflamed adipocytes secrete, both local and systemically, proinflammatory cytokines, which in turn alter the body metabolism and the normal function of the adipose tissue itself [255]. It has been shown that an increase of visceral adipose tissue is strongly linked to MetS [256] and the results obtained in our retrospective study on the Piancavallo cohort confirm this evidence, pointing out a clear implication of increased visceral adipose tissue and its altered metabolism in the worsening clinical picture of MUHO and MetS.

Given the impossibility to obtain visceral adipose tissue samples from the subjects of the study cohort and the invasiveness of the procedure, we designed a well-controlled experimental diet-induced obesity model in both male and female rats. Reproducing the gain of body weight and fat gain characteristic of human obesity with more reliability than with genetic models, the HFD model allows a better study of their development and their risk factors and components. In a general view, if global body weight is controlled nearly equally by genotype and environment, body fat percentage and distribution appear to be much more influenced by diet and sexual dimorphism, respectively, with repercussions on adipose tissue metabolism and its endocrine role in both humans and rats [257, 258].

The analysis of rat fat tissue and the experiments on adipocytes

could be helpful to detect a sex-specific metabolic profile induced by the HFD of the adipose tissue to better characterize the metabolic disturbances of MetS caused by the diet on the adipose tissue of the obese Piancavallo cohort. The first important correspondence between experimental rats and the human cohort was observed in the presence of sexual dimorphism in the distribution and increase of adipose tissue. Overall greater body weight gain was seen in male rats in comparison to females, with a significantly greater difference between CTL and HFD.

However, the mean weight difference of epididymal fat pads was not significant in male rats but weight differences between periovarian fat pads in rat females were statistically significant on average. As observed in humans, male rats tend to accumulate more visceral fat from a young age than females, regardless of the diet, although inevitably a high-calorie HFD exacerbates the process. Conversely, in female rats, the HFD appears to have a stronger effect on modifying fat distribution. The HFD would therefore seem to counteract and reduce the beneficial effect of estrogens in preventing the transformation of subcutaneous adipose tissue into visceral fat and protecting against the development of metabolic and cardiovascular diseases.

If anthropometrically sexual dimorphism seems to play an almost primary role, the metabolism and metabolic profile of the adipocytes under examination appears to be primarily and strongly modified by the diet, regardless of sex, which assumes a secondary, although important, role. Methionine/isoleucine constituted the metabolomic spectral area most significantly different between CTLs and HFDs, indicating methionine and isoleucine metabolism as the most modified in HFD adipocyte cell cultures, with lower excretion in the culture medium. It is known that

altered methionine metabolism is associated with weight gain in obesity and that restriction of dietary methionine intake seems to ameliorate lipid profiles, reduce fat deposition and improve metabolic flexibility [259]. Instead, isoleucine prevents the accumulation of tissue triglycerides [260] and may help to develop lean body mass and to control blood sugar preventing diet-induced weight gain in rodents. Moreover, acute-isoleucine administration reduces postprandial glucose levels [261].

Glutamine was the metabolite whose metabolomic spectral area differed more between CTL and HFD in adipose tissue organ cultures, resulting to be less excreted in the culture medium of the HFD-fed rats than in the CTL group. Glutamine resulted to be downregulated in obesity and it has been reported possible linker between obesity and inflammation in human white visceral adipose tissue. It is, in fact, inversely associated with the inflammation of white adipose tissue and macrophage activation, larger fat cell size and higher body fat percentage independently of BMI [262].

HFD animals had fat pads with bigger dimensions, a more compact consistency and a lighter colour due to increased cellular fatty acid storage and a lower density of the capillaries. This indicated a possible alteration in their metabolism probably related to a cell hypertrophy condition of the HFD adipocytes, hypoxia and inflammation. Evidence of hypoxia in white fat tissue has been previously determined in genetically obese mice and HFD-obese mice [263]. Hypoxia is also a stimulus for the inflammatory response of macrophages and inhibits the differentiation of adipocytes from preadipocytes through increased expression and secretion of several inflammation-related adipokines. Low oxygen tension also stimulates glucose utilisation by human adipocytes, suggesting that hypoxia has a pervasive effect on adipocyte metabolism and underlies the inflammatory

tissue response in obesity and the subsequent development of obesity-associated diseases, particularly DM2 and MetS [264]. Petrus *et al.*, combining studies on human and mouse cell cultures, observed that glutamine supplementation treatment counteracts insulin resistance and reduces macrophage infiltration and levels of pro-inflammatory genes and proteins in adipocytes and white adipose tissue [262]. This would recreate the physiological metabolism of adipose tissue cells and reduce low-grade inflammation of adipose tissue, thereby improving its function in obesity.

Most of the metabolic pathways were found to be common to those identified as altered in the MetS in the Piancavallo cohort. This confirms the importance of adipose tissue metabolism related to Western diets in the development of altered and pathological metabolic status and suggests the transferability of the *in vitro* results to humans, validating our retrospective study on the MetS. Moreover, it is well established that the metabolic state of a cell affects its transcriptional activity through intermediate metabolites, including glucose and glutamine, that constitute substrates or co-substrates for chromatin-modifying enzymes. This supports the idea that visceral fat tissue metabolic micro-environment impacts the function of several cell types, indicating an important relationship also with MetS' epigenetic aspects.

Specifically, *in vitro* results confirm the important consequences of diet in the development of obesity and the metabolism of adipocytes and adipose tissue due to not only calorie overconsumption but especially its nutrient type and composition. Triglycerides are accumulated in the adipose tissue by adipocytes as far as constituting 65 % of the adipose tissue and about 90 % of the adipocyte mass. This overaccumulation, typical in HFD diets, causes adipocytes' hypertrophic morphology, as

shown and confirmed by the visual analysis of our CTL and HFD rat adipocyte cultures, and alters the correct functioning of the adipose tissue. This leads to an alteration in visceral fat composition and a complication in the vascularization of the adipose tissue, as the capillary density is not able to support its growth request. Reduced blood perfusion leads to hypoxic adipocytes and a macrophage response, leading to inflammation [265]. At an early stage, and probably more successfully and efficiently in MHO subjects, hypoxia can stimulate vascular remodelling and promote systemic energy expenditure in obesity [266]. However, in the later stages and in most of MUHO and MetS people, chronic inflammation is established with the activation of macrophages in the adipose tissue, production of pro-inflammatory cytokines, and induction of insulin sensitivity with consequently insulin resistance [267, 268]. Furthermore, hypertrophy and inflammation together contribute to impaired metabolism and impaired endocrine function with repercussions on the entire body's metabolism.

This facilitates all the digestive processes of sugars, which lead to the accumulation of fat. As a consequence, a positive feedback effect is generated with a significant synergic increase in the static index of insulin resistance up to the onset of DM2 and metabolic alterations typical of MetS. Mannose (D-mannose) is a six-carbon sugar widely distributed in the body as an oligosaccharide constituent of glycoproteins. Free mannose is a normal constituent in blood circulation and serum mannose concentration has been related to the increase in diabetic patients and correlates closely with blood glucose [269] and triglyceride concentrations [270]. In our Piancavallo cohort mannose was the metabolite most discriminant between MHO and pathological condition for the strong change of its concentration, higher in MetS. Elevated levels are positively

related to DM2 and insulin resistance and have been found particularly involved in MetS and its clinical complications [189], probably representing a syndromic common ground in severe obesity.

Nevertheless, in our *in vitro* experiments on rat adipocyte cell cultures, mannose supplementation, at a dose mimicking that found in the disease group, did not modify the metabolism of adipocytes. This suggests that, at the tested dose, its effect does not come from adipocytes but other cell populations, such as macrophages, correlated with the lymphocyte response to chronic inflammation and that the process required different and more physiological conditions to activate and manifest. It was shown that mannose opposes the lipopolysaccharide (LPS) -induced macrophage activation effect because of the inhibition of glucose metabolism and suppression of succinate-mediated hypoxia-inducible factor 1- α (HIF-1 α) activation and that mannose supplementation, at safe supraphysiological doses, ameliorates some human disease states [271]. Moreover, the soluble mannose receptor (sMR), whose serum levels were observed to be increased in obese rodents and humans, seems directly correlated with body weight. It binds the transmembrane receptor CD45 on macrophages and inhibits its phosphatase activity, playing a direct functional role in both macrophage activation and meta-inflammation [272].

Inflammatory infiltration of adipose tissue, due to macrophages, is one of the most frequent evidence of conditions in which obesity is associated with MetS [273]. Our results, therefore, do not exclude an involvement of mannose, but different and more specific analyses, such as immunohistochemistry, might be necessary to test and verify the mannose's action and effects on our experimental animal model of obesity

and MetS.

The metabolomic impact of HFD was different between female and male rats. Methionine/Ile was the most significant metabolic area in female HFD rats, whilst 3-methyl-2-oxovalerate was the most significant metabolite in male rats. Interestingly, these results are according with those of Merino *et al.* who in a study on asymptomatic subjects from a general human population, reported that 3-methyl-2-oxovalerate, joint with the BCAA metabolite 4-methyl-2-oxopentanoate, showed a nominal significant interaction with visceral fat only in men [274]. Moreover, 3-methyl-2-oxovalerate is considered a strong predictor of impaired fasting glycemia independent of glucose [274], highly related to the future risk of diabetes and CVD.

Male rats' samples showed fewer differences in metabolites and only BCAAs showed statistical significance. This result agrees with different studies in which BCAAs appeared among the most contributing metabolites to MetS only for younger men, indicating that the disease has a worse effect on the metabolic core and an early predisposition to CVD in severe obesity [275]. Leucine, isoleucine and valine homeostasis is determined largely by their catabolic activities in tissues [276]. BCAAs dysregulation, whose catabolism occurs predominantly in the mitochondria, could be both a cause and consequence of mitochondrial dysfunction. Increased catabolism of BCAAs, effecting an increase in their catabolic intermediates, can impair mitochondrial oxidation of glucose and lipids, leading to mitochondrial stress and impaired insulin secretion and action [277]. These led to insulin resistance and DM2 in obese animals, among which some rodent models, and humans.

These results support the presence of sexual dimorphism that refer from animals to humans and highlight the need for more studies on the diet's sex-related metabolic effects in clinically severe obesity.

6.5. Our findings may be relevant in providing the basis for the introduction of specific preventive and therapeutic interventions to improve the prognosis and quality of life of severely obese patients.

The relevance of this work lies above all in the innovative investigative opportunities of current interest offered by the cohort under study. A general population is commonly used for this type of research and normal-weight subjects are compared with subjects suffering from obesity. Here, however, the Piacavallo cohort is composed of well-phenotyped subjects with extreme obesity. This altered background condition in all the subjects represented a challenge for the discovery of specific differences and effects of MetS. As known, MHO subjects, although not affected by the health complications related to MetS, cannot be considered as normal weighted people and this changes the basic parameters of comparison of anthropometric, metabolic and epigenetic variations associated with MetS in our study.

The study allows a better understanding of the factors that distinguish this pathological condition, regardless of extreme obesity presence, considering the sexual dimorphism of MetS impact in two age groups, equivalent to pre- and postmenopausal women, with a special focus on MetS' role in the interplay between metabolome and epigenome in elder ages.

One of the medical fields most interested in personalized medicine is about CVD and correlated pathology, such as extreme obesity. Globally they remain one of the leading causes of death in the world, affecting especially older adults, with a diagnosis that typically occurs seven to ten years earlier in men compared to women.

The metabolomics characterization of the MetS and MHO shows a different metabolic profile between men and women and confirming the presence of anthropometric, cardiometabolic and metabolomic differential patterns of MetS in severe obesity highly consistent with sex and age. Moreover, at the epigenetic level, MetS resulted in methylation alterations strongly related to hyperglycemia, hypercholesterolemia, diabetes and atherosclerosis, as well as premature ageing.

Our analysis enabled the identification of metabolic fingerprinting that may underlie the higher rates of cardiometabolic disease commonly observed among older men. It also highlighted that, although comparable in the clinical diagnosis by the number of pathological parameters and their correspondence, men and women are distinct at the metabolic and epigenetic level, responding certainly in a different way, and better for women, to the perturbations caused by obesity and MetS. Despite the prevalence of the disease rise strongly in postmenopausal women, their metabolomic profile and pathways involved in MetS appear to hold themselves in a sort of intermediate situation between men under 46 years and men of comparable age.

Moreover, although MetS has a sex-independent common basis, related to the production of cytokines and FFA from part of abdominal adipose tissue with consequent insulin resistance, hypertension and

dyslipidemia, women seem to require a higher degree of adiposity to achieve the same metabolic disorders of men. This is because they show a more favourable fat distribution that seems to guarantee them a sort of protection beyond menopause which is reflected in the constant gap between men's and women's metabolism. The switch from MHO to MUHO, and the worsening of the severity of the MetS, appears associated with a change in the energetic metabolism and a delayed visceral fat accumulation due, in women, to the modulation of sexual hormones. Interacting and modifying the metabolomic profile of the MetS from youth to menopause, estrogens provide some sort of protection that allows women to remain “metabolically younger” even in oldness when their influence is reduced. This protective effect can become the object of clinical treatments to improve their outcome.

This mechanism can be described as the Falconer threshold effect [278, 279], a liability threshold model often employed in medicine and genetics to model and intervene in risk factors that contribute to disease. The Falconer model, introducing the concept of the threshold effect, postulates the idea that each of us is capable of expressing a character and has its threshold value [280], which can be higher or lower, polygenic and Gaussian. People with MetS are exposed not only to genetics but also to an exposome, the set of internal and external "environmental factors" including epigenetic drift, body composition and fat distribution, diet and lifestyle, alteration of host/microbiota co-metabolism and metabolomic profile, endocrine action of adipose tissue, hormonal influence, sex and age, that would push toward the MetS development or counter it, with more or less strength, in a sort of "tug of war" similar effect. Subjects in which the susceptibility factors exceed a critical value will manifest the phenotype. In essence, when the threshold effect is exceeded, the MetS

occurs.

Although rarely, even people of normal weight can be “metabolically unhealthy normal-weight” (MUH-NW) [281], developing metabolic diseases and MetS. In people suffering from obesity, this "push" towards the threshold is exacerbated by obesity itself. For this reason, the risk assessment in severely obese patients with MetS must be considered separately from that of normal-weight patients and appropriately stratified, identifying at an early stage who has crossed the pathological threshold and the contributors or protectors involved. If these patients are subjected to proper treatment, one or more of the pushes that lead to the disease is reduced or cancelled and the clinical outcome is improved.

Basically, by acting on external environmental factors thanks to the treatment, there is a direct action on the metabolic factors. Since the latter interconnects with the epigenetic factors, there is, therefore, a reflected action on the latter as well, reducing the alterations affecting the epigenome and consequently the dangerous epigenetic drift (Figure D1).

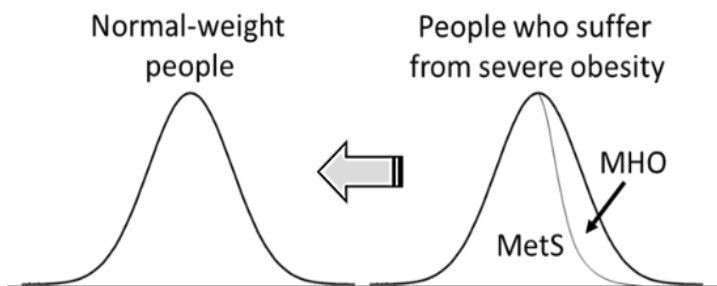


Figure D1. Graphic representation of the Falconer threshold effect [279] applied on the epigenetic drift in obesity.

In this contest, a diagnosis of MetS seems to be a preventive if not "curative" factor against epigenetic drift and its consequences. Moreover, the higher the number of MetS criteria, leading to worse disease diagnosis, the stronger the interventional treatment. The results obtained bring to light the need for studying in-depth metabolic and epigenetic changes and their specific biomarkers involved in the development and characterization of the disease in different stages of life and sex, as a fundamental step for identifying and stratifying people at risk, rather than just using current clinical parameters. This constitutes the premise for new preventive and therapeutic strategies and therapies based on nutritional interventions on host/microbiota co-metabolism based on the sum of patients' specific biological and clinical characteristics to understand how to act on them in a personalized way.

The well-controlled adipocyte cell culture from HFD or CTL diet can establish cause-and-effect relationships between diet and metabolic health, with a special focus on the impact of the HFD on the fat characteristics and metabolism which might be transferred to humans with MetS. Once again, diagnosis and treatment of MetS could have a beneficial effect, improving the quality and duration of life of the patients.

Larger resources should be invested, moreover, to improve the study of the effects of the diet on the epigenetic landscape and the possibility offered by methylation levels of estimating the real biological age, comparing it with the chronological one. In particular, the reduction in caloric intake without malnutrition, defined as caloric restriction (CR), has been demonstrated to increase the lifespan of several organisms [282] and delay age-related methylation drift [283]. Nutrition plays a significant role in epigenome modulation, and an increasing amount of data indicates that

dietary modifications can alter the epigenetic signs associated with ageing [284]. The reduction of oxidized lipids as an effect of CR [285] is particularly important because they were found to be the first metabolite involved in the MetS at a metabolomic level and significantly correlated to epigenetic alterations. As strong indicators of oxidative stress, damage, and inflammation directly related to ageing, their reduction contributes to improving life expectancy. Moreover, CR has been shown to reduce adiposity and improve the metabolic profile in primates ameliorating their survival and their lifespan [286]. These results suggested that similar effects might be transposed to humans [287]. Last but not least, sexual dimorphism must also be considered in the context of treatments based on nutrition due to the interaction between diet and sex hormones. A sex-specific diet, that also takes age into account, would lead to a greater reduction in metabolic ageing which would also be reflected in a "temporal advantage" on epigenetic ageing and would result in less risk of developing diseases related to ageing [288].

Even if further studies are necessary to discover how to act practically against the contributors to the pathological metabolism represented by MetS and their interactions, the information obtained in this thesis appears interesting and promising, and with high clinical relevance to improving severely obese patients' prognosis and their quality of life.

6.6. Limitations of the study.

This study has some structural and experimental limitations. Firstly, the subjects under study suffered all from clinically severe obesity. This condition, also in MHO subjects, already plays an important role in

epigenetic modifications, and correspondingly on the metabolomics landscape, that somehow could mask the effects of MetS. Moreover, all individuals were of Western European ancestry and it is difficult to extrapolate these data to other populations.

Secondly, we used MetS as an indicator of cardiometabolic dysregulation. It is important to realize that there are various definitions of MetS and this syndrome is heterogeneous. To optimize external validation, we used the most widely used definition from IDF.

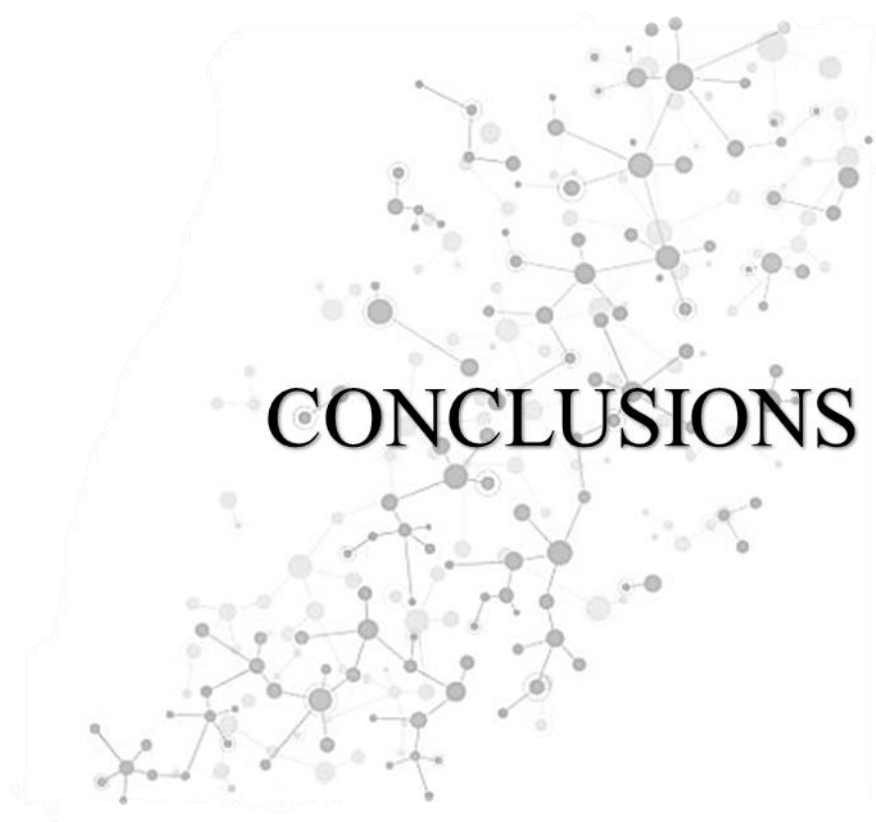
Thirdly, our cohort included an unequal number of men and women. However, we stratified the analysis by sex and age to overcome potential bias, assuming that the age range chosen (as inclusion criteria) could make men and women comparable, as postmenopausal women are no longer subjected to the action of estrogens. We did not assess the actual menopause, but the age of the group relative to the menopause transition, which could add some bias to the results in terms of interpretation. Numerous potential lifestyle factors could still influence the sex differences found in this study beyond biological mechanisms, such as adverse eating patterns, smoking behaviour, or alcohol consumption.

Fourthly, both metabolomics and epigenetics analyses of the human cohort were conducted only on the serum and the DNA of blood cells, respectively. On the contrary, in the HFD rat animal model, only the adipose tissue was analysed. So, even if the metabolomics analysis method was the same, the difference in the results obtained was probably caused by the tissue studied. Therefore, further studies of other tissues (eg adipose tissue in humans and serum samples in HFD rats) could be required to deepen and confirm these preliminary observations.

Fifth, the cohort enrolled in the study is vast but the results of the epigenetics analysis represent only a subset of subjects. We must

emphasize that a larger sample size could better estimate the normal DNA methylation ranges for each locus. For example, to explore the possibility that sex diversity is an epigenetic confounding variable it could be interesting to split the entire cohort by analysing men and women separately. While being aware that the split could be detrimental to statistical power, the epigenetic results obtained seem to support the hypothesis of a "temporal advantage" related to metabolic ageing provided to women by estrogens. Larger resources should be invested, moreover, to improve the study of the effects of the diet on the epigenetic landscape and the possibility offered by methylation levels of estimating the real biological age, comparing it with the chronological one.

Finally, current methods to study mature fat cell biology using primary cell cultures have limitations related to the difficulties of good maintenance of their viability and function. Rodent adipocytes, especially if hypertrophic, are more fragile than human adipocytes and the procedures for their isolation and seeding are complex. Collagenase digestion could be also liable for phenotypic changes such as the decrease in adipocyte marker gene expression and the induction of pro-inflammatory factors. Moreover, the inter-individual variability and the diversity among adipocytes within a fat depot, due to the presence of several populations of white and beige adipocytes with unique metabolic and endocrine properties, could result in differential responses to exogenous stimuli and cell treatments.



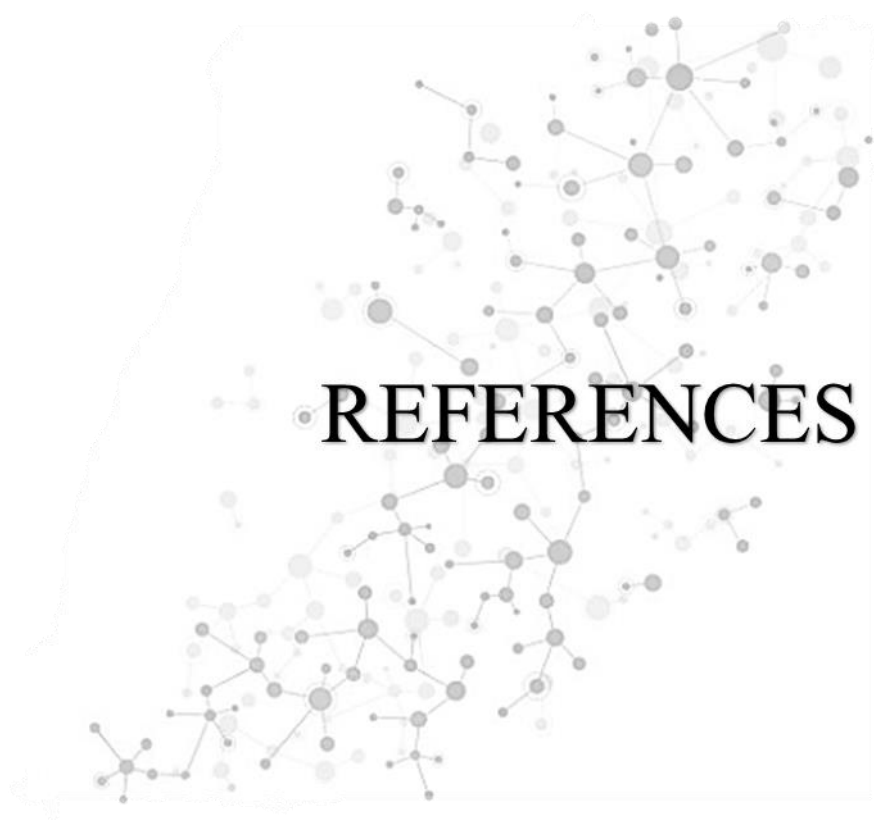
7. CONCLUSIONS

- 1) The prevalence of MetS in the Piancavallo cohort is higher in men than in women regardless of age and menopause status.
- 2) The metabolic profiles of the Piancavallo cohort showed age-dependent sex differences in the impact of MetS on host/microbiota co-metabolism and metabolic pathways involved which are consistent with the cardiometabolic characterization.
- 3) Although there is a common ground for MetS in the metabolome of severely obese individuals, the differences between women and men in the strong association between MetS and circulating metabolites indicate that their metabolic dysregulation is age- and sex-dependent.
- 4) Mannose and glycogen fragments could be potential novel biomarkers of MHO whereas the reduction of choline-containing compounds constituted the metabolite most significantly associated with MetS in the entire population.
- 5) The global metabolic profiles showed differences between MHO and MetS.5 at both age ranges. Whereas acetone and acetate and polyunsaturated fatty acids (PUFAs) were the metabolites most significantly associated with MetS.5 in younger ages whereas in older ages FACO₂, pyruvate and succinate showed the most important contribution in the older age group. Carbonyls in fatty acids (FACO₂), LDL particles, and acetate and derivatives revealed common trends regardless of age in the impact of MetS.5

CONCLUSIONS

- 6) The metabolic and epigenetic profiles of the Piancavallo cohort were in line with the difference between chronological age and biological (epigenetic) age between MHO and MUHO men and women, indicating that men older than 54 were affected more extensively and intensively.
- 7) The epigenetic analyses indicated that extreme MetS state and male sex correlate to accelerated ageing, whereas women seemed to be “metabolically/physiologically younger” thanks to estrogen's protective effect.
- 8) Epigenetic DNA methylation analyses, revealing hypermethylation of MYLIP and hypomethylation of TXNIP, and metabolomic analysis indicated an association between levels of protein carbonylation, oxidized lipids and severe obesity, suggesting an important role in oxidative stress and the development of MetS.
- 9) Severe obesity conditioned stochastic epigenetic mutations by enhancing hypomethylations rather than hypermethylations in MetS.5 compared to MHO. The decrease in epimutations in MetS.5 was positively associated with myoinositol, but negatively associated mainly with mannose, VLDL2, LDL2, FACO2, and creatinine. The decrease in SEMs in MetS.5 groups seemed to be much more pronounced in men than in women.
- 10) Experimental rat adipocyte models indicate that visceral adipose tissue metabolism appears to be influenced by diet and sexual dimorphism in a manner corresponding to humans and could clarify its endocrine role in the metabolic and metabolomic changes observed in severe human obesity and MetS.

- 11) HFD induced metabolic changes in cultured rat adipocytes that belonged to pathways that are shifted also in the differential profiles of MetS patients compared to MHO subjects, indicating the importance of diet in metabolic dysregulation.
- 12) Rat adipocyte cell assays could be used as a translational *in vitro* model to corroborate the hypotheses derived from the study on the Piancavallo cohort about identifying metabolomic biomarkers induced by diet and sexual dimorphism.
- 13) Metabolic profiling by NMR and epigenetic studies can be useful for the identification of new potential therapeutic targets through sex- and age-risk stratification and consequently retrieve on the clinically severe obese patient by the prevention, early detection, characterization of the disease, and the design of new therapies for a more personalized medicine



8. REFERENCES

1. World Health Organization. Obesity and Overweight Fact Sheet N. 311. WHO. 2016. Jun. Available from: www.who.int/mediacentre/factsheets/fs311/en/
2. Caballero B. The global epidemic of obesity: An overview. *Epidemiologic reviews* (2007); **29**(1):1-5. doi: 10.1093/epirev/mxm012
3. Agha M, Agha R. The rising prevalence of obesity: Part A: Impact on public health. *Int J Surg Oncol (N Y)* (2017); **2**(7):e17. doi: 10.1097/IJ9.000000000000017
4. Global Burden of Metabolic Risk Factors for Chronic Diseases Collaboration. Cardiovascular disease, chronic kidney disease, and diabetes mortality burden of cardiometabolic risk factors from 1980 to 2010: A comparative risk assessment. *Lancet Diabetes Endocrinol* (2014); **2**(8):634-47. doi: 10.1016/S2213-8587(14)70102-0
5. Wang W, Hu M, Liu H, Zhang X, Li H, Zhou F, Liu Y, Lei F, Qin J, Zhao Y, Chen Z, Liu W, Song X, Huang X, Zhu L, Ji Y, Zhang P, Zhang X, She Z, Yang J, Yang H, Cai J, Li H. Global burden of disease study 2019 suggests that metabolic risk factors are the leading drivers of the burden of ischemic heart disease. *Cell Metab* (2021); **33**(10):1943,1956.e2. doi: 10.1016/j.cmet.2021.08.005
6. Barness LA, Opitz JM, Gilbert-Barness E. Obesity: Genetic, molecular, and environmental aspects. *Am J Med Genet A* (2007); **143A**(24):3016-34. doi: 10.1002/ajmg.a.32035
7. Rothman KJ. BMI-related errors in the measurement of obesity. *Int J Obes (Lond)* (2008); **32 Suppl 3**:56. doi: 10.1038/ijo.2008.87
8. Daniels SR. The use of BMI in the clinical setting. *Pediatrics* (2009); **124 Suppl 1**:35. doi: 10.1542/peds.2008-3586F
9. Ghesmaty Sangachin M, Cavuoto LA, Wang Y. Use of various obesity measurement and classification methods in occupational safety and health research: A systematic review of the literature. *BMC Obes* (2018); **5** doi: 10.1186/s40608-018-0205-5

REFERENCES

10. Hales CM, Carroll MD, Fryar CD, Ogden CL. Prevalence of obesity and severe obesity among adults: United States, 2017-2018. *NCHS Data Brief* (2020); (360):1-8.
11. Ward ZJ, Bleich SN, Cradock AL, Barrett JL, Giles CM, Flax C, Long MW, Gortmaker SL. Projected U.S. state-level prevalence of adult obesity and severe obesity. *N Engl J Med* (2019); **381**(25):2440-50. doi: 10.1056/NEJMsa1909301
12. Nestle M, Jacobson MF. Halting the obesity epidemic: A public health policy approach. *Public Health Rep* (2000); **115**(1):12-24.
13. James WPT. The fundamental drivers of the obesity epidemic. *Obes Rev* (2008); **9 Suppl 1**:6-13. doi: 10.1111/j.1467-789X.2007.00432.x
14. Singla P, Bardoloi A, Parkash AA. Metabolic effects of obesity:A review. *World journal of diabetes* (2010); **1**(3):76-88. doi: 10.4239/wjd.v1.i3.76
15. Bleich S, Cutler D, Murray C, Adams A. Why is the developed world obese? *Annu Rev Public Health* (2008); **29**:273-95. doi: 10.1146/annurev.publhealth.29.020907.090954
16. Poirier P, Giles TD, Bray GA, Hong Y, Stern JS, Pi-Sunyer FX, Eckel RH. Obesity and cardiovascular disease: Pathophysiology, evaluation, and effect of weight loss. *Arterioscler Thromb Vasc Biol* (2006); **26**(5):968-76. doi: 10.1161/01.ATV.0000216787.85457.f3
17. Loos RJF, Bouchard C. FTO: The first gene contributing to common forms of human obesity. *Obes Rev* (2008); **9**(3):246-50. doi: 10.1111/j.1467-789X.2008.00481.x
18. Yang W, Kelly T, He J. Genetic epidemiology of obesity. *Epidemiol Rev* (2007); **29**:49-61. doi: 10.1093/epirev/mxm004
19. Espinoza García AS, Martínez Moreno AG, Reyes Castillo Z. The role of ghrelin and leptin in feeding behavior: Genetic and molecular evidence. *Endocrinol Diabetes Nutr (Engl Ed)* (2021); doi: 10.1016/j.endinu.2020.10.011

20. Álvarez-Castro P, Sangiao-Alvarellos S, Brandón-Sandá I, Cordido F. [Endocrine function in obesity]. *Endocrinol Nutr* (2011); **58**(8):422-32. doi: 10.1016/j.endonu.2011.05.015
21. Høgild ML, Bak AM, Pedersen SB, Rungby J, Frystyk J, Møller N, Jessen N, Jørgensen JOL. Growth hormone signaling and action in obese versus lean human subjects. *Am J Physiol Endocrinol Metab* (2019); **316**(2):E333-44. doi: 10.1152/ajpendo.00431.2018
22. Piaggi P. Metabolic determinants of weight gain in humans. *Obesity (Silver Spring)* (2019); **27**(5):691-9. doi: 10.1002/oby.22456
23. Oussaada SM, van Galen KA, Cooman MI, Kleinendorst L, Hazebroek EJ, van Haelst MM, Ter Horst KW, Serlie MJ. The pathogenesis of obesity. *Metabolism* (2019); **92**:26-36. doi: 10.1016/j.metabol.2018.12.012
24. Karelis AD, Faraj M, Bastard J, St-Pierre DH, Brochu M, Prud'homme D, Rabasa-Lhoret R. The metabolically healthy but obese individual presents a favorable inflammation profile. *J Clin Endocrinol Metab* (2005); **90**(7):4145-50. doi: 10.1210/jc.2005-0482
25. Zembic A, Eckel N, Stefan N, Baudry J, Schulze MB. An empirically derived definition of metabolically healthy obesity based on risk of cardiovascular and total mortality. *JAMA Netw Open* (2021); **4**(5):e218505. doi: 10.1001/jamanetworkopen.2021.8505
26. Appleton SL, Seaborn CJ, Visvanathan R, Hill CL, Gill TK, Taylor AW, Adams RJ. Diabetes and cardiovascular disease outcomes in the metabolically healthy obese phenotype: A cohort study. *Diabetes Care* (2013); **36**(8):2388-94. doi: 10.2337/dc12-1971
27. Chen G, Arthur R, Iyengar NM, Kamensky V, Xue X, Wassertheil-Smoller S, Allison MA, Shadyab AH, Wild RA, Sun Y, Banack HR, Chai JC, Wactawski-Wende J, Manson JE, Stefanick ML, Dannenberg AJ, Rohan TE, Qi Q. Association between regional body fat and cardiovascular disease risk among postmenopausal women with normal body mass index. *Eur Heart J* (2019); **40**(34):2849-55. doi: 10.1093/eurheartj/ehz391

28. Stefan N. Causes, consequences, and treatment of metabolically unhealthy fat distribution. *Lancet Diabetes Endocrinol* (2020); **8**(7):616-27. doi: 10.1016/S2213-8587(20)30110-8
29. Park J, Park D, Song Y, Kim JO, Choi J, Kwon Y, Kim S, Lee J, Hong K. Understanding the genetic architecture of the metabolically unhealthy normal weight and metabolically healthy obese phenotypes in a Korean population. *Sci Rep* (2021); **11**(1):2279. doi: 10.1038/s41598-021-81940-y
30. Sinatoro RV, Chagas EFB, Mattera FOP, Mellem LJ, Santos ARdOD, Pereira LP, Aranão ALdC, Guiguer EL, Araújo AC, Haber JFDS, Guissoni LC, Barbalho SM. Relationship of inflammatory markers and metabolic syndrome in postmenopausal women. *Metabolites* (2022); **12**(1) doi: 10.3390/metabo12010073
31. Galvão-Moreira LV, Nascimento ACB, D'Albuquerque IMSC, Sousa MAS, Brito HO, Nascimento MdDSB, da Costa Chein MB, Brito LMO. Hormonal, metabolic and inflammatory circulating biomarker profiles in obese and non-obese Brazilian middle-aged women. *PLoS One* (2019); **14**(9) doi: 10.1371/journal.pone.0222239
32. Zhou Z, Macpherson J, Gray SR, Gill JMR, Welsh P, Celis-Morales C, Sattar N, Pell JP, Ho FK. Are people with metabolically healthy obesity really healthy? A prospective cohort study of 381,363 UK biobank participants. *Diabetologia* (2021); **64**(9):1963-72. doi: 10.1007/s00125-021-05484-6
33. Kershaw EE, Flier JS. Adipose tissue as an endocrine organ. *J Clin Endocrinol Metab* (2004); **89**(6):2548-56. doi: 10.1210/jc.2004-0395
34. Arner P. Fat tissue growth and development in humans. *Nestle Nutr Inst Workshop Ser* (2018); **89**:37-45. doi: 10.1159/000486491
35. Zhu X, Ma S, Eirin A, Woollard JR, Hickson LJ, Sun D, Lerman A, Lerman LO. Functional plasticity of adipose-derived stromal cells during development of obesity. *Stem Cells Transl Med* (2016); **5**(7):893-900. doi: 10.5966/sctm.2015-0240
36. Charrière G, Cousin B, Arnaud E, André M, Bacou F, Penicaud L, Casteilla L. Preadipocyte conversion to macrophage. evidence of

- plasticity. *J Biol Chem* (2003); **278**(11):9850-5. doi: 10.1074/jbc.M210811200
37. Vykoukal D, Davies MG. Vascular biology of metabolic syndrome. *Journal of Vascular Surgery* (2011); **54**(3):819-31. doi: 10.1016/j.jvs.2011.01.003
38. Pi-Sunyer X. The medical risks of obesity. *Postgrad Med* (2009); **121**(6):21-33. doi: 10.3810/pgm.2009.11.2074
39. Haslam DW, James WPT. Obesity. *Lancet* (2005); **366**(9492):1197-209. doi: 10.1016/S0140-6736(05)67483-1
40. Eckel RH, Grundy SM, Zimmet PZ. The metabolic syndrome. *Lancet* (2005); **365**(9468):1415-28. doi: 10.1016/S0140-6736(05)66378-7
41. Kraemer FB, Ginsberg HN, Gerald M. reaven, MD: Demonstration of the central role of insulin resistance in type 2 diabetes and cardiovascular disease. *Diabetes Care* (2014); **37**(5):1178-81. doi: 10.2337/dc13-2668
42. Alberti KGMM, Zimmet P, Shaw J. The metabolic syndrome--a new worldwide definition. *Lancet* (2005); **366**(9491):1059-62. doi: 10.1016/S0140-6736(05)67402-8
43. Huang PL. A comprehensive definition for metabolic syndrome. *Dis Model Mech* (2009); **2**(5-6):231-7. doi: 10.1242/dmm.001180
44. Tenenbaum A, Motro M, Schwammenthal E, Fisman EZ. Macrovascular complications of metabolic syndrome: An early intervention is imperative. *Int J Cardiol* (2004); **97**(2):167-72. doi: 10.1016/j.ijcard.2003.07.033
45. Eckel-Mahan K, Ribas Latre A, Kolonin MG. Adipose stromal cell expansion and exhaustion: Mechanisms and consequences. *Cells* (2020); **9**(4) doi: 10.3390/cells9040863
46. Bonora BM, Marescotti M, Marcuzzo G, Avogaro A, Fadini GP. Synergistic interactions among metabolic syndrome components and homeostasis model assessment of insulin resistance in a middle-aged general population over time. *Metab Syndr Relat Disord* (2015); **13**(4):171-8. doi: 10.1089/met.2014.0163

REFERENCES

47. Povel CM. Components of the Metabolic Syndrome: Clustering and Genetic Variance [Ph.D. on the Internet]. Netherlands: Wageningen University and Research; 2012 Available from: <https://www.proquest.com/dissertations-theses/components-metabolic-syndrome-clustering-genetic/docview/2568605576/se-2?accountid=14777>
48. Faraj M, Lu HL, Cianflone K. Diabetes, lipids, and adipocyte secretagogues. *Biochem Cell Biol* (2004); **82**(1):170-90. doi: 10.1139/o03-078
49. Sowers JR. Insulin resistance and hypertension. *Am J Physiol Heart Circ Physiol* (2004); **286**(5):1597. doi: 10.1152/ajpheart.00026.2004
50. Huang PL. A comprehensive definition for metabolic syndrome. *Dis Model Mech* (2009); **2**(5-6):231-7. doi: 10.1242/dmm.001180
51. Sutherland JP, McKinley B, Eckel RH. The metabolic syndrome and inflammation. *Metab Syndr Relat Disord* (2004); **2**(2):82-104. doi: 10.1089/met.2004.2.82
52. Hotamisligil GS. Inflammation and metabolic disorders. *Nature* (2006); **444**(7121):860-7. doi: 10.1038/nature05485
53. Raparelli V., Sansone A., Napoleone L., Romiti G.F., Tucci C., Tosti G., Vernile A., Santoliquido M., Romanelli F., Basili S. La sindrome metabolica: Un modello clinico-terapeutico di endocrinologia di genere. *L'Endocrinologo* (2018); **19**:123–127. doi: 10.1007/s40619-018-0448-x
54. Miller VM. Why are sex and gender important to basic physiology and translational and individualized medicine? *Am J Physiol Heart Circ Physiol* (2014); **306**(6):781. doi: 10.1152/ajpheart.00994.2013
55. Tokatli MR, Sisti LG, Marziali E, Nachira L, Rossi MF, Amantea C, Moscato U, Malorni W. Hormones and sex-specific medicine in human physiopathology. *Biomolecules* (2022); **12**(3) doi: 10.3390/biom12030413
56. Ford ES, Giles WH, Dietz WH. Prevalence of the metabolic syndrome among US adults: Findings from the third national health and nutrition examination survey. *JAMA* (2002); **287**(3):356-9. doi: 10.1001/jama.287.3.356

57. Ervin RB. Prevalence of metabolic syndrome among adults 20 years of age and over, by sex, age, race and ethnicity, and body mass index: United States, 2003-2006. *Natl Health Stat Report* (2009); (13):1-7.
58. Kotani K, Tokunaga K, Fujioka S, Kobatake T, Keno Y, Yoshida S, Shimomura I, Tarui S, Matsuzawa Y. Sexual dimorphism of age-related changes in whole-body fat distribution in the obese. *Int J Obes Relat Metab Disord* (1994); **18**(4):207-2.
59. Cheung OK-, Cheng AS-. Gender differences in adipocyte metabolism and liver cancer progression. *Front Genet* (2016); **7**:168. doi: 10.3389/fgene.2016.00168
60. Muller M, Grobbee DE, den Tonkelaar I, Lamberts SWJ, van der Schouw YT. Endogenous sex hormones and metabolic syndrome in aging men. *The Journal of Clinical Endocrinology & Metabolism* (2005); **90**(5):2618-23. doi: 10.1210/jc.2004-1158
61. Kuk JL, Ardern CI. Age and sex differences in the clustering of metabolic syndrome factors: Association with mortality risk. *Diabetes Care* (2010); **33**(11):2457-61. doi: 10.2337/dc10-0942
62. Kelly DM, Jones TH. Testosterone: A metabolic hormone in health and disease. *J Endocrinol* (2013); **217**(3):25. doi: 10.1530/JOE-12-0455
63. Laughlin GA, Barrett-Connor E, May S. Sex-specific association of the androgen to oestrogen ratio with adipocytokine levels in older adults: The rancho bernardo study. *Clin Endocrinol (Oxf)* (2006); **65**(4):506-13. doi: 10.1111/j.1365-2265.2006.02624.x
64. Karim R, Stanczyk FZ, Brinton RD, Rettberg J, Hodis HN, Mack WJ. Association of endogenous sex hormones with adipokines and ghrelin in postmenopausal women. *J Clin Endocrinol Metab* (2015); **100**(2):508-15. doi: 10.1210/jc.2014-1839
65. Braveman P, Gottlieb L. The social determinants of health: It's time to consider the causes of the causes. *Public Health Rep* (2014); **129**(Suppl 2):19-31.
66. Stringhini S, Sabia S, Shipley M, Brunner E, Nabi H, Kivimaki M, Singh-Manoux A. Association of socioeconomic position with health

- behaviors and mortality. *JAMA* (2010); **303**(12):1159-66. doi: 10.1001/jama.2010.297
67. Izquierdo AG, Crujeiras AB. Chapter 10 - Epigenetic biomarkers in metabolic syndrome and obesity In: Sharma S, editor. Prognostic Epigenetics. *Academic Press* (2019); 269-87.
68. Xu W, Wang F, Yu Z, Xin F. Epigenetics and cellular metabolism. *Genet Epigenet* (2016); **8**:43-51. doi: 10.4137/GEG.S32160
69. Oliver SG, Winson MK, Kell DB, Baganz F. Systematic functional analysis of the yeast genome. *Trends Biotechnol* (1998); **16**(9):373-8. doi: 10.1016/s0167-7799(98)01214-1
70. Beecher CWW. The Human Metabolome. In: Harrigan G.G. GR(, editor. *Metabolic Profiling: Its Role in Biomarker Discovery and Gene Function Analysis*. Springer, Boston, MA. (2003);
71. Uppal K, Walker DI, Liu K, Li S, Go Y, Jones DP. Computational metabolomics: A framework for the million metabolome. *Chem Res Toxicol* (2016); **29**(12):1956-75. doi: 10.1021/acs.chemrestox.6b00179
72. Zamboni N, Saghatelian A, Patti GJ. Defining the metabolome: Size, flux, and regulation. *Mol Cell* (2015); **58**(4):699-706. doi: 10.1016/j.molcel.2015.04.021
73. Metallo CM, Heiden MG. Understanding metabolic regulation and its influence on cell physiology. *Mol Cell* (2013); **49**(3):388-98. doi: 10.1016/j.molcel.2013.01.018
74. Serrano-Carbajal EA, Espinal-Enríquez J, Hernández-Lemus E. Targeting metabolic deregulation landscapes in breast cancer subtypes. *Front Oncol* (2020); **10**:97. doi: 10.3389/fonc.2020.00097
75. Misselbeck K, Parolo S, Lorenzini F, Savoca V, Leonardelli L, Bora P, Morine MJ, Mione MC, Domenici E, Priami C. A network-based approach to identify deregulated pathways and drug effects in metabolic syndrome. *Nat Commun* (2019); **10**(1):5215. doi: 10.1038/s41467-019-13208-z

76. Barros SP, Offenbacher S. Epigenetics: Connecting environment and genotype to phenotype and disease. *J Dent Res* (2009); **88**(5):400-8. doi: 10.1177/0022034509335868
77. Berger SL, Kouzarides T, Shiekhattar R, Shilatifard A. An operational definition of epigenetics. *Genes Dev* (2009); **23**(7):781-3. doi: 10.1101/gad.1787609
78. Bird A. DNA methylation patterns and epigenetic memory. *Genes Dev* (2002); **16**(1):6-21. doi: 10.1101/gad.947102
79. Kornberg RD, Lorch Y. Twenty-five years of the nucleosome, fundamental particle of the eukaryote chromosome. *Cell* (1999); **98**(3):285-94. doi: 10.1016/s0092-8674(00)81958-3
80. Strahl BD, Allis CD. The language of covalent histone modifications. *Nature* (2000); **403**(6765):41-5. doi: 10.1038/47412
81. Inbar-Feigenberg M, Choufani S, Butcher DT, Roifman M, Weksberg R. Basic concepts of epigenetics. *Fertil Steril* (2013); **99**(3):607-15. doi: 10.1016/j.fertnstert.2013.01.117
82. Hoeijmakers L, Kempe H, Verschure PJ. Epigenetic imprinting during assisted reproductive technologies: The effect of temporal and cumulative fluctuations in methionine cycling on the DNA methylation state. *Mol Reprod Dev* (2016); **83**(2):94-107. doi: 10.1002/mrd.22605
83. Goll MG, Bestor TH. Eukaryotic cytosine methyltransferases. *Annu Rev Biochem* (2005); **74**:481-514. doi: 10.1146/annurev.biochem.74.010904.153721
84. Gujar H, Weisenberger DJ, Liang G. The roles of human DNA methyltransferases and their isoforms in shaping the epigenome. *Genes (Basel)* (2019); **10**(2) doi: 10.3390/genes10020172
85. Frías-Lasserre D, Villagra CA. The importance of ncRNAs as epigenetic mechanisms in phenotypic variation and organic evolution. *Front Microbiol* (2017); **8** doi: 10.3389/fmicb.2017.02483
86. Al Aboud NM, Tupper C, Jialal I. Genetics, Epigenetic Mechanism In: StatPearls. *StatPearls Publishing* (2022)

REFERENCES

87. Cooper DN, Mort M, Stenson PD, Ball EV, Chuzhanova NA. Methylation-mediated deamination of 5-methylcytosine appears to give rise to mutations causing human inherited disease in CpNpG trinucleotides, as well as in CpG dinucleotides. *Hum Genomics* (2010); **4**(6):406-10. doi: 10.1186/1479-7364-4-6-406
88. Takai D, Jones PA. Comprehensive analysis of CpG islands in human chromosomes 21 and 22. *Proc Natl Acad Sci U S A* (2002); **99**(6):3740-5. doi: 10.1073/pnas.052410099
89. Takai D, Jones PA. The CpG island searcher: A new WWW resource. *In Silico Biol* (2003); **3**(3):235-40.
90. Bock C, Walter J, Paulsen M, Lengauer T. CpG island mapping by epigenome prediction. *PLoS computational biology* (2007); **3**(6):e110. doi: 10.1371/journal.pcbi.0030110
91. Chadwick BP. Macrosatellite epigenetics: The two faces of DXZ4 and D4Z4. *Chromosoma* (2009); **118**(6):675-81. doi: 10.1007/s00412-009-0233-5
92. Thakur J, Packiaraj J, Henikoff S. Sequence, chromatin and evolution of satellite DNA. *Int J Mol Sci* (2021); **22**(9):4309. doi: 10.3390/ijms22094309
93. Dodge JE, Ramsahoye BH, Wo ZG, Okano M, Li E. De novo methylation of MMLV provirus in embryonic stem cells: CpG versus non-CpG methylation. *Gene* (2002); **289**(1-2):41-8. doi: 10.1016/s0378-1119(02)00469-9
94. Estécio MRH, Gallegos J, Vallot C, Castoro RJ, Chung W, Maegawa S, Oki Y, Kondo Y, Jelinek J, Shen L, Hartung H, Aplan PD, Czerniak BA, Liang S, Issa JJ. Genome architecture marked by retrotransposons modulates predisposition to DNA methylation in cancer. *Genome Res* (2010); **20**(10):1369-82. doi: 10.1101/gr.107318.110
95. Teschendorff AE, West J, Beck S. Age-associated epigenetic drift: Implications, and a case of epigenetic thrift? *Hum Mol Genet* (2013); **22**(R1):R7-R15. doi: 10.1093/hmg/ddt375

96. Wang Y, Karlsson R, Jylhävä J, Hedman ÅK, Almqvist C, Karlsson IK, Pedersen NL, Almgren M, Hägg S. Comprehensive longitudinal study of epigenetic mutations in aging. *Clin Epigenetics* (2019); **11**(1):187. doi: 10.1186/s13148-019-0788-9
97. Issa J. Aging and epigenetic drift: A vicious cycle. *J Clin Invest* (2014); **124**(1):24-9. doi: 10.1172/JCI69735
98. Fraga MF, Ballestar E, Paz MF, Ropero S, Setien F, Ballestar ML, Heine-Suñer D, Cigudosa JC, Urioste M, Benitez J, Boix-Chornet M, Sanchez-Aguilera A, Ling C, Carlsson E, Poulsen P, Vaag A, Stephan Z, Spector TD, Wu Y, Plass C, Esteller M. Epigenetic differences arise during the lifetime of monozygotic twins. *Proc Natl Acad Sci U S A* (2005); **102**(30):10604-9. doi: 10.1073/pnas.0500398102
99. Hamilton OKL, Zhang Q, McRae AF, Walker RM, Morris SW, Redmond P, Campbell A, Murray AD, Porteous DJ, Evans KL, McIntosh AM, Deary IJ, Marioni RE. An epigenetic score for BMI based on DNA methylation correlates with poor physical health and major disease in the lothian birth cohort. *International journal of obesity (2005)* (2019); **43**(9):1795-802. doi: 10.1038/s41366-018-0262-3
100. Wahl S, Drong A, Lehne B, Loh M, Scott WR, Kunze S, Tsai P, Ried JS, Zhang W, Yang Y, Tan S, Fiorito G, Franke L, Guarrera S, Kasela S, Kriebel J, Richmond RC, Adamo M, Afzal U, Ala-Korpela M, Albeti B, Ammerpohl O, Apperley JF, Beekman M, Bertazzi PA, Black SL, Blancher C, Bonder M, Brosch M, Carstensen-Kirberg M, de Craen AJM, de Lusignan S, Dehghan A, Elkalaawy M, Fischer K, Franco OH, Gaunt TR, Hampe J, Hashemi M, Isaacs A, Jenkinson A, Jha S, Kato N, Krogh V, Laffan M, Meisinger C, Meitinger T, Mok ZY, Motta V, Ng HK, Nikolakopoulou Z, Nteliopoulos G, Panico S, Pervjakova N, Prokisch H, Rathmann W, Roden M, Rota F, Rozario MA, Sandling JK, Schafmayer C, Schramm K, Siebert R, Slagboom PE, Soininen P, Stolk L, Strauch K, Tai E-, Tarantini L, Thorand B, Tigchelaar EF, Tumino R, Uitterlinden AG, van Duijn C, van Meurs JBJ, Vineis P, Wickremasinghe AR, Wijmenga C, Yang T, Yuan W, Zhernakova A, Batterham RL, Smith GD, Deloukas P, Heijmans BT, Herder C, Hofman A, Lindgren CM, Milani L, van der Harst P, Peters A, Illig T, Relton CL, Waldenberger M, Jarvelin M, Bollati V, Soong R, Spector TD, Scott J, McCarthy MI, Elliott P, Bell JT, Matullo G, Gieger C, Kooner JS, Grallert H, Chambers JC. Epigenome-wide association study of body mass index, and the adverse outcomes of adiposity. *Nature* (2017); **541**(7635):81-6. doi: 10.1038/nature20784

REFERENCES

101. Marioni RE, Shah S, McRae AF, Ritchie SJ, Muniz-Terrera G, Harris SE, Gibson J, Redmond P, Cox SR, Pattie A, Corley J, Taylor A, Murphy L, Starr JM, Horvath S, Visscher PM, Wray NR, Deary IJ. The epigenetic clock is correlated with physical and cognitive fitness in the lothian birth cohort 1936. *Int J Epidemiol* (2015); **44**(4):1388-96. doi: 10.1093/ije/dyu277
102. Arneson A, Haghani A, Thompson MJ, Pellegrini M, Kwon SB, Vu H, Maciejewski E, Yao M, Li CZ, Lu AT, Morselli M, Rubbi L, Barnes B, Hansen KD, Zhou W, Breeze CE, Ernst J, Horvath S. A mammalian methylation array for profiling methylation levels at conserved sequences. *Nat Commun* (2022); **13**(1):1-13. doi: 10.1038/s41467-022-28355-z
103. Horvath S. DNA methylation age of human tissues and cell types. *Genome Biol* (2013); **14**(10):R115. doi: 10.1186/gb-2013-14-10-r115
104. Bergsma T, Rogaeva E. DNA methylation clocks and their predictive capacity for aging phenotypes and healthspan. *Neurosci Insights* (2020); **15**:2633105520942221. doi: 10.1177/2633105520942221
105. Lu AT, Quach A, Wilson JG, Reiner AP, Aviv A, Raj K, Hou L, Baccarelli AA, Li Y, Stewart JD, Whitsel EA, Assimes TL, Ferrucci L, Horvath S. DNA methylation GrimAge strongly predicts lifespan and healthspan. *Aging (Albany NY)* (2019); **11**(2):303-27. doi: 10.18632/aging.101684
106. Al Muftah WA, Al-Shafai M, Zaghlool SB, Visconti A, Tsai P, Kumar P, Spector T, Bell J, Falchi M, Suhre K. Epigenetic associations of type 2 diabetes and BMI in an arab population. *Clin Epigenetics* (2016); **8**:13. doi: 10.1186/s13148-016-0177-6
107. Horvath S, Erhart W, Brosch M, Ammerpohl O, von Schönfels W, Ahrens M, Heits N, Bell JT, Tsai P, Spector TD, Deloukas P, Siebert R, Sipos B, Becker T, Röcken C, Schafmayer C, Hampe J. Obesity accelerates epigenetic aging of human liver. *Proc Natl Acad Sci U S A* (2014); **111**(43):15538-43. doi: 10.1073/pnas.1412759111
108. Quach A, Levine ME, Tanaka T, Lu AT, Chen BH, Ferrucci L, Ritz B, Bandinelli S, Neuhauser ML, Beasley JM, Snetselaar L, Wallace RB, Tsao PS, Absher D, Assimes TL, Stewart JD, Li Y, Hou L, Baccarelli AA, Whitsel EA, Horvath S. Epigenetic clock analysis of diet, exercise,

education, and lifestyle factors. *Aging (Albany NY)* (2017); **9**(2):419-46. doi: 10.18632/aging.101168

109. Park YJ, Han SM, Huh JY, Kim JB. Emerging roles of epigenetic regulation in obesity and metabolic disease. *Journal of Biological Chemistry* (2021); **297**(5):101296. doi: 10.1016/j.jbc.2021.101296

110. Pant R, Fimal P, Shah VK, Alam A, Chattopadhyay S. Epigenetic regulation of adipogenesis in development of metabolic syndrome. *Front Cell Dev Biol* (2021); **8** doi: 10.3389/fcell.2020.619888

111. Mendelson MM, Marioni RE, Joehanes R, Liu C, Hedman ÅK, Aslibekyan S, Demerath EW, Guan W, Zhi D, Yao C, Huan T, Willinger C, Chen B, Courchesne P, Multhaup M, Irvin MR, Cohain A, Schadt EE, Grove ML, Bressler J, North K, Sundström J, Gustafsson S, Shah S, McRae AF, Harris SE, Gibson J, Redmond P, Corley J, Murphy L, Starr JM, Kleinbrink E, Lipovich L, Visscher PM, Wray NR, Krauss RM, Fallin D, Feinberg A, Absher DM, Fornage M, Pankow JS, Lind L, Fox C, Ingelsson E, Arnett DK, Boerwinkle E, Liang L, Levy D, Deary IJ. Association of body mass index with DNA methylation and gene expression in blood cells and relations to cardiometabolic disease: A mendelian randomization approach. *PLoS Med* (2017); **14**(1):e1002215. doi: 10.1371/journal.pmed.1002215

112. Reed ZE, Suderman MJ, Relton CL, Davis OSP, Hemani G. The association of DNA methylation with body mass index: Distinguishing between predictors and biomarkers. *Clin Epigenetics* (2020); **12**(1):50. doi: 10.1186/s13148-020-00841-5

113. Carson C, Lawson HA. Epigenetics of metabolic syndrome. *Physiol Genomics* (2018); **50**(11):947-55. doi: 10.1152/physiolgenomics.00072.2018

114. Kuneš J, Vaněčková I, Mikulášková B, Behuliak M, Maletínská L, Zicha J. Epigenetics and a new look on metabolic syndrome. *Physiol Res* (2015); **64**(5):611-20. doi: 10.33549/physiolres.933174

115. Micheel, CM, Nass, SJ, Omenn, GS, Trials, Committee on the Review of Omics-Based Tests for Predicting Patient Outcomes in Clinical, Services, BoHC, Policy, BoHS, Medicine, Io. Omics-Based Clinical

Discovery: Science, Technology, and Applications. *National Academies Press (US)* (2012)

116. Yu L, Li K, Zhang X. Next-generation metabolomics in lung cancer diagnosis, treatment and precision medicine: Mini review. *Oncotarget* (2017); **8**(70):115774-86. doi: 10.18632/oncotarget.22404

117. Ahmadzadehfar H, Gholamrezanezhad A. A multi-omics investigation of the molecular characteristics and classification of six metabolic syndrome relevant diseases. *PET clinics* (2021); **16**(3) doi: 10.1016/S1556-8598(21)00031-6

118. Petersen A, Zeilinger S, Kastenmüller G, Römisch-Margl W, Brügger M, Peters A, Meisinger C, Strauch K, Hengstenberg C, Pagel P, Huber F, Mohny RP, Grallert H, Illig T, Adamski J, Waldenberger M, Gieger C, Suhre K. Epigenetics meets metabolomics: An epigenome-wide association study with blood serum metabolic traits. *Human molecular genetics* (2014); **23**(2):534-45. doi: 10.1093/hmg/ddt430

119. Nicholson JK. Global systems biology, personalized medicine and molecular epidemiology. *Mol Syst Biol* (2006); **2**:52. doi: 10.1038/msb4100095

120. Faber JH, Malmödin D, Toft H, Maher AD, Crockford D, Holmes E, Nicholson JK, Dumas ME, Baunsgaard D. Metabonomics in diabetes research. *J Diabetes Sci Technol* (2007); **1**(4):549-57.

121. Dumas M. Metabolome 2.0: Quantitative genetics and network biology of metabolic phenotypes. *Mol Biosyst* (2012); **8**(10):2494-502. doi: 10.1039/c2mb25167a

122. Cirulli ET, Guo L, Leon Swisher C, Shah N, Huang L, Napier LA, Kirkness EF, Spector TD, Caskey CT, Thorens B, Venter JC, Telenti A. Profound perturbation of the metabolome in obesity is associated with health risk. *Cell Metab* (2019); **29**(2):488,500.e2. doi: 10.1016/j.cmet.2018.09.022

123. Hoult DI, Busby SJ, Gadian DG, Radda GK, Richards RE, Seeley PJ. Observation of tissue metabolites using ³¹P nuclear magnetic resonance. *Nature* (1974); **252**(5481):285-7. doi: 10.1038/252285a0

124. Segers K, Declerck S, Mangelings D, Heyden YV, Eeckhaut AV. Analytical techniques for metabolomic studies: A review. *Bioanalysis* (2019); **11**(24):2297-318. doi: 10.4155/bio-2019-0014
125. Wishart DS, Knox C, Guo AC, Eisner R, Young N, Gautam B, Hau DD, Psychogios N, Dong E, Bouatra S, Mandal R, Sinelnikov I, Xia J, Jia L, Cruz JA, Lim E, Sobsey CA, Shrivastava S, Huang P, Liu P, Fang L, Peng J, Fradette R, Cheng D, Tzur D, Clements M, Lewis A, De Souza A, Zuniga A, Dawe M, Xiong Y, Clive D, Greiner R, Nazyrova A, Shaykhtudinov R, Li L, Vogel HJ, Forsythe I. HMDB: A knowledgebase for the human metabolome. *Nucleic Acids Res* (2009); **37**(Database issue):603. doi: 10.1093/nar/gkn810
126. Clish CB. Metabolomics: An emerging but powerful tool for precision medicine. *Cold Spring Harb Mol Case Stud* (2015); **1**(1) doi: 10.1101/mcs.a000588
127. García-Villaescusa A, Morales-Tatay JM, Monleón-Salvadó D, González-Darder JM, Bellot-Arcis C, Montiel-Company JM, Almerich-Silla JM. Using NMR in saliva to identify possible biomarkers of glioblastoma and chronic periodontitis. *PLOS ONE* (2018); **13**(2):e0188710. doi: 10.1371/journal.pone.0188710
128. Waddington CH. Genetic assimilation of an acquired character. *Evolution* (1953); **7**(2):118-26. doi: 10.1111/j.1558-5646.1953.tb00070.x
129. Rauscher FJ. It is time for a human epigenome project. *Cancer Res* (2005); **65**(24):11229. doi: 10.1158/0008-5472.CAN-65-24-ED1
130. Turunen TA, Väänänen M-, Ylä-Herttua S. Epigenomics In: Vasan RS, Sawyer DB, editors. *Encyclopedia of Cardiovascular Research and Medicine*. Elsevier (2018); 258-65.
131. Flanagan JM. Epigenome-wide association studies (EWAS): Past, present, and future. *Methods Mol Biol* (2015); **1238**:51-63. doi: 10.1007/978-1-4939-1804-1_3
132. Stephens CR, Easton JF, Robles-Cabrera A, Fossion R, de la Cruz L, Martínez-Tapia R, Barajas-Martínez A, Hernández-Chávez A, López-Rivera JA, Rivera AL. The impact of education and age on metabolic

REFERENCES

disorders. *Front Public Health* (2020); **8**:180. doi: 10.3389/fpubh.2020.00180

133. Guo Y, Musani SK, Sims M, Pearson TA, Deboer MD, Gurka MJ. Assessing the added predictive ability of a metabolic syndrome severity score in predicting incident cardiovascular disease and type 2 diabetes: the Atherosclerosis Risk in Communities Study and Jackson Heart Study. *Springer Science and Business Media LLC* (2018); **10** doi: 10.1186/s13098-018-0344-3

134. Grundy SM, Cleeman JI, Daniels SR, Donato KA, Eckel RH, Franklin BA, Gordon DJ, Krauss RM, Savage PJ, Smith SC, Spertus JA, Costa F. Diagnosis and management of the metabolic syndrome. an american heart association/national heart, lung, and blood institute scientific statement. executive summary. *Cardiol Rev* (2005); **13**(6):322-7.

135. Swarup S, Goyal A, Grigorova Y, Zeltser R. Metabolic Syndrome In: StatPearls. *StatPearls Publishing* (2022);

136. Bagheri P, Khalili D, Seif M, Rezaianzadeh A. Dynamic behavior of metabolic syndrome progression: a comprehensive systematic review on recent discoveries. *Springer Science and Business Media LLC* (2021); **21** doi: 10.1186/s12902-021-00716-7

137. Wijndaele K, Beunen G, Duvigneaud N, Matton L, Duquet W, Thomis M, Lefevre J, Philippaerts RM. A continuous metabolic syndrome risk score: Utility for epidemiological analyses. *Diabetes Care* (2006); **29**(10):2329. doi: 10.2337/dc06-1341

138. Vasquez-Avila K, Pacheco-Barrios K, de Melo PS, Fregni F. Addressing the critical role of gender identity and sex in the planning, analysis, and conduct of clinical trials. *Princ Pract Clin Res* (2021); **7**(2):59-62. doi: 10.21801/ppcrj.2021.72.7

139. Alex L, Fjellman Wiklund A, Lundman B, Christianson M, Hammarström A. Beyond a dichotomous view of the concepts of 'sex' and 'gender' focus group discussions among gender researchers at a medical faculty. *PLoS One* (2012); **7**(11):e50275. doi: 10.1371/journal.pone.0050275

140. Santos AC, Ebrahim S, Barros H. Gender, socio-economic status and metabolic syndrome in middle-aged and old adults. *BMC Public Health* (2008); **8**:62. doi: 10.1186/1471-2458-8-62
141. Yi Y, An J. Sex differences in risk factors for metabolic syndrome in the Korean population. *Int J Environ Res Public Health* (2020); **17**(24) doi: 10.3390/ijerph17249513
142. Gurka MJ, Lilly CL, Oliver MN, DeBoer MD. An examination of sex and racial/ethnic differences in the metabolic syndrome among adults: A confirmatory factor analysis and a resulting continuous severity score. *Metabolism* (2014); **63**(2):218-25. doi: 10.1016/j.metabol.2013.10.006
143. Canello R, Soranna D, Brunani A, Scacchi M, Tagliaferri A, Mai S, Marzullo P, Zambon A, Invitti C. Analysis of predictive equations for estimating resting energy expenditure in a large cohort of morbidly obese patients. *Frontiers in endocrinology (Lausanne)* (2018); **9**:367. doi: 10.3389/fendo.2018.00367
144. Leopoldo AS, Lima-Leopoldo AP, Nascimento AF, Luvizotto RaM, Sugizaki MM, Campos DHS, da Silva DCT, Padovani CR, Cicogna AC. Classification of different degrees of adiposity in sedentary rats. *Braz J Med Biol Res* (2016); **49**(4):e5028. doi: 10.1590/1414-431X20155028
145. Luong Q, Huang J, Lee KY. Deciphering white adipose tissue heterogeneity. *Biology (Basel)* (2019); **8**(2) doi: 10.3390/biology8020023
146. Lindon JC, Holmes E, Bollard ME, Stanley EG, Nicholson JK. Metabonomics technologies and their applications in physiological monitoring, drug safety assessment and disease diagnosis. *Biomarkers* (2004); **9**(1):1-31. doi: 10.1080/13547500410001668379
147. Emwas AH. The strengths and weaknesses of NMR spectroscopy and mass spectrometry with particular focus on metabolomics research. In *J. T. Bjerrum (Ed.), Metabonomics methods and protocols*. New York, NY: Springer. (2015); :161–193.
148. Emwas A, Roy R, McKay RT, Ryan D, Brennan L, Tenori L, Luchinat C, Gao X, Zeri AC, Gowda GAN, Raftery D, Steinbeck C, Salek RM, Wishart DS. Recommendations and standardization of biomarker quantification using NMR-based metabolomics with particular focus on

REFERENCES

- urinary analysis. *J Proteome Res* (2016); **15**(2):360-73. doi: 10.1021/acs.jproteome.5b00885
149. Assenov Y, Müller F, Lutsik P, Walter J, Lengauer T, Bock C. Comprehensive analysis of DNA methylation data with RnBeads. *Nat Methods* (2014); **11**(11):1138-40. doi: 10.1038/nmeth.3115
150. Müller F, Scherer M, Assenov Y, Lutsik P, Walter J, Lengauer T, Bock C. RnBeads 2.0: Comprehensive analysis of DNA methylation data. *Genome Biol* (2019); **20**(1):55. doi: 10.1186/s13059-019-1664-9
151. Teschendorff AE, Marabita F, Lechner M, Bartlett T, Tegner J, Gomez-Cabrero D, Beck S. A beta-mixture quantile normalization method for correcting probe design bias in illumina infinium 450 k DNA methylation data. *Bioinformatics* (2013); **29**(2):189-96. doi: 10.1093/bioinformatics/bts680
152. Pevsner, J. Bioinformatics and functional genomics. *Wiley-Blackwell, New York*. (2009)
153. Yousefi P, Huen K, Aguilar Schall R, Decker A, Elboudwarej E, Quach H, Barcellos L, Holland N. Considerations for normalization of DNA methylation data by illumina 450K BeadChip assay in population studies. *Epigenetics* (2013); **8**(11):1141-52. doi: 10.4161/epi.26037
154. Houseman EA, Accomando WP, Koestler DC, Christensen BC, Marsit CJ, Nelson HH, Wiencke JK, Kelsey KT. DNA methylation arrays as surrogate measures of cell mixture distribution. *BMC Bioinformatics* (2012); **13**:86. doi: 10.1186/1471-2105-13-86
155. Fiorito G, McCrory C, Robinson O, Carmeli C, Rosales CO, Zhang Y, Colicino E, Dugué P, Artaud F, McKay GJ, Jeong A, Mishra PP, Nøst TH, Krogh V, Panico S, Sacerdote C, Tumino R, Palli D, Matullo G, Guarrera S, Gandini M, Bochud M, Dermitzakis E, Muka T, Schwartz J, Vokonas PS, Just A, Hodge AM, Giles GG, Southey MC, Hurme MA, Young I, McKnight AJ, Kunze S, Waldenberger M, Peters A, Schwettmann L, Lund E, Baccarelli A, Milne RL, Kenny RA, Elbaz A, Brenner H, Kee F, Voortman T, Probst-Hensch N, Lehtimäki T, Elliot P, Stringhini S, Vineis P, Polidoro S. Socioeconomic position, lifestyle habits and biomarkers of epigenetic aging: A multi-cohort analysis. *Aging (Albany NY)* (2019); **11**(7):2045-70. doi: 10.18632/aging.101900

156. Gentilini D, Garagnani P, Pisoni S, Bacalini MG, Calzari L, Mari D, Vitale G, Franceschi C, Di Blasio AM. Stochastic epigenetic mutations (DNA methylation) increase exponentially in human aging and correlate with X chromosome inactivation skewing in females. *Aging (Albany NY)* (2015); **7**(8):568-78. doi: 10.18632/aging.100792
157. Gentilini D, Scala S, Gaudenzi G, Garagnani P, Capri M, Cescon M, Grazi GL, Bacalini MG, Pisoni S, Dicitore A, Circelli L, Santagata S, Izzo F, Di Blasio AM, Persani L, Franceschi C, Vitale G. Epigenome-wide association study in hepatocellular carcinoma: Identification of stochastic epigenetic mutations through an innovative statistical approach. *Oncotarget* (2017); **8**(26):41890-902. doi: 10.18632/oncotarget.17462
158. Guida V, Calzari L, Fadda MT, Piceci-Sparascio F, Digilio MC, Bernardini L, Brancati F, Mattina T, Melis D, Forzano F, Briuglia S, Mazza T, Bianca S, Valente EM, Salehi LB, Prontera P, Pagnoni M, Tenconi R, Dallapiccola B, Iannetti G, Corsaro L, De Luca A, Gentilini D. Genome-wide DNA methylation analysis of a cohort of 41 patients affected by oculo-auriculo-vertebral spectrum (OAVS). *Int J Mol Sci* (2021); **22**(3) doi: 10.3390/ijms22031190
159. Morris TJ, Butcher LM, Feber A, Teschendorff AE, Chakravarthy AR, Wojdacz TK, Beck S. ChAMP: 450k chip analysis methylation pipeline. *Bioinformatics* (2014); **30**(3):428-30. doi: 10.1093/bioinformatics/btt684
160. Wang K, Li M, Hakonarson H. ANNOVAR: Functional annotation of genetic variants from high-throughput sequencing data. *Nucleic Acids Res* (2010); **38**(16):e164. doi: 10.1093/nar/gkq603
161. Bujak R, Dagher-Wojtkowiak E, Kaliszan R, Markuszewski MJ. PLS-based and regularization-based methods for the selection of relevant variables in non-targeted metabolomics data. *Front Mol Biosci* (2016); **3** doi: 10.3389/fmolb.2016.00035
162. Johnson RA, WD. Applied Multivariate Statistical Analysis. (2002)
163. Fraley C, Raftery AE. Model-based clustering, discriminant analysis, and density estimation. *Journal of the American Statistical Association* (2002); **97**(458):611-31.

REFERENCES

164. R Core Team (2020). — European Environment Agency. Available from: <https://www.eea.europa.eu/data-and-maps/indicators/oxygen-consuming-substances-in-rivers/r-development-core-team-2006>
165. Trygg J, Holmes E, Lundstedt T. Chemometrics in metabonomics. *J Proteome Res* (2007); **6**(2):469-79. doi: 10.1021/pr060594q
166. Mandrekar JN. Receiver operating characteristic curve in diagnostic test assessment. *J Thorac Oncol* (2010); **5**(9):1315-6. doi: 10.1097/JTO.0b013e3181ec173d
167. Pang Z, Chong J, Zhou G, de Lima Morais DA, Chang L, Barrette M, Gauthier C, Jacques P, Li S, Xia J. MetaboAnalyst 5.0: Narrowing the gap between raw spectra and functional insights. *Nucleic Acids Res* (2021); **49**(W1):W388-96. doi: 10.1093/nar/gkab382
168. Shannon P, Markiel A, Ozier O, Baliga NS, Wang JT, Ramage D, Amin N, Schwikowski B, Ideker T. Cytoscape: A software environment for integrated models of biomolecular interaction networks. *Genome Res* (2003); **13**(11):2498-504. doi: 10.1101/gr.1239303
169. Beissbarth T, Speed TP. GOstat: Find statistically overrepresented gene ontologies within a group of genes. *Bioinformatics* (2004); **20**(9):1464-5. doi: 10.1093/bioinformatics/bth088
170. Huang DW, Sherman BT, Tan Q, Collins JR, Alvord WG, Roayaei J, Stephens R, Baseler MW, Lane HC, Lempicki RA. The DAVID gene functional classification tool: A novel biological module-centric algorithm to functionally analyze large gene lists. *Genome Biol* (2007); **8**(9):R183. doi: 10.1186/gb-2007-8-9-r183
171. Supek F, Bošnjak M, Škunca N, Šmuc T. REVIGO summarizes and visualizes long lists of gene ontology terms. *PLoS One* (2011); **6**(7) doi: 10.1371/journal.pone.0021800
172. Honda T, Chen S, Yonemoto K, Kishimoto H, Chen T, Narazaki K, Haeuchi Y, Kumagai S. Sedentary bout durations and metabolic syndrome among working adults: A prospective cohort study. *BMC Public Health* (2016); **16**(1):888. doi: 10.1186/s12889-016-3570-3

173. Tune JD, Goodwill AG, Sassoon DJ, Mather KJ. Cardiovascular consequences of metabolic syndrome. *Transl Res* (2017); **183**:57-70. doi: 10.1016/j.trsl.2017.01.001
174. Gesteiro E, Megía A, Guadalupe-Grau A, Fernandez-Veledo S, Vendrell J, González-Gross M. Early identification of metabolic syndrome risk: A review of reviews and proposal for defining pre-metabolic syndrome status. *Nutr Metab Cardiovasc Dis* (2021); **31**(9):2557-74. doi: 10.1016/j.numecd.2021.05.022
175. Miccoli R, Bianchi C, Odoguardi L, Penno G, Caricato F, Giovannitti MG, Pucci L, Del Prato S. Prevalence of the metabolic syndrome among italian adults according to ATP III definition. *Nutr Metab Cardiovasc Dis* (2005); **15**(4):250-4. doi: 10.1016/j.numecd.2004.09.002
176. Damiri B, Abualsoud MS, Samara AM, Salameh SK. Metabolic syndrome among overweight and obese adults in palestinian refugee camps. *Diabetol Metab Syndr* (2018); **10** doi: 10.1186/s13098-018-0337-2
177. Nguyen SN, Tran VD, Mai Le TT, Nga HT, Thi Thi Tho N. High prevalence of metabolic syndrome among overweight adults in Vietnam based on different criteria: Results from a community-based study. *Clinical Epidemiology and Global Health* (2021); **12**:100852. doi: 10.1016/j.cegh.2021.100852
178. Ahmed A, Khan TE, Yasmeen T, Awan S, Islam N. Metabolic syndrome in type 2 diabetes: Comparison of WHO, modified ATP III & IDF criteria. *J Pak Med Assoc* (2012); **62**(6):569-74.
179. Ross R, Neeland IJ, Yamashita S, Shai I, Seidell J, Magni P, Santos RD, Arsenault B, Cuevas A, Hu FB, Griffin BA, Zambon A, Barter P, Fruchart J, Eckel RH, Matsuzawa Y, Després J. Waist circumference as a vital sign in clinical practice: A consensus statement from the IAS and ICCR working group on visceral obesity. *Nat Rev Endocrinol* (2020); **16**(3):177-89. doi: 10.1038/s41574-019-0310-7
180. Welch AA, Hayhoe RPG, Cameron D. The relationships between sarcopenic skeletal muscle loss during ageing and macronutrient metabolism, obesity and onset of diabetes. *Proc Nutr Soc* (2020); **79**(1):158-69. doi: 10.1017/S0029665119001150

181. Gill LE, Bartels SJ, Batsis JA. Weight management in older adults. *Curr Obes Rep* (2015); **4**(3):379-88. doi: 10.1007/s13679-015-0161-z
182. Shah NR, Braverman ER. Measuring adiposity in patients: The utility of body mass index (BMI), percent body fat, and leptin. *PLoS one* (2012); **7**(4):e33308. doi: 10.1371/journal.pone.0033308
183. Srikanthan K, Feyh A, Visweshwar H, Shapiro JI, Sodhi K. Systematic review of metabolic syndrome biomarkers: A panel for early detection, management, and risk stratification in the west Virginian population. *Int J Med Sci* (2016); **13**(1):25-38. doi: 10.7150/ijms.13800
184. Zhang Z, Monleon D, Verhamme P, Staessen JA. Branched-chain amino acids as critical switches in health and disease. *Hypertension* (2018); **72**(5):1012-22. doi: 10.1161/HYPERTENSIONAHA.118.10919
185. Pallares-Méndez R, Aguilar-Salinas CA, Cruz-Bautista I, Del Bosque-Plata L. Metabolomics in diabetes, a review. *Ann Med* (2016); **48**(1-2):89-102. doi: 10.3109/07853890.2015.1137630
186. Pisoni S, Marrachelli VG, Morales JM, Maestrini S, Di Blasio AM, Monleón D. Sex dimorphism in the metabolome of metabolic syndrome in morbidly obese individuals. *Metabolites* (2022); **12**(5) doi: 10.3390/metabo12050419
187. Holmes D. Biomarkers: Mannose levels predict insulin resistance. *Nat Rev Endocrinol* (2016); **12**(9):496. doi: 10.1038/nrendo.2016.119
188. Mardinoglu A, Stančáková A, Lotta LA, Kuusisto J, Boren J, Blüher M, Wareham NJ, Ferrannini E, Groop PH, Laakso M, Langenberg C, Smith U. Plasma mannose levels are associated with incident type 2 diabetes and cardiovascular disease. *Cell Metab* (2017); **26**(2):281-3. doi: 10.1016/j.cmet.2017.07.006
189. Ferrannini E, Bokarewa M, Brembeck P, Baboota R, Hedjazifar S, Andersson K, Baldi S, Campi B, Muscelli E, Saba A, Sterner I, Wasen C, Smith U. Mannose is an insulin-regulated metabolite reflecting whole-body insulin sensitivity in man. *Metabolism* (2020); **102**:153974. doi: 10.1016/j.metabol.2019.153974

190. Chen M, Yang Z, Gan H, Wang Y, Li C, Gao Y. Investigation into potential mechanisms of metabolic syndrome by integrative analysis of metabolomics and proteomics. *PLoS One* (2022); **17**(7):e0270593. doi: 10.1371/journal.pone.0270593
191. Cani PD, Delzenne NM. Interplay between obesity and associated metabolic disorders: New insights into the gut microbiota. *Curr Opin Pharmacol* (2009); **9**(6):737-43. doi: 10.1016/j.coph.2009.06.016
192. Alsoud LO, Soares NC, Al-Hroub HM, Mousa M, Kasabri V, Bulatova N, Suyagh M, Alzoubi KH, El-Huneidi W, Abu-Irmaileh B, Bustanji Y, Semreen MH. Identification of insulin resistance biomarkers in metabolic syndrome detected by UHPLC-ESI-QTOF-MS. *Metabolites* (2022); **12**(6) doi: 10.3390/metabo12060508
193. Holvoet P. Relations between metabolic syndrome, oxidative stress and inflammation and cardiovascular disease. *Verh K Acad Geneesk Belg* (2008); **70**(3):193-219.
194. Cai H, Li D, Song L, Xu X, Han Y, Meng K, Wen Z, Yang P. Metabolomic characteristics of liver and cecum contents in high-fat-diet-induced obese mice intervened with lactobacillus plantarum FRT10. *Foods* (2022); **11**(16) doi: 10.3390/foods11162491
195. Sookoian S, Pirola CJ. Alanine and aspartate aminotransferase and glutamine-cycling pathway: Their roles in pathogenesis of metabolic syndrome. *World J Gastroenterol* (2012); **18**(29):3775-81. doi: 10.3748/wjg.v18.i29.3775
196. Newgard CB, An J, Bain JR, Muehlbauer MJ, Stevens RD, Lien LF, Haqq AM, Shah SH, Arlotto M, Slentz CA, Rochon J, Gallup D, Ilkayeva O, Wenner BR, Yancy WE, Eisensohn H, Musante G, Surwit R, Millington DS, Butler MD, Svetkey LP. A branched-chain amino acid-related metabolic signature that differentiates obese and lean humans and contributes to insulin resistance. *Cell Metab* (2009); **9**(4):311-26. doi: 10.1016/j.cmet.2009.02.002
197. Agus A, Clément K, Sokol H. Gut microbiota-derived metabolites as central regulators in metabolic disorders. *Gut* (2021); **70**(6):1174-82. doi: 10.1136/gutjnl-2020-323071

REFERENCES

198. Koeth RA, Wang Z, Levison BS, Buffa JA, Org E, Sheehy BT, Britt EB, Fu X, Wu Y, Li L, Smith JD, DiDonato JA, Chen J, Li H, Wu GD, Lewis JD, Warrier M, Brown JM, Krauss RM, Tang WHW, Bushman FD, Luskis AJ, Hazen SL. Intestinal microbiota metabolism of L-carnitine, a nutrient in red meat, promotes atherosclerosis. *Nat Med* (2013); **19**(5):576-85. doi: 10.1038/nm.3145
199. Ley RE, Bäckhed F, Turnbaugh P, Lozupone CA, Knight RD, Gordon JI. Obesity alters gut microbial ecology. *Proc Natl Acad Sci U S A* (2005); **102**(31):11070-5. doi: 10.1073/pnas.0504978102
200. Thingholm LB, Rühlemann MC, Koch M, Fuqua B, Laucke G, Boehm R, Bang C, Franzosa EA, Hübenthal M, Rahnavard A, Frost F, Lloyd-Price J, Schirmer M, Luskis AJ, Vulpe CD, Lerch MM, Homuth G, Kacprowski T, Schmidt CO, Nöthlings U, Karlsen TH, Lieb W, Laudes M, Franke A, Huttenhower C. Obese individuals with and without type 2 diabetes show different gut microbial functional capacity and composition. *Cell Host Microbe* (2019); **26**(2):252,264.e10. doi: 10.1016/j.chom.2019.07.004
201. Zhang N. Role of methionine on epigenetic modification of DNA methylation and gene expression in animals. *Anim Nutr* (2018); **4**(1):11-6. doi: 10.1016/j.aninu.2017.08.009
202. Elshorbagy AK, Smith AD, Kozich V, Refsum H. Cysteine and obesity. *Obesity (Silver Spring)* (2012); **20**(3):473-81. doi: 10.1038/oby.2011.93
203. Connelly PJ, Casey H, Montezano AC, Touyz RM, Delles C. Sex steroids receptors, hypertension, and vascular ageing. *J Hum Hypertens* (2022); **36**(2):120-5. doi: 10.1038/s41371-021-00576-7
204. Khalil RA. Sex hormones as potential modulators of vascular function in hypertension. *Hypertension* (2005); **46**(2):249-54. doi: 10.1161/01.HYP.0000172945.06681.a4
205. Palmu J, Tikkanen E, Havulinna AS, Vartiainen E, Lundqvist A, Ruuskanen MO, Perola M, Ala-Korpela M, Jousilahti P, Würtz P, Salomaa V, Lahti L, Niiranen T. Comprehensive biomarker profiling of hypertension in 36985 Finnish individuals. *J Hypertens* (2022); **40**(3):579-87. doi: 10.1097/HJH.0000000000003051

206. Frank AP, de Souza Santos R, Palmer BF, Clegg DJ. Determinants of body fat distribution in humans may provide insight about obesity-related health risks. *Journal of Lipid Research* (2019); **60**(10):1710-9. doi: 10.1194/jlr.R086975
207. Silvestris E, de Pergola G, Rosania R, Loverro G. Obesity as disruptor of the female fertility. *Reprod Biol Endocrinol* (2018); **16**(1):22. doi: 10.1186/s12958-018-0336-z
208. Pascot A, Lemieux S, Lemieux I, Prud'homme D, Tremblay A, Bouchard C, Nadeau A, Couillard C, Tchernof A, Bergeron J, Després JP. Age-related increase in visceral adipose tissue and body fat and the metabolic risk profile of premenopausal women. *Diabetes Care* (1999); **22**(9):1471-8. doi: 10.2337/diacare.22.9.1471
209. Mancuso P, Bouchard B. The impact of aging on adipose function and adipokine synthesis. *Front Endocrinol* (2019); **0** doi: 10.3389/fendo.2019.00137
210. Pucci G, Alcidi R, Tap L, Battista F, Mattace-Raso F, Schillaci G. Sex- and gender-related prevalence, cardiovascular risk and therapeutic approach in metabolic syndrome: A review of the literature. *Pharmacol Res* (2017); **120**:34-42. doi: 10.1016/j.phrs.2017.03.008
211. Sundarakumar JS, Stezin A, Menesgere AL, Ravindranath V. Rural-urban and gender differences in metabolic syndrome in the aging population from southern India: Two parallel, prospective cohort studies. *EClinicalMedicine* (2022); **47**:101395. doi: 10.1016/j.eclinm.2022.101395
212. Jiang B, Zheng Y, Chen Y, Chen Y, Li Q, Zhu C, Wang N, Han B, Zhai H, Lin D, Lu Y. Age and gender-specific distribution of metabolic syndrome components in east china: Role of hypertriglyceridemia in the SPECT-china study. *Lipids Health Dis* (2018); **17** doi: 10.1186/s12944-018-0747-z
213. Krebs HA. The regulation of the release of ketone bodies by the liver. *Adv Enzyme Regul* (1966); **4**:339-54. doi: 10.1016/0065-2571(66)90027-6
214. Cantrell CB, Mohiuddin SS. Biochemistry, Ketone Metabolism In: StatPearls. *StatPearls Publishing* (2021);

215. Borrás C, Sastre J, García-Sala D, Lloret A, Pallardó FV, Viña J. Mitochondria from females exhibit higher antioxidant gene expression and lower oxidative damage than males. *Free Radic Biol Med* (2003); **34**(5):546-52. doi: 10.1016/s0891-5849(02)01356-4
216. Ko S, Kim H. Menopause-associated lipid metabolic disorders and foods beneficial for postmenopausal women. *Nutrients* (2020); **12**(1) doi: 10.3390/nu12010202
217. Karakelides H, Irving BA, Short KR, O'Brien P, Nair KS. Age, obesity, and sex effects on insulin sensitivity and skeletal muscle mitochondrial function. *Diabetes* (2010); **59**(1):89-97. doi: 10.2337/db09-0591
218. Guasch-Ferré M, Hu FB, Ruiz-Canela M, Bulló M, Toledo E, Wang DD, Corella D, Gómez-Gracia E, Fiol M, Estruch R, Lapetra J, Fitó M, Arós F, Serra-Majem L, Ros E, Dennis C, Liang L, Clish CB, Martínez-González MA, Salas-Salvadó J. Plasma metabolites from choline pathway and risk of cardiovascular disease in the PREDIMED (prevention with mediterranean diet) study. *Journal of the American Heart Association* (2017); **6**(11):e006524. doi: 10.1161/JAHA.117.006524
219. Zhu W, Gregory JC, Org E, Buffa JA, Gupta N, Wang Z, Li L, Fu X, Wu Y, Mehrabian M, Sartor RB, McIntyre TM, Silverstein RL, Tang WHW, DiDonato JA, Brown JM, Luscis AJ, Hazen SL. Gut microbial metabolite TMAO enhances platelet hyperreactivity and thrombosis risk. *Cell* (2016); **165**(1):111-24. doi: 10.1016/j.cell.2016.02.011
220. Fuente IMDI, Cortes JM, Perez-Pinilla MB, Ruiz-Rodriguez V, Veguillas J. The metabolic core and catalytic switches are fundamental elements in the self-regulation of the systemic metabolic structure of cells. *PLoS One* (2011); **6**(11):e27224. doi: 10.1371/journal.pone.0027224
221. Greco EA, Lenzi A, Migliaccio S, Gessani S. Epigenetic modifications induced by nutrients in early life phases: Gender differences in metabolic alteration in adulthood. *Front Genet* (2019); **10** doi: 10.3389/fgene.2019.00795
222. Wang J, Wu Z, Li D, Li N, Dindot SV, Satterfield MC, Bazer FW, Wu G. Nutrition, epigenetics, and metabolic syndrome. *Antioxid Redox Signal* (2012); **17**(2):282-301. doi: 10.1089/ars.2011.4381

223. Alhawiti NM, Al Mahri S, Aziz MA, Malik SS, Mohammad S. TXNIP in metabolic regulation: Physiological role and therapeutic outlook. *Curr Drug Targets* (2017); **18**(9):1095-103. doi: 10.2174/1389450118666170130145514
224. Chong C, Chan WPA, Nguyen TH, Liu S, Procter NEK, Ngo DT, Sverdlov AL, Chirkov YY, Horowitz JD. Thioredoxin-interacting protein: Pathophysiology and emerging pharmacotherapeutics in cardiovascular disease and diabetes. *Cardiovasc Drugs Ther* (2014); **28**(4):347-60. doi: 10.1007/s10557-014-6538-5
225. Domingues A, Jolibois J, Marquet de Rougé P, Nivet-Antoine V. The emerging role of TXNIP in ischemic and cardiovascular diseases; A novel marker and therapeutic target. *Int J Mol Sci* (2021); **22**(4) doi: 10.3390/ijms22041693
226. Soriano-Tárraga C, Jiménez-Conde J, Giralt-Steinhauer E, Mola-Caminal M, Vivanco-Hidalgo RM, Ois A, Rodríguez-Campello A, Cuadrado-Godia E, Sayols-Baixeras S, Elosua R, Roquer J. Epigenome-wide association study identifies TXNIP gene associated with type 2 diabetes mellitus and sustained hyperglycemia. *Hum Mol Genet* (2016); **25**(3):609-19. doi: 10.1093/hmg/ddv493
227. Zhang D, Cheng C, Cao M, Wang T, Chen X, Zhao Y, Wang B, Ren Y, Liu D, Liu L, Chen X, Liu F, Zhou Q, Tian G, Li Q, Guo C, Li H, Wang J, Cheng R, Hu D, Zhang M. TXNIP hypomethylation and its interaction with obesity and hypertriglyceridemia increase type 2 diabetes mellitus risk: A nested case-control study. *J Diabetes* (2020); **12**(7):512-20. doi: 10.1111/1753-0407.13021
228. Tsai H, Shen C, Ho C, Hsu S, Tantoh DM, Nfor ON, Chiu S, Chou Y, Liaw Y. Interaction between a diabetes-related methylation site (TXNIP cg19693031) and variant (GLUT1 rs841853) on fasting blood glucose levels among non-diabetics. *J Transl Med* (2022); **20**(1):87. doi: 10.1186/s12967-022-03269-y
229. Zhang C, Tian Y, Zhang M, Tuo Q, Chen J, Liao D. IDOL, inducible degrader of low-density lipoprotein receptor, serves as a potential therapeutic target for dyslipidemia. *Med Hypotheses* (2016); **86**:138-42. doi: 10.1016/j.mehy.2015.11.010

230. Wang H, Ma L, Pan X, Du Z, Chen Y. Novel associations of SNPs MYLIP rs3757354 and ABCA1 2230806 gene with early-onset-preeclampsia: A case-control candidate genetic study. *Pregnancy Hypertens* (2021); **23**:185-90. doi: 10.1016/j.preghy.2020.12.005
231. Hedman ÅK, Mendelson MM, Marioni RE, Gustafsson S, Joehanes R, Irvin MR, Zhi D, Sandling JK, Yao C, Liu C, Liang L, Huan T, McRae AF, Demissie S, Shah S, Starr JM, Cupples LA, Deloukas P, Spector TD, Sundström J, Krauss RM, Arnett DK, Deary IJ, Lind L, Levy D, Ingelsson E. Epigenetic patterns in blood associated with lipid traits predict incident coronary heart disease events and are enriched for results from genome-wide association studies. *Circ Cardiovasc Genet* (2017); **10**(1):e001487. doi: 10.1161/CIRCGENETICS.116.001487
232. Liang C, Wang X, Peng K, Lai P, Liu Z, Ma J, Chen X, Liu G, Zheng M, Wang Y, Yang H, Liu G, Xian X, Gao M. Idol depletion protects against spontaneous atherosclerosis in a hamster model of familial hypercholesterolemia. *Oxid Med Cell Longev* (2022); **2022**:1889632. doi: 10.1155/2022/1889632
233. Teslovich TM, Musunuru K, Smith AV, Edmondson AC, Stylianou IM, Koseki M, Pirruccello JP, Ripatti S, Chasman DI, Willer CJ, Johansen CT, Fouchier SW, Isaacs A, Peloso GM, Barbalic M, Ricketts SL, Bis JC, Aulchenko YS, Thorleifsson G, Feitosa MF, Chambers J, Orho-Melander M, Melander O, Johnson T, Li X, Guo X, Li M, Shin Cho Y, Jin Go M, Jin Kim Y, Lee J, Park T, Kim K, Sim X, Tzee-Hee Ong R, Croteau-Chonka DC, Lange LA, Smith JD, Song K, Hua Zhao J, Yuan X, Luan J, Lamina C, Ziegler A, Zhang W, Zee RYL, Wright AF, Witteman JCM, Wilson JF, Willemssen G, Wichmann H-, Whitfield JB, Waterworth DM, Wareham NJ, Waeber G, Vollenweider P, Voight BF, Vitart V, Uitterlinden AG, Uda M, Tuomilehto J, Thompson JR, Tanaka T, Surakka I, Stringham HM, Spector TD, Soranzo N, Smit JH, Sinisalo J, Silander K, Sijbrands EJG, Scuteri A, Scott J, Schlessinger D, Sanna S, Salomaa V, Saharinen J, Sabatti C, Ruukonen A, Rudan I, Rose LM, Roberts R, Rieder M, Psaty BM, Pramstaller PP, Pichler I, Perola M, Penninx BWJH, Pedersen NL, Pattaro C, Parker AN, Pare G, Oostra BA, O'Donnell CJ, Nieminen MS, Nickerson DA, Montgomery GW, Meitinger T, McPherson R, McCarthy MI, McArdle W, Masson D, Martin NG, Marroni F, Mangino M, Magnusson PKE, Lucas G, Luben R, Loos RJF, Lokki M, Lettre G, Langenberg C, Launer LJ, Lakatta EG, Laaksonen R, Kyvik KO, Kronenberg F, König IR, Khaw K, Kaprio J, Kaplan LM, Johansson A, Jarvelin M, Janssens ACJW, Ingelsson E, Igl W, Kees Hovingh G,

Hottenga J, Hofman A, Hicks AA, Hengstenberg C, Heid IM, Hayward C, Havulinna AS, Hastie ND, Harris TB, Haritunians T, Hall AS, Gyllenstein U, Guiducci C, Groop LC, Gonzalez E, Gieger C, Freimer NB, Ferrucci L, Erdmann J, Elliott P, Ejebe KG, Döring A, Dominiczak AF, Demissie S, Deloukas P, de Geus EJC, de Faire U, Crawford G, Collins FS, Chen YI, Caulfield MJ, Campbell H, Burt NP, Bonnycastle LL, Boomsma DI, Boehholdt SM, Bergman RN, Barroso I, Bandinelli S, Ballantyne CM, Assimes TL, Quertermous T, Altshuler D, Seielstad M, Wong TY, Tai E-, Feranil AB, Kuzawa CW, Adair LS, Taylor HA, Borecki IB, Gabriel SB, Wilson JG, Holm H, Thorsteinsdottir U, Gudnason V, Krauss RM, Mohlke KL, Ordoñas JM, Munroe PB, Kooner JS, Tall AR, Hegele RA, Kastelein JJP, Schadt EE, Rotter JI, Boerwinkle E, Strachan DP, Mooser V, Stefansson K, Reilly MP, Samani NJ, Schunkert H, Cupples LA, Sandhu MS, Ridker PM, Rader DJ, van Duijn CM, Peltonen L, Abecasis GR, Boehnke M, Kathiresan S. Biological, clinical and population relevance of 95 loci for blood lipids. *Nature* (2010); **466**(7307):707-13. doi: 10.1038/nature09270

234. Sayols-Baixeras S, Irvin MR, Arnett DK, Elosua R, Aslibekyan SW. Epigenetics of lipid phenotypes. *Curr Cardiovasc Risk Rep* (2016); **10**(10) doi: 10.1007/s12170-016-0513-6

235. Parker DC, Wan M, Lohman K, Hou L, Nguyen AT, Ding J, Bertoni A, Shea S, Burke GL, Jacobs DR, Post W, Corcoran D, Hoeschele I, Parks JS, Liu Y. Monocyte miRNAs are associated with type 2 diabetes. *Diabetes* (2022); **71**(4):853-61. doi: 10.2337/db21-0704

236. Weissglas-Volkov D, Calkin AC, Tusie-Luna T, Sinsheimer JS, Zelcer N, Riba L, Tino AMV, Ordoñez-Sánchez ML, Cruz-Bautista I, Aguilar-Salinas CA, Tontonoz P, Pajukanta P. The N342S MYLIP polymorphism is associated with high total cholesterol and increased LDL receptor degradation in humans. *J Clin Invest* (2011); **121**(8):3062-71. doi: 10.1172/JCI45504

237. Chen Y, Kassam I, Lau SH, Kooner JS, Wilson R, Peters A, Winkelmann J, Chambers JC, Chow VT, Khor CC, van Dam RM, Teo Y, Loh M, Sim X. Impact of BMI and waist circumference on epigenome-wide DNA methylation and identification of epigenetic biomarkers in blood: An EWAS in multi-ethnic Asian individuals. *Clin Epigenetics* (2021); **13** doi: 10.1186/s13148-021-01162-x

238. Ling C, Rönn T. Epigenetics in human obesity and type 2 diabetes. *Cell Metab* (2019); **29**(5):1028-44. doi: 10.1016/j.cmet.2019.03.009
239. Dekkers KF, Slagboom PE, Jukema JW, Heijmans BT. The multifaceted interplay between lipids and epigenetics. *Curr Opin Lipidol* (2016); **27**(3):288-94. doi: 10.1097/MOL.0000000000000301
240. Yara S, Lavoie J, Levy E. Oxidative stress and DNA methylation regulation in the metabolic syndrome. *Epigenomics* (2015); **7**(2):283-300. doi: 10.2217/epi.14.84
241. Feng B, Ruiz MA, Chakrabarti S. Oxidative-stress-induced epigenetic changes in chronic diabetic complications. *Can J Physiol Pharmacol* (2013); **91**(3):213-20. doi: 10.1139/cjpp-2012-0251
242. Reddy P, Lent-Schochet D, Ramakrishnan N, McLaughlin M, Jialal I. Metabolic syndrome is an inflammatory disorder: A conspiracy between adipose tissue and phagocytes. *Clin Chim Acta* (2019); **496**:35-44. doi: 10.1016/j.cca.2019.06.019
243. Chait A, den Hartigh LJ. Adipose tissue distribution, inflammation and its metabolic consequences, including diabetes and cardiovascular disease. *Front Cardiovasc Med* (2020); **7**:22. doi: 10.3389/fcvm.2020.00022
244. Luebeck EG, Curtius K, Hazelton WD, Maden S, Yu M, Thota PN, Patil DT, Chak A, Willis JE, Grady WM. Identification of a key role of widespread epigenetic drift in Barrett's esophagus and esophageal adenocarcinoma. *Clin Epigenetics* (2017); **9** doi: 10.1186/s13148-017-0409-4
245. Armani A, Berry A, Cirulli F, Caprio M. Molecular mechanisms underlying metabolic syndrome: The expanding role of the adipocyte. *FASEB J* (2017); **31**(10):4240-55. doi: 10.1096/fj.201601125RRR
246. Nevalainen T, Kananen L, Marttila S, Jylhävä J, Mononen N, Kähönen M, Raitakari OT, Hervonen A, Jylhä M, Lehtimäki T, Hurme M. Obesity accelerates epigenetic aging in middle-aged but not in elderly individuals. *Clin Epigenetics* (2017); **9**:20. doi: 10.1186/s13148-016-0301-7

247. Włodarczyk M, Nowicka G. Obesity, DNA damage, and development of obesity-related diseases. *Int J Mol Sci* (2019); **20**(5) doi: 10.3390/ijms20051146
248. Setayesh T, Nersesyan A, Mišík M, Ferk F, Langie S, Andrade VM, Haslberger A, Knasmüller S. Impact of obesity and overweight on DNA stability: Few facts and many hypotheses. *Mutat Res Rev Mutat Res* (2018); **777**:64-91. doi: 10.1016/j.mrrev.2018.07.001
249. Salvestrini V, Sell C, Lorenzini A. Obesity may accelerate the aging process. *Front Endocrinol (Lausanne)* (2019); **10** doi: 10.3389/fendo.2019.00266
250. Valdes AM, Andrew T, Gardner JP, Kimura M, Oelsner E, Cherkas LF, Aviv A, Spector TD. Obesity, cigarette smoking, and telomere length in women. *Lancet* (2005); **366**(9486):662-4. doi: 10.1016/S0140-6736(05)66630-5
251. von Zglinicki T. Oxidative stress shortens telomeres. *Trends Biochem Sci* (2002); **27**(7):339-44. doi: 10.1016/s0968-0004(02)02110-2
252. Epel ES, Blackburn EH, Lin J, Dhabhar FS, Adler NE, Morrow JD, Cawthon RM. Accelerated telomere shortening in response to life stress. *Proc Natl Acad Sci U S A* (2004); **101**(49):17312-5. doi: 10.1073/pnas.0407162101
253. Lin J, Epel E, Blackburn E. Telomeres and lifestyle factors: Roles in cellular aging. *Mutat Res* (2012); **730**(1-2):85-9. doi: 10.1016/j.mrfmmm.2011.08.003
254. Jung UJ, Choi M. Obesity and its metabolic complications: The role of adipokines and the relationship between obesity, inflammation, insulin resistance, dyslipidemia and nonalcoholic fatty liver disease. *International journal of molecular sciences* (2014); **15**(4):6184-223. doi: 10.3390/ijms15046184
255. Kawai T, Autieri MV, Scalia R. Adipose tissue inflammation and metabolic dysfunction in obesity. *Am J Physiol Cell Physiol* (2021); **320**(3):C375-91. doi: 10.1152/ajpcell.00379.2020

256. Bilgin Göçer D, Baş M, Çakır Biçer N, Hajhamidiasl L. Predicting metabolic syndrome by visceral adiposity index, body roundness index, dysfunctional adiposity index, lipid accumulation product index, and body shape index in adults. *Nutr Hosp* (2022); **39**(4):794-802. doi: 10.20960/nh.03966
257. Maric I, Krieger J, van der Velden P, Börchers S, Asker M, Vujicic M, Wernstedt Asterholm I, Skibicka KP. Sex and species differences in the development of diet-induced obesity and metabolic disturbances in rodents. *Front Nutr* (2022); **9** doi: 10.3389/fnut.2022.828522
258. Boulet N, Briot A, Galitzky J, Bouloumié A. The sexual dimorphism of human adipose depots. *Biomedicines* (2022); **10**(10) doi: 10.3390/biomedicines10102615
259. Plaisance EP, Greenway FL, Boudreau A, Hill KL, Johnson WD, Krajcik RA, Perrone CE, Orentreich N, Cefalu WT, Gettys TW. Dietary methionine restriction increases fat oxidation in obese adults with metabolic syndrome. *J Clin Endocrinol Metab* (2011); **96**(5):E836-40. doi: 10.1210/jc.2010-2493
260. Nishimura J, Masaki T, Arakawa M, Seike M, Yoshimatsu H. Isoleucine prevents the accumulation of tissue triglycerides and upregulates the expression of PPARalpha and uncoupling protein in diet-induced obese mice. *J Nutr* (2010); **140**(3):496-500. doi: 10.3945/jn.109.108977
261. O'Rielly R, Li H, Lim SM, Yazbeck R, Kritas S, Ullrich SS, Feinle-Bisset C, Heilbronn L, Page AJ. The effect of isoleucine supplementation on body weight gain and blood glucose response in lean and obese mice. *Nutrients* (2020); **12**(8) doi: 10.3390/nu12082446
262. Petrus P, Lecoutre S, Dollet L, Wiel C, Sulen A, Gao H, Tavira B, Laurencikiene J, Rooyackers O, Checa A, Douagi I, Wheelock CE, Arner P, McCarthy M, Bergo MO, Edgar L, Choudhury RP, Aouadi M, Krook A, Rydén M. Glutamine links obesity to inflammation in human white adipose tissue. *Cell Metab* (2020); **31**(2):375,390.e11. doi: 10.1016/j.cmet.2019.11.019
263. Ye J, Gao Z, Yin J, He Q. Hypoxia is a potential risk factor for chronic inflammation and adiponectin reduction in adipose tissue of ob/ob and

dietary obese mice. *Am J Physiol Endocrinol Metab* (2007); **293**(4):1118. doi: 10.1152/ajpendo.00435.2007

264. Trayhurn P, Wang B, Wood IS. Hypoxia in adipose tissue: A basis for the dysregulation of tissue function in obesity? *Br J Nutr* (2008); **100**(2):227-35. doi: 10.1017/S0007114508971282

265. Netzer N, Gatterer H, Faulhaber M, Burtscher M, Pramsohler S, Pesta D. Hypoxia, oxidative stress and fat. *Biomolecules* (2015); **5**(2):1143-50. doi: 10.3390/biom5021143

266. Ye J. Adipose tissue vascularization: Its role in chronic inflammation. *Curr Diab Rep* (2011); **11**(3):203-10. doi: 10.1007/s11892-011-0183-1

267. Hamada M, Abe M, Miyake T, Kawasaki K, Tada F, Furukawa S, Matsuura B, Hiasa Y, Onji M. B cell-activating factor controls the production of adipokines and induces insulin resistance. *Obesity (Silver Spring)* (2011); **19**(10):1915-22. doi: 10.1038/oby.2011.165

268. Zeyda M, Farmer D, Todoric J, Aszmann O, Speiser M, Györi G, Zlabinger GJ, Stulnig TM. Human adipose tissue macrophages are of an anti-inflammatory phenotype but capable of excessive pro-inflammatory mediator production. *Int J Obes (Lond)* (2007); **31**(9):1420-8. doi: 10.1038/sj.ijo.0803632

269. Pitkänen E. Mannose, mannitol, fructose and 1,5-anhydroglucitol concentrations measured by gas chromatography/mass spectrometry in blood plasma of diabetic patients. *Clin Chim Acta* (1996); **251**(1):91-103. doi: 10.1016/0009-8981(96)06284-5

270. Pitkänen OM, Vanhanen H, Pitkänen E. Metabolic syndrome is associated with changes in D-mannose metabolism. *Scand J Clin Lab Invest* (1999); **59**(8):607-12. doi: 10.1080/00365519950185094

271. Torretta S, Scagliola A, Ricci L, Mainini F, Di Marco S, Cuccovillo I, Kajaste-Rudnitski A, Sumpton D, Ryan KM, Cardaci S. D-mannose suppresses macrophage IL-1 β production. *Nat Commun* (2020); **11** doi: 10.1038/s41467-020-20164-6

272. Embgenbroich M, van der Zande HJP, Hussaarts L, Schulte-Schrepping J, Pelgrom LR, García-Tardón N, Schlautmann L, Stoetzel I,

REFERENCES

Händler K, Lambooj JM, Zawistowska-Deniziak A, Hoving L, de Ruiter K, Wijngaarden M, Pijl H, Willems van Dijk K, Everts B, van Harmelen V, Yazdanbakhsh M, Schultze JL, Guigas B, Burgdorf S. Soluble mannose receptor induces proinflammatory macrophage activation and metaflammation. *Proc Natl Acad Sci U S A* (2021); **118**(31) doi: 10.1073/pnas.2103304118

273. Hajer GR, van Haefen TW, Visseren FLJ. Adipose tissue dysfunction in obesity, diabetes, and vascular diseases. *Eur Heart J* (2008); **29**(24):2959-71. doi: 10.1093/eurheartj/ehn387

274. Merino J, Leong A, Liu C, Porneala B, Walford GA, von Grotthuss M, Wang TJ, Flannick J, Dupuis J, Levy D, Gerszten RE, Florez JC, Meigs JB. Metabolomics insights into early type 2 diabetes pathogenesis and detection in individuals with normal fasting glucose. *Diabetologia* (2018); **61**(6):1315-24. doi: 10.1007/s00125-018-4599-x

275. Díaz A, López-Grueso R, Gambini J, Monleón D, Mas-Bargues C, Abdelaziz KM, Viña J, Borrás C. Sex differences in age-associated type 2 diabetes in rats-role of estrogens and oxidative stress. *Oxid Med Cell Longev* (2019); **2019**:6734836. doi: 10.1155/2019/6734836

276. Wang J, Liu Y, Lian K, Shentu X, Fang J, Shao J, Chen M, Wang Y, Zhou M, Sun H. BCAA catabolic defect alters glucose metabolism in lean mice. *Front Physiol* (2019); **10**:1140. doi: 10.3389/fphys.2019.01140

277. Menni C, Fauman E, Erte I, Perry JRB, Kastenmüller G, Shin S, Petersen A, Hyde C, Psatha M, Ward KJ, Yuan W, Milburn M, Palmer CNA, Frayling TM, Trimmer J, Bell JT, Gieger C, Mohny RP, Broxnan MJ, Suhre K, Soranzo N, Spector TD. Biomarkers for type 2 diabetes and impaired fasting glucose using a nontargeted metabolomics approach. *Diabetes* (2013); **62**(12):4270-6. doi: 10.2337/db13-0570

278. Falconer D. The inheritance of liability to certain diseases, estimated from the incidence among relatives. *Annals of Human Genetics* (2007); **29**:51-76. doi: 10.1111/j.1469-1809.1965.tb00500.x

279. Falconer DS. The inheritance of liability to diseases with variable age of onset, with particular reference to diabetes mellitus. *Ann Hum Genet* (1967); **31**(1):1-20. doi: 10.1111/j.1469-1809.1967.tb01249.x

280. Benckek PH, Morris NJ. How meaningful are heritability estimates of liability? *Hum Genet* (2013); **132**(12) doi: 10.1007/s00439-013-1334-z
281. Eckel N, Mühlenbruch K, Meidtner K, Boeing H, Stefan N, Schulze MB. Characterization of metabolically unhealthy normal-weight individuals: Risk factors and their associations with type 2 diabetes. *Metabolism* (2015); **64**(8):862-71. doi: 10.1016/j.metabol.2015.03.009
282. Liang Y, Liu C, Lu M, Dong Q, Wang Z, Wang Z, Xiong W, Zhang N, Zhou J, Liu Q, Wang X, Wang Z. Calorie restriction is the most reasonable anti-ageing intervention: A meta-analysis of survival curves. *Sci Rep* (2018); **8**(1):5779. doi: 10.1038/s41598-018-24146-z
283. Maegawa S, Lu Y, Tahara T, Lee JT, Madzo J, Liang S, Jelinek J, Colman RJ, Issa JJ. Caloric restriction delays age-related methylation drift. *Nat Commun* (2017); **8**(1):539. doi: 10.1038/s41467-017-00607-3
284. Gensous N, Franceschi C, Santoro A, Milazzo M, Garagnani P, Bacalini MG. The impact of caloric restriction on the epigenetic signatures of aging. *Int J Mol Sci* (2019); **20**(8) doi: 10.3390/ijms20082022
285. Ibero-Baraibar I, Abete I, Navas-Carretero S, Massis-Zaid A, Martinez JA, Zulet MA. Oxidised LDL levels decreases after the consumption of ready-to-eat meals supplemented with cocoa extract within a hypocaloric diet. *Nutr Metab Cardiovasc Dis* (2014); **24**(4):416-22. doi: 10.1016/j.numecd.2013.09.017
286. Colman RJ, Anderson RM, Johnson SC, Kastman EK, Kosmatka KJ, Beasley TM, Allison DB, Cruzen C, Simmons HA, Kemnitz JW, Weindruch R. Caloric restriction delays disease onset and mortality in rhesus monkeys. *Science* (2009); **325**(5937):201-4. doi: 10.1126/science.1173635
287. López-Otín C, Galluzzi L, Freije JMP, Madeo F, Kroemer G. Metabolic control of longevity. *Cell* (2016); **166**(4):802-21. doi: 10.1016/j.cell.2016.07.031
288. Artegoitia VM, Krishnan S, Bonnel EL, Stephensen CB, Keim NL, Newman JW. Healthy eating index patterns in adults by sex and age predict cardiometabolic risk factors in a cross-sectional study. *BMC Nutr* (2021); **7** doi: 10.1186/s40795-021-00432-4



9. ANNEXES

ANNEX I: Ethics Review Committee approval



MINUTES OF THE MEETING OF THE ETHICS REVIEW COMMITTEE OF ISTITUTO AUXOLOGICO ITALIANO ON 10TH DECEMBER, 2008

The Ethics Review Committee, duly called by its president, convened on 10th December, 2008 at 5 p.m. in Milan, Via Mosè Biamchi 90, to discuss the following agenda:

1. **President's Communications**
2. **Research Protocols**
3. **Amendments**
4. **Any other issues**

The Ethics Committee of Istituto Auxologico Italiano is so composed:

<i>Prof. Giovanni Ancarani</i>	Expert in Law and Insurance, President
<i>Prof. Alberto Zanchetti MD</i>	Scientific Director of the Institute, ex officio member
<i>Prof. Father Ferdinando Citterio</i>	Expert in Bioethics
<i>Mr Goffredo Grassani, Lawyer</i>	Expert in Bioethics, representative of voluntary services and patient protection associations; Vice-President
<i>Prof. Mario Chirico MD</i>	Expert in Health Organization
<i>Prof. Francesco Morabito MD</i>	Expert in Research on Minors
<i>Prof. Luciano Martini</i>	Expert in Pharmacology
<i>Prof. Virgilio Melchiorre</i>	Expert in Bioethics
<i>Prof. Adriano Propersi</i>	Expert in Health Economics
<i>Mr. Marino Pron MA</i>	Expert in Management Control
<i>Mr. Mario Colombo MA</i>	Expert in Law and Insurance, Sexcretary
<i>Mrs. Elisabetta Sala PhD</i>	Biostatistician
<i>Mr. Alfredo Di Rocco MD</i>	Hospital Director, ex-officio member
<i>Mr. Alberto Pozzi MD</i>	Practitioner
<i>Mrs. Cinzia D'Angelo PhD</i>	Pharmacist, ex-officio member
<i>Mrs. Carla Amiconi DNursing</i>	Representative of Nurses



The following persons have justified their absence: Mario Colombo, Luciano Martini, Adriano Propersi, Cinzia D'Angelo. Mrs. Antonella Eliana Sorgente, Lawyer will act as Secretary.

Omissis

2. Research Protocols

Omissis

2.3 Study Title

"Genome-Wide study to identify new loci associated with the development of severe obesity" (Geoitaly)

Sponsor : Istituto Auxologico Italiano

Proponente : Laboratory for Molecular Biology Research

Study Responsible (Principal Investigator): Prof. Antonio Liuzzi

Co-Investigator : Mrs. Anna Maria Di Blasio MD

Prof. Antonio Liuzzi, asks the Istituto Auxologico Italiano Ethics Review Committee for opinion and approval of an investigation titled "Genome-Wide study to identify new loci associated with the development of severe obesity" (Geoitaly)

Study objectives

Study aim is to compare the genetic profile of patient with severe obesity to that of normal-weight subjects to identify genetic variants associated with an increased susceptibility to severe obesity

The study will be conducted at the IRCCS Ospedale San Giuseppe, at the IRCCS San Michele and at the Centre for Researches and Biomedical Technologies.

The Ethics Reviewer Committee, having examined the documentation received



Fondazione riconosciuta con DPR 6 Dicembre 1963, N.1883 - Iscr. Reg. Pers. Giur. Prefettura di Milano N. 194
Sede Legale: Via L. Ariosto, 13 - 20145 Milano - C.F. e P. IVA 02703120160 - Tel. 02.61911.1 Fax 02.61911.2480



- √ Having considered that the structure is adequate for study coordination
- √ Having found the principal investigator and his collaborators well suited for coordinating the study
- √ Having found the patient's information and consensus forms exhaustive and adequate
- √ Having found that the sponsor is providing adequate insurance
- √ Having found that the study is in accordance with other legal requirements

**UNANIMOUSLY EXPRESSES A FAVOURABLE OPINION TO THE STUDY
CONDUCTANCE**

In particular, approval is given for the following documents:

- Study protocol in English, draft of 20th November 2008
- Protocol synopsis in Italian, draft of 3rd December 2008
- Information and consensus forms for patients, draft of 20th November 2008
- Letter requesting evaluation

Formally entrusts

The responsibility of the conductance, coordination and management of the investigation to the Study Responsible (Principal Investigator), Prof. Antonio Liuzzi, and eventually to his collaborators, who should be identified by writing and will operate under his direct responsibility.

REQUIRES THAT THE PRINCIPAL INVESTIGATOR AND THE SPONSOR

- Keep the Committee informed by writing about the beginning and the end of the study as well as by its eventual premature interruption and its causes.
- Keep the Committee informed about any successive protocol amendments, adverse events, serious or unexpected, occurring during the study, and any other issue that may influence the patient's safety and the continuation of the study.
- Do not effect any protocol deviation or changes without the Ethical Review Committee has expressed by writing a favourable opinion to any specific amendment, except for



Fondazione riconosciuta con DPR 6 Dicembre 1963, N.1883 - Iscr. Reg. Pers. Giur. Prefettura di Milano N. 194
Sede Legale: Via L. Ariosto, 13 - 20145 Milano - C.F. e P. IVA 02703120150 - Tel. 02.61911.1 Fax 02.61911.2480

ANNEX II: Experimental rat's diets composition sheets

2014

++++
ENVIGO

Teklad Global 14% Protein Rodent Maintenance Diet

Product Description - 2014 is a fixed formula, non-autoclavable diet manufactured with high quality ingredients and designed to promote longevity and normal body weight in rodents. 2014 does not contain alfalfa or soybean meal, thus minimizing the occurrence of natural phytoestrogens. Typical isoflavone concentrations (daidzein + genistein aglycone equivalents) range from non-detectable to 20 mg/kg. Exclusion of alfalfa reduces chlorophyll, improving optical imaging clarity. Absence of animal protein and fish meal minimizes the presence of nitrosamines. Also available certified (2014C) and irradiated (2914). For autoclavable diet, refer to 2014S (Sterilizable).

Macronutrients		
Crude Protein	%	14.3
Fat (ether extract) ^a	%	4.0
Carbohydrate (available) ^b	%	48.0
Crude Fiber	%	4.1
Neutral Detergent Fiber ^c	%	18.0
Ash	%	4.7
Energy Density ^d	kcal/g (kJ/g)	2.9 (12.1)
Calories from Protein	%	20
Calories from Fat	%	13
Calories from Carbohydrate	%	67
Minerals		
Calcium	%	0.7
Phosphorus	%	0.6
Non-Phytate Phosphorus	%	0.3
Sodium	%	0.1
Potassium	%	0.6
Chloride	%	0.3
Magnesium	%	0.2
Zinc	mg/kg	70
Manganese	mg/kg	100
Copper	mg/kg	15
Iodine	mg/kg	6
Iron	mg/kg	175
Selenium	mg/kg	0.23
Amino Acids		
Aspartic Acid	%	0.9
Glutamic Acid	%	2.9
Alanine	%	0.9
Glycine	%	0.7
Threonine	%	0.5
Proline	%	1.2
Serine	%	0.7
Leucine	%	1.4
Isoleucine	%	0.6
Valine	%	0.7
Phenylalanine	%	0.7
Tyrosine	%	0.4
Methionine	%	0.3
Cystine	%	0.3
Lysine	%	0.7
Histidine	%	0.4
Arginine	%	0.8
Tryptophan	%	0.2

Teklad Diets are designed and manufactured for research purposes only.

©2015 Envigo



Ingredients (in descending order of inclusion)-Wheat middlings, ground wheat, ground corn, corn gluten meal, calcium carbonate, soybean oil, dicalcium phosphate, iodized salt, L-lysine, vitamin E acetate, DL-methionine, magnesium oxide, choline chloride, manganese oxide, ferrous sulfate, menadione sodium bisulfite complex (source of vitamin K activity), zinc oxide, copper sulfate, niacin, calcium pantothenate, calcium iodate, pyridoxine hydrochloride, riboflavin, thiamin mononitrate, vitamin A acetate, vitamin B₁₂ supplement, folic acid, cobalt carbonate, biotin, vitamin D₃ supplement.

Standard Product Form: Pellet

Vitamins		
Vitamin A ^{1,7}	IU/g	6.0
Vitamin D ₃ ^{8,9}	IU/g	0.6
Vitamin E	IU/kg	120
Vitamin K ₃ (menadione)	mg/kg	20
Vitamin B ₁ (thiamin)	mg/kg	12
Vitamin B ₂ (riboflavin)	mg/kg	6
Niacin (nicotinic acid)	mg/kg	54
Vitamin B ₆ (pyridoxine)	mg/kg	10
Pantothenic Acid	mg/kg	17
Vitamin B ₁₂ (cyanocobalamin)	mg/kg	0.03
Biotin	mg/kg	0.26
Folate	mg/kg	2
Choline	mg/kg	1030
Fatty Acids		
C16:0 Palmitic	%	0.5
C18:0 Stearic	%	0.1
C18:1ω9 Oleic	%	0.7
C18:2ω6 Linoleic	%	2.0
C18:3ω3 Linolenic	%	0.1
Total Saturated	%	0.6
Total Monounsaturated	%	0.7
Total Polyunsaturated	%	2.1
Other		
Cholesterol	mg/kg	--

^a Ether extract is used to measure fat in pelleted diets, while an acid hydrolysis method is required to recover fat in extruded diets. Compared to ether extract, the fat value for acid hydrolysis will be approximately 1% point higher.

^b Carbohydrate (available) is calculated by subtracting neutral detergent fiber from total carbohydrates.

^c Neutral detergent fiber is an estimate of insoluble fiber, including cellulose, hemicellulose, and lignin. Crude fiber methodology underestimates total fiber.

^d Energy density is a calculated estimate of metabolizable energy based on the Atwater factors assigning 4 kcal/g to protein, 9 kcal/g to fat, and 4 kcal/g to available carbohydrate.

^e Indicates added amount but does not account for contribution from other ingredients.

¹ 1 IU vitamin A = 0.3 µg retinol

⁸ 1 IU vitamin D = 25 ng cholecalciferol

For nutrients not listed, insufficient data is available to quantify.

Nutrient data represent the best information available, calculated from published values and direct analytical testing of raw materials and finished product. Nutrient values may vary due to the natural variations in the ingredients, analysis, and effects of processing.

Figure A1. Composition of the standard diet. Teklad 2014 (Harlan).

Teklad Custom Diet

TD.08811

45%kcal Fat Diet (21% MF, 2% SBO)

++++
ENVIGO


Formula	g/Kg	Key Features
Casein	195.0	+ Purified Diet
L-Cystine	3.0	+ Diet Induced Obesity
Sucrose	340.0	+ Anhydrous Milkfat
Corn Starch	56.86	+ Sucrose
Maltodextrin	60.0	
Anhydrous Milkfat	210.0	
Soybean Oil	20.0	
Cellulose	50.0	
Mineral Mix, AIN-93G-MX (94046)	43.0	
Vitamin Mix, AIN-93-VX (94047)	19.0	
Choline Bitartrate	3.0	
TBHQ, antioxidant	0.04	
Green Food Color	0.1	
Footnote		Key Planning Information
Designed with similarities to TD 88137 Western Diet with 21% anhydrous milk fat and 34% sucrose. 2% soybean oil is included to supplement essential fatty acids and the more modern AIN-93 mineral and vitamin mixes are used. Modified corn starch (maltodextrin) replaces a portion of the regular corn starch to improve pellet quality. Approximate fatty acid profile (% of total fat): 61% SFA, 30% MUFA, 9% PUFA.		+ Products are made fresh to order + Store product at 4°C or lower + Use within 6 months (applicable to most diets) + Box labeled with product name, manufacturing date, and lot number + Replace diet at minimum once per week <i>More frequent replacement may be advised</i> + Lead time: · 2 weeks non-irradiated · 4 weeks irradiated
Selected Nutrient Information¹		Product Specific Information
	% by weight	% kcal from
Protein	17.3	14.7
Carbohydrate	47.6	40.7
Fat	23.2	44.6
Kcal/g	4.7	
¹ Values are calculated from ingredient analysis or manufacturer data		+ 1/2" Pellet or Powder (free flowing) + Minimum order 3 Kg + Irradiation available upon request
Speak With A Nutritionist		Options (fees will apply)
+ (800) 483-5523 + askanutritionist@envigo.com		+ Rush order (pending availability) + Irradiation (see Product Specific Information) + Vacuum packaging (1 and 2 Kg)
Teklad diets are designed & manufactured for research purposes only.		Contact Us
© 2016 Envigo		Obtain pricing - Check order status + teklad@envigo.com + (800) 483-5523
		
		International Inquiry (outside USA or Canada)
		+ askanutritionist@envigo.com
		Place Your Order (USA & Canada)
		Please Choose One + www.envigo.com/teklad-orders + tekladorders@envigo.com + (800) 483-5523 + (608) 277-2066 facsimile

Figure A2. Composition of the HFD. Teklad Custom Diet TD08811 from Harlan.